DISSECTING OUT THE MECHANISMS TO LONGEVITY THROUGH EATING LESS

Lorna Mulvey

B.A. (Honours), M.Sc.

SUBMITTED IN FULFILLMENT OF THE REQUIREMENTS FOR THE DEGREE OF DOCTOR OF PHILOSOPHY

SCHOOL OF LIFE SCIENCES

COLLEGE OF MEDICAL, VETERINARY AND LIFE SCIENCES

UNIVERSITY OF GLASGOW

SEPTEMBER 2017

Abstract

We are currently in the midst of a revolution in ageing research, with several dietary, genetic and pharmacological interventions now known to modulate ageing in model organisms. Whilst it has been known for almost 100 years that dietary restriction (DR) extends lifespan across wide evolutionary distances, the mechanisms through which it acts are still unknown. Using three different recombinant inbred ILSXISS mouse strains, which vary in response to DR; from lifespan extension to lifespan shortening, my PhD has sought to identify the mechanisms involved in DR-induced lifespan extension. Ultimately by exploiting the genetic heterogeneity of these mouse strains may help identify the mechanisms through which DR acts to slow ageing. During my PhD I (1) examined how these animals respond metabolically to DR, (2) determined the impact of DR on mitochondrial function, as mitochondrial dysfunction is a well characterised hallmark of ageing, and DR is known to attenuate age-related mitochondrial dysfunction, and (3) investigated proteostasis in these mice using isotopic labelling. A number of metabolic changes were found to be important to lifespan extension with DR, namely maintenance of gonadal white adipose tissue (WAT) stores and increases in brown adipose tissue (BAT). Conversely, large losses of WAT was associated with lifespan truncation following 40% long-term DR. Surprisingly, enhanced glucose homeostasis was not found to be a prerequisite to lifespan extension with DR. Hepatic mitochondrial dysfunction associated with reduced lifespan of TejJ114 mice under 40% DR, but similar dysfunction was not apparent in skeletal muscle mitochondria, highlighting tissue-specific differences in the mitochondrial response in ILSXISS mice to DR. Increased proteostasis as measured by the ^{new}protein/^{new}DNA ratio, was increased following short-term DR, highlighting increased synthesis of cytoplasmic proteins in the skeletal muscle as important to DR-induced lifespan extension, however results were both tissue and protein specific. The evidence produced in this thesis strongly suggests that numerous aspects of metabolism and mitochondrial function are associated with lifespan shortening, and that the inability for metabolic adaptability may be detrimental to lifespan. This thesis helps to elucidate the impact of genotype on key hallmarks of DR and highlights the importance of utilising both genders and genetically heterogeneous murine strains in order to understand the shared features of slowed ageing.

Table of Contents

List of Tables

List of Figures

List of Accompanying Material:

Appendix I: Supplementary data related to Chapter 4

Appendix II: L. Mulvey, A. Sinclair and C. Selman. ‘Lifespan modulation in mice and the confounding effects of genetic background’. Journal of Genetics and Genomics. 2014. 41(9): 497-503.

Appendix III: L. Mulvey, W. Sands, K. Salin, A. Carr, C. Selman. ‘Disentangling the effect of dietary restriction on mitochondrial function using recombinant inbred mice’. Molecular and Cellular Endocrinology. 2016. 1-13

Bibliography

Acknowledgements

I would like to give a special thank you to my supervisor Colin Selman for his patience and guidance throughout my PhD. Without his support, encouragement and attention to detail this would not have been possible. I am especially grateful to him for many of the great opportunities that he made possible during my PhD, and for pushing me, even if at times I did not want to be pushed. Thank you to Karine Salin for her expert opinion, knowledge and help with the mitochondrial studies and to William Sands for his advice and expertise. Many thanks to the college of Medical, Veterinary and Life Sciences for funding this PhD. One of the highlights of my PhD was my trip to Colorado, where I was hosted by Benjamin Miller and Karyn Hamilton at Colorado State University. A huge thank you to both for enabling me to visit them and learn a new technique, for their help with sample processing and analysis, proof reading and for making my time in Colorado such a pleasant experience. Thanks to past post-docs Holly Birchenough and Amy Sinclair, for their assistance in a number of my experiments, but also for making the lab such a friendly place to work. Thanks to Tony and Denis for assisting in the care of so many hungry mice. Also, a big thank you to all my friends and colleagues in the department who have made this PhD so enjoyable particularly Calum, and Jess for being such lovely office cohabitants, and to my flat mate Becca, who always had time for a chat. Lastly, a massive thank you to my family and friends, especially my best friends Bryan and Siobhan, boyfriend Kris, and parents Giselle and Declan, who were invaluable to me in terms of advice and support. I am sure are almost as happy as I to see this thesis complete!

Candidate Declaration

I declare that work recorded in this thesis is entirely my own composition and that research described herein was carried out by me unless otherwise stated or acknowledged. No part of this thesis has been submitted for another degree. I hereby give my consent, for my thesis, if accepted, to be available for photocopy and interlibrary loan.

Lorna Mulvey

September 2017

Chapter 1: General Introduction

1. Overview

The ageing process is characterised by progressive loss in cellular homeostasis and a decline in physiological function, resulting in a decline in fecundity and increased risk of mortality over time (Balcombe & Sinclair 2001). While ageing was historically believed to be an inevitable and intractable process (for discussion see (Kirkwood & Holliday 1979; Kirkwood 2005; Kirkwood 2008; Munch et al. 2008), we now know that ageing can be modulated through various environmental, genetic and pharmacological interventions including dietary restriction (DR) (Kenyon 2005; Mair & Dillin 2008; Rikke et al. 2010; Swindell 2012; Gems & Partridge 2013). DR is defined here in this thesis as a reduction in overall energy intake, or in specific components of the diet, relative to that consumed normally by individuals with *ad libitum* (AL) access to food. DR has been repeatedly shown to extend lifespan in a wide range of taxonomically diverse organisms (Mair & Dillin 2008; Selman 2014a), although the specific mechanism(s) through which DR induces its beneficial effects remains unclear. More recently pharmacological interventions, many of which appear to act as DR mimetics; including rapamycin and metformin, have been shown to extend lifespan in model organisms (Harrison et al. 2009; Anisimov et al. 2008; Bjedov & Partridge 2011). This has led to renewed hope in identifying realistic, efficacious and safe pharmacological interventions that will increase healthspan, which is the period of our life free from age-related diseases (Selman 2014a). Excitingly, evidence exists that some molecular processes altered by different lifespan interventions may overlap, thereby suggesting some level of commonality (Selman et al. 2009; Yan et al. 2012), although such commonality has not been reported in all comparisons (Masternak et al. 2004; Bhattacharya et al. 2012; Fok et al. 2014).

In humans, DR is associated with a number of physiological and metabolic improvements to health, although the impact on human longevity remains unclear (Fontana & Partridge 2015). Moreover, the level of DR required to induce beneficial effects in humans and the chronic nature of typical DR regimes suggest that it is unlikely to be a feasible lifestyle choice for most humans. Therefore the development of mimetics which capture the beneficial effects of DR, but circumvent the unrealistic levels of self-restraint required, will be instrumental in the

improvement of human health during ageing (as discussed in Fontana & Partridge 2015). One other potentially confounding factor in the efficacy of DR in studies, with particular relevance to human studies, is the impact of genetic heterogeneity on the responsiveness of individuals to DR. Most DR studies are conducted using inbred mice (specifically C57BL/6), but evidence is emerging to suggest that the effectiveness of DR in slowing ageing is highly sensitive to the effects of genetic background (Mitchell et al. 2016; Liao et al. 2010; Rikke et al. 2010; see Swindell 2012 for review).

1.1 Background and History of DR

Humans are now the longest-lived land-based mammal, with an exponential increase in life expectancy observed over the past century. In 2010, 524 million people globally were estimated to be 65 years of age or older, with this number predicted to increase to 1.5 billion by 2050, representing 16% of the world's population (WHO data, see also Suzman et al. 2015 for discussion). This increased proportion of elderly in the population has been coined "the silver tsunami" (See Fig 1.1) (Mitchell 2014; Barusch 2013).

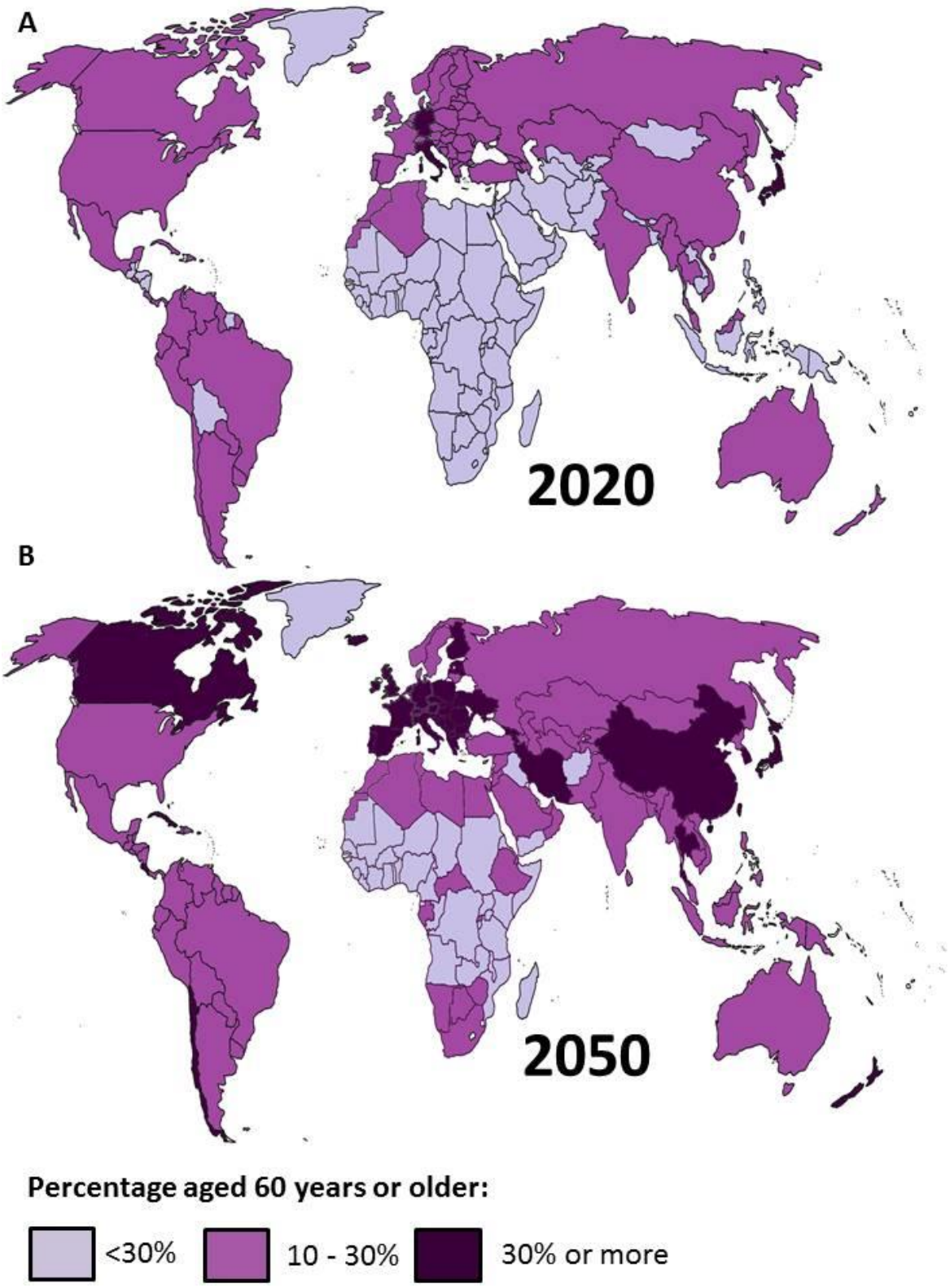

Figure 1.1: Predicted proportion of the population over the age of 60 by (A) 2020 and (B) 2050. Adapted from World Health Organisation data (http://www.who.int/ageing/en/).

However, while human life expectancy continues to grow, there is currently a growing disconnect between longevity and healthspan; healthspan defined here as the period of life free from age-related disease (Figure 1.2). Ageing is the primary risk factor for a host of maladies including obesity, sarcopenia, atherosclerosis, cancer, type II diabetes mellitus and neurodegenerative disorders (Dietz et al. 2015). Furthermore, type II diabetes predisposes to vascular and non-vascular dementia (Chatterjee et al. 2016), thus highlighting the prevalence of comorbidities associated with old age. As the number of elderly individuals in the population continues to increase, and thus the proportion of the population suffering from age-related disease increases, this is undoubtedly going to lead to significant socio-economic implications in terms of increased costs of health and social care (Bartels & Naslund 2013), with fewer people of working age available for care and support. In order to enhance the wellbeing of the aged populous, but also to alleviate some of the societal strain, it will be imperative to attempt to bridge the gap between lifespan and healthspan, in order to compress this period of morbidity and to maintain health and vitality in old age.

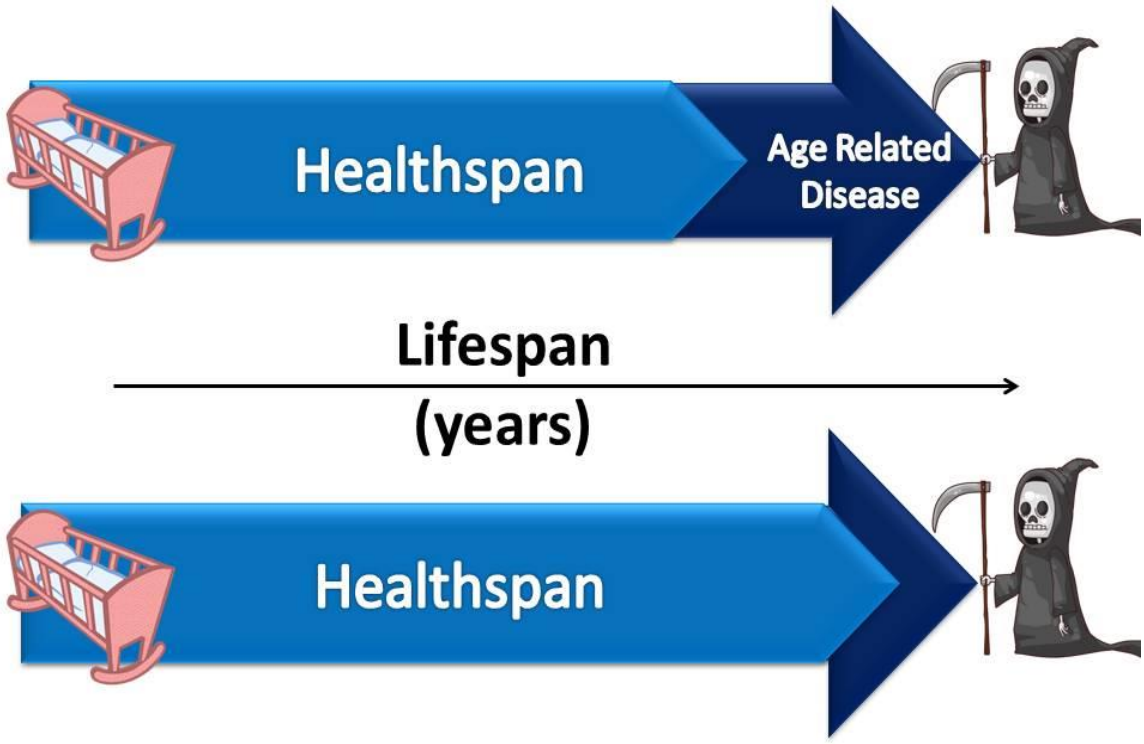

Figure 1.2: Aim of gerontological research; to compress the period of morbidity and to extend the period of life free from age-related disease.

The rate at which organisms age is not universal, with huge variation in life expectancy across taxa; from the Greenland shark (*Somniosus microcephalus*), which can live for over 400 years (Nielsen et al. 2016), to the Mayfly (*Ephemeroptera*) which typically lives for 1-2 days (Carey 2002). Furthermore, bats and birds live substantially longer on average than non-flying mammals of similar body size. Even within mammals, significant variation in ageing rate is observed, with rodents of similar sizes having highly variable life expectancies. For example, the typical laboratory rat (*Rattus norvegicus*), lives on average 2 years, the red squirrel (*Sciurus vulgaris*) lives 10 years in captivity, the grey squirrel (*Sciurus carolinensis*) 20 years in captivity and the naked mole rat (*Heterocephalus glaber*) which lives up to 32 years in captivity (Lifespan data from anAge:The animal longevity data base; http://genomics.senescence.info/species/). Organisms such as hydra, or the immortal jellyfish (*Turritopsis dohrnii*), appear to forgo the classical ageing process and exhibit negligible senescence. Consequently comparative biological approaches has been employed relatively successfully to help understand

the ageing process, by utilising species with exceptionally slow or rapid ageing (Austad 2010).

1.2 Experimental DR

DR-induced lifespan extension was first reported approximately one century ago, by Osborne *et al*. in their seminal paper (Osborne et al. 1917), in which they reported that restriction of food intake in rats, below that of AL fed counterparts, dramatically extended lifespan but decreased reproductive output. Similarly, in 1935 McCay e*t al.*, reported that 40% DR in white rats, from the age of weaning, resulted in a significant increase in longevity (McCay et al. 1935). Subsequently, numerous studies in a range of species, but most notably in mice, have shown that reductions of food intake ranging from 5% to 50% below that eaten by AL controls have a significantly greater median and maximal lifespan (Weindruch 1996; Weindruch et al. 2001; Ladiges et al. 2009; Kim et al. 2008). In addition to rodents, DR has shown beneficial lifespan effects in a wide range of species, spanning several animal taxa (as discussed in Mair & Dillin 2008; Masoro 2005) from yeast (*Sacchromyces cerevisiae*) (Fabrizio & Longo 2003), to the nematode worm (*Caenorhabditis elegans*) (Braeckman et al. 2006), to the fruit fly (D*rosophila melanogaster)* (Partridge et al. 2005). This has led to the widely held belief that DR-induced longevity is mediated by an evolutionarily conserved mechanism (Le Bourg & Rattan 2006; Le Bourg 2010; Mair & Dillin 2008). Furthermore, reports in non-model organisms such as cattle (*Bos Taurus*) (Pinney et al. 1972), dogs (*Canis domesticus*) (Lawler et al. 2008) and non-human primates (*Macaca mulatta*) (Mattison et al. 2017) further bolster this premise (Figure 1.3). Therefore, if the beneficial effects of DR are ubiquitous, the argument is that it should confer significant longevity benefits to humans (Fontana & Partridge 2015).

However, despite the well-publicised beneficial effects of DR on lifespan and a wealth of candidate mechanisms (see Table 1.1) being proposed as driving DR-induced longevity, the precise processes through which DR act mechanistically, remains elusive. It has been proposed that the lack of consensus regarding determining the mechanistic basis of DR relates to the fact that most candidate hypothesis focus on a single underlying mechanism, whereas in reality DR is most likely underpinned by a number of interconnected mechanistic processes (Masoro 2009). To further confuse the issue, the beneficial effect of DR on lifespan has not

been reported in house-flies, rotifers or in several mouse strains (Kirk 2001; Cooper et al. 2004; Harper et al. 2006; Forster et al. 2003).

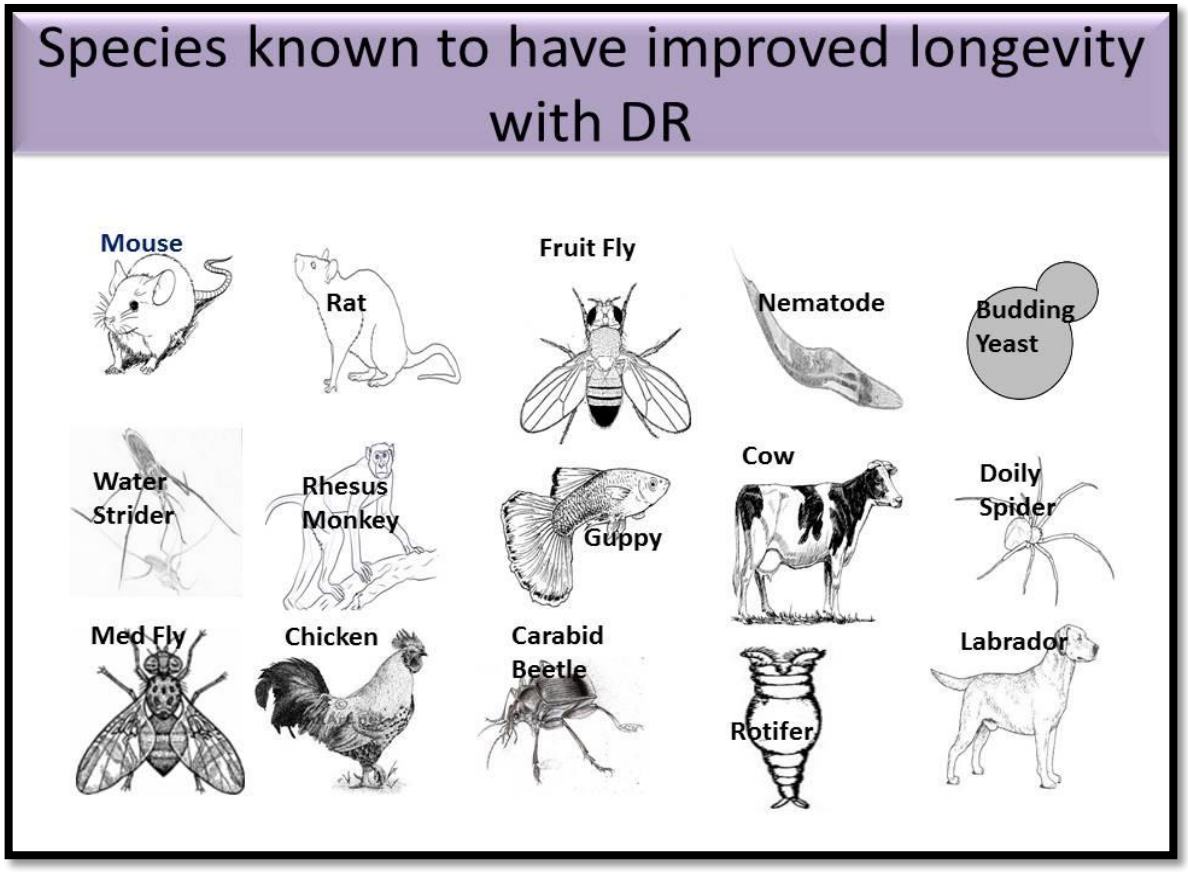

Figure 1.3: DR improves longevity in a host of taxonomically diverse organisms.

1.3 Variation in DR protocols

Model systems are invaluable to DR studies, in helping to identify common mechanisms which are evolutionary conserved across taxa, and in discerning the potential processes underlying DR extension. However, several differences in DR protocols arise across species, as a consequence of variation in life history traits, making it difficult to directly compare results across model organisms. *Saccharomyces Cervisae, Caenorhabditis Elegans* and *Drosophila Melanogaster*, are typically restricted through dilution of the diet through some indigestible component (See Table 1.1 for definitions). However, different DR regimes are likely to alter lifespan through different, yet potentially overlapping, mechanisms (Greer & Brunet 2009), making it difficult to recapitulate the likely responses to DR in mammals. Even within mammals, numerous variations have arisen in restriction protocols, and these protocol differences are likely to influence the outcome of DR (Anson et al. 2005). For example, age at onset of restriction is likely to impact response to DR (Selman 2014). An additional issue that arises in DR studies is that certain strains of over eat and AL controls may experience reduced lifespan as a result of obesity (Keenan et al. 1996; Keenan et al. 1997). To overcome this, numerous studies restrict the AL controls (by 5-10%) (Mattison et al. 2012; Mattison et al. 2017), however it has been found that even mild restriction (8%) has a host of beneficial effects in Fischer 344 rats (Kim et al. 2008). Other restriction protocols such as alternate day fasting or intermittent fasting (IF) involve periodic cycles of DR, also result in lifespan extension in rodents but do not lead to loss of body mass, (Mattson et al. 2014; Goodrick et al. 1990; Anson et al. 2003). Furthermore, time sensitive feeding; restricting food access to 8 hours during the active phase (during dark hours) or for only 4 hours during the light phase, is sufficient to see beneficial effects in both health and on lifespan in mice (Chaix et al. 2014; Asher & Sassone-Corsi 2015). Despite calorie intake being equal to AL counterparts, the mice subject to time restricted feeding are afforded protection against hepatic steatosis, hyperinsulinemia and obesity. Moreover, mice maintained on high-sugar or high-fat diets but subject to daily fasting intervals, are found to do better in endurance testing than AL non-fasted mice on regular diet (Chaix et al. 2014).

Classic DR involves the percentage reduction in the overall nutrient intake of the experimental group of animals, calculated from the intake of the AL control group, without causing malnutrition. As a result the DR mice experience reduction

in their gross calorific intake. Caloric restriction (CR) refers solely to the restriction of calories, whereas DR can encapsulate the reduced intake of both calories and micro/macro-nutrients, as an overall reduction in dietary nutrients will result in reduced calorie intake by proxy. Numerous variations on DR have come into existence since classical restriction in 1917, including, but not limited to, protein restriction, methionine restriction, macronutrient manipulation (definitions summarised in Table 1). Protein restriction (PR) results in decreased IGF-1 levels in middle-aged humans, a common outcome seen in animals following DR, and is associated with reduced incidence of cancer and all-cause mortality in mice and humans (Levine et al. 2014). Wistar rats on 40% PR for 7 weeks had decreased hepatic mitochondrial reactive oxygen species (ROS) production and reduced oxidative damage to nuclear and mitochondrial DNA (mtDNA), and increased lifespan (Sanz et al. 2004; Ayala et al. 2007). In these same studies, similar changes were also observed under 40% DR, suggesting that at least some of the beneficial effects of DR can be related to nutritional intake over calories, however response was smaller than with 40% DR (Sanz et al. 2004; Ayala et al. 2007). Findings that alterations in the ratio of macronutrient intake, in terms of carbohydrate and protein content, in mice suggest an association between macronutrient intake and lifespan, with confirmed health and longevity benefits detected with a low protein, high carbohydrate diet (Solon-Biet et al. 2015). Restriction of the single amino acid, methionine, extends longevity in numerous model systems from yeast to rodents (Madeo et al. 2015; Edwards et al. 2015; Grandison et al. 2009). Restriction of dietary methionine by 80%, leads to a reduction of ROS production by mitochondria (Sanz et al. 2006; Pamplona & Barja 2006), restores a younger metabolic phenotype to adult mice, in terms of body mass, adiposity and insulin resistance, (Lees et al. 2014) and leads to an increase in lifespan in rats (Orentreich et al. 1993; Richie et al. 1994) and mice (Sun et al. 2009; Miller et al. 2005). Thus numerous methods of restriction, such as time-restricted restriction, or restriction of dietary components, have the potential to induce health benefits without adhering to chronic DR. However, as is the case with DR, the question remains as to what mechanistic processes are involved in order to identify effective dietary interventions for beneficial effects on health and lifespan.

Table1.1: Summary of definitions used in DR literature

Abbreviation	Name	Definition
AL	*Ad libitum*	Food freely available. Animals can potentially over consume
WM	Weight Maintenance	As AL, however animals are prevented from over consuming through slight restriction (5-10%). Weight is maintained but development of obesity is prevented
DD	Dietary Dilution	Diet is diluted to a variable extent with inert indigestible component, e.g. cellulose and water (*Drosophila*)
CD	Calorie Dilution	Diet is diluted to reduce caloric content. Shortfall in calories offset by increase in protein
PD	Protein Dilution	Diet is diluted to reduce protein content. Protein content can vary <20% = PD, >20% = Protein Enrichment
DR	Dietary Restriction	Reduction in overall intake, without causing malnutrition, but insufficient to make daily energy demands. Includes alterations of micro and macro-nutrients. Food is same composition as fed to AL controls
CR	Caloric Restriction	Deficit in calories alone. Insufficient calories to make daily energy demands. Food is same composition as fed to AL controls
PR	Protein Restriction	Restriction of protein intake
MR	Methionine Restriction	Restriction of dietary essential amino acid methionine
IF	Intermittent Fasting	Fasting period of 24hs where food is not provided. The number of 24h fasting periods is equal to or less than 50% of the total days
EOD	Every Other Day Feeding	Fasting period of 24hs where food is not provided, every other day. The number of 24h fasting periods is less than 50% of the total days

2. Effects of DR

2.1 Lifespan extension and DR

Enhanced mouse longevity in response to DR has been reported extensively (Forster et al. 2003; Rikke et al. 2003; Rikke & Johnson 2007; Turturro et al. 1999; Weindruch & Walford 1988) (Figure 1.4). However, it is becoming increasingly apparent that lifespan extension with DR is modulated by a number of factors. For instance, differences in DR protocol, including magnitude and age of onset, appear to be important to DR outcome. Reports of DR induced lifespan extension being dose-dependent, implicate magnitude of DR as important to the extent of the longevity effect, with higher magnitudes of DR appearing to promote greater increases in lifespan extension to an upper limit (Figure 1.4) (Weindruch et al. 1986). In addition, the age at which DR is initiated appears to impact lifespan, with a greater longevity effect apparent when initiated earlier, compared to a diminishing effect (Dhahbi et al. 2004; Weindruch & Walford 1982), no effect (Lipman et al. 1995), and even a negative effect (Forster et al. 2003), when initiated in middle-age or later in life. A meta-analysis, which set out to investigate DR lifespan response across gender and taxa found that DR was more effective at extending lifespan in model-species (fruit fly, nematode worm, yeast, mice and rats) than non-model species (Nakagawa et al. 2012). This may suggest a co-adaptive response to DR under laboratory conditions, and may explain some of the apparent lack of effects seen in some non- model organisms following DR, or alternatively, perhaps a lack of power in non-model studies. Moreover, DR was found to generally be more effective at extending female lifespan in all species (Nakagawa et al. 2012).

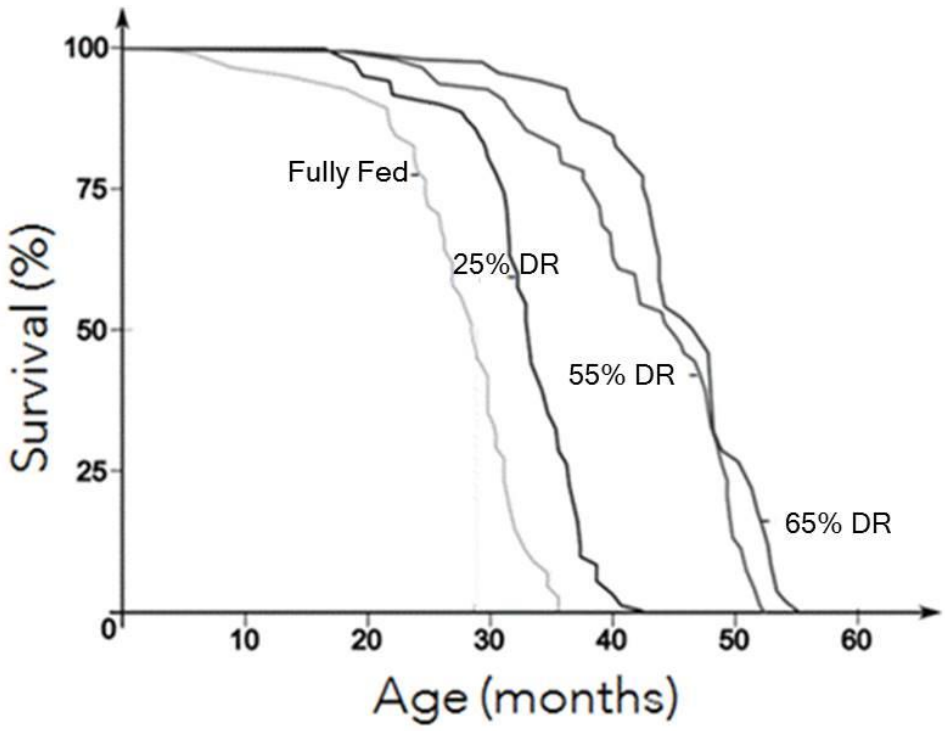

Figure 1.4: Dose-dependent response in C3B10RF mice (Females from the C3H.SW/Sn inbred strain X males from the C57BL10.RIII/Sn inbred strain) in response to varying levels of DR (Data adapted from Weindruch et al. 1986).

The C57BL/6 mouse has a robust and reproducible pro-longevity effect with DR (Turturro et al. 1999; Weindruch & Walford 1988) and is the most commonly used strain in ageing research. However, recently, questions have been raised about the translatability of mouse research, the majority of which has been carried out on this one strain, to a genetically heterogeneous population, such as humans (Miller 2016). A recent study sought to address this problem, and investigate reproducibility of results when genetic background is altered slightly. Male C57BL/6J mice heterozygous for null alleles of Cacna1c and Tcf7l2 were crossed with wild-type females from 30 inbred laboratory strains to produce an F1 cross (Sittig et al. 2016). They found genetic background to be a key determinant of phenotype, more so than gender, and found that altering genotype sometimes gave opposite conclusions on certain interactions than on the classic C57BL/6 background. Indeed the importance of genotype in DR research is becoming increasingly apparent, with genetic background appearing to be a crucial factor in both the magnitude and direction of the DR response. The DBA/2 mouse for example, has previously been reported as unresponsive to DR-induced lifespan extension (Fernandes et al. 1976), but has also reported to show a shortening of lifespan under DR (Forster et al. 2003). However, in a recent comprehensive assessment of different magnitudes of DR on lifespan and healthspan in the DBA/2 and C57BL/6 mouse (Mitchell et al. 2016), it was found that the strains had different optimal levels of DR on which lifespan was maximised. The DBA/2 mouse was found to have better survival, relative to AL controls, when subject to 20% DR rather than 40% DR, unlike the C57BL/6 mouse. Moreover, the DR effects in the DBA/2 mouse are less than that of the C57BL/6 mouse. These results indicate that magnitude of DR is a key mediating variable in lifespan extension with DR, and that the degree of restriction can exert strain-specific lifespan responses. Aside from the monopoly of research being carried out on one genotype to date (C57BL/6), the majority of DR studies have been carried out on male animals and the role of gender has largely been overlooked. In addition to genotype differences, Mitchell *et al* highlight a number of sex-specific responses to DR (Mitchell et al. 2016). For instance, C57BL/6 females did not show DR-induced lifespan extension under 40% DR, relative to AL controls, unlike male animals from this strain, and had higher percentage increase in lifespan under 20% DR than males. DBA/2 females had no further benefits from 20% to 40% DR, thus, implicating gender as important to DR response (Mitchell et al. 2016).

2.2 Healthspan

In addition to enhanced longevity, DR has been shown repeatedly to elicit numerous health benefits. Reports of positive effects on age-associated diseases, attenuation of functional decline, and inhibition of malignant tumour growth have been detected in a number of species (Gross & Dreyfuss 1984; Kritchevsky 2002; Tannenbaum 1940; Richard Weindruch & Sohal 1997; Weindruch et al. 1986). DR protects animals against a range of age-related and non-age-related pathologies, including various cancers, glaucoma, glucose intolerance and sarcopenia (Weindruch & Walford 1982; Sheldon, Warbritton, et al. 1995; Sheldon, Bucci, et al. 1995; McKiernan et al. 2004; Hempenstall et al. 2010). Furthermore, DR decreases pathogenesis and increases survival in a range of mouse disease models of disease including a model of neuronal loss used to mimic Parkinson's disease (C57BL/6 mice administered the toxin 1-methyl-4-phenyl-1,2,3,6-tetrahydropyridine (MPTP) (Duan & Mattson 1999), as well as mouse models for Alzheimer's disease (3xTgAD mice) (Halagappa et al. 2007), viral myocarditis (obese KKAy mice) (Kanda et al. 2007) and pancreatic cancer (LSL-KrasG12D/+; Pdx-1/Cre mice) (Lanza-Jacoby et al. 2013). The positive effects of DR on healthspan also extend to Rhesus monkeys, where the incidence of cancer, cardiovascular disease, type-II diabetes mellitus and brain atrophy during are reduced in DR monkeys relative to AL controls (Colman et al. 2014; Mattison et al. 2017; Colman et al. 2009; Mattison et al. 2012).

However, as with the effect of DR on lifespan, DR-induced effects on healthspan also show considerable sexual dimorphism. Sex-specific differences in glucose homeostasis and in relation to magnitude of DR (20% or 40%) in both C57BL/6 mice and DBA/2 mice have been reported (Mitchell et al. 2016). While improvements in fasting plasma insulin were observed in male mice of both strains following DR, females did not undergo any changes in insulin levels. In rats, following 3 months of 30% DR, mitochondrial function in terms of bioenergetics, oxidative balance and respirations was found to be sex-specific under both AL and DR conditions (Valle et al. 2008), and females were found to have an advantageous metabolic efficiency compared to males following DR (Valle et al. 2005). Moreover, following DR rhesus macaque monkeys exhibit a sexually dimorphic glucose response, in terms of fasting blood glucose levels. Additionally, females displayed a different association between food intake and body weight than males, although

the effects were found to change with age, highlighting gender-specific differences in the allocation of nutritional resources influencing both body composition and metabolism (Mattison et al. 2017). It is difficult to directly compare results between male and female responses to DR owing to the traditional heavy historical bias towards use of male animals in DR studies, and a lack of side-by-side comparisons of male and females in response to DR. In May 2014, the NIH issued a policy statement promising to redress this imbalance (Clayton & Collins 2014). In terms of biomedical research, the inclusion of both sexes is compulsory as results from one gender cannot be reliably extended to the other (Austad & Bartke 2015).

Accumulating evidence reports that DR has numerous protective health effects against comorbidities of ageing. DR protects against obesity, type 2 diabetes and coronary heart disease in humans (Fontana et al. 2007), and reduces risk factors associated with cardio vascular disease (Fontana et al. 2004). Furthermore, DR has been shown to have beneficial effects on cardiac function (Stein et al. 2012), glucose tolerance and insulin action, in terms of reduced insulin levels, as well as improved insulin sensitivity (Weiss et al. 2006), and reportedly ameliorates age-associated decline in diastolic function (Meyer et al. 2006). DR additionally results in a reduction in circulating levels of inflammatory cytokines and adipokines, anabolic hormones and growth factors, several of which are associated with increased cancer risk, and DR can inhibit the development of tumour growth in human models (Fontana et al. 2013). One year of 20% DR in humans decreased body mass, as well as visceral and subcutaneous fat (Racette et al. 2006), while 6 months of 25% DR improves mitochondrial function in young non-obese adults (Civitarese et al. 2007). Brown adipose tissue is decreased in elderly humans, compared to young individuals (Saito et al. 2009), and while DR induces browning of white adipose tissue in mice (Fabbiano, Suá Rez-Zamorano, et al. 2016), the impact of DR on BAT in humans remains to be determined.

2.3 DR- A Universal Modulator of Ageing?

In order for DR research to be translatable to humans, the mechanistic basis through which DR acts to slow ageing needs to be conserved across distantly related organisms, or taxonomically diverse species (Partridge & Gems 2002). These mechanisms are therefore public, that is shared across large evolutionary distances. Conversely, private mechanisms of ageing are specific to particular species, taxa, or even particular genetic backgrounds. As data emerge from multiple

model systems, and murine strains, debate grows over the ubiquitous nature of DR on lifespan extension. The use of genetically heterogeneous mouse models will be important to DR research in identifying universal mechanisms of slowed ageing.

2.4 ILSXISS Mice

Recently, lifespan was assayed in heterogeneous ILSXISS recombinant inbred (RI) mice derived from eight distinct mouse strains (Liao et al. 2010; Rikke et al. 2010). In two separate studies undertaken by the Universities of Texas and Colorado, clear lifespan differences existed between distinct ILSXISS lines under 40% DR. The Liao *et al*. study examined 39 female lines and 41 male lines under DR and reported that only 21% of female and 5% of male lines showed a significant lifespan extension under DR (Liao et al. 2010). In this study, a higher number of lines (26% and 27% for males and females, respectively) showed a significant shortening of lifespan under DR (Figure 1.5). Similarly, Rikke *et al.* examined 42 separate female lines and reported a significant strain-specific difference lifespan following DR, with 21% of females showing lifespan extension and 19% showing significant truncation of lifespan under DR (Rikke et al. 2010) (Figure 1.6). While surprising, these results are not actually unprecedented. Several DR studies have reported no lifespan extension following DR; white rats (McCay et al. 1939), certain inbred mouse strains (e.g. C57BL/6 and DBA/2) (Cheney et al. 1980; Harrison & Archer 1987; Forster et al. 2003), and laboratory-reared descendants of wild-caught mice (Harper 2008). These genotype-dependant lifespan responses have been proposed as a means of probing candidate mechanisms of DR induced lifespan extension, i.e. by comparing responses between “positive” and “negative” DR responders (Sohal et al. 2009; discussed in Swindell 2012). Furthermore, comparisons across strains with differential lifespan responses to DR would allow the uncoupling of lifespan/healthspan benefits. By disentangling DR responses which co-occur with lifespan extension from those that occur following DR in strains which experience lifespan truncation following DR, additional insight into how DR acts to slow ageing can be gleaned (Selman 2014a). Indeed, the strain-specificity of these mice has been utilised previously in order to draw conclusions on how genotype may alter well characterised DR responses. For instance, it is widely established that DR leads to a reduction in body temperature (T_b), first described in rodents by Weindruch *et al* (Weindruch et al. 1979), and subsequently by numerous

other rodent studies (Carrillo & Flouris 2011; Turturro & Hart 1991; Ferguson et al. 2007), humans (Soare et al. 2011) and in non-human primates (Lane et al 1996). This reduction of T_b has been suggested to play a direct mechanistic role in the beneficial effect of DR on lifespan (Turturro & Hart 1991; Jin & Koizumi 1994). Utilising the strain-specific lifespan response of the ILSXISS RI mice, 28 lines of female mice were maintained on 40% DR to assess the link between reduced T_b with DR and life extension (Rikke et al. 2003). Not only was significant strain variation observed, ranging from a 1.5^0 C to a 5^0 C reduction in T_b relative to AL controls, but reductions correlated well with lifespan response, enabling Rikke *et al* to conclude that that maintenance of T_b above a critical threshold is important to the beneficial effects of DR.

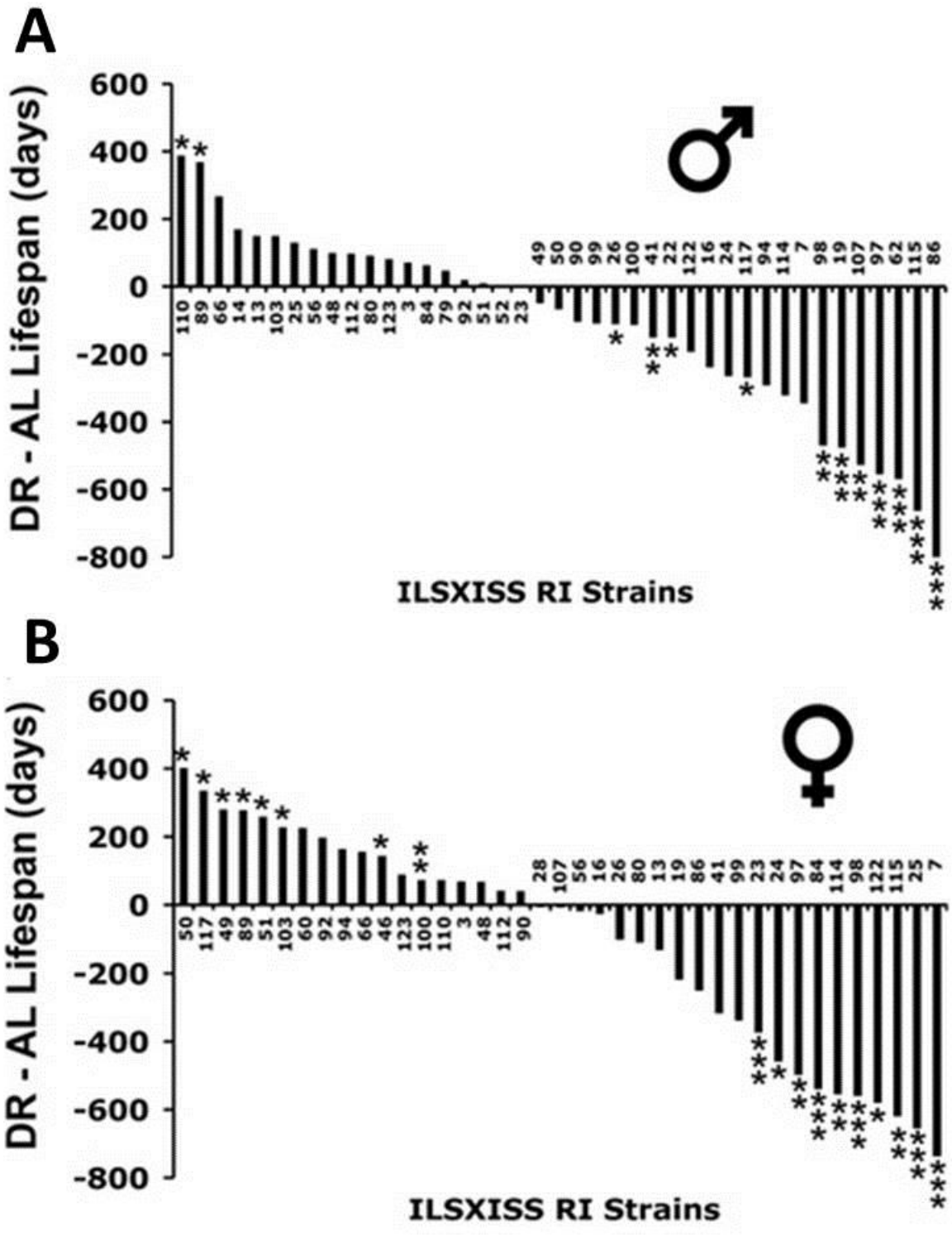

Figure 1.5: Lifespan response following 40% DR across a panel of 39 female and 41 male strains of recombinant inbred ILSXISS mice. Variation in lifespan in response to DR ranges from lifespan extension, no effect on lifespan, to lifespan shortening. *=statistically significant from AL controls. (Data taken from Liao et al. 2010).

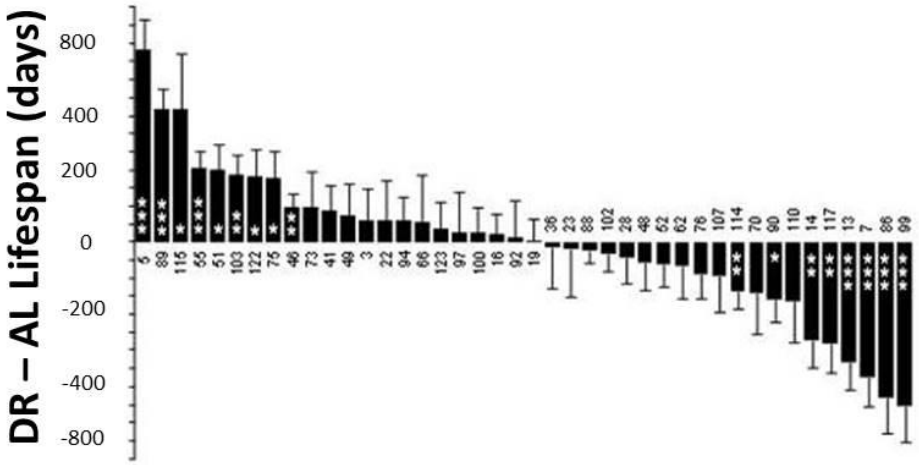

Figure 1.6 : Lifespan response following 40% DR across a panel of 42 strains of recombinant inbred female ILSXISS mice. Variation in lifespan in response to DR ranges from lifespan extension, no effect on lifespan, to lifespan shortening. *=statistically significant from AL controls. (Data taken from Rikke et al. 2010).

3. Candidate Mechanisms of DR

A number of mechanisms have been proposed as mediating the DR response (Fontana & Partridge 2015; Shimokawa & Trindade 2010; Masoro 2005; Hine et al. 2015; Anderson & Weindruch 2010). For instance, DR promotes proteostasis (Cuervo 2008), reduces insulin/insulin-like growth factor 1 (IGF-1) signalling, reduces oxidative stress and /or increases antioxidant protection (Cohen et al. 2004), and enhances mitochondrial function (López-Lluch et al. 2008; Nisoli et al. 2005). Furthermore, there are nine described hallmarks of ageing; genomic instability, telomere attrition, epigenetic alterations, loss of proteostasis, deregulated nutrient sensing, mitochondrial dysfunction, cellular senescence, stem cell exhaustion, and altered intercellular communication (Lopez-Otin et al. 2013). These hallmarks encompass shared characteristics of ageing across the animal kingdom, with special emphasis on mammalian aging. Several of these hallmarks are known to be positively affected with DR, such as enhanced mitochondrial function (López-Lluch et al. 2008; Nisoli et al. 2005) and proteostasis (Cuervo 2008), and have therefore become extensively studied as candidate mechanisms for lifespan extension.

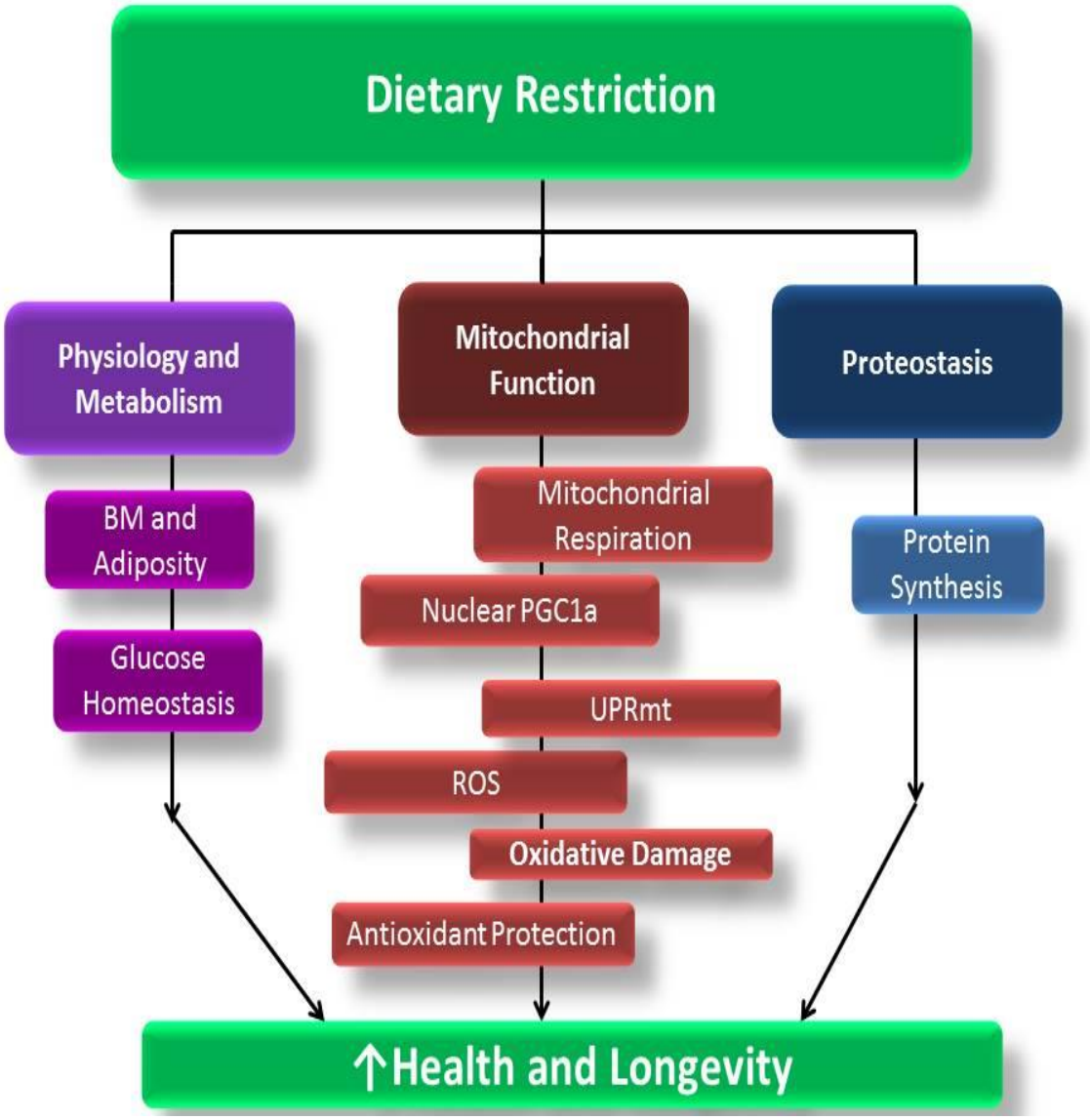

Figure 1.7: Plausible candidate pathways through which DR may act to improve health and longevity.

3.1 Physiology

3.1.1 DR induced changes in body mass and adiposity

Ageing is characterised by increased body mass, obesity, decline in organ function and increased mortality risk (Fontana et al. 2007; Klein et al. 2002; Fontaine et al. 2003). DR is associated with a reduction in body mass and body fat, and thus decreases in both have been proposed as relating to DR-induced longevity (Berg & Simms 1960; Masoro 2005). Excess visceral adiposity is associated with insulin resistance, type II diabetes, and metabolic syndrome in mammals (Després & Lemieux 2006; Bartke & Brown-Borg 2004). It remains unclear, however, as to how alterations in body mass and adiposity relate to the underlying molecular and physiological mechanisms through which DR acts to extend lifespan. The reduction of fat hypothesis, originally posited by Berg and Simms (Berg & Simms 1960), proposed that decreased fat stores underpin DR-induced longevity following reports of increased lifespan in rats following either 33% or 46% DR to be associated with reduced fat accumulation. Following on from this it was later proposed that alterations in adiposity following DR, specifically reductions in visceral fat depots, underlie DR-induced longevity (Muzumdar et al. 2008). However, the role of reduced fat mass in the life-extending effect is a complex one and there are several arguments which contest the relevance to DR (Bertrand et al. 1980; Harrison et al. 1984; Liao et al. 2011). Moreover, a positive association between body weight and survival outcome has been observed in several murine studies, including C57BL/6J mice, wild mice, and recombinant inbred ILXISS strains (Goodrick et al. 1990; Harper et al. 2006; Rikke et al. 2010; Weindruch et al. 1986). Indeed, survival outcomes of C57BL/6 and DBA/2 mice maintained on 20% and 40% were highest in individuals which better preserved fat mass in the second year of life (Mitchell et al. 2016), suggesting ability to maintain fat as important to lifespan extension. Strain-specific losses of fat mass in response to DR exist and have been linked to the direction of lifespan response. ILSXISS recombinant inbred mouse strains with the smallest reductions in fat mass under DR, relative to their appropriate AL controls, were more likely to show life extension and those with the greatest reductions were more likely to have truncation of lifespan (Liao et al. 2011). This suggests that loss of body fat, beyond a critical threshold, as detrimental to lifespan extension with DR. One potential pitfall of this association however, discussed in Speakman *et al*. (Speakman & Mitchell 2011), highlights that the association would not uphold if

carried out in the “positive responding” strains alone. Therefore the association between the lifespan effect of DR and change in body fatness is only detected in the strains where DR impacts negatively on lifespan (Speakman & Mitchell 2011).

DR invariably leads to a reduction in BM and alterations in body composition. However, what is clear is that the weight loss following DR is not uniform between different tissue and organs. For example loss of white adipose tissue (WAT) is disproportionately large compared to reductions in lean and organ mass (Bertrand et al. 1980; Speakman & Mitchell 2011), with WAT preferentially utilised as an energy source whilst under DR (Mitchell et al. 2015a). Up until relatively recently this was considered the primary function of adipose tissue, however it has become clear that adipose tissue performs many vital endocrine roles (Ahima & Flier 2000), and therefore it is important that not all stocks become depleted when faced with DR. Instead reductions at other sites, such as reductions in lean mass, and organs with a high metabolic demand, have been reported under DR (Hempenstall et al. 2010; Mitchell et al. 2015a), presumably as a way to reduce energy expenditure. Furthermore, brown adipose tissue has been implicated as crucial to thermoregulation, and the ability to effectively thermoregulate has been shown to be important to DR-induced longevity in ILSXISS mice (Rikke et al. 2003). BAT is specialised for the dissipation of energy through the production of heat. Increased levels of WAT are characteristic of ageing (Barzilai & Gupta 1999a; Das et al. 2004; Masoro 1999). Smaller BAT depots are associated with old age in mice (Rogers et al. 2012), whereas larger phenotypes associated with a healthier metabolic phenotype in humans (Saely et al. 2011). Therefore interventions which increase BAT have been proposed as a means of affording protecting against diseases of ageing and improved insulin sensitivity (Mattson 2010; Dionne et al. 2016; Stanford et al. 2013). BAT catabolises lipids to produce heat, a function that is mediated via a unique biochemical property of the mitochondria in brown adipocytes; uncoupling protein 1 (UCP1), in a process known as non-shivering thermogenesis. DR is found to increase BAT mass and DR animals are found to have an increased capacity for thermogenic activity in brown adipose tissue (Fabbiano, Suarez-Zamorano, et al. 2016; Valle et al. 2008; Himms-Hagen 1985). Moreover, DR is associated with enhanced fatty acid biosynthesis (Okita et al. 2012; Bruss et al. 2010). Okita *et al.* propose that under DR, WAT and BAT work synergistically together to enable a metabolically efficient switch from glucose as an energy source to fatty acid oxidation, using WAT as an energy reservoir.

Strain-specific responses in fat loss may be relevant to the DR response in mice (Liao et al. 2010; Mitchell et al. 2016) however, precisely how genetic background mediates adiposity, as well as reductions in BM, with DR remains to be elucidated. Sex-specific mechanisms have been reported to regulate energy balance and adiposity (Shi et al. 2007), and it is therefore likely that the sexually dimorphic strategies involved in regulation of body weight will have an impact on DR response. In most instances, females are longer lived than males (Austad & Bartke 2015) and at reduced risk of mortality from the metabolic complications of obesity, despite being more obesity prone (Palmer & Clegg 2015; Vague 1947). In rats, changes in UCP1 and BAT levels related to the ability of females to deactivate facultative thermogenesis to a greater degree than males following DR (Valle et al. 2005). This ability may have advantages for female survival whilst on DR or during times of nutrient scarcity, but also highlights gender specific responses in fat depots under DR.

3.1.2 Glucose Homeostasis

Ageing is accompanied by a marked increase in skeletal muscle and hepatic resistance to the action of insulin. In male F344 rats lifespan extension with DR is found to be associated with reduced levels of plasma glucose and fasting plasma insulin, (Masoro et al. 1992) and reported in, in mice following long-term DR (Masoro et al. 1992; Rincon et al. 2005; Berryman et al. 2008; Hempenstall et al. 2012), as well as in monkeys (Kemnitz et al. 1994; Lane et al. 1995), and humans (Fontana et al. 2010). This has led to the widely accepted theory that reduced levels of plasma glucose and insulin underlie the life-extending effect of DR (Masoro 2005).

Reductions of circulating levels of plasma insulin-like growth factor-1 (IGF-1) are widely observed in rats and mice following DR (Argentino et al. 2005; Mitchell et al. 2015b; Mitchell et al. 2016). Furthermore, IGF-1 appears to be more sensitive to DR than fasting plasma insulin levels, with 3 weeks of 30% DR in both C57BL/6 and DBA/2 male mice, resulting in markedly lower levels of IGF-1, but having no effect on insulin levels (Hempenstall et al. 2010). Long-lived Ames, Snell and GHRKO dwarf mice have markedly lower levels of plasma IGF-1 than wildtype litter mates, suggesting an association between longevity and reduced plasma IGF-1 (Brown-Borg et al. 1996; Bartke et al. 2001; Flurkey et al. 2001; Coschigano et al. 2000). Thus, the reduction of plasma IGF-1 in mice on DR is proposed as having a crucial role in the life-extending effect. However, despite the widespread association

of reduced glucose, insulin and IGF-1 levels there are a number of observations which dispute the universality of this relationship with DR. Firstly, humans, unlike rodents do not experience a reduction in serum IGF-1 (Fontana et al. 2008; Fontana et al. 2016) following DR. Secondly, strain-specific differences in metabolism exist between C57BL/6 and DBA/2 mice (Sohal et al. 2009), and it is well established that DBA/2 mice vary in numerous parameters (including insulin sensitivity and glucose tolerance) under both AL and DR feeding when compared to C57BL/6 mice (Funkat et al. 2004; Berglund et al. 2008; Goren et al. 2004; Hempenstall et al. 2010). Consequently, exactly how metabolic profiles of different genetic backgrounds relate to lifespan extension with DR remains to be fully examined.

In addition to strain-specific DR responses sex-specific responses in fasting plasma insulin have also been reported. In a study examining the effects of 20% and 40% DR on C57BL/6 and DBA/2, females, unlike males were not found to have a reduction in fasting plasma insulin following DR, suggesting that lower levels of insulin is not critical to enhance longevity (Mitchell et al. 2016). Moreover, a number of studies show that male rodents tend to be more insulin resistant than females (Goren et al. 2004; Macotela et al. 2009).

3.2 Mitochondrial Function and DR

The primary function of the mitochondria is the generation of cellular energy through the production of adenosine triphosphate (ATP) (See Figure 1.8), and mitochondrial dysfunction appears to play a crucial role in the ageing process (Wang & Hekimi 2015). Ageing is associated with altered mitochondrial morphology, reduced mitochondrial oxidative capacity and ATP production, increased mitochondrial-derived reactive oxygen species (ROS) generation and greater oxidative damage (Wang & Hekimi 2015). Mitochondrial dysfunction is a hallmark of ageing (Lopez-Otin et al. 2013), and it has been proposed that the gradual accumulation of mitochondrial derived ROS-induced damage underlies the ageing process (Nicholls 2004; Salvioli et al. 2001; Lenaz et al. 2000; Sohal et al. 1990). Dysfunctional mitochondria are associated with the functional decline of organs and tissues during ageing (Riera et al. 2016) and with a number of age-related diseases such as cardiovascular disease, liver and kidney disease, diabetes and cancer (Lane et al. 2015; Payne & Chinnery 2015; Ryan et al. 2015; Wallace 2012). Maintenance of mitochondrial function in old age, has therefore been posited as one explanation of how DR works to induce health and lifespan benefits (Ruetenik &

Barrientos 2015; Lanza et al. 2012). Consequently, significant research effort has investigated whether DR can induce beneficial effects on the mitochondrial function, such as maintaining mitochondrial function during ageing, reducing ROS production and attenuating oxidative damage. Numerous studies have shown DR to attenuate damage from oxidative stress and to effectively decrease electron and proton leak in the mitochondria of mammalian cells (Sohal et al. 1990; Weindruch 1996; Masoro 2000; Masoro 2009; Lopez-Torres et al. 2002; Ramsey J. et al. 2000).

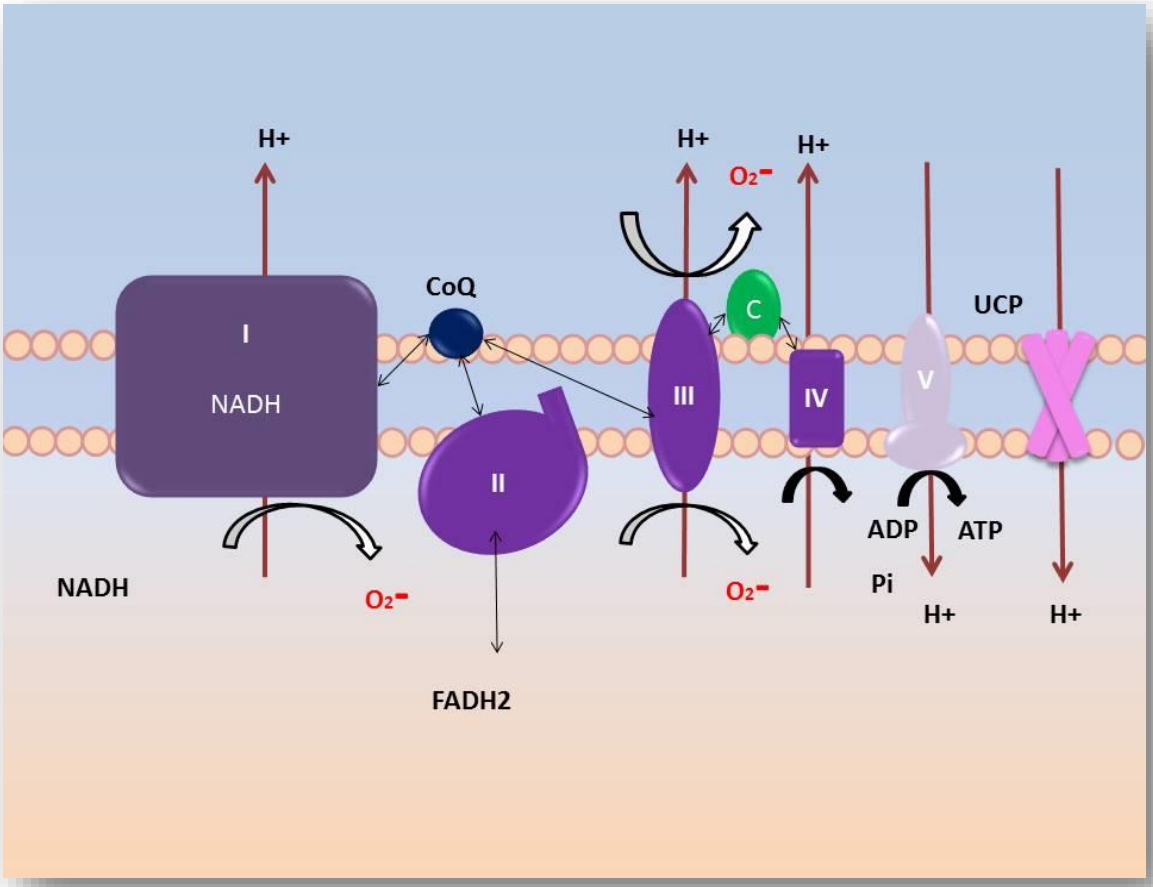

Figure 1.8: Schematic of electron transport chain; **1**. Complex I is the site of the initial oxidation of NADH, generated by associated Krebs cycle dehydrogenases. The energy generated by the transfer of the electrons from NADH to oxidised coenzyme Q (the first mobile electron acceptor), is dissipated by the ejection of protons. **2**. At complex II FADH can donate electrons to Coenzyme Q (*thereby bypassing CI and one proton ejection site).* **3**. Complex III receives electrons donated by coenzyme Q to cytochrome b, in a process that is in a near potential energy neutral process. Electrons are passed to cytochrome C1 with the dissipative ejection of protons.**4**. At Complex IV, following the transfer of electrons from Cytochrome C1 to the second mobile element in the cytochrome chain, cytochrome c. COX (cytochrome oxidase) is reduced, and ultimately results in the reduction of molecular oxygen from water. This final dissipation of the redox energy in NADH/FADH at site IV is also associated with a final ejection of protons. **5**. In this manner, the cytochrome chain transforms the redox energy of the rather stable molecules NADH and FADH into a $\Delta\Psi$ across the inner mitochondrial membrane.

Reports of increased mitochondrial respiration with DR in yeast (Lin et al. 2002) and in male C57BL/6 mice (Hempenstall et al. 2012) suggest a link between DR and improved mitochondrial function. Mitochondrial biogenesis has also been proposed as being critical to the beneficial effects of DR (López-Lluch et al. 2006; López-Lluch et al. 2008; Lanza et al. 2012; Nisoli et al. 2005), with increases in mitochondrial DNA content, increased expression of mitochondrial associated genes (e.g. peroxisome proliferator-activated receptor gamma co-activator (Pgc-1α), nuclear respiratory factor-1 (Nrf-1) and mitochondrial transcription factor A (Tfam) has been reported in a range of mouse tissues (Nisoli et al. 2005), and in human skeletal muscle (Civitarese et al. 2007). PGC-1α regulation is proposed as driving an adaptive response to DR in mitochondrial function that protects against age-associated DNA damage and loss of mitochondria (Hancock et al. 2011). Indeed, increased expression of PGC-1α has been described in the skeletal muscle of C57BL/6 mice (Hempenstall et al. 2012) and rats with DR (Hepple et al. 2005). Recently a mitohormetic response, called the unfolded protein response (UPR^{mt}) has been implicated as an important regulator of longevity (Houtkooper et al. 2013; Mouchiroud et al. 2013; Baqri et al. 2014; Hill & Van Remmen 2014a). It is proposed that when subject to acute stress, which may lead to an accumulation of damaged or misfolded proteins, the UPR^{mt} is triggered and returns the mitochondria to a state of homeostasis. The UPR^{mt} is induced by DR mimetics rapamycin and resveratrol in mouse hepatocytes in vitro (Houtkooper et al. 2013), and enhanced longevity is reportedly linked to the activation of the UPR^{mt} by nicotinamide riboside (Zhang et al. 2016; Gariani et al. 2016), suggesting that the UPR^{mt} is associated with ageing in mammals. In BXD mice DR protects against the age related reduction in mitochondrial ribosomal protein S5 (Mrps5) in skeletal muscle (Houtkooper et al. 2013), reduced expression of which is associated with ageing. Mrps5 is proposed as triggering the UPR^{mt}, and if this is the case implicates the UPR^{mt} as an overarching longevity pathway conserved across many species (Houtkooper et al. 2013). However, the role of UPR^{mt}, as measured by mitonuclear imbalance, and the association with lifespan extension, has yet to be determined in mice.

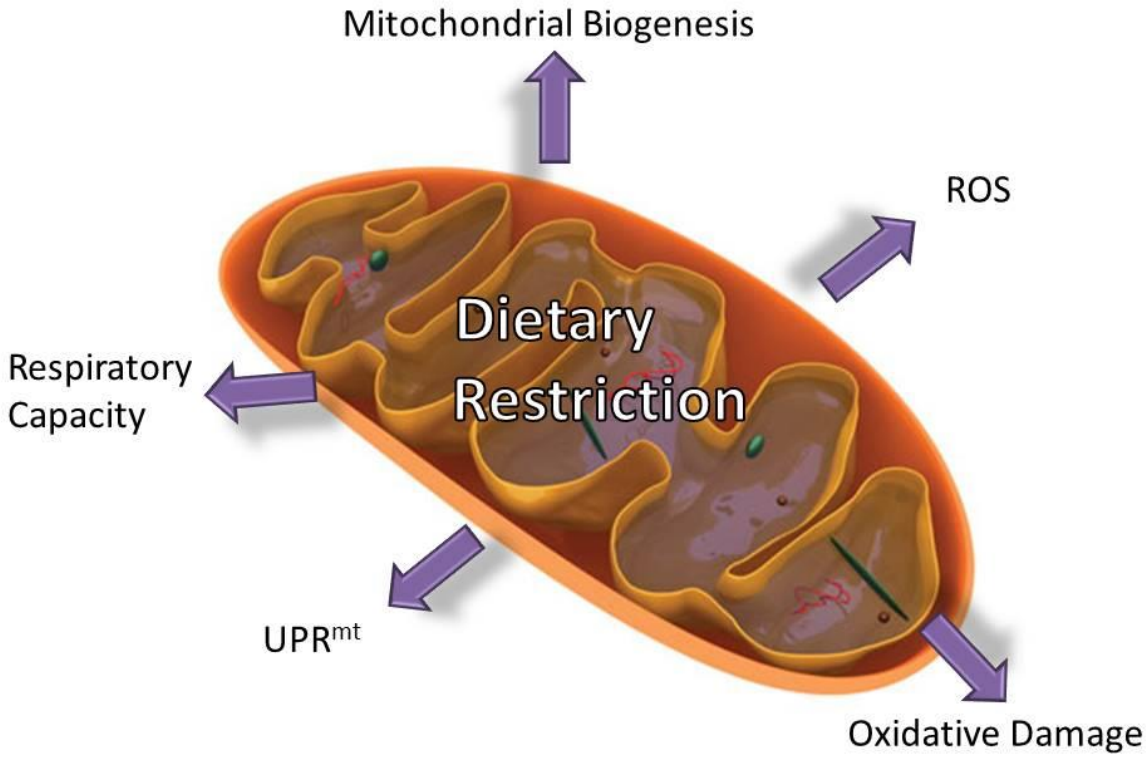

Figure 1.9: Proposed mechanisms through which DR acts to improve mitochondrial function

Despite reports in support of enhanced mitochondrial function as a mediator of longevity with DR, the precise mechanisms are difficult to determine with substantial lack of consensus between studies. For instance, the mitochondrial theory of ageing proposes that accumulation of damage to mitochondria and mitochondrial DNA (mtDNA), induced by reactive oxygen species (ROS), is the cause of ageing (Wei et al. 2001). Indeed, numerous studies support a role for decreased mitochondrial ROS as underlying the lifespan benefits of DR (Sohal & Weindruch 1996; Masoro 2000). However, a recent meta-analysis of rodent response following DR found that the majority of studies reported no change in ROS levels relative to AL controls (Walsh et al 2014), with only 4% of these studies carried out on female or mixed populations. The impact of DR on mitochondrial respiration in rodents is also unclear, with an increase (Hempenstall et al. 2012; A. J. Lambert et al. 2004; Nisoli et al. 2005; Lanza et al. 2012) decrease (Agarwal & Sohal 1994), or no effect reported relative to AL controls (Gredilla et al.

2001). Similarly debate arises over the role of mitochondrial biogenesis as a mediator of DR with reports that mRNA levels of several mitochondrial associated genes in muscle, heart or liver and PGC-1α protein were unchanged by DR in male Wistar rats (Hancock et al. 2011). Both Hempenstall *et al* and Lanza *et al.* reported no evidence of mitochondrial biogenesis and proposed that DR preserves mitochondrial function by protecting the integrity and function of existing cellular components (Hempenstall et al. 2012; Lanza et al. 2012). Although mitochondrial biogenesis is poorly defined, it can be inferred that protein synthesis is necessary for the making of new mitochondria. Humans and animals under DR exhibit decreased protein synthesis rates (Henderson et al. 2010; Giroud et al. 2010), and these findings challenge the some-what counter intuitive idea of increased mitochondrial biogenesis whilst experiencing chronic nutrient deprivation. Numerous methods of assessing mitochondrial biogenesis exist, however argument has arisen over the best means of quantification suggesting that some means of assessment are not reflective of protein synthesis (Miller et al. 2012), and may relate to the inconsistent effect of DR on mitochondrial biogenesis. The reason for ambiguity between DR studies is unclear, however comparison between various tissues (A. J. Lambert et al. 2004; Zangarelli et al. 2006; Miller et al. 2012), different sampling techniques (e.g. measurements taken in isolated mitochondria versus permeabilised muscle fibres) (Picard et al. 2011; Picard et al. 2010), as well as across different genotypes and genders, make direct comparisons across studies difficult (Hunt et al. 2006).

3.3 DR and Protein Synthesis

Ageing is associated with a progressive loss of protein synthesis (Lopez-Otin et al. 2013), which is likely the primary cause of the increased number of damaged proteins in old age (Wolff et al. 2014). Furthermore, mitochondrial proteins are particularly important to ageing, in terms of maintaining a healthy pool of mitochondria, and their synthesis has been shown to decrease by middle-age in humans (Rooyackers et al. 1996). This encapsulates the protein turnover theory of ageing, which postulates that a major mechanism underlying ageing is the increased number of aberrant proteins in old age, which consequently reduces the rate of protein turnover. The proteome is maintained by the removal of damaged proteins, and replacement with new proteins, and therefore both the rate of protein synthesis and degradation determines the rate of protein turnover. Indeed an increase in the

concentration of damaged proteins (Stadtman 1992), and decline in synthesis rates is well documented during ageing in a variety of organisms (Makrides 1983; Rattan 1996; Ward 2000).

Loss of proteostasis is a hallmark of ageing (Lopez-Otin et al. 2013) but is reportedly prevented by DR (Kaushik & Cuervo 2015). Therefore DR-induced changes in protein synthesis rates have been linked as a mechanism mediating lifespan extension with DR (Tavernarakis & Driscoll 2002; Zangarelli et al. 2006; Lambert & Merry 2000), although exactly how DR alters protein synthesis rate is unclear. While it has been established that aged rats undergo a progressive decline in the rate of protein synthesis and degradation (Goldspink et al. 1987) it has been reported that under DR protein turnover is elevated in rodent tissues, including skeletal muscle and liver (el Haj et al. 1986; Ward & Richardson 1991). Following DR primary rat hepatocyte cultures are protected from decline in protein turnover (Lambert & Merry 2000), while conversely in mouse skeletal muscle DR is associated with an increased turnover rate (Lee et al. 1999). However other DR studies report no changes in (Lanza et al. 2012) or even decreased rates of protein synthesis (Henderson et al. 2010; Giroud et al. 2010).

In an investigation into the effect of different magnitudes on important hallmarks of DR in both male and female C57BL/6 and DBA/2 mice, proteasome activity was found to be lower in DR animals, leading the authors to propose that autophagy is a more important proteostatic mechanism under DR (Mitchell et al. 2016). Protein turnover is the sum of both protein synthesis and degradation and consequently measuring protein synthesis in isolation may not provide an accurate measure of protein turnover rate (Miller et al. 2014). For example, during cell division sufficient increases in protein synthesis are essential to account for distribution of proteins between daughter cells and for dilution of protein damage (Eden et al. 2011). Furthermore, cell replication is not essential to cellular homeostasis, while increases in protein synthesis are, which suggests a dynamic rate of synthesis and degradation. In order to combat this issue, Miller *et al* suggest a method of simultaneously assessing both protein and DNA synthesis through deuterium oxide incorporation (D_2O), and using the ratio between protein and DNA synthesis to accurately determine proteostatic mechanisms. D_2O is an isotopically labelled marker, with free access to all pools of body water, and as hydrogen from water is almost universally associated with biosynthetic processes it allows for a reliable

measurement of numerous tissues and proteins. Using this means of assessment, proteostatic mechanisms were found to be enhanced in a long-lived mouse model (Drake et al. 2015), following treatment with rapamycin (Drake et al. 2013) , a crowded-litter model (Drake et al. 2014), and following short-term DR in B6D2F1male mice (Miller & Hamilton 2012; Miller et al. 2013) relative to controls. Such reports implicate increased proteostatic mechanisms as a shared feature of slowed ageing and suggest that enhanced protein synthesis is associated with DR-induced lifespan extension.

4. Aims of Thesis

Evidence suggests that genetic background may impact on the responsiveness to DR in both mice (Rikke et al. 2010; Liao et al. 2010; Mitchell et al. 2016) and monkeys (Mattison et al. 2017). However, while lifespan responses following DR in recombinant inbred ILSXISS mice have been reported (Liao et al. 2010; Rikke et al. 2010), the impact of genotype on metabolism, mitochondrial function and protein synthesis rates following DR are as of yet undetermined in these strains. Moreover, although a wealth of research has been carried out to determine candidate mechanisms mediating the anti-ageing effects of DR, few of these have included female mice, making it difficult to identify universal modulators of slowed ageing.

This thesis set out to investigate this by employing a comparative approach, utilising the distinct DR-induced lifespan responses of three genetically heterogeneous strains of female ILSIXSS RI mice (Figure 1.9). My PhD sought to examine metabolism, mitochondrial function and protein synthesis, three important hallmarks of ageing (Lopez-Otin et al. 2013), under the premise that if a candidate mechanism was similarly affected in all three strains then it was not an important mechanism underlying DR-induced longevity. The objective of this thesis was to probe the mechanistic basis of DR, and to gain novel insights into the effect of genotype on DR response. This was achieved by addressing the following questions:

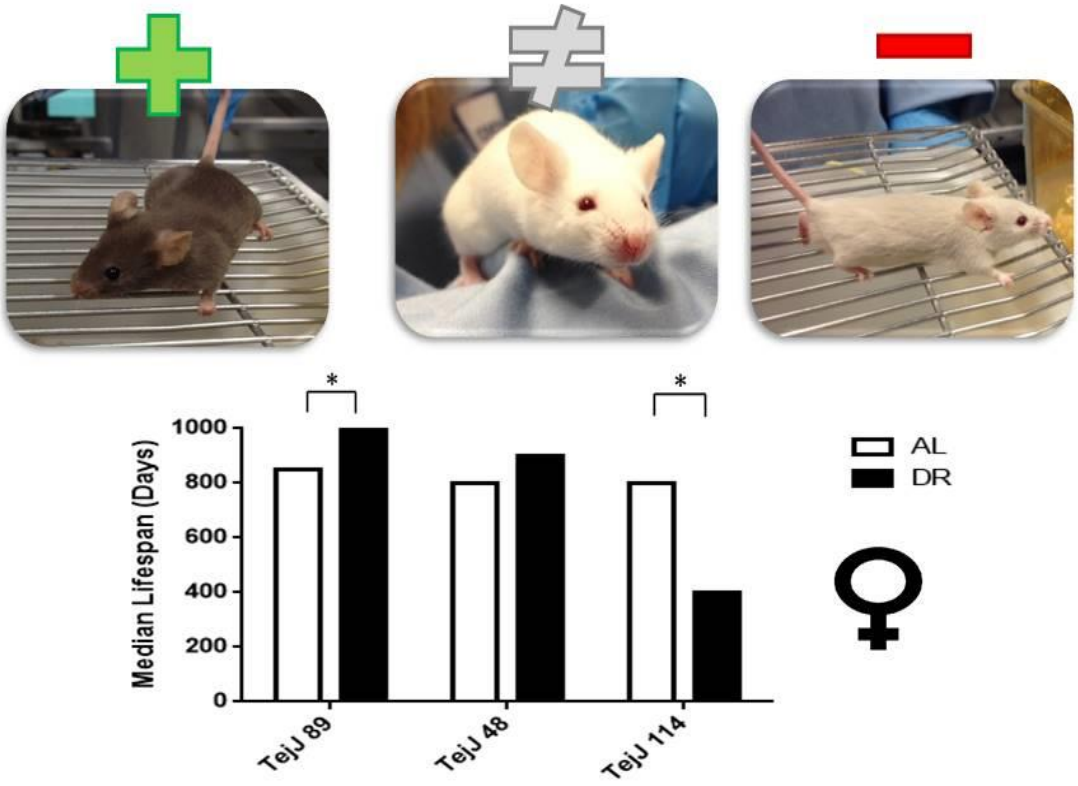

Figure 1.10: Strain-specific lifespan responses following 40% DR in TejJ89 (positive responder), TejJ48 (non-responder) and TejJ114 (negative responder) female ILSXISS RI mice. (Data from Liao et al. 2010; and Rikke et al. 2010).

1. **What is the effect of short and long-term DR on metabolic characteristics in female recombinant inbred ILSXISS mice?**

In Chapter 3 I examined the impact of both short- (2 months) and long-term (10 months) 40% DR on body mass, adiposity (white adipose and brown adipose tissue mass) and food intake. In addition, glucose homeostasis was determined by measuring fed and fasted blood glucose levels, glucose tolerance, fasting plasma insulin, insulin resistance (HOMA-IR), and fasting plasma IGF-1.

2. **Is enhanced mitochondrial function a candidate mechanism underlying lifespan extension with DR?**

I investigated the impact of DR on mitochondrial function within liver and skeletal muscle of female ILSXISS mice following both short and long-term DR. Oxygen consumption rates (OCR) were determined in isolated mitochondria from skeletal muscle and liver tissue for each strain using the Seahorse XF24 Flux analyser. Hepatic protein levels of PGC-1a (regulator of mitochondrial biogenesis), TFAM (key activator of mitochondrial transcription), OXPHOS (oxidative phosphorylation in the mitochondrial complexes) and the UPR^{mt} (mitonuclear protein imbalance; nDNA:mtDNA ratio) were measured. Mitochondrial ROS (Hydrogen peroxide) production was quantified in liver and skeletal muscle tissue, and both oxidative damage (protein carbonyl and 4 HNE) and antioxidant defences (Superoxide dismutase and total glutathione) were determined.

3. **Is enhanced proteostasis associated with DR-induced lifespan?**

Following short-term DR protein synthesis rates were assessed in each strain using deuterium oxide (D_2O) as an isotopically stable marker to label proteins. Protein synthesis was assessed in three different subcellular fractions (mitochondrial, cytoplasmic and mixed proteins) in the skeletal muscle (gastrocnemius), heart and liver.

Chapter 2: Materials and Methods

2.1 Animals

2.1.1 ILSXISS mice

ILSXISS recombinant inbred (RI) mouse strains were derived from a cross between inbred long sleep (ILS) and inbred short sleep (ISS) mice (Williams et al. 2004). Originally the founding ILS and ISS strains were generated through an eight-way cross from heterogeneous stock; A, AKR, BALB/c, C3H/2, C57BL, DBA/2, IsBi, RIII (see Figure 2.1) and bred based on their ethanol sensitivity, thus giving rise to the long and short sleep models. Following 20 or more successive generations of brother/sister matings of the progenitor strains (ILS X ISS), over 75 ILSXISS RI lines were generated (See Figure 2.1 for schematic representation) (Williams et al. 2004). As each RI strain is inbred, every genetic locus contains either an ISS or ILS allele, meaning that each strain has a unique arrangement of ISS and ILS alleles, resulting in each line being genetically distinct from one another (Liao et al. 2013). This genetic variation creates a unique tool for exploring the differential responses of dietary restriction (DR), and can be used to probe the mechanisms which underlie DR-induced lifespan extension (Rikke & Johnson 2007; Williams et al. 2004; Liao et al. 2013). Mice from three of these strains; TejJ89 (increase in lifespan with DR; positive responder), TejJ48 (no effect of DR on lifespan; non-responder) and TejJ114 (decrease in lifespan with DR; negative responder) were purchased from a commercial breeder (The Jackson Laboratory, Bar Harbour, Maine, URL: http://www.informatics.jax.org). 3 males and 3 females from each strain were purchased and paired, resulting in 3 breeding pairs per strain. The rationale for studying these particular strains was that in addition to the repeatable effect of DR on lifespan across two independent studies (Rikke et al. 2010; Liao et al. 2010), no strain-specific differences in median lifespan were observed upon *ad libitum* (AL) feeding (See Figure 2.2 Rikke et al. 2010; Liao et al. 2010).

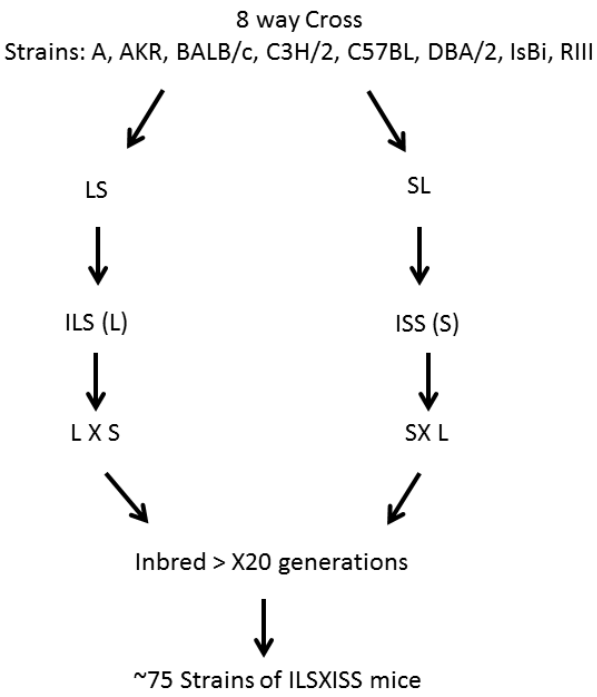

Figure 2.1: Generation of ILSXISS RI strains through an 8-way cross from heterogeneous stock. Generations of inbreeding resulted in the panel of RI ILSXISS mice (Adapted from Williams et al. 2004).

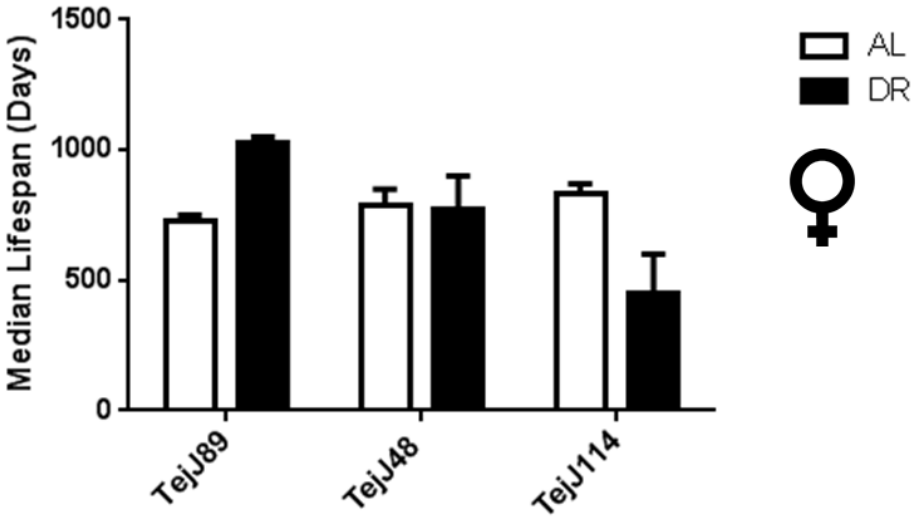

Figure 2.2: Median AL and DR lifespan in female ILSXISS mice from strains TejJ89, TejJ48 and TejJ114, highlighting the differential impact of 40% DR for each strain and the non-strain specific response under AL feeding (Adapted from Rikke et al. 2010; Liao et al. 2010).

2.1.2 Husbandry, Dietary Restriction (DR) and Experimental Design

Female ILSXISS mice from three genetically distinct strains, shown to have repeatable lifespan responses to 40% DR in two independent studies (TejJ89, TejJ48 and TejJ114, see Figure 2.3), were used in this study. Mice were kept in groups of 4 post-weaning in shoebox cages (48cm×15cm×13cm), with AL access to water and standard chow (CRM(P), Research Diets Services, LBS Biotech, UK; Atwater Fuel Energy- protein 22%, carbohydrate 69%, fat 9%) and maintained on a 12L/12D cycle (lights on 0700–1900h) at an ambient temperature of 22±2°C. At 9 weeks of age, cages were randomly assigned to either an AL or DR group, with no difference in body mass observed between treatment groups at this time (TejJ89 AL vs. DR $t=0.056$, $p=0.583$, TejJ48 AL vs. DR $t=0.677$, $p=0.509$, TejJ114 AL vs. DR $t=0.289$, $p=0.777$). Mice were introduced to DR in a graded fashion (as described in Hempenstall et al. 2010); at 10 weeks of age mice were exposed to 10% DR (90% of AL feeding), at 11 weeks this was increased to 20% DR, and from 12 weeks of age, until the termination of the experiment, mice were exposed to 40% DR, relative to their appropriate strain-specific AL controls. Mice were maintained on 40% DR for a period of either 2 months (equivalent to 5 months of age), or 10 months (equivalent to 13 months of age), (See Figure 2.4 for schematic of experimental design). Short-term DR, defined here as a period of 2 months 40% DR, and long term DR, a period of 10 months of 40% DR were chosen with previously published lifespan data on these strains on DR, in mind (Rikke et al. 2010; Liao et al. 2010). 10 months of DR was fixed as the upper limit of restriction in this study in order to examine the effect of DR on candidate mechanisms, and not late life health. Total food intake of AL mice from each strain was measured weekly (±0.01g) and food intake of the DR cohort calculated from the average AL intake per mouse over the preceding week (Hempenstall et al. 2010). DR mice were fed daily at 1800hrs, with the food placed directly onto the cage floor in order to reduce any competition for the food. No evidence of fighting or dominance hierarchies was observed in any cage.

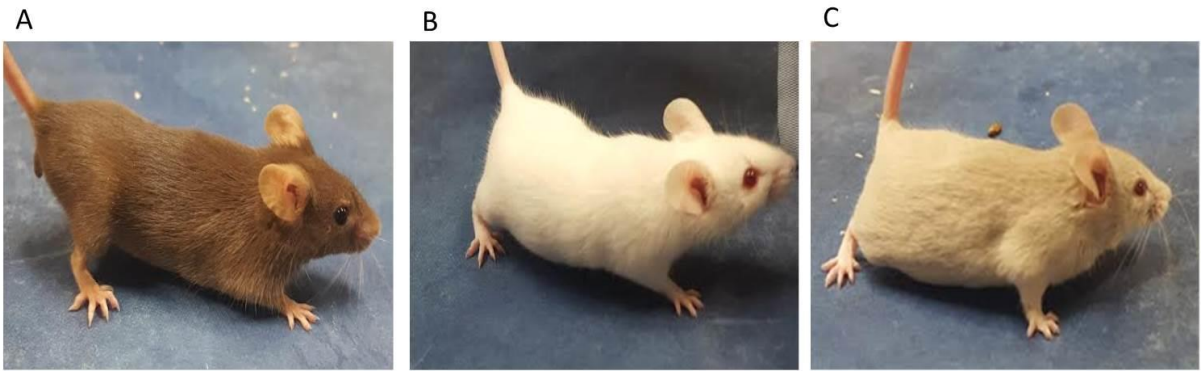

Figure 2.3: ILSXISS mice; positive responder TejJ89 (A), non responder TejJ48 (B) and negative responder TejJ114 (C).

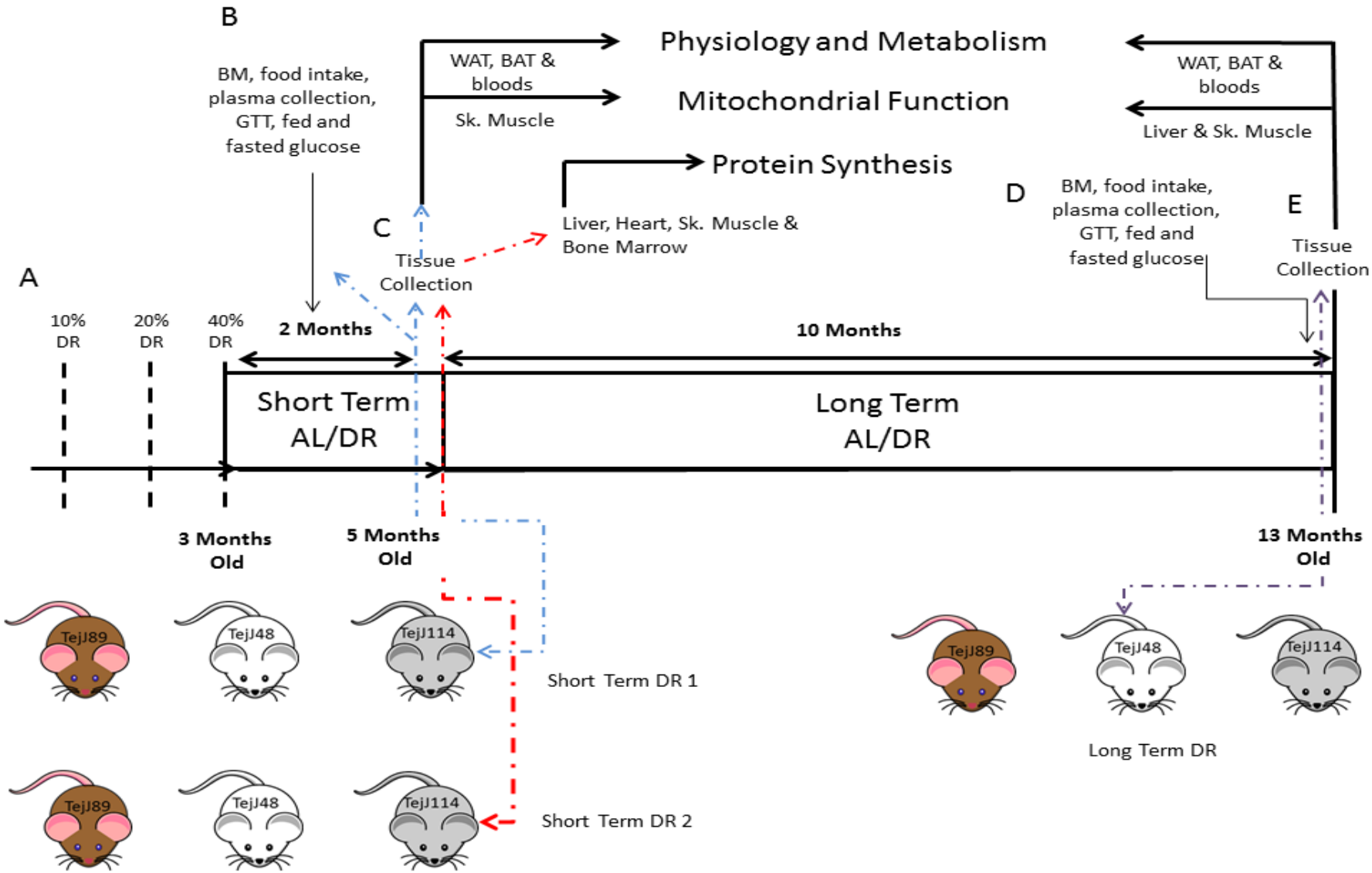
B
BM, food intake, plasma collection, GTT, fed and fasted glucose
WAT, BAT & bloods
Sk. Muscle
Physiology and Metabolism
Mitochondrial Function
Protein Synthesis
WAT, BAT & bloods
Liver & Sk. Muscle
D
BM, food intake, plasma collection, GTT, fed and fasted glucose
E
Tissue Collection
C
Tissue Collection
Liver, Heart, Sk. Muscle & Bone Marrow
A
10% DR
20% DR
40% DR
2 Months
10 Months
Short Term AL/DR
Long Term AL/DR
3 Months Old
5 Months Old
13 Months Old
TejJ89
TejJ48
TejJ114
Short Term DR 1
Short Term DR 2
Long Term DR

Figure 2.4: Schematic of experimental design. (A) 2 cohorts of mice were maintained on AL or DR treatment for a period of 2 months; Short-Term DR 1 and Short-Term DR 2. (B) Over the 2 month period numerous metabolic and physiological measurements were taken on Short-Term DR 1 animals, including measurements on body mass, food intake, fed and fasted plasma collection, fed and fasted glucose measurements and a glucose tolerance test. Short-Term DR 2 animals were maintained on short-term DR, prior to administration of isotopically labelled water, for the assessment of protein turnover. (C) Samples were collected at 5 months of age for both Short-Term DR 1 and Short-Term DR 2 animals, following 2 months of DR. Skeletal muscle, WAT, BAT and blood were collected from the Short-Term DR 1 cohort for downstream physiological and metabolic assays. Liver, heart, skeletal muscle, plasma and bone marrow were dissected and snap frozen from the Short-Term DR 2 cohort for protein synthesis assays. (D) Over the course of 10 months, measurements were taken on body mass, food intake, fed and fasted plasma collection, fed and fasted glucose measurements and a glucose tolerance test in the Long-Term DR cohort. (E) After 13 months liver, skeletal muscle, WAT, BAT and blood were collected for physiological and mitochondrial experiments.

At 5 months (2 months of 40% DR) and 13 months (10 months of 40% DR) AL and DR mice from Short-term DR 1 and Long-term DR, were fasted overnight and weighed prior to being culled by schedule one cervical dislocation. At 5 months AL and DR mice from Short-term DR 2 were fasted overnight and culled by cardiac puncture and dissection as described in section 2.4. Following cervical dislocation Short-term DR 1 and Long-term DR mice were decapitated and trunk blood was collected in a petri dish. Fasting blood glucose was recorded with a glucometer (OneTouch Ultra, Lifescan, UK) and the remaining blood pipetted into an EDTA coated tube, and spun at 10,000 x g for 10 minutes at 4°C, with the resultant supernatant (plasma) collected. All plasma samples were stored at -80°C. The brain, hypothalamus, kidneys, heart, WAT, BAT, two lobes of liver and gastrocnemius muscle from one hind limb, were rapidly excised, snap frozen in liquid nitrogen and stored at -80°C. The remaining gastrocnemius muscle and lobe of liver were dissected and subsequently used for the assessment of mitochondrial function (See Table 2.1 for tissues and experimental end point). Functional assessment of isolated mitochondria was carried out only in the muscle for the short-term DR animals. Liver mitochondrial function was also assessed in liver for the long-term DR assay in order to compare the effect of DR on a mitotic tissue (liver) with a post mitotic tissue (skeletal muscle). A total of 4 mice per day were culled, with the time between dissection, mitochondrial isolation and mitochondrial analysis kept as uniform as possible. For the long-term DR study the particular tissue (liver or skeletal muscle) processed and analysed was alternated each day. All experiments were carried out under a licence from the UK Home Office (Project Licence 60/4504) and followed the “principles of laboratory animal care” (NIH Publication No. 86-23, revised 1985) (See Figure 2.4 for schematic).

Table 2.1: All samples and tissues taken for both long and short term studies and description of experimental destination

Experiment	Sample Type	Action
Short Term DR (1)		
Physiology	WAT	Dissected & weighed - Adiposity
	BAT	Dissected & weighed - Adiposity
	Body Mass	Longitudinal measurement
	Food intake	Longitudinal measurement
	Plasma	Fed & fasting glucose, insulin sensitivity, IGF-1 –glucose homeostasis
	Blood	GTT –glucose homeostasis
Other	Heart	Snap Frozen
	Brain	Snap Frozen
	Hypothalamus	Snap Frozen
	Fur	Snap Frozen
	Kidney	Snap Frozen
Mitochondria	Skeletal Muscle (Fresh – isolated mitochondria)	Mitochondrial Respiration & ROS
	Skeletal Muscle (Snap Frozen)	Western Blot
Short Term DR (2)		
Protein synthesis n=8	Liver	Snap Frozen
	Heart	Snap Frozen
	Sk.Muscle	Snap Frozen
	Bone Marrow	Femur dissected and marrow flushed and frozen
	Blood/Plasma	Cardiac puncture (See section 2.4.1)
Long Term DR		
Physiology	WAT	Dissected & weighed - Adiposity
	BAT	Dissected & weighed - Adiposity
	Body Mass	Longitudinal measurement
	Food intake	Longitudinal measurement
	Plasma	Fed & fasting glucose, insulin sensitivity, IGF-1 –glucose homeostasis
	Blood	GTT –glucose homeostasis
Other	Heart	Snap Frozen
	Brain	Snap Frozen
	Hypothalamus	Snap Frozen
	Fur	Snap Frozen
	Kidney	Snap Frozen
Mitochondria	Liver (Fresh – isolated mitochondria)	Mitochondrial Respiration & ROS
	Liver (Snap Frozen)	Oxidative damage & antioxidant defence ELISAs, PGC-1α, UPR^{mt} & OXPHOS western blot, qPCR
	Skeletal Muscle (Fresh – isolated mitochondria)	Mitochondrial Respiration & ROS
	Skeletal Muscle (Snap Frozen)	PGC-1α western blot, UPR^{mt} & OXPHOS western blot
	Heart (Snap Frozen)	UPR^{mt} & OXPHOS western blot

2.2 Physiology

2.2.1 Body Mass, Food intake and Adiposity

Body mass (BM) was measured daily for 8 weeks from the introduction of 10% DR, and weekly thereafter, for both AL and DR mice. Total food intake of AL mice from each strain was recorded each week (±0.01g) by weighing the contents of food in the hopper of each cage. Intake per AL mouse, per day, for each strain was calculated based on the quantity of food consumed the preceding week and the daily DR allowance was determined according to this (Hempenstall et al. 2010). BM and food intake were measured at the same time, on the same day, every week. Adiposity was measured by collecting and weighing gonadal WAT and intrascapular BAT depots.

2.2.2 Glucose tolerance, fasting glucose and fed glucose

All animals (AL and DR) were fasted overnight in a fresh cage with AL access to water (1800 to 0800hrs) at 5 months (2 months 40% DR) and 13 months of age (10 months 40% DR). DR mice were fed at ~1500hrs on the afternoons immediately prior to a glucose tolerance test (GTT), to ensure feeding prior to the overnight fast (Hempenstall et al. 2010). Glucose tolerance was measured according to standard protocols (Selman et al. 2008). On the morning of the glucose tolerance test a 20% glucose solution for injection was prepared in a tissue culture hood by adding 5 g of pre-weighed glucose powder (Sigma Aldrich, Dorset, UK) incrementally to 20ml of sterile water, mixing regularly to ensure complete dissolution of glucose powder, and adding water to bring the final volume to 25ml. A heat box, with four chambers, was switched on to heat up prior to performing the GTT. Each mouse was weighed, marked on the tail for identification purposes, and placed in the heat box at 38°C. The animals were heated for approximately 15 minutes in order for vasodilation to occur; the dilation of the veins, which makes them more visible. Following this, each mouse was taken, held in a restrainer, and fasting blood glucose measurements were taken by venosection. With the tail protruding from the restrainer a clean razor blade was used to lightly cut across the caudal vein, and then 5µl of blood was added to a blood glucose strip of a glucometer (OneTouch Ultra, Lifescan, UK), and the resulting blood glucose (mmol/L) level recorded. Following which, mice were returned to the hot box. Injectate volume was calculated based on body mass for each animal (2g of glucose/kg body mass) and made up in a 1ml syringe and needle

(25cc), prepared with the glucose solution. Glucose was administered by intraperitoneal injection (IP) to each mouse, with a 30 second gap between IPs to each animal. Mice were returned to the heat box immediately following IP and glucose readings were taken by venosection at 15, 30, 60 and 120 minutes post injection. Animals were returned to their cages after the 60 minute reading for water, and placed back in the hot box 20 minutes prior to the 120 minute time point. After the procedure all animals were placed back in their original cage with access to water, and food in the case of the AL mice. DR mice were fed at the usual time (1800hr) following the procedure. All mice were checked the evening following a GTT. Glucose tolerance was expressed as the area under the curve over a 120 minute period following the IP injection of glucose. Similarly, fed glucose was recorded by venosection with the glucometer, blood was collected per mouse directly into an EDTA coated tube and spun at room temperature at 10,000 x g for 10 minutes, and stored long term at -80°C. Blood from AL mice was collected at 1100hrs and from DR mice at 1800hrs, following an early feeding at 1500hrs, to ensure mice were post-prandial (Hempenstall et al. 2010).

2.2.3 Fasting plasma insulin levels, insulin sensitivity and IGF-1 levels

2.2.3 (A) Fasting plasma insulin levels

Fasting plasma insulin levels were determined using a 96 well plate mouse insulin ELISA kit (EMD Millipore Corporation, USA Catalogue #EZRMI-13K) precoated in monoclonal insulin antibodies, in order to bind to insulin molecules from plasma samples. The plate was washed 3 times with 300 µl of wash buffer (provided by the manufacturer made up by a 10X dilution in deionised water) before use. The wash buffer was added to each well using a multichannel pipette (Gilson™ PIPETMAN™ Multichannel Pipettes) and subsequently decanted in the sink. Any residual wash buffer was removed by inverting the plate and tapping on absorbent towels, without letting the well dry out completely. 10 µl of assay buffer (provided by the manufacturer) was added to each well, followed by the addition of 10 µl of standard, control or sample in duplicate to the appropriate well. 80µl of anti-insulin “detection” antibody was added to each well to bind the insulin molecules, the plate was covered and incubated at room temperature for 2 hours on a plate shaker at 400 rpm. The plate was washed, as previously described, 3 times with wash buffer and thoroughly aspirated. 100µl of enzyme solution, containing horseradish peroxidase (HRP) conjugate, was added to each well. The plate was covered once

again and incubated at room temperature on a plate shaker 30 minutes on a plate shaker at 400 rpm. The plate was washed and aspirated, as described, a total of 6 times. Following this 100 µl of substrate solution was added to each well, covered and sealed on a plate shaker for 10 minutes. A blue colour develops over time, following the addition of substrate solution which catalyses the reaction, with insulin intensity being directly proportional to increasing insulin concentration. 100 µl of stop solution was then added to each well and a colour change from blue to yellow was observed, following acidification from the stop solution. The colour change was proportional to the amount of insulin protein per sample and was quantified spectrophotometrically, using a plate reader at an absorbance of 450nm and 590nm. The average absorbance was calculated for each sample and standard, and the difference in absorbance between 450nm and 590nm was used to calculate the standard curve. By comparing the absorbance of the standards of known insulin concentration, the standard curve was used to determine the insulin concentration of each sample.

2.2.3 (B) Insulin Sensitivity

Immediately following 2 and 10 months of DR (5 and 13 months of age respectively), all mice were fasted overnight, weighed and culled. Blood was collected and the resultant plasma stored at -80°C. Insulin sensitivity was estimated using the updated homeostatic model assessment (HOMA2) model (Wallace et al. 2004), a method used to quantify insulin resistance and beta-cell function from fasting glucose and insulin concentrations. This calculator is based on a mathematical equation that describes glucose regulation as a feedback loop, and the software solves the equation so that insulin resistance can be estimated from known fasting glucose and insulin levels (Matthews et al. 1985). Using fasting blood glucose (mmol/L) and insulin (pM/L) measurements the HOMA2 calculator (version 2.2.3) determined HOMA IR, a measure of insulin resistance, in all strains, following short and long term treatment.

2.2.3 (C) Fasting IGF-1 levels

Fasting plasma IGF-1 levels were determined using a mouse IGF-1 ELISA kit (Catalogue #MG100, Quantikine, R and D Systems Inc., USA). Employing the quantitative sandwich enzyme immunoassay technique, a 96 well microplate was pre-coated with a monoclonal antibody specific for mouse IGF-1. Standards were

made up following the manufacturers guidelines, and plasma was diluted 500 fold in calibrator diluent RDF5-38 (a buffered protein solution provided with the kit). Following this 50 µl of standards, control and samples were pipetted into each well in duplicate. At this point any mouse IGF-1 present in the samples were bound and immobilised by the antibody. The plate was covered with an adhesive strip and incubated at room temperature for 2 hours on a plate shaker set at 500 rpm. The plate was washed and aspirated a total of 5 times. This was done by adding 400µl of wash buffer (a buffered surfactant, made up by adding 20mls of wash buffer, provided with the kit, to 480 ml of deionised water) to each well. Following this all liquid was removed by decanting and drying on absorbent surface, the removal of all liquid ensured the removal of any unbound substances. Following the wash step, 100µl of secondary antibody, a polyclonal antibody against mouse IGF-1 conjugated to horseradish peroxidase, was added to each well. The plate was covered with a fresh adhesive strip, and incubated for 2 hours at room temperature (RT) on a shaker. The plate was washed and aspirated 5 times, as previously described, and 100 µl of substrate solution (equal volumes of stabilised hydrogen peroxide and stabilised chromogen, provided by the manufacturer) was added to each well before being incubated for 30 minutes at room temperature. The plate was protected from light for these 30 minutes by covering in tin foil. 100µl of stop solution was added to each well, and a colour change from blue to yellow was observed. The optical density of each well was assessed immediately using a microplate reader set to 450nm. Readings were subtracted from readings made at 540nm in order to correct for optical imperfections on the plate. The intensity of the colour measured is in proportion to the amount of mouse IGF-I bound in the initial step. The sample values were then read off the standard curve.

2.3 Mitochondria

2.3.1 (A) Isolation of mouse liver mitochondria

Liver mitochondria were isolated following previously published protocols (Brand & Nicholls 2011; Rogers et al. 2011). The liver was weighed and washed in ice-cold MSHE+BSA buffer (210mM mannitol, 70mM sucrose, 5mM HEPES, 1mM EGTA and 0.5% (w/v) fatty acid free bovine serum albumin (pH 7.2), all from Sigma Aldrich). On ice the liver was rapidly minced with scissors in 10 volumes of chilled MSHE+BSA buffer before homogenisation (2-3 strokes) using a chilled glass-glass homogeniser (Fisher Scientific, Loughborough, UK). Liver mitochondria were then

isolated using differential centrifugation following a previously described protocol (Brand & Nicholls 2011). In brief, the liver homogenate was initially centrifuged at 8,000 x g for 10 minutes at a temperature of 4°C. The lipid bilayer was then aspirated off and the supernatant subsequently passed through two layers of cheesecloth. The filtrate was collected in a 50 ml centrifuge tube and spun at 8,000 x g for 10 minutes at 4°C. Following this spin, the supernatant was discarded and 5mls of MSE+BSA buffer was added (without disturbing the pellet) and spun for a second time at 8,000 x g. The supernatant was once again discarded, and the resulting pellet was gently resuspended in a minimal volume (250 µl) of buffer (MSHE with no BSA) buffer prior to protein quantification (see section 2.3.1 (B) below).

2.3.1 (B) Isolation of mouse skeletal muscle mitochondria

As with the liver, gastrocnemius muscle was harvested, weighed, washed and then minced in ice-cold isolation buffer (100 mM sucrose, 100 mM KCL, 50 mM Tris HCl, 1 mM KH2PO4, 0.1 mM EGTA, 0.2% BSA (pH 7.4), all from Sigma Aldrich), as previously described (Garcia-Cazarin et al. 2011). The minced muscle was rinsed three times in 1 ml of ice cold fresh isolation buffer, before 1 ml of 2% (w/v) Proteinase Type XXIV (Sigma Aldrich, Dorset, UK) was added and the sample vortexed for 1 minute at RT, followed by a 1 minute incubation on ice. Samples were then added to a glass homogeniser containing 4 ml of isolation buffer before homogenisation (10 strokes with a glass-glass homogeniser). Through differential centrifugation mitochondria were isolated in the form of a pellet from the muscle (Garcia-Cazarin et al. 2011). The homogenate was spun at 700 x g for 10 minutes at 4°C in the first instance. The supernatant was transferred to a fresh tube and spun for a second time at 10,500 x g for 10 minutes, once again at 4°C. Following this the supernatant was discarded and the pellet was resuspended in a minimal volume of isolation buffer (200 µl). After a final 3 minute spin at 7,000 x g, the supernatant was discarded and the pellet was resuspended in 50 µl of suspension buffer (225 mM Mannitol, 75 mM sucrose, 10 mM Tris, 0.1 mM EDTA (pH 7.4).

Total liver and skeletal muscle mitochondrial protein (mg/ml) were determined using the Bradford assay (Sigma Aldrich, Dorset, UK). The Bradford assay is based on the absorbance shift of the dye, (coomassie brilliant blue G-250), to its bluer form, through the binding of the protein being assayed (Bradford 1976). The blue colour is given from reflected light and of lower wavelength than the absorbance measured in the green/yellow area of the spectrum. Thus the density

of the blue colour is effectively directly proportional to the amount of protein in the sample and is measured using a plate reader at 595nm. The absorbance of standards, of known BSA protein concentration (0 mg/ml-2mg/ml), were compared to the samples and the standard curve was used to determine the total mitochondrial protein for both liver and muscle.

2.3.2 XF Assay – Plate preparation

Isolated mitochondria were diluted 10X in mitochondrial assay solution (MAS; 70 mM sucrose, 220 mM mannitol, 10 mM KH2PO4, 5 mM MgCl2, 2 mM HEPES, 1.0 mM EGTA and 0.2% (w/v) fatty acid-free BSA, pH 7.2, all from Sigma Aldrich) containing substrate (10 mM pyruvate, 2 mM malate – Sigma Aldrich), and subsequently diluted to produce a mitochondrial suspension which were then added to a Seahorse XF assay plate (Agilent Technologies, CA, USA) at a concentration of 10µg per well. The plate was then centrifuged at 2000 x g for 20 minutes at 4°C. A XF cartridge (Agilent Technologies) was prepared as described by Brand et al. (Brand & Nicholls 2011), (see Figure 2.5). The plate was incubated at 37°C for 6 minutes before being transferred to a XF24 Analyser (Agilent Technologies) (See Figure 2.6) and the experiment initiated as previously described (Rogers et al. 2011) (See Figure 2.7 for schematic of workflow and Table 2.2 for XF24 protocol). Basal Oxygen consumption rate (OCR) was measured in substrate (10 mM pyruvate, 2 mM malate). Following this OCR was sequentially recorded for state 3 (addition of ADP (4 mM)), state 4 (addition of oligomycin (2.5 µg/ml)), state 3u (FCCP (4 µM Carbonyl cyanide 4-(trifluoromethoxy) phenylhydrazone)), and finally in the presence of Antimycin A and rotenone (4 µM) to determine non-mitochondrial respiratory capacity (Rogers et al. 2011) (See Figure 2.8 for data output figure, all stocks from Sigma Aldrich). Analysis was carried out using Seahorse XF software (www.seahorsebio.com).

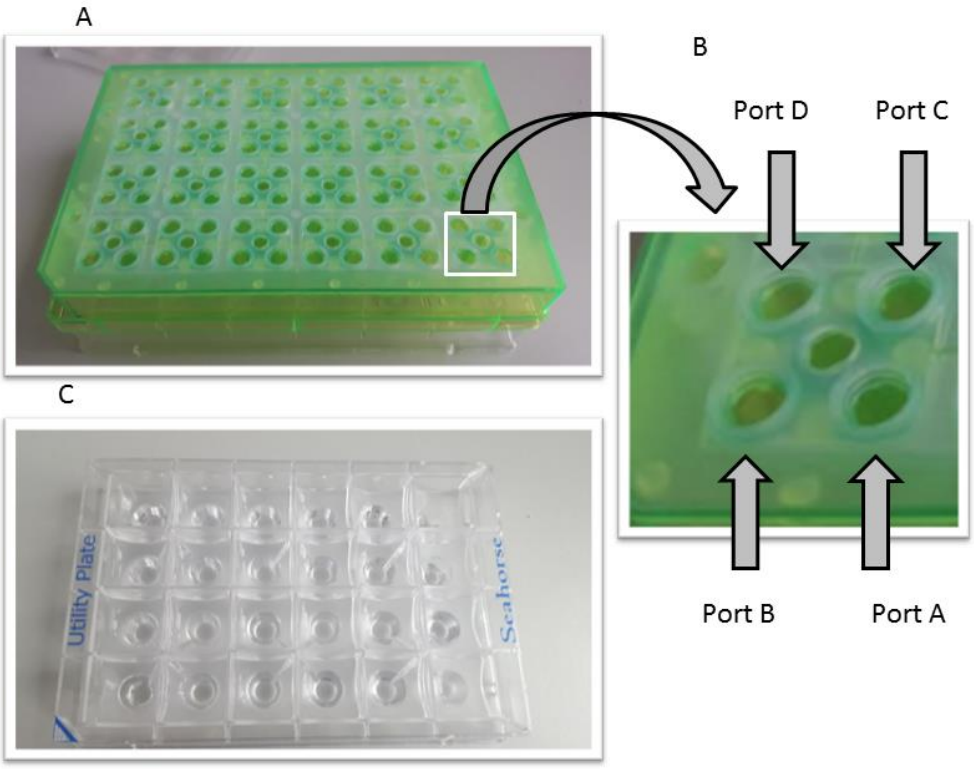

Figure 2.5: (A) The XF24 cartridge was hydrated the night before the respiration assay. (B) On the day of the assay compounds were prepared and loaded into Port D (4 mM ADP), Port C (2.5 µg/ml Oligomycin), Port B (4 µM FCCP) and Port A (4 µM Antimycin A and Rotenone) and the cartridge was loaded onto the XF24 flux analyser for calibration. (C) Isolated mitochondria are added to each well of the XF24 utility plate, each set of ports on the cartridge sits directly on top of a well containing isolated mitochondria and sequential injections are made into each well.

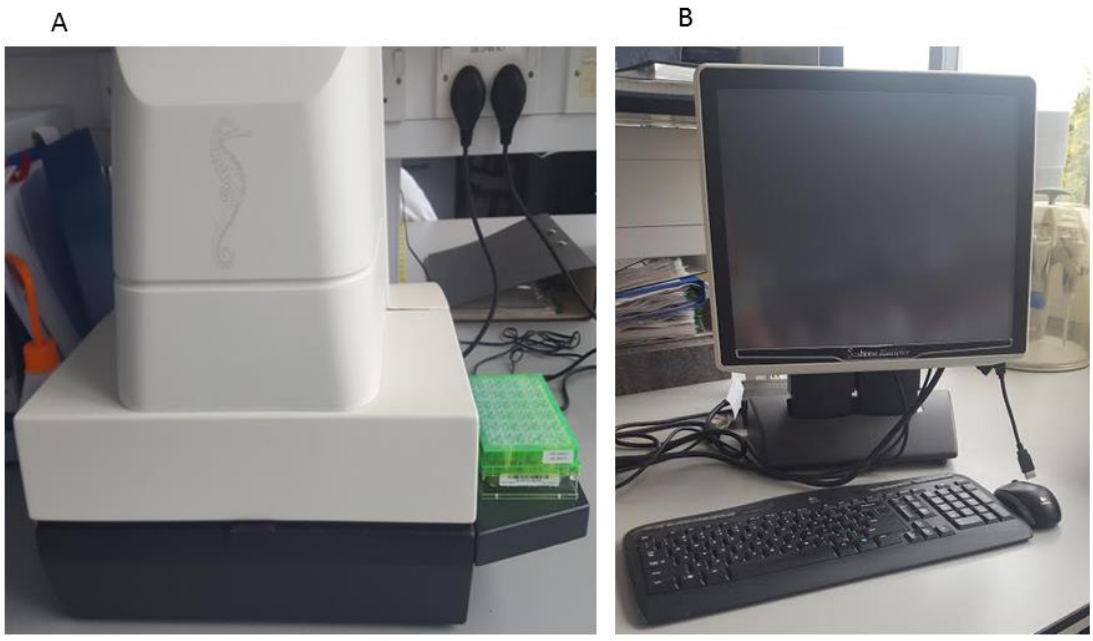

Figure 2.6: (A) XF24 Flux analyser with cartridge prior to loading of cartridge containing compounds and 24 well plate containing isolated mitochondria, (B) XF24 user console.

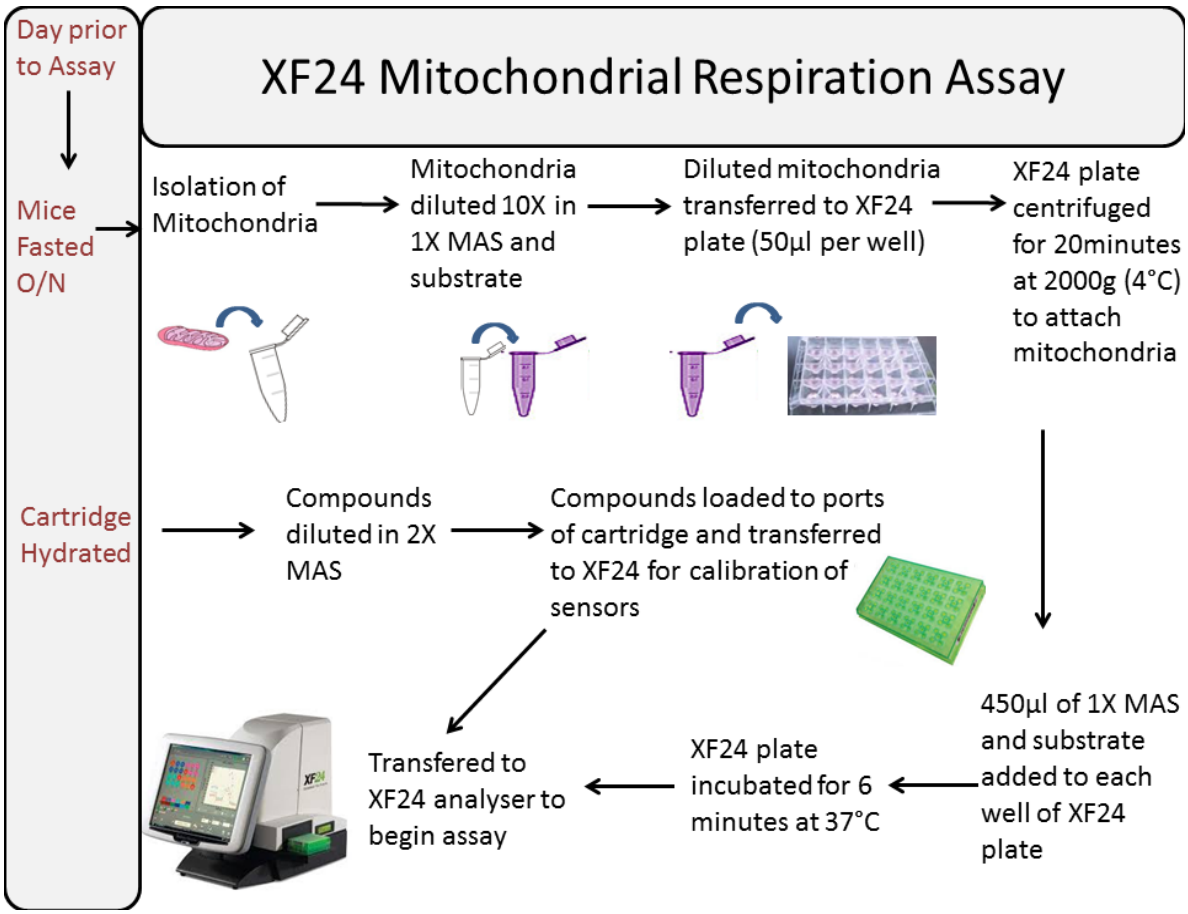

Figure 2.7: Schematic of experimental procedure used to measure oxygen consumption rates of isolated mitochondria using an XF24 analyser.

Table 2.2: XF24 mitochondrial respiration protocol including mix, wait and measure cycle times and order of compound injection.

Command	Time	Port
Calibrate		
Mix	1	
Wait	3	
Mix	1	
Wait	3	
Mix	0.5	
Measure	3	
Mix	0.5	
Inject		D – ADP (4 mM)
Mix	1	
Measure	3	
Mix	1	
Inject		C – Oligomycin (2.5 µg/ml)
Mix	0.5	
Measure	3	
Mix	1	
Inject		B – FCCP (4 µM)
Mix	0.5	
Measure	3	
Mix	1	
Inject		A – Antimycin A and Rotenone (4 µM)
Mix	0.5	
Measure	3	

Firstly the contents of each well were mixed, followed by a wait period. The machine then recorded the respiration rate before the injection of any compounds, to get the basal respiration rate. Following the injection of each compound a series of mixing

and measuring occurs, recording the oxygen consumption rate of the mitochondria in response to each compound (Rogers et al. 2011).

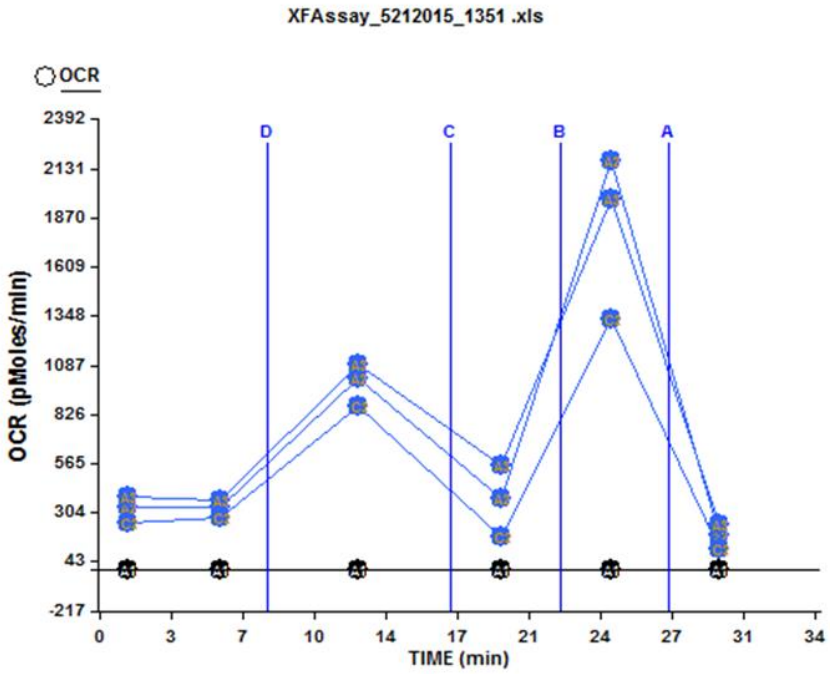

Figure 2.8: Representative trace of data output from XF24 analyser. Mitochondrial oxygen consumption rate (OCR (pMoles/min)) was measured over time (minutes). Mitochondria respired at a basal rate until injection of ADP (Port D) where an increase in respiration was observed (State 3). Following an injection of Oligomycin (Port C), respiration rate dropped through inhibition of ATP synthase (State 4o). A subsequent injection of FCCP (Port B), a mitochondrial uncoupler, caused mitochondria to respire at their maximal rate (State 3u) before non-mitochondrial OCR was determined through the addition of Antimycin A and Rotenone (Port A).

2.3.3 Protein extraction for western blotting

Liver, skeletal muscle and heart tissue were suspended in 1ml of ice cold RIPA buffer (Radio Immuno Precipitation Assay buffer, 150 mM sodium chloride, 1.0% NP-40 or Triton X-100, 0.5% sodium deoxycholate, 0.1% SDS (sodium dodecyl sulphate), 50 mM Tris, pH 8.0) containing protease inhibitors (Halt™ Protease and Phosphatase Inhibitor Cocktail, Thermo Fisher Scientific, UK). The liver and heart were rapidly minced on ice with scissors prior to homogenisation in 1 ml of RIPA, using a glass-glass homogeniser (Fisher Scientific, UK). A stainless steel bead (Catalogue #69989, QIAGEN, Manchester, UK), was added to the eppendorf containing the skeletal muscle tissue and RIPA buffer, and then homogenised at maximum speed (30Hz) for 4 minutes on the RETSCH MM 400 mixer mill (Catalogue #10573034, Fisher Scientific). Following homogenisation all lysates were incubated on ice for 40-60 minutes before being centrifuged at 16,000 x g for 10 minutes at 4°C, and total protein levels subsequently determined using the BCA protein assay (G Biosciences, MO, USA). The BCA protein assay is based on the reduction of copper (Cu^{2+}) by the protein sample. The amount of CU^{2+} reduced is proportional to the amount of protein in the sample. 25 µl of standards and samples were added to the wells of the 96 well plate. 200 µl of working solution (50 parts BCA solution to 1 part copper solution) was added to each well. The plate was wrapped in tinfoil to protect from light and incubated at 37°C for 30 minutes. The plate was read at an absorbance of 562nm and a standard curve was prepared to determine the protein concentration of each sample. The amount of protein present in a sample was calculated by measuring the absorption spectra of each lysate and comparing with protein solutions of known concentrations (0-2mg/ml).

2.3.4 Extraction of nuclear and cytoplasmic proteins

Nuclear and cytoplasmic fractionation of liver and skeletal muscle was undertaken using the ReadyPrep™ Protein Extraction (Cytoplasmic/Nuclear) Kit (Catalogue #163-2089, Bio-Rad, UK). Briefly, ~50mg of tissue was homogenised together with 0.75 ml of cold cytoplasmic protein extraction buffer (CPEB) containing protease inhibitors using a chilled Wheaton Dounce tissue homogeniser (Catalogue #62400-595, VWR, West Sussex, UK). The tissue was broken up with 10 strokes of the loose fitting pestle, followed by 10 strokes with the tight pestle, in order to release the nuclei from the cells. The homogenate was chilled on ice for 1 minute, to allow large fragments to settle, and the supernatant was transferred to a fresh tube. The

supernatant was subsequently spun at 1000 x g for 10 minutes at 4°C. The supernatant was immediately transferred to a fresh tube. The original tube was spun for a further 10 seconds at the same speed, and the supernatant was pooled with the supernatant from the first spin. This was the cytoplasmic protein fraction and was stored at -80^0 C until further use. The pellet, containing the nuclei, was washed with 250 µl of CPEB, vortexed gently and incubated on ice for 10 minutes. Following this the samples were spun at 1000 x g for 10 minutes at 4°C in order to concentrate the nuclei. The supernatant was discarded following this spin. Following the protocol supplied with the kit complete PSB (Protein Solubilisation Buffer) was prepared by adding 2 ml of the provided 2-D rehydration/sample buffer, with 1.1 ml of PSB diluent and 1 g of PSB powder. Following this 15.4 mg of DTT (50mM) (BioRad), 20µl of 100X Bio-Lyte (0.2 %(w/v) (BioRad) and 4µl 1% Bromophenol Blue (0.002 %(w/v)) was added to the mixture making up complete PSB. The nuclei were suspended in 500ul of complete PSB and vortexed 4 times, 60 seconds each. The sample was centrifuged at 12,000 x g for 20 minutes at room temperature in order to pellet the genomic DNA. The supernatant was transferred into a fresh tube and labelled Nuclear Protein Fraction. The pellet was resuspended in 250 µl of PSB and centrifuged again at 12,000 x g for 20 minutes at room temperature. The supernatant was collected, pooled with the previous supernatant in the tube marked nuclear protein fraction and stored at -80°C until future use. The protein concentration of each fraction determined using the BCA protein assay (G Biosciences).

2.3.5 Western Blot Analysis

Equal volumes of tissue protein extract (50 µg) in Laemmli sample buffer (Biorad) were loaded onto 4-12% Bis-Tris pre-cast polyacrylamide gels (Life Technologies, Paisley, UK). Following this, proteins were transferred to polyvinylidene difluoride membranes (BioRad). Ponceau staining (ThermoFisher Scientific, UK) was used to ensure equal loading of protein and for normalisation purposes. Membranes were incubated in Tris-buffered saline Tween^{20} (Sigma-Aldrich, UK) (1X TBST) containing 5% BSA for 1h^{-1}. Blots were then washed in TBST (5×5minutes), incubated with primary antibody for 24h^{-1} (4°C), washed again (TBST) and incubated with secondary antibody for 1h^{-1} at room temperature. Blots were visualised using Clarity™ Western ECL Substrate (BioRad) and a ChemiDoc™XRS system (BioRad).

Antibodies for peroxisome proliferator-activated receptor-gamma co-activator 1 alpha (PGC-1α) and the oxidative phosphorylation complex antibody (OXPHOS cocktail; CI subunit NDUFB8, CII-30kDa (SDH), CIII-Core protein 2 (UQCRC2), CIV subunit I (MTCO1) and CV alpha subunit (ATP5A) were from Abcam, Cambridge, UK. Antibody H2B was purchased from Cell Signalling (New England BioLabs, UK) and used as a control when blotting for nuclear PGC-1α to ensure that the nucleic protein fraction was not contaminated with cytoplasmic proteins. Mitochondrial transcription factor A (TFAM) and secondary (anti-rabbit and anti-mouse) antibodies from Santa Cruz Biotechnology Inc. (Santa Cruz, CA, USA), and HSP60 and HSP90 from BD Biosciences (BD Biosciences, Oxford, UK. Mitochondrial nuclear imbalance (nDNA: mtDNA ratio) was determined by the ratio of nuclear encoded SDHB (Complex II)) to mitochondrial-encoded MTCO1 (Complex IV) (Houtkooper et al. 2013). Antibodies for uncoupling protein 1 (UCP-1) were purchased from Abcam, Cambridge, UK.

2.3.6 Mitochondrial ROS production

Mitochondrial ROS production was assayed in mitochondria isolated from skeletal muscle and liver (See Figure 2.9 for diagram of ROS production) by Dr Karine Salin. Fresh respiratory medium (MAS; 70 mM sucrose, 220 mM mannitol, 10 mM KH2PO4, 5 mM MgCl2, 2mM HEPES, 1.0 mM EGTA and 0.2% (w/v) fatty acid-free BSA, pH 7.2) was supplemented with 1 U/ml horseradish peroxidase and 10uM Amplex® Red reagent (ThermoFisher Scientific, UK) as previously described (Zhou et al 1997). 90µl of this medium was then added to each well of a standard 96 well plate (Costar®, Sigma Aldrich, UK) and heated for two minutes at 37°C. Fluorescence was then measured at 15 second intervals for 2-3 minutes using a spectrophotometer (Clariostar microplate reader, BMG Labtech) at excitation and emission wavelength of 563 and 587nm respectively. A sequential protocol was then run simultaneously for each sample in triplicate and completed within 15 minutes. First the baseline fluorescence was measured by adding 10 µl of mitochondrial suspension, and then mitochondrial hydrogen peroxide production from all complexes was determined by adding a saturating concentration of succinate (10 mM), and then rotenone added (0.5 uM; an inhibitor of complex I). The fluorescence signal was calibrated using 176 nM of hydrogen peroxide, and then hydrogen peroxide production was calculated following background correction.

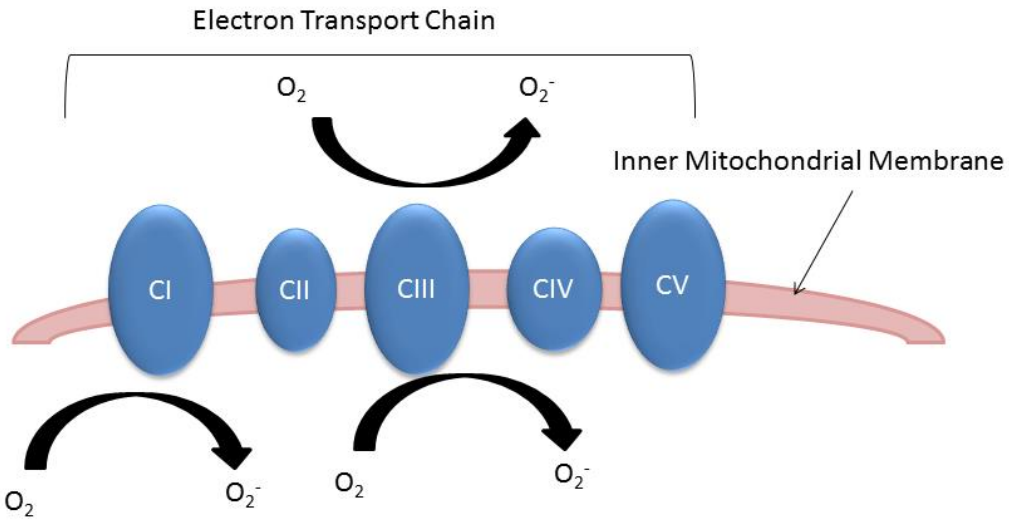

Figure 2.9: Complex I-V of the electron transport chain located in the inner membrane of the mitochondria. CI and CIII are major sites of oxygen metabolism and so the main site of ROS production.

2.3.7 Oxidative damage and antioxidant levels

Protein carbonyl (PC) content and 4-Hydroxynonenal (HNE)-protein adduct levels are commonly used biomarkers for oxidative damage (Chevion et al. 2000; Castro et al. 2017). NADPH oxidase generates superoxide through electron transfer and can also be used as a marker for oxidative damage. Glutathione (GSH) and total Superoxide dismutase content are considered important indicators of antioxidant defence against ROS and are used as markers of antioxidant levels (Singh 2002; Serra et al. 2003).

2.3.7 (A) Sample Preparation

A fragment of liver was homogenised at maximum speed (30Hz) for 4 minutes on the RETSCH MM 400 mixer mill (Fisher Scientific) (as mentioned in section 2.3.2) in 1 ml of cold assay buffer (PC and GSH homogenate buffer: 50 mM MES, 1 mM EDTA, pH6.7; SOD homogenate buffer: 20 mM HEPES, 1 mM EGTA, 210 mM mannitol and 70 mM sucrose, pH 7.2; 4-HNE & NADPH oxidase homogenate buffer 1 ml RIPA buffer and 10 µl of protein and phosphatase inhibitors (as described in section 2.3.2 protein extraction) using one stainless steel bead (QIAGEN) per sample. All samples were centrifuged at 10,000 x g for 15 minutes at 4°C following homogenisation and stored at -80°C until required. Total protein was calculated for each sample using the BCA assay (G Biosciences).

2.3.7 (B) Protein Carbonyl content

Hepatic protein carbonyl (PC) content was measured using a commercially available kit (Carbonyl assay kit, Catalogue #10005020, Cayman, Estonia). The assay measured the reaction between 2,4-dinitrophenylhdrazine (DNPH) and protein carbonyls, and the reaction was analysed spectrophotometrically to determine protein carbonyl content. Prior to the assay the absorbance of each sample was checked for nucleic acid content. This was done by measuring the absorbance of each sample at 280nm and 260nm, however as the ratio (280/260) of all samples was greater than 1, no further action was required with the samples (as per specification in the manufacturer protocol). 200µl of sample was added to two 2 ml tubes. One tube was labelled C for control and the other S for sample, along with the corresponding sample ID number. 800 µl of DNPH was added to the tube marked S for sample, and 800 µl of 2.5M HCL was added to the tube labelled C for control. Both tubes were incubated in the dark, by covering in tinfoil, at room

temperature for 1 hour. Each tube, both sample and control, was vortexed every 15 minutes during this 1 hour period. Following this 1 ml of 20% (w/v) TCA (trichloroacetic acid, provided by the manufacturer) was added to each tube and vortexed. All samples were subsequently incubated on ice for 5 minutes. Samples were centrifuged at 10000 x g for 10 minutes at 4°C. Following this, the supernatant was discarded and the pellet was resuspended in 1 ml of 10% w/v TCA. Samples were put on ice for 5 minutes following this. Samples were centrifuged for a second time, at 10000 x g for 10 minutes at 4°C. As before, the supernatant was discarded. This time the pellet was resupsended in 1 ml of (1:1) ethanol/ethyl acetate mixture. The pellet was resuspended, vortexed, and centrifuged for 10 minutes at 10000 x g, 4^0 C. This step was repeated twice more, before resuspending the pellets in 500 µl of guanidine hydrochloride (supplied with the kit) and vortexing. The samples were centrifuged at 10000 x g for 10 minutes at 4°C, in order to remove any remaining debris. 220 µl of supernatant from S and C samples were added to the plate in duplicate. The absorbance was measured at a wavelength of 360nm using a plate reader (Clariostar microplate reader, BMG Labtech). The average of absorbance was calculated for each sample and control. The average absorbance of the controls was subtracted from the average absorbance of the samples. This was called the Corrected Absorbance (CA). The concentration of the carbonyls was calculated using the following equation:

Protein Carbonyl (nmol/ml) = [(CA)/ (*0.011um^{-1})] (500µl/200µl)

2.3.7 (C) 4-HNE protein content

Hepatic 4-Hydroxynonenal (HNE)-protein adduct levels were determined using an anti-HNE-His mouse IgG protein binding plate (OxiSelect™ HNE Adduct Competitive ELISA Kit, Catalogue #STA-838, Cell Biolabs Inc., CA, USA). This assay is an enzyme immunoassay in 96 well format, the primary antibody was added to the plate and incubated overnight at 4°C. The quantity of HNE-His adduct in protein samples was determined by comparing the absorbance with that of a known HNE-BSA standard curve. On the day of the assay 100 µl of standard and sample was added to each well in duplicate and incubated at 37°C for 2 hours. The well was washed and aspirated twice with 250 µl of phosphate buffered saline (PBS, Sigma-Aldrich UK) per well. 200 µl of assay diluent was added and incubated at room temperature for 2 hours on an orbital shaker. Following this the plate was washed 3 times with 250 µl of wash buffer and aspirated thoroughly. 100µl of anti-

HNE antibody was added to each well and incubated for 1 hour at room temperature on an orbital shaker. The plate was washed and aspirated as previously described and 100 µl of secondary antibody-HRP conjugate was added to each well and incubated for 1 hour at room temperature on an orbital shaker. The plate was washed and aspirated once again before adding 100 µl of substrate solution to each well and incubated at room temperature on an orbital shaker for 10 minutes. 100 µl of stop solution was added to each well to stop the enzyme reaction and the plate was read immediately at 450nm using a plate reader. 4-HNE was calculated using the standard curve and expressed relative to protein content as µg/ml, quantified using a BCA assay (G Biosciences).

2.3.7 (D) NADPH Oxidase content

NADPH oxidase levels were determined using a commercially available kit (mouse NADPH oxidase ELISA kit, Catalogue #abx255148, Abbexa ltd, Cambridge, UK). Nox1 (NADPH oxidase 1) antibody came pre-coated on a 96 well plate. The plate was twice washed with wash buffer before the addition of 100µl of the standards and samples to each well. The plate was then covered and incubated at 37°C for 90 minutes. Following this the contents of the plate were discarded but the plate was not washed in this instance and 100 µl of Biotin conjugated antibody, used as the detection antibody, or secondary, was added to each well. The plate was sealed and incubated at 37°C for 60 minutes. Following this the plate was washed three times with wash buffer and thoroughly aspirated, through decanting and drying on absorbent towels. Each well was filled with wash buffer and allowed to soak for 2 minutes before discarding the liquid in the wells. Any unbound conjugates were removed through this process and the soaking procedure was carried out a total of three times. 100 µl of working solution was added to each well, the plate sealed and incubated for 30 minutes at 37°C, and washed 5 more times with wash buffer subsequently. 90 µl of TMB (3,3',5,5'-Tetramethylbenzidine) substrate was used to visualise the HRP enzymatic reaction. The plate was incubated at 37°C in the dark for 15 minutes and during this time the TMB is catalysed by HRP to produce a blue colour product that changes into yellow after adding 50 µl of stop solution. The absorbance was measured at 450nm on a microplate reader, and then the concentration of Nox1 was calculated from the standard curve.

2.3.7 (E) Total GSH content

Total glutathione (GSH) (Glutathione assay kit, Catalogue #703002 Cayman) was measured using an assay that makes use of an enzymatic recycling method, using glutathione reductase for the quantification of GSH. The sulfhydryl group of GSH reacts with DTNB (5,5'-dithio-bis-2-(nitrobenzoic acid) and produces a yellow coloured 5-thio-2nitrobenzoic acid (TNB). The rate of TNB production is directly proportional to this recycling reaction which is in turn directly proportional to the concentration of GSH in the sample. Samples required deproteination, to avoid interference with the assay, before analysis. In order to do this 5mg of metaphosphoric acid (Sigma-Aldrich Item no. 239275) was dissolved in dH_2O, this was called the MPA reagent. An equal volume of MPA reagent was added to the sample. The mixture of sample and MPA was left to stand at room temperature for 5 minutes and then centrifuged at 2000 x g for 2 minutes. The supernatant was carefully collected. 50µl of TEAM reagent, made up of 4M solution of triethanolamine (Sigma-Aldrich Item no. T58300) by mixing 531 µl of triethanolamine with 469 µl of dH_2O, was added per ml of supernatant and vortexed immediately. At this point the samples were ready for immediate analysis of total GSH. 50 µl of standards and samples were added to the appropriate wells of the 96 well plate. The plate was covered with the protective adhesive provided. The assay cocktail was prepared as per assay protocol, by mixing 11.25 ml of MES buffer (consisting of 0.4M 2-(N-morpholino) ethanesulphonic acid,), 0.1 M phosphate and 2 mM EDTA, pH6.0. Entire mixture diluted 1:2 with dH_2O for MES buffer), 0.45 ml of reconstituted Cofactor mixture, 2.1ml of reconstituted enzyme mixture, 2.3 ml of dH_2O, and 0.45 ml of DTNB. The plate cover was removed and 150 µl of the assay cocktail was added to all wells using a multichannel pipette (Gilson™ PIPETMAN™ Multichannel Pipettes). The plate was covered with a new protective cover, covered in tinfoil to protect from light, and left on an orbital shaker for 25 minutes. At this point the plate was read at 405nm using a plate reader. The average absorbance was calculated for all standards and samples. The absorbance value of standard A (0 µM) was subtracted from itself and from all other values. This was the corrected absorbance (CA). The corrected absorbance was plotted as a function of the concentration of total GSH. The total GSH was calculated from the standard curve, and all values were expressed relative to total protein concentration.

$$\text{Total GSH} = \left[\frac{(\text{Absorbance at } 405 - 414\text{nm}) - (\text{y} - \text{intercept})}{\text{Slope}}\right] \text{ x 2 x Sample Dilution}$$

2.3.7(F) Total superoxide dismutase activity

Total superoxide dismutase (SOD) activity was measured using a commercially available kit (Total SOD activity assay kit, Catalogue #706002, Cayman). This assay utilises a tetrazolium salt for detection of superoxide radicals generated by xanthine oxidase and hyposanthine. One unit of SOD is defined as the amount of enzyme needed to exhibit 50% dismutation of the superoxide radical. 200 µl of the diluted radical detector (diluted tetrazolium salt solution, prepared as per manufacturer guidelines) was added to each of the 96 wells on the plate. Standards of known concentration were provided and labelled A- G, A being the lowest known concentration and G being the highest (0-0.05 U/ml total SOD). 10 µl of standard and sample was added to the appropriate well. The reaction was initiated by adding 20 µl of diluted Xanthine oxidase to all the wells, as quickly as possible, to avoid time differences between addition to first well and last well. The plate was covered with an adhesive cover, and shaken for a few seconds to mix. The plate was incubated on a shaker for 30 minutes at room temperature. The absorbance was read at 440nm using a plate reader. The average absorbance was calculated for each standard and sample. The linearised rate (LR) was determined by dividing standard A's absorbance by all the other standards, and by all the sample absorbance's. The linearised rate was plotted as a function of final SOD activity (U/ml). The SOD activity of the samples was calculated using the equation (See below) obtained from the linear regression of the standard curve and substituting in the LR value for each sample.

$$\text{SOD(U/ml)} = \left(\frac{\text{Sample LR} - \text{y intercept}}{\text{Slope}}\right) \text{ x } \frac{0.23\text{ml}}{0.01\text{ml}} \text{ x sample dilution}$$

All assays were read on a plate reader (BMG Labtech, UK) and expressed relative to protein content (mg/ml).

2.4 Protein Synthesis

We employed a method using a stable isotope, deuterium oxide (^2H_2O Catalogue #756822, Sigma), to assess the rate of protein turnover and DNA synthesis. Skeletal muscle, heart and liver were examined, to allow a comparison of tissues representative of post mitotic, semi-mitotic and mitotic tissues, in order to give a more complete assessment of the impact of short term DR on protein and DNA synthesis in three genetically heterogeneous mouse strains. The *in vivo* labelling with ^2H_2O gave a measure of proteostatic mechanisms through the concurrent measurement of both protein (Busch et al. 2006; Drake et al. 2013; Miller et al. 2012; Miller et al. 2013; Robinson et al. 2011) and DNA synthesis (Drake et al. 2013; Miller et al. 2012; Miller et al. 2013; Robinson et al. 2011; Neese et al. 2002). The ratio of protein:DNA synthesis is indicative of the proteostatic process, and gives insight to cellular processes that may be concealed by measurements of DNA or protein concentration alone (Hamilton & Miller 2017; Miller et al. 2014). Following an injection, enrichment of the body water pool with ^2H_2O is rapidly established, and the ^2H label is incorporated at multiple sites. Newly synthesised metabolites incorporate deuterium into stable Carbon-Hydrogen (C-H) bonds, and ^2H incorporation can be measured by gas chromatography mass spectrometry (GC/MS). The label is incorporated into deoxyribose (dR), which has 7 C-H bonds available for the incorporation of ^2H_2O and a given amino acid (AA), in this case alanine, with 4 C-H bonds available (compared with 2 available C-H bonds in AA glycine and 1 C-H bond in AA leucine, see Busch *et al* 2006 for in depth description), and allows for the determination of rates of newly synthesised DNA and protein. One advantage to this method is that it can be dispensed over prolonged periods of time. This allows measurement of proliferation of cells with a slow rate of turnover, and provides information on processes over the course of the labelling period rather than one metabolic moment in time, without interfering with daily movements of the experimental animals (Miller & Hamilton 2012; Miller et al. 2014; Hamilton & Miller 2017).

2.4.1 Experimental Design and Labelled Water

At 5 months of age (2 months of 40% DR), AL and DR animals were fasted overnight, in a fresh cage, with AL access to normal drinking water. DR mice were given an initial intraperitoneal injection (IP) of 99% ^2H_2O to rapidly enrich the pool of body water with deuterium. Enrichment was then maintained by *ad libitum* access

to drinking water enriched with 8% $^{2}H_2O$ for a 2-week period (Miller et al. 2012; Neese et al. 2002). Following this 2-week enrichment period, the mice were fasted overnight, and sacrificed under HO licence following CO_2 inhalation. Blood was collected by cardiac puncture (0.1 ml – 1 ml) followed by dissection and snap freezing of the heart, liver and the gastrocnemius of both hind limbs. All tissues were stored at −80°C. Bone marrow was collected to represent a fully turned over population of cells. The marrow was extracted by taking the femur and cutting both ends. 1ml of PBS was drawn into a 3cc syringe with a 25 gauge needle. The femur, with both ends removed, was held over a fresh tube, the syringe stuck in the hole on one end of the bone and the marrow flushed out and collected in the tube. All bone marrow samples were stored at -20°C. Samples were shipped on dry ice to the Translational Research on Aging and Chronic Disease Laboratory at Colorado State University for analysis (See Figure 2.10 for experimental design).

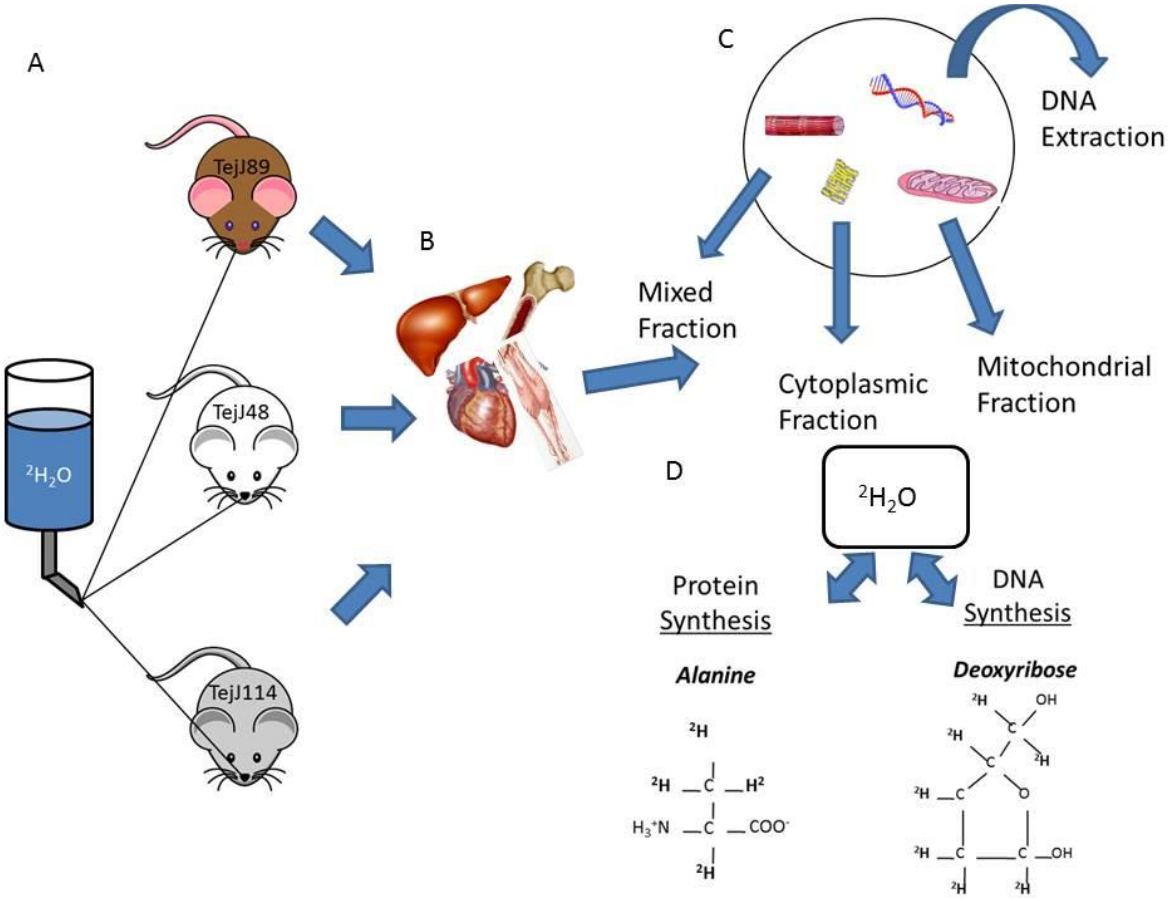

Figure 2.10: Schematic of experimental design used to determine the synthesis of DNA and protein at 5 months of age (Short Term DR 2). (A) (^2H_2O) was administered through AL access to drinking water for 2 weeks following IP injection. (B) Liver, heart, gastrocnemius and bone marrow were collected and (C) through a series of differential centrifugation steps and DNA extraction procedure, DNA was extracted and tissue separated into the mixed (consisting of primarily of contractile proteins), cytoplasmic and mitochondrial protein fractions. (D) It was possible to measure the rates of newly synthesised proteins and DNA, assessed through the incorporation of deuterium from body water (Adapted from Miller et al. 2014).

2.4.2 Tissue Isolation and DNA Extraction

Fractionation of heart, liver and skeletal muscle tissue was carried out according to a series of differential centrifugation steps, as described in previously published protocols (Robinson et al. 2010; Miller et al. 2012), under the supervision of, and with the assistance of collaborators at Colorado State University (CSU), CO, USA. Tissues were powdered using a pestle and mortar, under liquid nitrogen. Tissue was weighed out (50-70mg) and homogenised, using a bead homogenizer (Next Advance Inc., Averill Park NY), 1:10 in isolation buffer (100 mM KCl, 40 mM Tris HCl, 10 mM Tris Base, 5 mM MgCl2, 1 mMEDTA, 1 mM ATP, pH=7.5) with phosphatase and protease inhibitors (HALT, Thermo Scientific). Subcellular fractions of myofibrillar/mixed (Mixed; consisting of nuclei and of essential contractile components in muscle tissues), cytosolic (Cyto) and mitochondrial (Mito) proteins were isolated following homogenisation as previously described (Miller et al 2012, Miller et al 2015).

2.4.2 (A) Mixed (Myofibrillar) Fraction:

The homogenate was centrifuged at 4°C, 800 x g, for 10 minutes. The supernatant was removed for the isolation of the Mito fraction and the resulting pellet was washed with 500 µl 100% EtOH and spun at 100 x g for 1 minute. The supernatant was removed, discarded and subsequently washed with 5 00µl of dH2O, before being spun again at 100 x g for 1 minute. This series of wash steps was repeated once more.

2.4.2 (B) Mito Fraction:

The supernatant from the 800 x g spin was transferred to a fresh tube labelled Mito, and subsequently centrifuged at 9000 x g for 30 minutes. The supernatant was removed and set aside for the isolation of the Cyto fraction. The pellet from this spin contained the mitochondrial fraction to which 200 µl of mitochondrial buffer (100 mM KCl, 10 mM Tris HCl, 10 mM Tris Base, 1 mM MgCl2, 0.1 mM EDTA, 0.02 mM ATP, 1.5% (w/v) BSA, pH 7.5) was added followed by centrifugation at 8000 x g for 10 minutes at 4°C. The supernatant from this spin was discarded and 100 µl of mitochondrial buffer was added to the pellet, without resuspending, followed by centrifugation at 6000 x g for 10 minutes at 4°C. The supernatant from this spin was discarded and the remaining pellet was washed in 1 ml of water.

2.4.2 (C) Cyto Fraction:

Following the spin at 9000 x g for 30 minutes, 400 µl of supernatant was removed and transferred to a new tube labelled Cyto. An equal volume (400 µl) of 14% SSA was added to each Cyto tube for deproteinisation, followed by 1 hour incubation on ice. After the incubation the Cyto sample was centrifuged at 16000 x g for 10 minutes at 4°C. The supernatant was removed and discarded. Each pellet was washed with 500 µl 100% EtOH and centrifuged at 100 x g for 1 minute. The supernatant was removed, discarded and subsequently washed with 500 µl of dH2O, before being spun again at 100 x g for 1 minute. This series of wash steps was repeated once more.

The Mixed, Cyto and Mito samples were solubilized with the addition of 250 µl of 1M NaOH followed by incubation for 15 minutes on a shaker at 50°C at 900rpms to obtain a homogeneous solution.

2.4.2 (D) DNA Isolation

For DNA, ~8 µg of total DNA was extracted following the manufacturer's protocol (MiniDNA kit, Qiagen) from approximately 30 mg tissue. This process involved leaving the tissue overnight in lysis buffer at 37°C to access DNA in the nucleus. The sample was prepared, loaded to a spin column, and centrifuged, through a series of purification steps. The DNA was eluted, to ensure the removal of nuclei from the spin column, into 200µl TE buffer (10 mM Tris, 1 mM EDTA, pH 8.0) and stored at -20°C until preparation for analysis via GC/MS. Bone marrow suspension was centrifuged for 10 minutes at 2,000 x g. The pellet was treated the same as the tissue DNA isolation.

2.4.3 Sample Preparation and Analysis of derivatised amino acids via Gas chromatography–mass spectrometry (GC/MS).

To hydrolyse the protein samples, 3 ml (Cyto and Mix) or 750 µl (Mito) of 6N HCL was added to 13X100 glass tubes, labelled to correspond with the appropriate samples followed by incubation for 24 h at 120°C.

All subsequent steps described for this protocol were carried out by collaborators at CSU. The hydrolysates were ion exchanged, dried under vacuum, and resuspended in 1 ml molecular biology grade H_2O. Derivation of 500µl of suspended samples (500 µl acetonitrile, 50 µl 1M K2HPO4 (pH 11), and 20 µl of

pentafluorobenzyl bromide (Pierce Scientific, Rockford, IL)) was carried out, samples were sealed and left to incubate for 1h at 100°C. Ethyl acetate was used to extract derivatives. Through drying by N2 and subsequent vacuum centrifugation, the organic layer was removed, and samples were reconstituted in 1 ml of ethyl acetate prior to GC/MS analysis. Negative chemical ionisation (NCI) was used to analyse derivatised amino acids (AA) on a DB225 gas chromatograph column, with a starting temperature of 100°C, and increased to 220°C by increasing 10°C per minute. An Agilent 7890A GC coupled to an Agilent 5975C MS (Drake et al. 2014; Miller et al. 2012; Miller et al. 2013) was employed and mass spectrometry using NCI with helium as the carrier gas and methane as the reagent gas. The mass-to-charge ratios of 448,449 and 450 were recorded for the pentafluorobenzyl-N,N-di(pentafluorobenzyl) derivative of alanine. Primary daughter ions that included all of the original hydrocarbon bonds from the given amino acid, were represented by these mass-to-charge ratios. ^{2}H enrichment was calculated as set out in previously described protocols (Fanara et al. 2004). Briefly, a reaction with calcium carbide was used to transfer protons from plasma water to acetylene. Using a Series 3000 cycloidal mass spectrometer (Monitor Instruments, Cheswick, PA), modified to record ions at m/z 26 and 27 (M0 and M1) and calibrated against a standard curve prepared by mixing 99.9% $^{2}H_2O$ with unlabelled water. acetylene samples were analysed (Fanara et al. 2004). The newly synthesised fraction (f) of proteins was calculated from the true precursor enrichment (p) with plasma analysed for $^{2}H_2O$ enrichment and adjusted by mass isotopomer distribution analysis (MIDA: see Hellerstein & Neese 1999; Busch et al. 2006). Protein synthesis was calculated the change in enrichment of deuterium-labelled alanine (Busch et al. 2006) bound in muscle proteins over the entire labelling period and expressed as the common unit for protein synthesis rates ($\%*h^{-1}$) (Drake et al. 2015; Miller et al. 2013).

To determine body water enrichment, 125 µl of plasma was placed into the inner well of o-ring screw on cap and placed inverted on heating block overnight. Next, 2 µl of 10 M NaOH and 20 µl of acetone were added to all samples and 20 µl 0%–20% D_2O standards and capped immediately. Samples were vortexed at low speed and kept overnight at room temperature. Samples were extracted with addition of 200 µl hexane, and the organic layer was transferred through anhydrous Na_2SO_4 into gas chromatography vials and analysed via EI mode using a DB-17MS column.

2.4.4 DNA synthesis measurement

Determination of ^{2}H incorporation into purine deoxyribose (dR) of DNA was performed, as previously described (Drake et al. 2014; Neese et al. 2002; Miller et al. 2013), by collaborators at CSU. Nuclease S1 and potato acid phosphatase was used to hydrolyse DNA isolated from whole tissue at 37°C overnight. Pentafluorobenzyl hydroxylamine and acetic acid were reacted with hydrolysates and then acetylated with acetic anhydride and 1-methylimidazole. Dichloromethane extracts were dried, resuspended in ethyl acetate, and analysed by GC/MS as previously described (Drake et al. 2014; Neese et al. 2002; Miller et al. 2013), on a DB-17MS column with NCI, using helium as a carrier and methane as the reagent gas. Using ChemStation software, the fractional molar isotope abundances at m/z 435 (M0, mass isotopomer) and 436 (M1) of the pentafluorobenzyl triacetyl derivative of purine dR. The analysed sample and an unenriched pentafluorobenzyl triacetyl purine dR derivative standard, were referred to as sample and standard respectively. The fractional synthesis rate (f) was calculated by a comparison with bone marrow cells in the same animal, which represents an essentially fully turned over population of cells (Miller et al. 2012; Drake et al. 2013). The calculation for excess fractional M+1 enrichment (EM1) was:

$$EM1 = \frac{(\text{abundance}m/\text{z}436)\text{sample}}{(\text{abundance}m/\text{z}435 + \text{z}436)\text{sample}} - \frac{(\text{abundance}m/\text{z}436)\text{std}}{(\text{abundance}m/\text{z}435 + \text{z}436)\text{std}}$$

2.5 Statistical Analysis

All statistical analyses were performed using R and figures were produced using GraphPad Prism (GraphPad Inc., La Jolla, CA, USA, version 5) software. Data were checked for normality using the Shapiro–Wilks test and a logarithmic transformation was undertaken if data not normally distributed. Following transformation, if the data was not normally distributed an appropriate non-parametric test was applied. Results are reported as mean±standard error of the mean (SEM), with $p<0.05$ regarded as statistically significant.

A linear model (lm) was used for the analysis of the effect of either short-term or long-term DR. Strain and treatment were considered explanatory variables in the lm, with all experimental parameters input as single response variables and assessed within each strain; AL vs. DR. All non-significant interaction effects ($p > 0.05$) were removed to obtain the best-fit model in each case, with only significant interactions reported. Post-hoc Tukey tests were performed to examine directional differences, although it should be noted that these analyses do not take into account the treatment or treatment*strain effects. A one way ANOVA was used to assess strain effects within treatment AL and DR groups. For example AL treatment group as TejJ89 vs. TejJ48 vs. TejJ114 after 2 and 10 months of treatment. Results are reported as mean ± standard error of the mean (SEM), with n = 8 per group and with $p < 0.05$ regarded as statistically significant. * denotes $p < 0.05$, **$p<0.01$, ***$p<0.001$. t= treatment effect; t=$p<0.05$, tt=$p<0.01$, ttt denotes $p<0.001$, S= strain effect; S=$p<0.05$, SS=$p<0.01$, SSS denotes $p<0.001$.

2.5.1 Metabolic Characteristics:

WAT and BAT were corrected for body mass prior to analysis. The impact of short and long-term DR on starting body mass (g), end body mass (g), WAT/body mass (g), BAT/body mass, glucose tolerance, fed and fasting glucose levels, fasting plasma insulin, HOMA IR and fasting plasma IGF-1 levels was determined using an lm as described in section 2.5.

2.5.2 Mitochondrial Function:

Mitochondrial function was analysed the same way, by employing a linear model (lm) to determine oxygen consumption rate (OCR), ROS production, PGC-1-α, oxidative damage, antioxidant defence and the UPR^{mt} response following long-

term DR in liver, skeletal muscle or heart tissue. Nuclear and cytosolic PGC1-α protein levels, Tfam, OXPHOS and Heat shock proteins assessed by western blot were all normalised to total protein by Ponceau staining, prior to analysis.

2.5.3 Protein Synthesis:

% Fractional synthesis rates of proteins and % DNA synthesis rates for skeletal muscle, heart and liver were determined by collaborators at CSU. From the synthesis rates of protein and DNA, the ^{new}protein/^{new}DNA ratio was calculated. A two way ANOVA was employed by collaborators in order to determine treatment and strain effects in each tissue. I repeated the analysis here using a linear model to ensure consistency between previous analyses, although lm and 2 way ANOVA are essentially the same test.

Chapter 3: The impact of short and long-term dietary restriction on metabolic characteristics in female recombinant inbred ILSXISS mice

3.1 Abstract

To investigate potential differences underlying the DR response in female ILSXISS RI mice, I examined several metabolic parameters in strain TejJ89 (lifespan increased under DR), TejJ48 (lifespan unaffected by DR) and TejJ114 (lifespan decreased under DR) following short- (2 months) and long-term (10 months) 40% DR. Short-term DR decreased body mass (BM) in all strains, with largest losses observed in strain TejJ114. White adipose tissue (WAT) and brown adipose tissue (BAT) were not reduced by DR, although surprisingly WAT was higher in strain TejJ114 relative to AL controls. Following long-term DR BM was reduced in all strains, again with largest losses reported in strain TejJ114. WAT levels were unaffected by DR in TejJ89 and TejJ48 relative to strain-specific AL controls, but decreased by DR in TejJ114. BAT was increased in strain TejJ89 with long-term DR but unchanged in TejJ48 or TejJ114. Short-term DR decreased fed and fasting blood glucose levels in TejJ48, and increased fasting blood glucose in strain TejJ114. No alterations in any parameters of glucose homeostasis were changed with short-term DR in strain TejJ89. Following long-term DR fasting blood glucose was increased in all three strains, and fed blood glucose was reduced in TejJ48 and TejJ114 but unchanged in TejJ89. Surprisingly strain TejJ89 had increased insulin resistance, as measured by HOMA IR, and were hyperinsulinaemic compared to TejJ48 and TejJ114 following DR, with no changes in insulin resistance or insulin levels apparent in the other strains. Moreover, short or long-term DR had no effect on insulin-like growth factor-1 (IGF-1) levels in any strain. My findings indicate that reductions in WAT were associated with reduced lifespan of TejJ114 mice under 40% DR, while ability for strain TejJ89 to maintain WAT teamed with an increase in BAT mass, may be important to lifespan extension. These strain-specific differences in body composition may underlie the reported lifespan truncation of TejJ114 mice to DR. Surprisingly I report a delineation in the response of glucose, insulin and IGF-1 mice and find no evidence to suggest that improved glucose homeostasis is necessary for lifespan extension with DR.

3.2 Introduction

The impact of dietary restriction (DR) on organisms is multifarious, from effects on whole-animal physiology to changes at the tissue, organelle and molecular level. Not only is DR well established as a means of lifespan extension (Fontana & Partridge 2015; Masoro 2005; Speakman & Mitchell 2011) but it also induces positive effects on healthspan, such as affording protection against disease (Omodei & Fontana 2011), including in human subjects (Fontana et al. 2004; Cava & Fontana 2013). Ageing in mammals is characterised by an overall increase in adiposity (Huffman & Barzilai 2009) and an impairment in glucose tolerance and insulin resistance (DeFronzo 1981; Stout 1994), with both short and long-term DR found to ameliorate these age-related features (Mitchell et al. 2015a; Mitchell et al. 2016; Hempenstall et al. 2010). Consequently, reductions in adiposity and improvements in glucose homeostasis following DR have been proposed as being critical to DR's beneficial effects on lifespan and healthspan (Berg & Simms 1960; Barzilai & Gupta 1999b; Masoro et al. 1992). However, despite DR being the most widely used intervention used to slow ageing the precise mechanism(s) underlying the beneficial effects of DR on lifespan and healthspan have yet to be defined. To further complicate the picture, the status of DR as a ubiquitous means of lifespan extension is in some dispute, with evidence suggesting that DR does not increase lifespan in all species, such as flies or rotifers, (Carey et al. 2002; Cooper et al. 2004; Kirk 2001), or all murine strains (Harper et al. 2006; Sohal et al. 2009; Rikke et al. 2010; Liao et al. 2010). Genetic background, gender and magnitude of DR are emerging as key determinants in lifespan extension, suggesting that the mechanisms involved in DR-induced longevity, and the overlapping processes involved in ageing, may be more complex than first thought (Mitchell et al. 2016; Hayflick 2010; Selman 2014a).

3.2.1 DR and Genetic Background

C57BL/6 mice are the most widely used murine model in ageing research, showing repeatable pro-longevity effects under DR (Turturro et al. 1999; Weindruch & Walford 1988). Accumulating evidence has implicated genetic background as a potentially important factor that mediates DR response (Selman 2014b; Mulvey et al. 2014; Partridge 2012; Swindell 2012), with several studies reporting little or no effect of DR on lifespan (Fernandes et al. 1976; Forster et al. 2003; Goodrick et al. 1990; Harper et al. 2006; Harrison & Archer 1987; Liao et al. 2010; Rikke et al.

2010), which in turn raises the question as to whether the relationship between DR and lifespan can be accurately inferred from studies of a single genotype. For example, the DBA/2 mouse was once considered to have an ambiguous longevity response with DR, with reports of no effect (Fernandes et al. 1976) and negative impact on lifespan (Forster et al. 2003). However, recently it has been proposed that responses to DR are context dependent, and that the ideal context for DR is mediated by factors such as genotype and/or gender (Mitchell et al. 2016). Indeed, DBA/2 mice subject to 20% DR had an improved survival outcome over 40% DR, relative to AL controls. The DBA/2 mouse was not only responsive to DR but also had a strain-specific optimal magnitude of DR, which may explain some previously reported unresponsiveness in this strain (Mitchell et al. 2016). In addition this study highlighted the importance of gender in DR response, reporting a number of sexually dimorphic outcomes. For example, C57BL/6 females did not show DR induced lifespan extension with 40% DR, relative to AL controls, unlike male DR counterparts. DR studies have traditionally been biased towards the use of male mice, making it difficult to accurately predict female response, and identify public modulators of ageing. Genetic background was unequivocally linked to survival outcome following 40% DR based on reports from two independent studies studying ILSXISS recombinant inbred (RI) mice. These genetically heterogeneous strains exhibit extensive genetic variation in the lifespan response to DR (Liao et al. 2010; Rikke et al. 2010), from lifespan lengthening to lifespan shortening. Furthermore, the genotype-dependent response of the ILSXISS mice provide a comparative model to examine the role of candidate mechanisms in life extension with DR, and provide insight into how these mechanisms may be regulated during slowed ageing.

3.2.2 DR, Body Mass and Ageing

DR leads to a reduction in body mass as well as alterations in body composition and adiposity. Reports of reduced BM are widespread across taxa and extend to both non-human primates and humans (Mattison et al. 2017; Fontana et al. 2004). Similarly reductions in adiposity are widely reported with DR, specifically reductions in visceral fat such as the white adipose tissue (WAT) (Mitchell et al. 2015a). As a result reductions in BM and adiposity have been proposed to underlie DR-induced longevity (Berg & Simms 1960; Muzumdar et al. 2008). Reductions in WAT appear to be a key component of longevity induced by DR, as mice manipulated to have reduced levels of WAT are long-lived and protected from age-

related obesity (Blüher et al. 2003). Surgical excision of visceral fat both ameliorates insulin resistance (Barzilai et al. 1998; Das et al. 2004) and increases longevity in one strain of rat (Muzumdar et al. 2008) and high levels of visceral fat are associated with an increased risk of type 2 diabetes and mortality (Carey et al. 1997; Wang et al. 2005; Nicklas et al. 2006; Ross et al. 2008). However, not all fat depots are reduced with DR. Brown adipose tissue (BAT), for instance, is subject to an age-related reduction in mass, yet DR has been found to slow this decline (Valle et al. 2008). In addition to this, higher levels of BAT mass are associated with a leaner phenotype, and reduced insulin resistance (Lowell et al. 1993; Mattson 2010; Rogers et al. 2012) and DR has been proposed as driving a shift from WAT to BAT stores as a source of energy (Dionne et al. 2016; Okita et al. 2012; Fabbiano, Suarez-Zamorano, et al. 2016). A recent study found 40% DR in male C57BL/6 and BALB/C mice promoted the development of beige fat (Fabbiano, Suarez-Zamorano, et al. 2016) suggesting that promotion of brown fat development as a potentially common feature of DR, and involved in the prolongevity effect.

However, the impact of DR on BM and adiposity is not a straightforward one, and genotype appears important. Strain-specific differences in BM and body composition exist under both AL and DR conditions. For instance, under AL conditions DBA/2 mice with unrestricted access to normal chow have higher weight gain and larger fat depots compared to age-matched C57BL/6 and 129T2 mice (Funkat et al. 2004). In addition to this strain-specific losses of fat in the ILSXISS RI following 40% DR have been reported previously (Liao et al. 2011). These losses have been found to correlate to lifespan data for these strains, such that increased lifespan was associated with increased fat mass, while conversely lifespan shortening was linked to reduced fat mass following DR. This resulted in the proposal that maintenance of adiposity with DR, instead of reduction of fat (as proposed by Berg & Simms 1960), is key to DR induced lifespan extension. Moreover, this positive correlation between fat mass and lifespan has been reported in a number of rodent studies, including wild mice, C57BL/6 mice, DBA/2 mice and F344 rats (Harper et al. 2006; Mitchell et al. 2016; Bertrand et al. 1980). While changes in adiposity with DR have been previously examined in ILSXISS mice (Liao et al. 2011), changes in WAT and BAT mass have yet to be determined. Therefore the question as to how alterations in body mass and adiposity relate to lifespan extension with DR, and the role genotype plays, remains to be elucidated.

3.2.3 Glucose Homeostasis

Glucose intolerance and insulin resistance are well characterised hallmarks of mammalian ageing (Masoro 2005; Barzilai et al. 2012), and enhanced glucose tolerance, reduced fasting levels of insulin and insulin-like growth factor (IGF-1) and insulin sensitivity, have all been observed under DR (Anson et al. 2003; Argentino et al. 2005; Colman et al. 2014; Mattison et al. 2017). Enhanced glucose homeostasis, in particular increased insulin sensitivity, has been considered a conserved characteristic of DR in mammals and has led to the proposal that maintenance of glucose homeostasis as a key underlying mechanism of DR-mediated lifespan extension (Barzilai et al. 1998; Barzilai et al. 2012).

Improvements to glucose tolerance and insulin sensitivity are almost universally associated with DR response (Anson et al. 2003; Masoro 2009; Speakman & Mitchell 2011). However, a number of strain-specific differences have been reported in murine strains following DR and may relate to lifespan response. The DBA/2 mouse for example has a number of metabolic differences when compared to the C57BL/6 strain both under AL and DR conditions (Kooptiwut et al. 2002; Andrikopoulos et al. 2005; Goren et al. 2004). Under short-term 30% DR male DBA/2 mice are hyperinsulinaemic and relatively insulin resistant, but with improved glucose tolerance, and reduced fed blood glucose levels relative to the C57BL/6 strain (Hempenstall et al. 2010). Moreover, the impact of gender is emerging as key in DR response. Female DBA/2 mice, unlike male counterparts, reportedly have no changes in circulating insulin levels following 20% or 40% DR (Mitchell et al. 2016). This may indicate that improvements in insulin sensitivity are not important to survival outcome in female mice following DR. In contrast to fasting plasma insulin, IGF-1 appears much more responsive to DR, with reductions observed in both strains, under short and long-term DR (Hempenstall et al. 2010; Mitchell et al. 2016). Thus IGF-1 may be a more relevant candidate for driving DR-induced longevity. To the best of our knowledge the metabolic phenotype of ILSXISS recombinant inbred (RI) mouse strains has not been examined. Previously strain-specific differences in body temperature and fat maintenance in the ILSXISS mice have been described in response to 40% DR and have been found to correspond to lifespan data of these strains (Liao et al. 2011; Rikke et al. 2003). Investigations into the strain-specific responses with short and long-term DR in ILSXISS mice will offer insight as to

whether improvements to glucose homeostasis underlies enhanced longevity with DR.

3.2.4 Predictions and Aims

In order to investigate the physiological correlates of DR, a comparative approach was employed utilising the strain-specific longevity observed in ILSXISS RI mouse strains under 40% DR (Liao et al. 2010; Rikke et al. 2010). We examined the response of three strains of age-matched female ILSXISS mice following short (animals were 5 months of age, maintained on DR for a period of 2 months) or long-term (animals were 13 months of age, maintained on DR for a period of 10 months) 40% DR initiated at 3 months of age. Body weight, fat mass (weight of gonadal WAT and interscapular BAT depots) and glucose homeostasis (glucose tolerance, fed and fasting blood glucose, fasting plasma insulin levels, insulin sensitivity, insulin resistance and fasting plasma IGF-1 levels), were determined. We compared females from strain TejJ89 (increased lifespan with DR relative to AL fed controls), TejJ48 (lifespan unaffected by DR) and TejJ114 (lifespan reduced with DR), which have shown repeatable responses to DR across two independent studies (Rikke et al. 2010; Liao et al. 2010). We predicted that DR would positively influence body composition and enhance glucose homeostasis in strain TejJ89 that DR would have no effect on these parameters in strain TejJ48, and that DR would be detrimental to these parameters, and negatively impact glucose homeostasis, in the negative responder TejJ114.

3.3 Materials and Methods

3.3.1 Animal Husbandry, Dietary Restriction (DR) and Experimental Design

This study used 3 ILSXISS recombinant inbred (RI) mouse strains originally developed to analyse genetic variation in alcohol sensitivity (Williams et al. 2004). The animal husbandry was described in Chapter 2 (Figure 2.1). Briefly, these strains have well documented lifespan responses under both *ad libitum* (AL) feeding conditions and 40% DR (Liao et al. 2010; Rikke et al. 2010). Mice from three of these strains; TejJ89 (increase in lifespan with DR; positive responder), TejJ48 (no effect of DR on lifespan; non-responder) and TejJ114 (decrease in lifespan with DR; negative responder) were purchased from a commercial breeder (The Jackson Laboratory, Bar Harbour, Maine, URL: http://www.informatics.jax.org).

Mice were kept in groups of 4 post-weaning in shoebox cages (48cm×15cm×13cm), with AL access to water and standard chow (CRM(P), Research Diets Services, LBS Biotech, UK; Atwater Fuel Energy- protein 22%, carbohydrate 69%, fat 9%) and maintained on a 12L/12D cycle (lights on 0700–1900h) at an ambient temperature of 22±2°C. At 9 weeks of age, cages were randomly assigned to either an AL or DR group, with no difference in body mass observed between treatment groups at this time (TejJ89 AL vs. DR $t=0.056$, $p=0.583$, TejJ48 AL vs. DR $t=0.677$, $p=0.509$, TejJ114 AL vs. DR $t=0.289$, $p=0.777$). Mice were introduced to DR in a graded fashion (as described in Hempenstall et al. 2010); at 10 weeks of age mice were exposed to 10% DR (90% of AL feeding), at 11 weeks this was increased to 20% DR, and from 12 weeks of age, until the termination of the experiment, mice were exposed to 40% DR, relative to their appropriate strain-specific AL controls. Mice were maintained on 40% DR for a period of either 2 months (equivalent to 5 months of age), or 10 months (equivalent to 13 months of age), (See Figure 2.4 for schematic of experimental design in Chapter 2). We defined 2 months of 40% DR as short-term DR and 10 months of 40% DR as long-term DR and n was 8 mice per group.

There were two distinct cohorts termed Short-term 1 and Long-term. Short-term 1 animals were culled following 2 months of AL or DR feeding (short-term) in November 2014. Long-term animals were maintained on an AL or DR regime for a period of 10 months (long-term) and culled in April 2015, thus both cohorts were analysed on different occasions. The extent of the long-term DR protocol was based

on previously published lifespan data on these strains following DR (Rikke et al. 2010; Liao et al. 2010) (see Figure 3.2). Hence 10 months of DR was fixed as the upper limit of restriction in this study in order to examine the effect of DR on candidate mechanisms of enhanced ageing and not late life pathology, given the reported truncation of lifespan in strain TejJ114 with 40% DR, approximately 400 days median lifespan with DR. Total food intake of AL mice from each strain was measured weekly (±0.01g) and food intake of the DR cohort calculated from the average AL intake per mouse over the preceding week (Hempenstall et al. 2010). DR mice were fed daily at 1800hrs, with the food placed directly onto the cage floor in order to reduce any competition for the food. No evidence of fighting or dominance hierarchies was observed in any cage.

Following short and long-term DR, both, AL and DR mice were fasted overnight and then culled by schedule one cervical dislocation. Mice were decapitated and trunk blood was collected. Fasting blood glucose was recorded with a glucometer (OneTouch Ultra, Lifescan, UK). The remaining blood pipetted into an EDTA coated tube, and spun at 10,000 x g for 10 minutes at 4°C, with the resultant supernatant (plasma) collected. All plasma samples were stored at -80°C. A total of 4 mice per day were culled a day and samples for mitochondrial studies (as described in Chapter 4) were collected. All experiments were carried out under a licence from the UK Home Office (Project Licence 60/4504) and followed the “principles of laboratory animal care” (NIH Publication No. 86-23, revised 1985)

3.3.2 Body Mass, Food intake and Adiposity

Body mass (BM) was measured daily for 8 weeks from the introduction of 10% DR, and weekly thereafter, for both AL and DR mice. BM and food intake were measured at the same time, on the same day, every week. Adiposity was measured by collecting and weighing (±0.001g) gonadal WAT and BAT, which were subsequently snap frozen liquid nitrogen and stored at -80°C.

3.3.3 Fed glucose, fasting glucose and glucose tolerance

Glucose tolerance was determined after an overnight fast, described in full in Chapter 2, section 2.2.2. All animals (AL and DR) were fasted overnight in a fresh cage with AL access to water (1800 to 0800hrs) following short and long-term DR.

DR mice were fed at ~1500hrs on the afternoons immediately prior to a glucose tolerance test (GTT), to ensure feeding prior to the overnight fast (Hempenstall et al. 2010). Glucose tolerance was measured according to standard protocols (as described in Chapter 2) (Selman et al. 2008; Lees et al. 2015). Mice were weighed and a fasting blood glucose measurement was taken with a blood glucose strip using a glucometer (OneTouch Ultra, Lifescan, UK). Mice were injected intraperitoneally (IP) with 20% D-glucose (2g kg^{-1}) and blood glucose levels collected from tail vein samples as previously described (Cantley et al. 2009). Glucose tolerance was expressed as the area under the curve over a 120 minute period following the IP injection of glucose. Fed blood glucose was recorded with a blood glucose strip using a glucometer. Blood from AL mice was collected at 1100hrs and from DR mice at 1800hrs, following an early feeding at 1500hrs, to ensure mice were post-prandial (Hempenstall et al. 2010).

3.3.4 Fasting plasma insulin levels, insulin sensitivity and IGF-1 levels

Fasting plasma insulin levels were determined using a mouse insulin ELISA kit (EMD Millipore Corporation, USA Catalogue #EZRMI-13K). Insulin sensitivity was estimated using the updated homeostatic model assessment (HOMA2) model (Wallace et al. 2004), a method used to quantify insulin resistance from fasting glucose and insulin concentrations. Fasting plasma IGF-1 levels were determined using a mouse IGF-1 ELISA kit (Catalogue# MG100, Quantikine, R and D Systems Inc., USA).

3.3.5 UCP-1 protein levels

Protein was extracted from liver tissue as described in Chapter 2 (section 2.3.3). Equal volumes of tissue protein extract (50 µg) in Laemmli sample buffer were loaded onto 4–12% Bis-Tris pre-cast polyacrylamide gels (Life Technologies, Paisley, UK). Following this, proteins were transferred to polyvinylidene difluoride membranes (BioRad). Ponceau staining (Thermo Fisher Scientific, UK) was used to ensure equal loading of protein and for normalisation purposes. Membranes were incubated in Tris-buffered saline Tween (1X TBST) containing 5% BSA for 1 h^{-1}. Blots were then washed in TBST (5 × 5min), incubated with primary antibody for 24 h^{-1} (4 °C), washed again (TBST) and incubated with secondary antibody for 1 h^{-1} at

room temperature. Blots were visualised using Clarity™ Western ECL Substrate (BioRad) and a ChemiDoc™XRS system (BioRad). Antibodies for uncoupling protein -1 and secondary (anti-rabbit) antibodies were purchased from Abcam (Cambridge, UK) and Santa Cruz Biotechnology Inc. (Santa Cruz, CA, USA) respectively.

3.3.6 Statistical Analysis

All statistical analyses were performed using R and Graphpad Prism (GraphPad Inc., La Jolla, CA, USA, version 5). Figures were produced using GraphPad Prism software. One-way analysis of variance and linear modelling (lm) were used as appropriate. Lm was employed with strain (TejJ89, TejJ48, TejJ114) and treatment (AL or DR) as fixed factors. All non-significant variables ($p>0.05$) were removed from the lm analyses in order to obtain the minimum adequate model. Multiple comparisons were obtained through Tukey's post-hoc test. Data were checked for normality using the Shapiro–Wilks test and a logarithmic transformation was undertaken if data not normally distributed. Results are reported as mean±standard error of the mean (SEM), with $p<0.05$ regarded as statistically significant.

3.4 Results

Table 3.1 denotes treatment effects on a range of metabolic parameters following short- and long-term 40% DR.

Table 3.1 Summary of treatment effects within each strain (AL vs DR)

Strain	Duration	BM	WAT	BAT	Fasting B.G.	Fed B.G.	AUC	Fasting Insulin	HOMA IR	IGF-1
TejJ 89	ST	↓	ns	ns	ns	ns	ns	ns	ns	ns
TejJ 48	ST	↓	ns	ns	↓	↓	ns	ns	ns	ns
TejJ 114	ST	↓	↑	ns	↑	ns	ns	ns	ns	ns
TejJ 89	LT	↓	ns	↑	↑	ns	ns	ns	↑	ns
TejJ 48	LT	↓	ns	ns	↑	↓	ns	ns	ns	ns
TejJ 114	LT	↓	↓	ns	ns	↓	ns	ns	ns	ns

ST = Short-term DR

Long-term DR

ns=non-significant

↓= decreased with DR

↑= increased with DR

Fasted B.G = Fasting blood glucose

Fed B.G = Fed blood glucose

AUC = Area under the Curve

F. Insulin = Fasting insulin

3.4.1 Effects of Short-term DR on the metabolic phenotype of female ILSXISS mice

3.4.1 (A) Body Mass

Initial body mass (BM) (Figure 3.1), prior to introduction of DR protocol, was dependent on strain, with strain TejJ114 being significantly lighter at 9 weeks of age than either strain TejJ89 ($t=4.569$, $p<0.001$) or strain TejJ48 ($t=-6.539$, $p<0.001$). No difference was observed between strains TejJ89 and TejJ48 ($t=-0.374$, $p=0.7108$). BM across all 3 strains was significantly reduced, relative to their appropriate *ad libitum* (AL) controls, following 1 week of 20% DR (12 weeks of age), and remained significantly reduced in the DR mice for the remainder of the study (Figure 3.2A-C; TejJ89 $t=4.404$, $p<0.001$ (Fig. 3.2A), TejJ48 $t=3.182$, $p=0.007$ (Fig. 3.2B), TejJ114 $t=2.606$, $p=0.021$ (Fig. 3.2C)). A significant treatment ($F= 77.66$, $p < 0.001$), strain ($F = 20.41$, $p < 0.001$) and an interaction effect, between treatment and strain, ($F= 3.323$, $p = 0.0456$) on BM was observed following 2 months of DR (Figure 3.3 A).

At the termination of the experiment (5 months of age), no strain-specific differences in BM was observed in the AL mice (Figure 3.3 B), but a significant strain-specific effect was detected in the DR mice (Figure 3.3C; $F=4.562$, $=0.031$); strain TejJ114 lost significantly more BM under 40% DR when compared with strains TejJ89 and TejJ48, with strain TejJ89 having the highest BM following short-term DR. When expressed as percentage loss in BM relative to the relevant AL mice, strain TejJ114 lost a greater percentage (~22%) of BM compared to either strain TejJ89 (~12%) or strain TejJ48 (~18%). No differences in average weekly food intake were detected over the duration of the study in the AL mice (Figure 3.4).

.

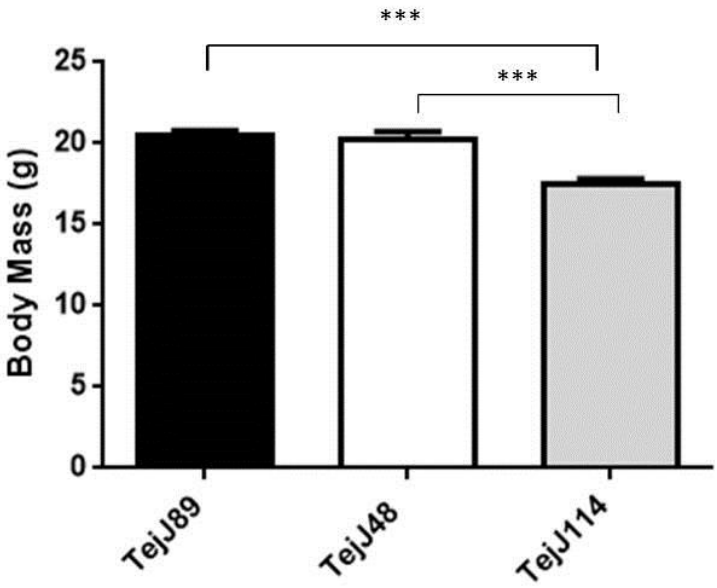

Figure 3.1: Initial body mass (BM) of strains TejJ89, TejJ48 and TejJ114 immediately before the start of the DR experiment (9 weeks of age) TejJ114 was significantly lighter than the other 2 strains at this time. Values are expressed as mean ± SEM, with n = 8 per group, *** denotes $p<0.001$.

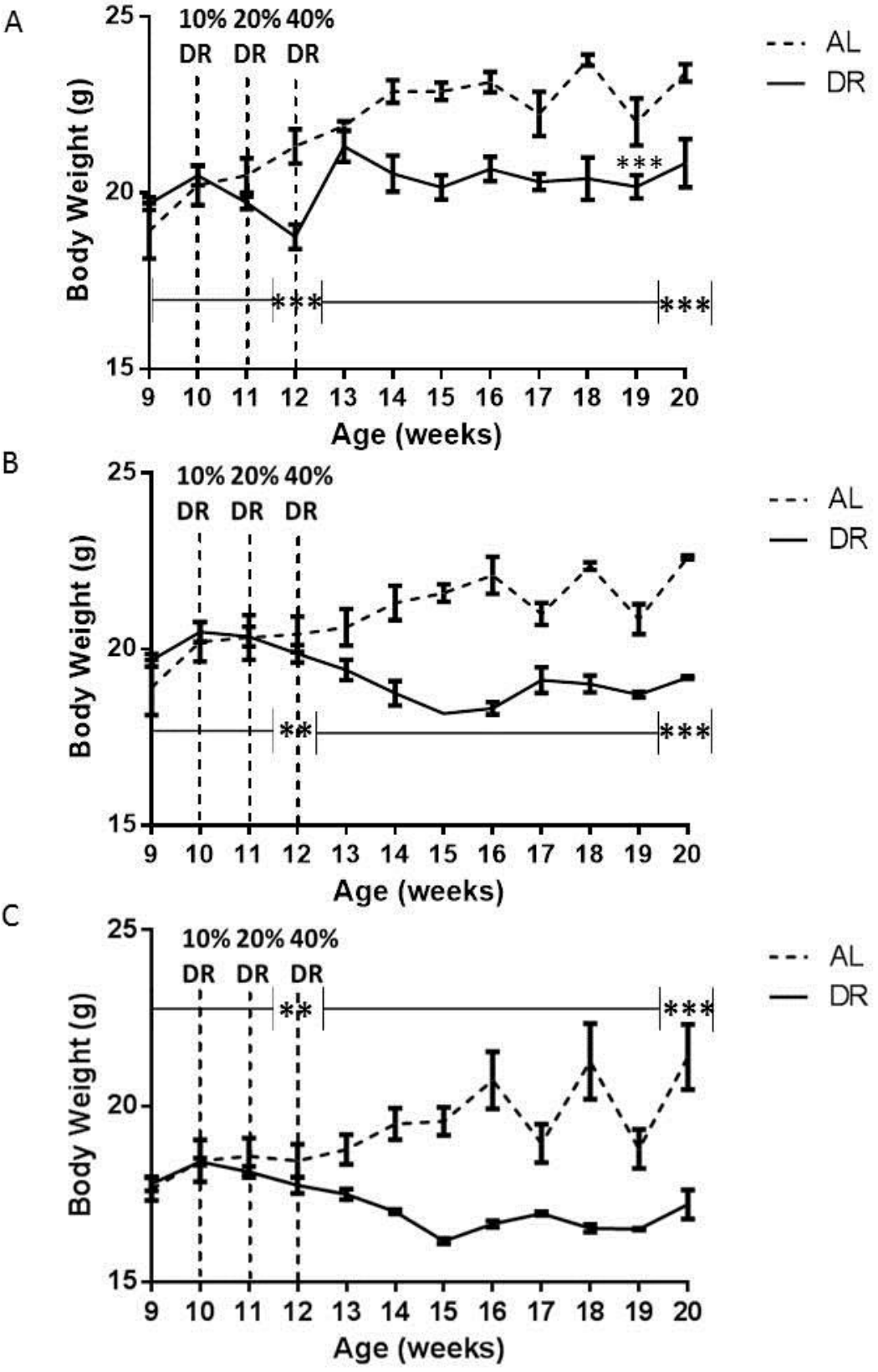

Figure 3.2: Body mass (BM) of female TejJ89 (A), TejJ48 (B) and TejJ114 (C) ILSXISS mice fed an *ad libitum* (AL) or 40% dietary restricted (DR) diet for 2 months. Values are expressed as mean ± SEM, with n = 8 per group. * denotes **p<0.01, ***p<0.001.

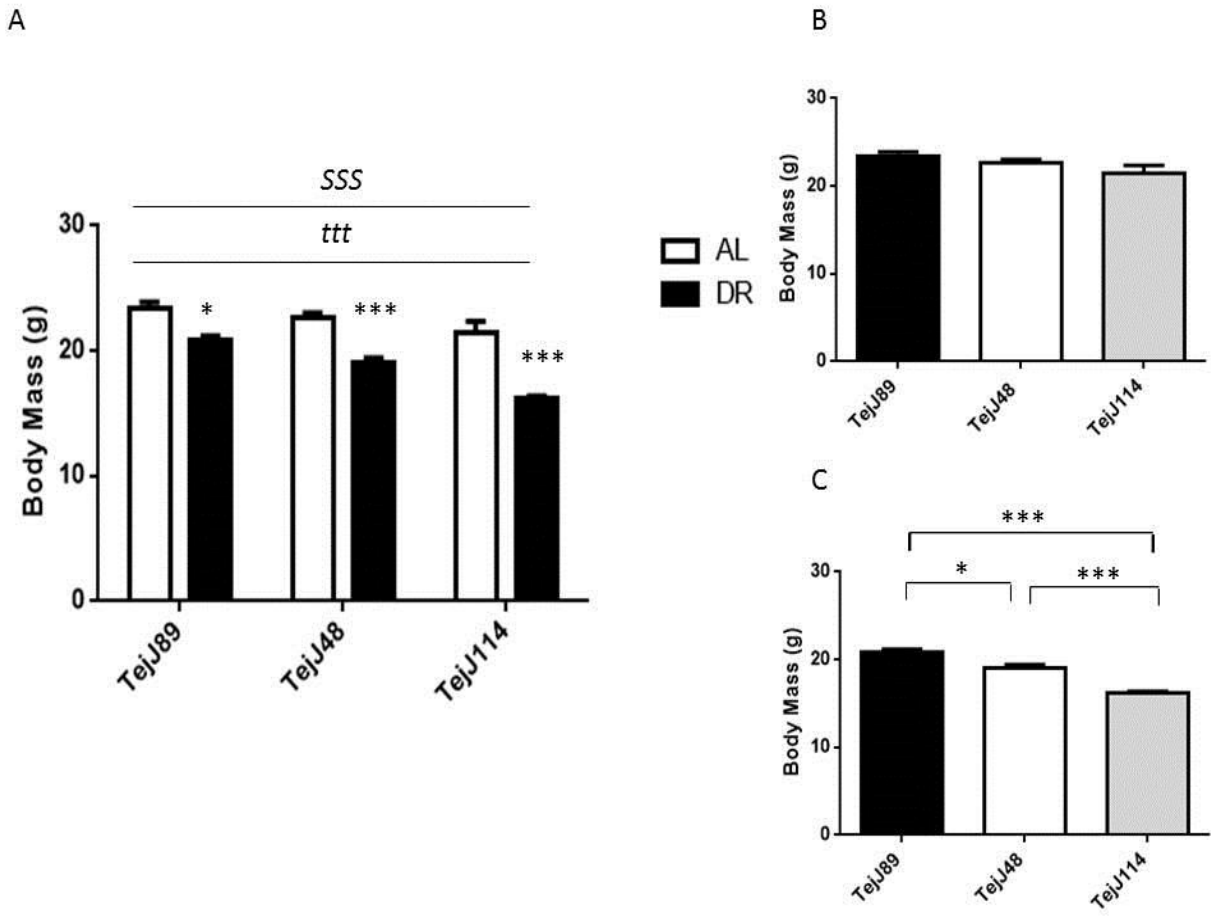

Figure 3.3: Body mass (BM) of female TejJ89, TejJ48 and TejJ114 ILSXISS mice fed an *ad libitum* (AL) or 40% dietary restricted (DR) diet for 2 months. (A) BM was significantly reduced in all strains of mice following DR. (B) No strain-specific differences in BM were observed within AL mice, but within the DR group (C) a significant strain-effect was detected in BM. Values are expressed as mean ± SEM, with n = 8 per group. * denotes $p < 0.05$, **$p<0.01$, ***$p<0.001$. t= treatment effect; ttt denotes $p<0.001$, S= strain effect; SSS denotes $p<0.001$.

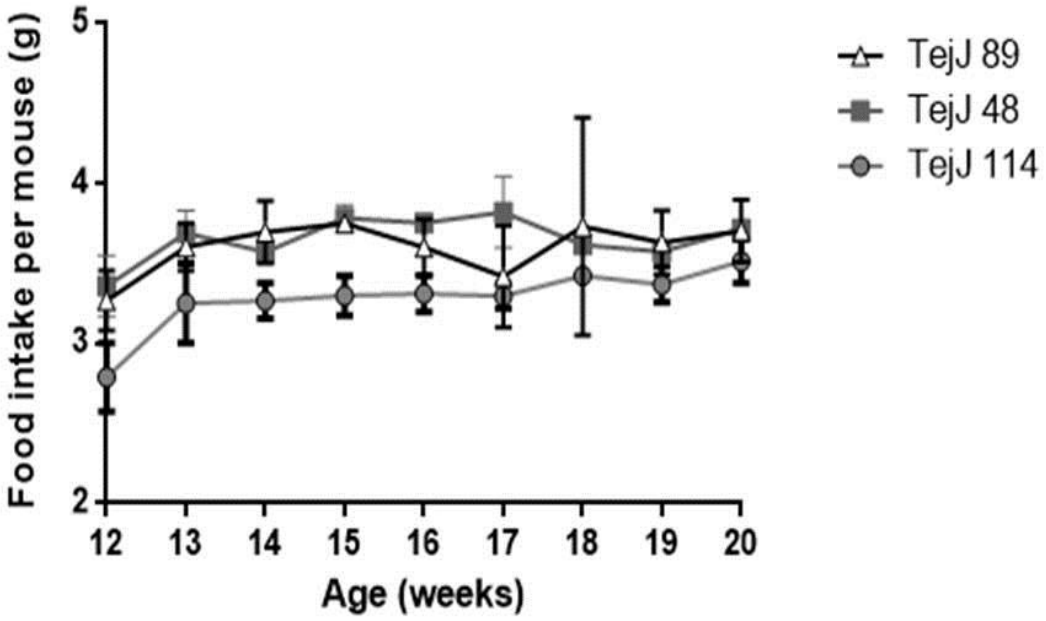

Figure 3.4: Food intake per mouse (g) of AL female ILSXISS mice from 12 weeks of age until 20 weeks of age. No differences in food intake were observed at any point between any strains. Values are expressed as mean ± SEM, with n = 8 per group.

3.4.1 (B) White Adipose Tissue

Gonadal white adipose tissue (WAT) data was corrected for BM and all analysis performed on corrected data. WAT mass (expressed as a percentage of BM) was affected by treatment ($F=16.24$, $p<0.001$), strain ($F=9.563$, $p<0.001$) and a significant treatment*strain interaction was also observed ($F = 8.603$, $p= 0.001$) following short-term DR (Figure 3.5 A). Strain TejJ114 was found to have increased gonadal fat mass under DR relative to its AL control ($p<0.001$). While no strain specific-differences were apparent between the AL group (Figure 3.5 B), a significant strain effect was detected between the DR mice ($F=13.18$, $p<0.001$), with strain TejJ48 having a reduced WAT mass relative to both TejJ89 ($p<0.05$) and TejJ114 ($p<0.001$), (Figure 3.5 C).

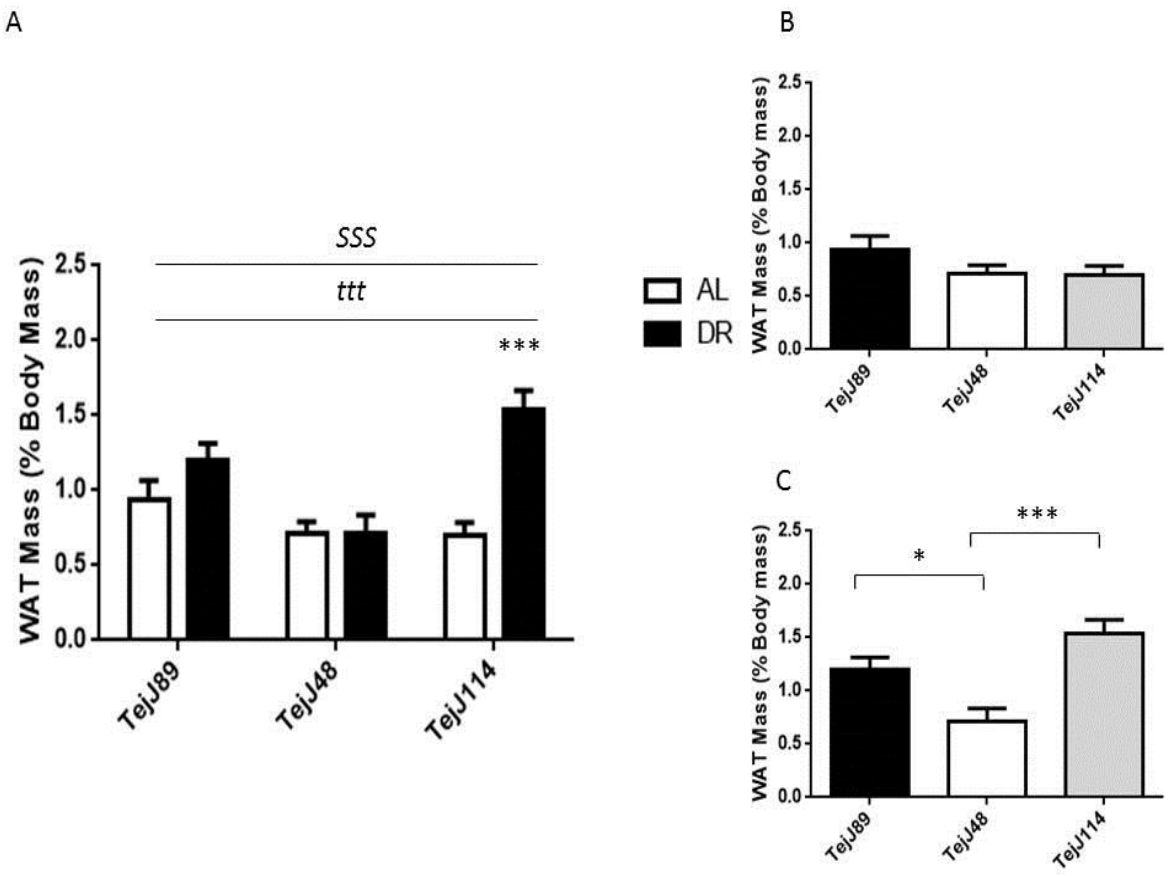

Figure 3.5: Gonadal white adipose tissue (WAT) mass of female TejJ89, TejJ48 and TejJ114 ILSXISS mice fed an *ad libitum* (AL) or 40% dietary restricted (DR) diet for 2 months (A). WAT was increased with DR in strain TejJ114. (B) WAT levels in the AL and (C) DR mice. Values are expressed as mean ± SEM, with n = 8 per group. * denotes $p < 0.05$, ***$p<0.001$, t= treatment effect; ttt denotes $p<0.001$, S= strain effect; SSS denotes $p<0.001$.

3.4.1 (C) Brown Adipose Tissue

Brown adipose tissue (BAT) data was corrected for BM and all analysis performed on corrected data. No treatment effect was observed following short-term DR on interscapular BAT mass (expressed as a % of body mass), (Figure 3.6 A). A significant strain effect was detected overall ($F = 4.312$, $p = 0.022$), however when analysed independently of treatment no strain effects were apparent within the AL mice (Figure 3.6 B) or DR animals (Figure 3.6 C).

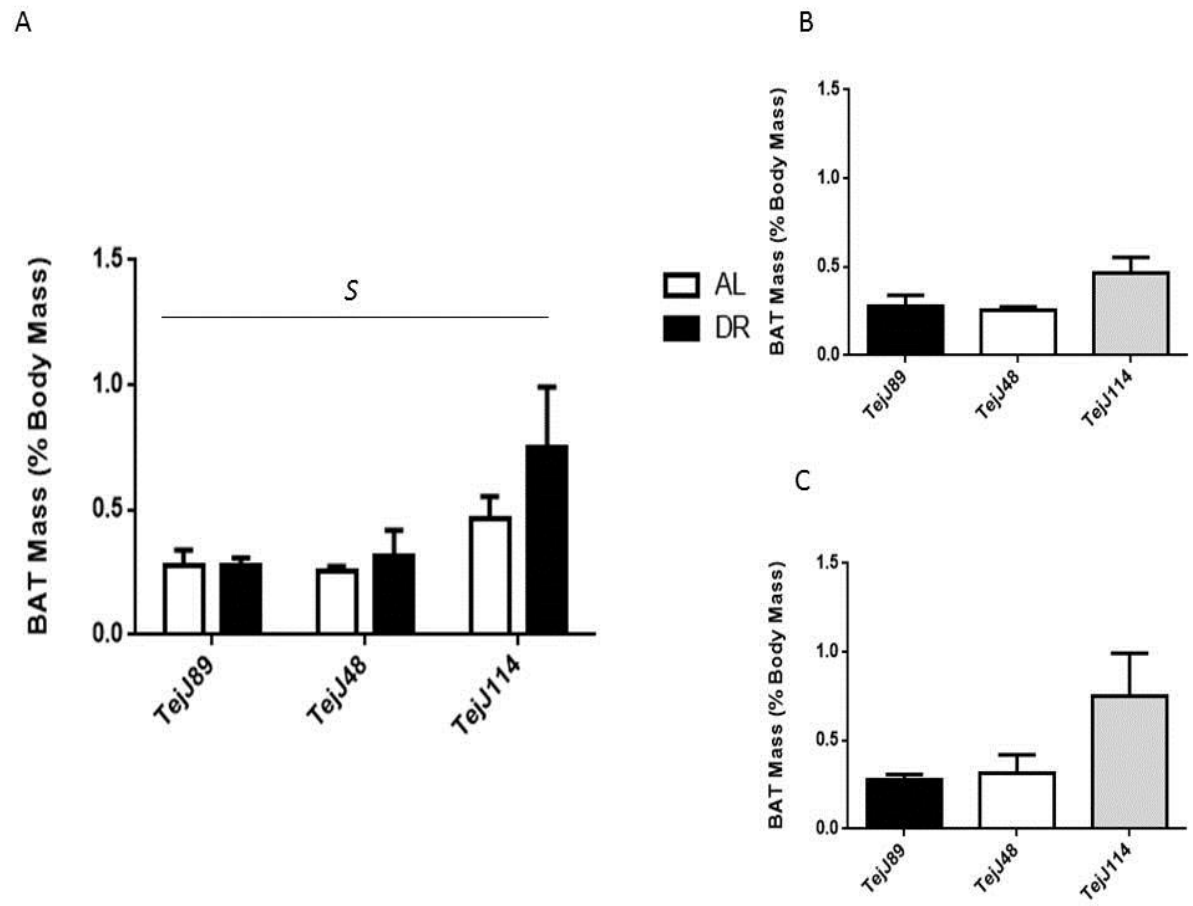

Figure 3.6: Brown adipose tissue (BAT) mass in female ILSXISS mice following 2 months of 40% DR or AL feeding (A). No changes in BAT were observed in the AL (B) or DR (C) mice. Values are expressed as mean ± SEM, with n = 8 per group. S= strain effect; SSS denotes $p<0.05$.

3.4.1 (D) Fasting blood glucose

Significant treatment ($F=8.65$, $p=0.005$), strain ($F=3.547$, $p=0.037$) and an interaction between treatment and strain ($F= 24.9$, $p<0.001$) on fasting blood glucose (FBG) levels was observed following short-term DR (Figure 3.7 A). FBG levels were significantly decreased under DR in strain TejJ48 ($p<0.05$) but increased significantly by DR in strain TejJ114 ($p<0.001$) relative to AL controls. Within AL mice strain had a significant effect on FBG ($F=38.55$, $p<0.001$) with an elevated FBG observed in strain TejJ48 compared to the other two strains (Figure 3.7 B). Within DR mice, strain-specific differences were similarly apparent ($F=3.889$, $p=0.036$), but strain TejJ114 having a higher FBG level compared to strain TejJ48 (Figure 3.7 C).

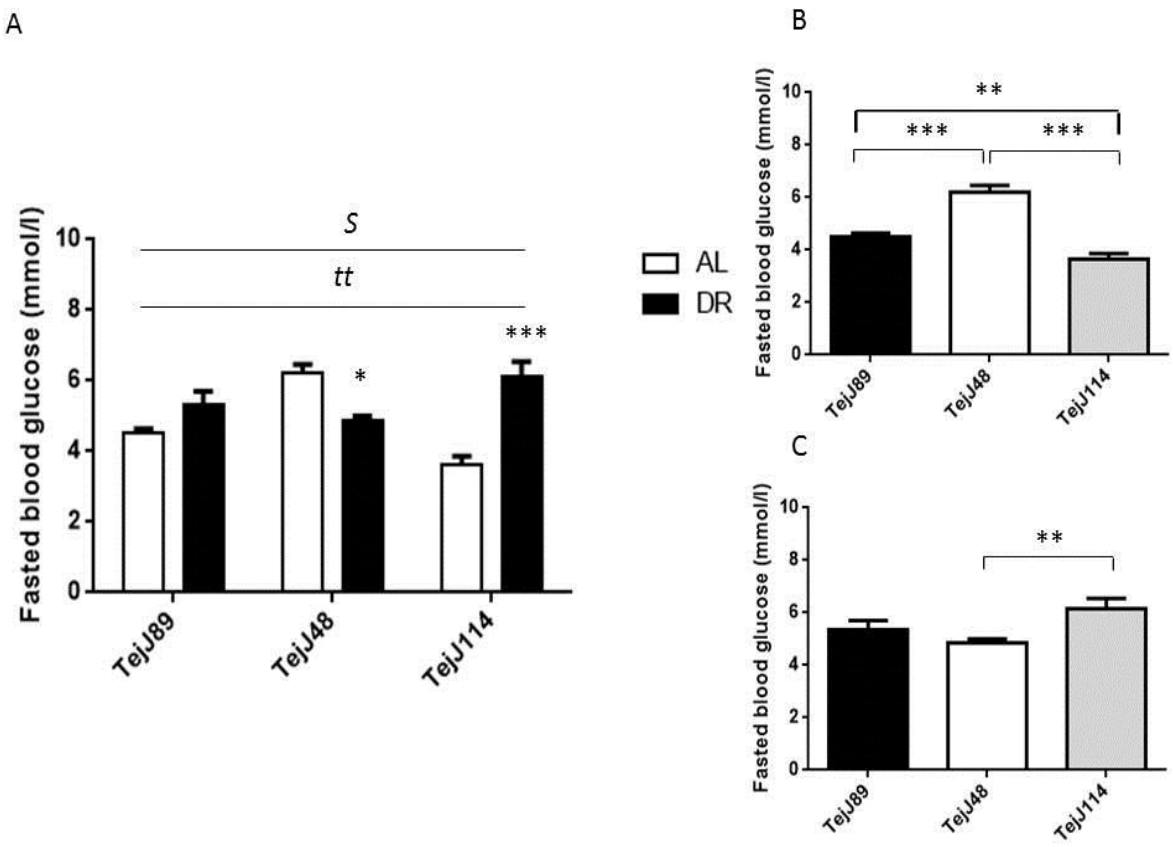

Figure 3.7: Fasting blood glucose levels in female ILSXISS mice following 2 months of 40% DR or AL feeding (A). A significant treatment and strain effect was detected on fasting blood glucose levels. Fasted blood glucose in the AL (B) and DR (C) mice. Values are expressed as mean ± SEM, with n = 8 per group. * denotes $p < 0.05$, **$p<0.01$, ***$p<0.001$, t= treatment effect; tt denotes $p<0.01$, S= strain effect; S denotes $p<0.05$.

3.4.1 (E) Fed Blood Glucose

Fed blood glucose levels were significantly affected by both treatment ($F = 8.575$, $p = 0.005$) and strain ($F = 8.679$, $p < 0.001$). DR significantly reduced fed blood glucose levels in strainTejJ48 ($p<0.05$) only (Figure 3.8A). Within the AL mice a significant strain-effect was detected ($F=6.495$, $p<0.001$), with strain TejJ89 having significantly increased fed blood glucose levels compared to TejJ114 mice (Figure 3.8 B). In the DR mice ($F=4.836$, $p=0.019$), strain TejJ48 had reduced fed blood glucose levels relative to both TejJ89 and TejJ114 (Figure 3.8 C).

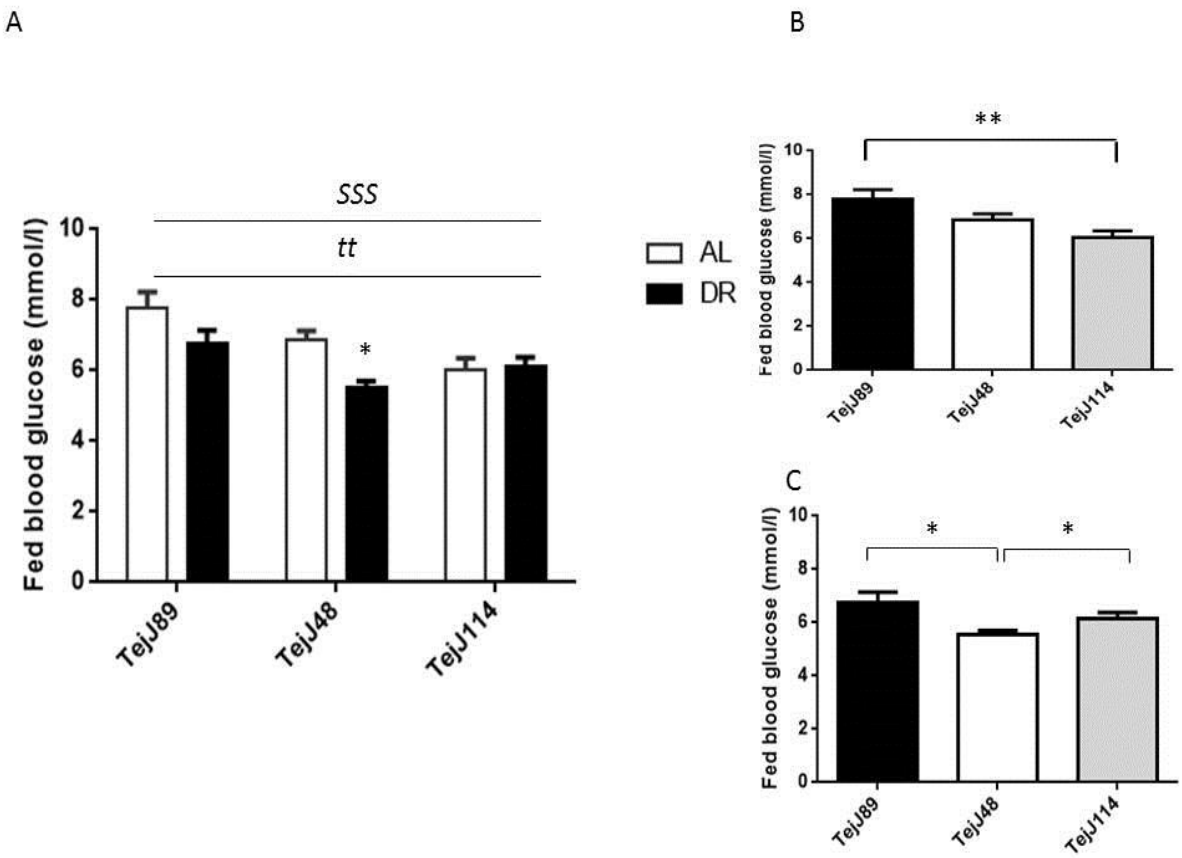

Figure 3.8: Fed blood glucose levels in female ILSXISS mice following 2 months of 40% DR or AL feeding (A). Treatment and strain were found to have a significant effect on fed blood glucose levels. Strain differences were observed within both AL (B) and DR mice (C). Values are expressed as mean ± SEM, with n = 8 per group. * denotes $p < 0.05$, **$p<0.01$, t= treatment effect; tt denotes $p<0.01$, S= strain effect; SSS denotes $p<0.001$.

3.4.1 (F) Glucose Tolerance

Following an intraperitoneal injection of glucose, glucose tolerance (as determined by area under curve (AUC)) showed a significant treatment effect ($F=14.28$, $p<0.001$), with DR mice of all strains following short-term DR appearing to have impaired glucose tolerance. However, when analysed with Post-hoc tests, DR mice were not more glucose intolerant compared to AL controls within each strain (Figure 3.9A). No strain-specific effects on glucose tolerance were observed within either the AL (Figure 3.9B) or DR (Figure 3.9 C) mice. (See Figure 3.10 for glucose tolerance response curves).

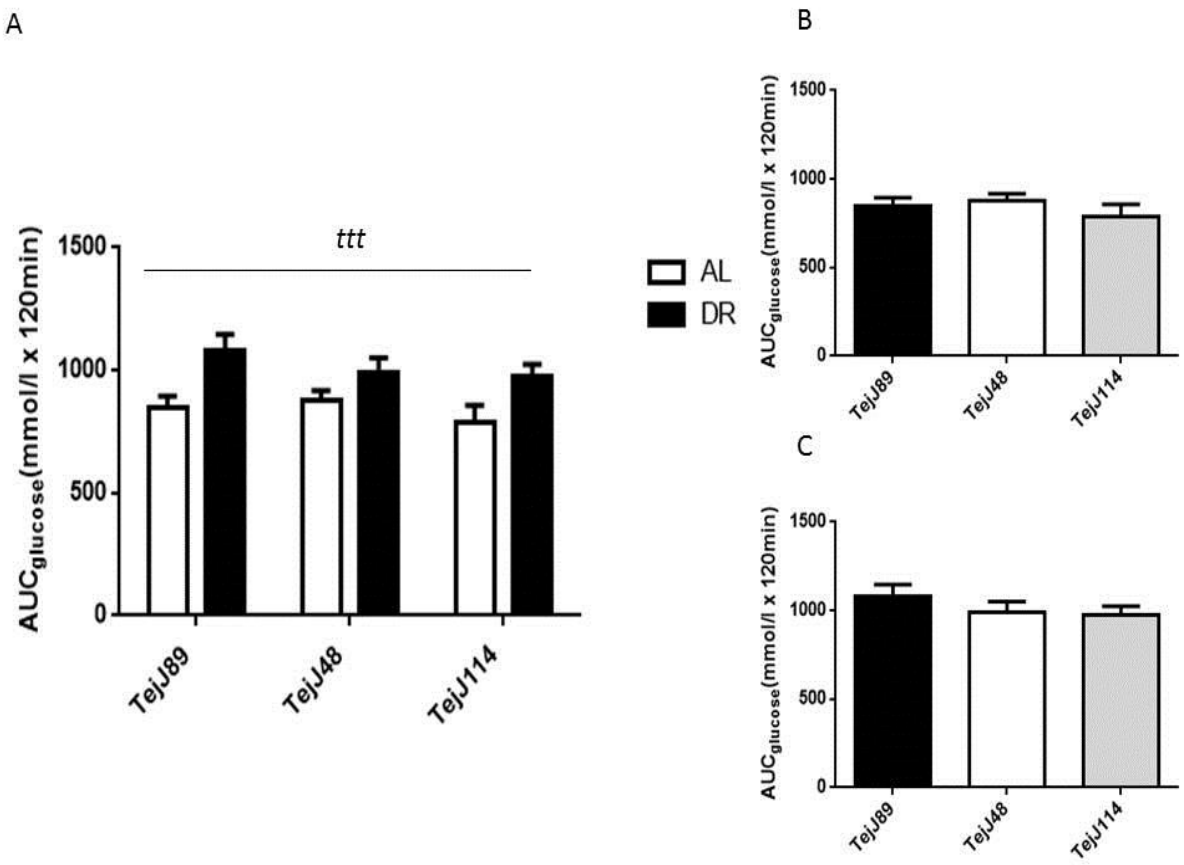

Figure 3.9: Glucose tolerance (denoted by area under the curve (AUC) following a glucose injection) in female ILSXISS mice after 2 months of 40% DR or AL feeding. Glucose tolerance was increased with treatment (A). No effect of strain was observed in the AL (B) or DR (C) mice. Values are expressed as mean ± SEM, with n = 8 per group. t= treatment effect; ttt denotes $p<0.001$.

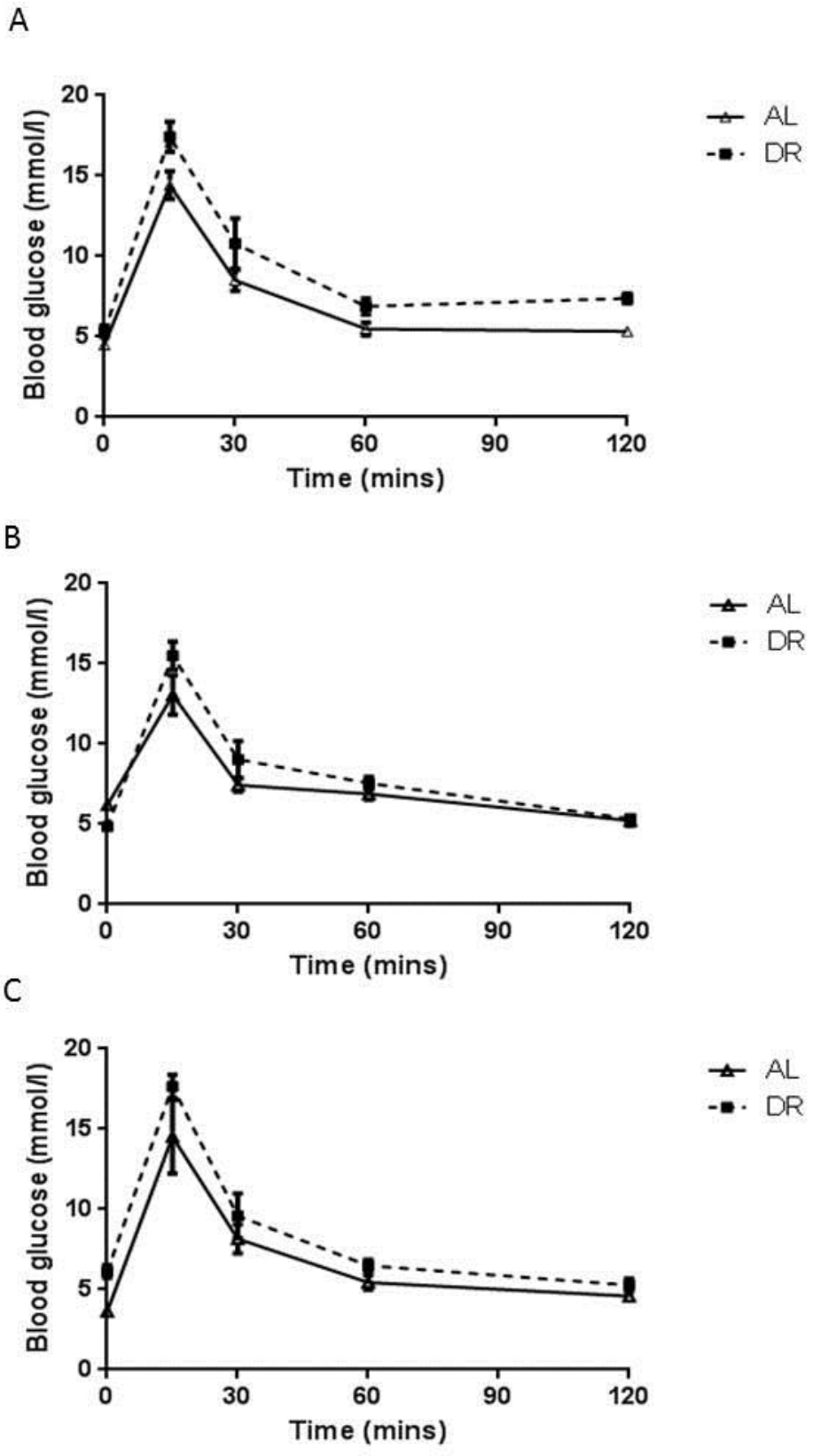

Figure 3.10: Glucose tolerance curves for strain TejJ89 (A), TejJ48 (B) and TejJ114 (C) following an IP injection of 20% glucose (2g kg^{-1}). Values are expressed as mean ± SEM, with n = 8 per group.

3.4.1 (G) Fasting Plasma Insulin

No treatment effect on fasting plasma insulin levels was detected, but a significant strain effect was observed ($F = 3.854$, $p = 0.031$), being higher, albeit non-significantly, in strain TejJ114. However, no strain-specific effects were detected within the AL (Figure 3.11 B) or DR (Figure 3.11 C) mice.

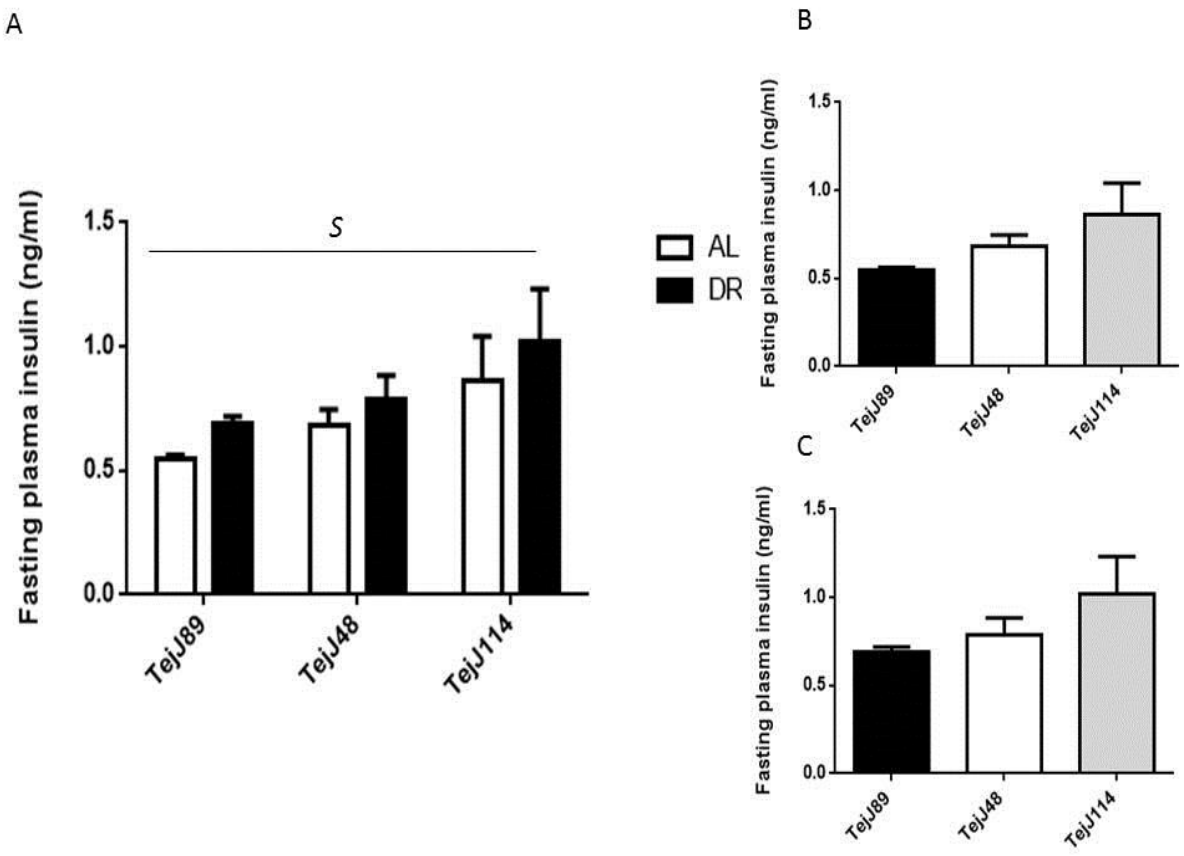

Figure 3.11: Fasting plasma insulin levels in female ILSXISS mice following 2 months of 40% DR or AL feeding. Fasting plasma insulin levels (A) were unaffected by treatment, however a significant strain effect was apparent. No strain effects were observed at 5 months of age within the AL (B) or DR (C) mice. Values are expressed as mean ± SEM, with n = 8 per group. S= strain effect; S denotes $p<0.05$.

3.4.1 (H) Insulin resistance - HOMA IR

No treatment effect was apparent following short-term DR on insulin resistance, as assessed using the homeostasis model assessment of insulin (HOMA2) (Figure 3.12 A). However, a significant strain-effect existed ($F = 3.336$, $p = 0.048$), with strain TejJ114 appearing more insulin resistant relative to the other strains, however with post-hoc testing this was not statistically significant. When analysed independently of treatment, no strain-specific effects were observed in either the AL (Figure 3.12 B) or DR (Figure 3.12 C) mice.

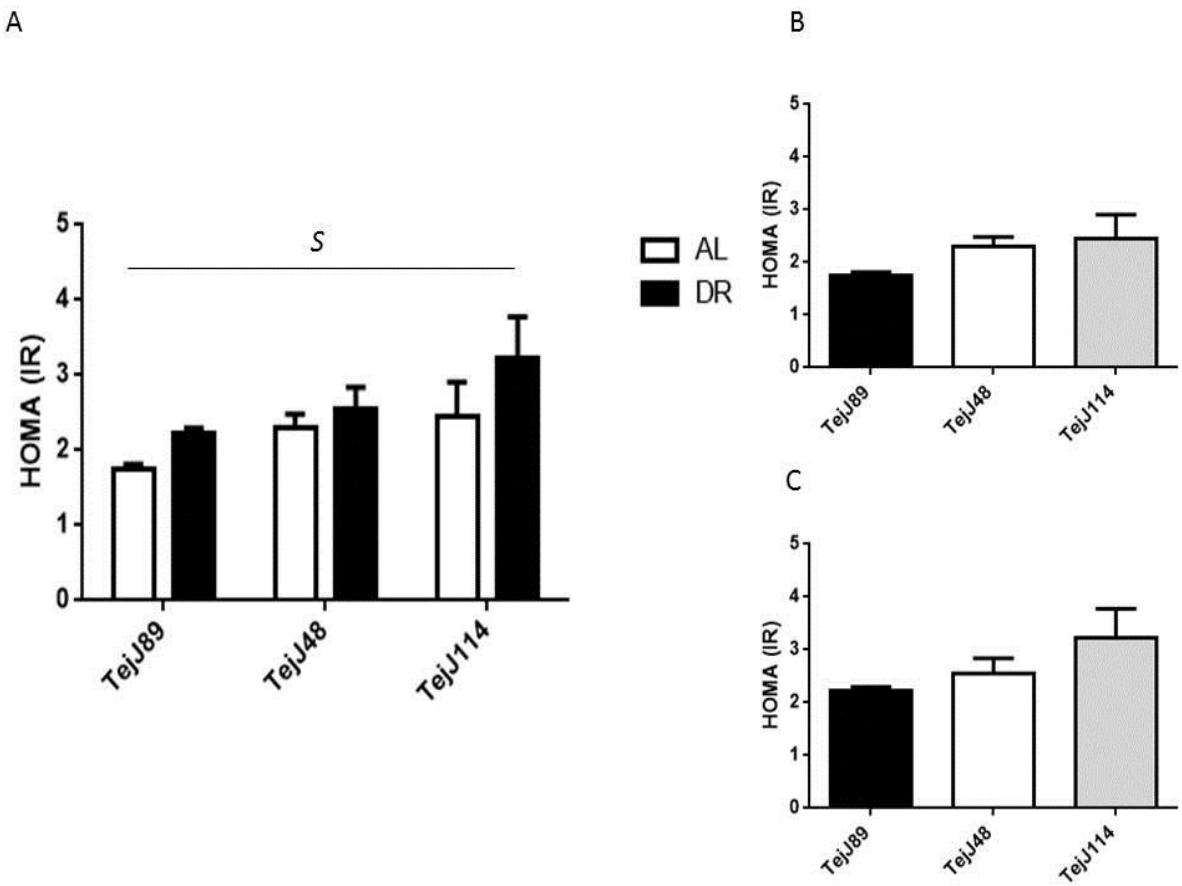

Figure 3.12: Homeostatic Model of Assessment (HOMA) of insulin resistance (IR) in female ILSXISS mice following 2 months of 40% DR or AL feeding. Treatment had no effect on HOMA IR, however strain was found to have an effect on HOMA IR (A). No strain effect was found within the AL (B) or DR (C) mice. Values are expressed as mean ± SEM, with n = 8 per group. S= strain effect; S denotes $p<0.05$.

3.**4.1 (I) Fasting plasma IGF-1**

No treatment or strain effect on fasting plasma IGF-1 levels were detected (Figure 3.13 A). Similarly no strain effect was found, with plasma IGF-1 levels in the AL (Figure 3.13B) or DR (Figure 3.13C) mice.

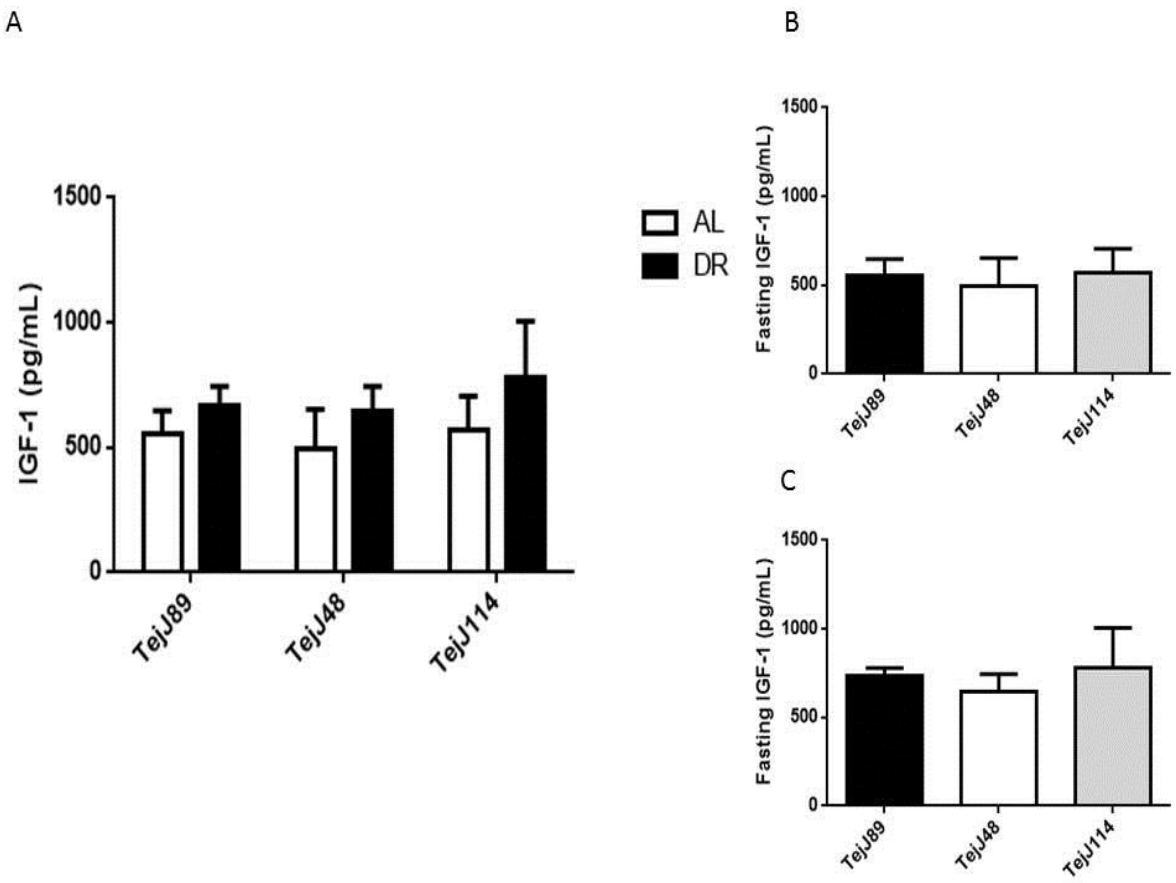

Figure 3.13: Fasting plasma IGF-1 levels in female ILSXISS mice following 2 months of 40% DR or AL feeding (A). No strain effect was found in AL (B) or DR (C) mice at 5 months of age. Values are expressed as mean ± SEM, with n = 8 per group.

3.4.2 Effects of Long-term DR on the metabolic phenotype of female ILSXISS mice

3.4.2 (A) Body Mass

As with the mice in the short-term DR study (Short-term 1), BM was reduced significantly from 12 weeks of age onwards in the Long-term study. Following 10 months of DR (13 months of age; Figure 3.14 A- C) all mice subject to DR were significantly lighter than their respective AL controls (AL vs. DR TejJ89; 25.3g vs. 17.8g t=11.66, p< 0.001, TejJ48; 24.7g vs. 19.3g t=11.98, p< 0.001, TejJ114; 25.6g vs. 14.9g t=12.40, p< 0.001; mean+/- SEM). A significant treatment (F=410.0, p<0.001), strain (F=7.277, p=0.002) and strain*treatment interaction (F=15.22, p<0.001) were observed (Figure 3.15 A). While no strain-specific differences in BM were observed between the AL mice (Figure 3.15B), a significant strain-effect existed in the DR mice (Figure 3.15C); strain TejJ114 was significantly lighter than both TejJ89 (p<0.01) and TejJ48 (p<0.001). The loss in BM following DR over the course of the experiment (relative to their AL controls) was greatest in strain TejJ114 (~52.3%) compared to the respective losses in BM in strain TejJ89 (~34.5%) and TejJ48 (~24.6 %). Average weekly food intake in the AL mice over the duration of the experiment, did not differ between the strains (Figure 3.16).

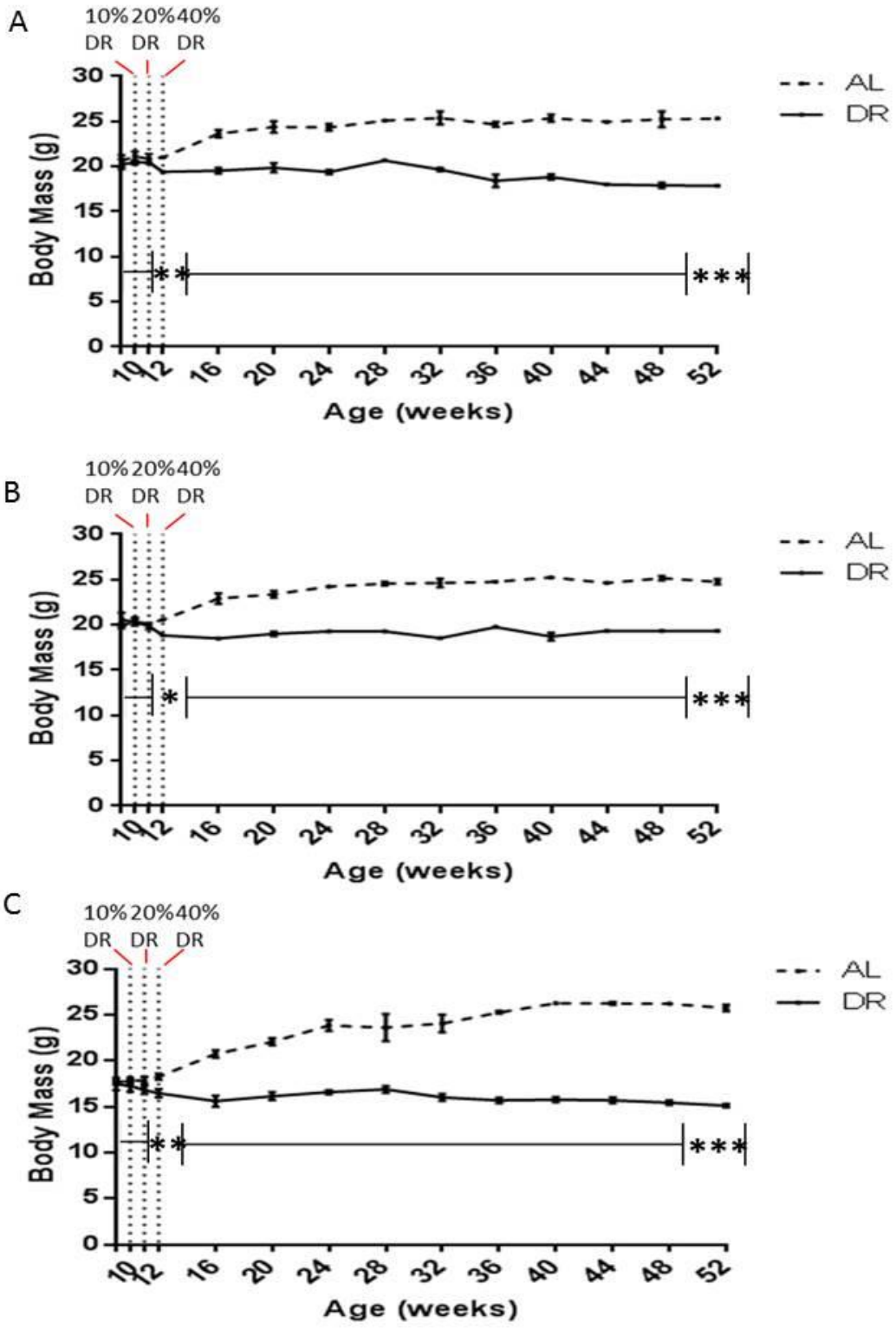

Figure 3.14: Body mass (BM) of female TejJ89 (A), TejJ48 (B) and TejJ114 (C) ILSXISS mice fed an *ad libitum* (AL) or 40% dietary restricted (DR) over a 10 month period (equivalent to 13 months of age). BM differed significantly with treatment from 20% onwards. Values are expressed as mean ± SEM, with n = 8 per group. * denotes $p < 0.05$, **$p<0.005$, ***$p<0.0001$.

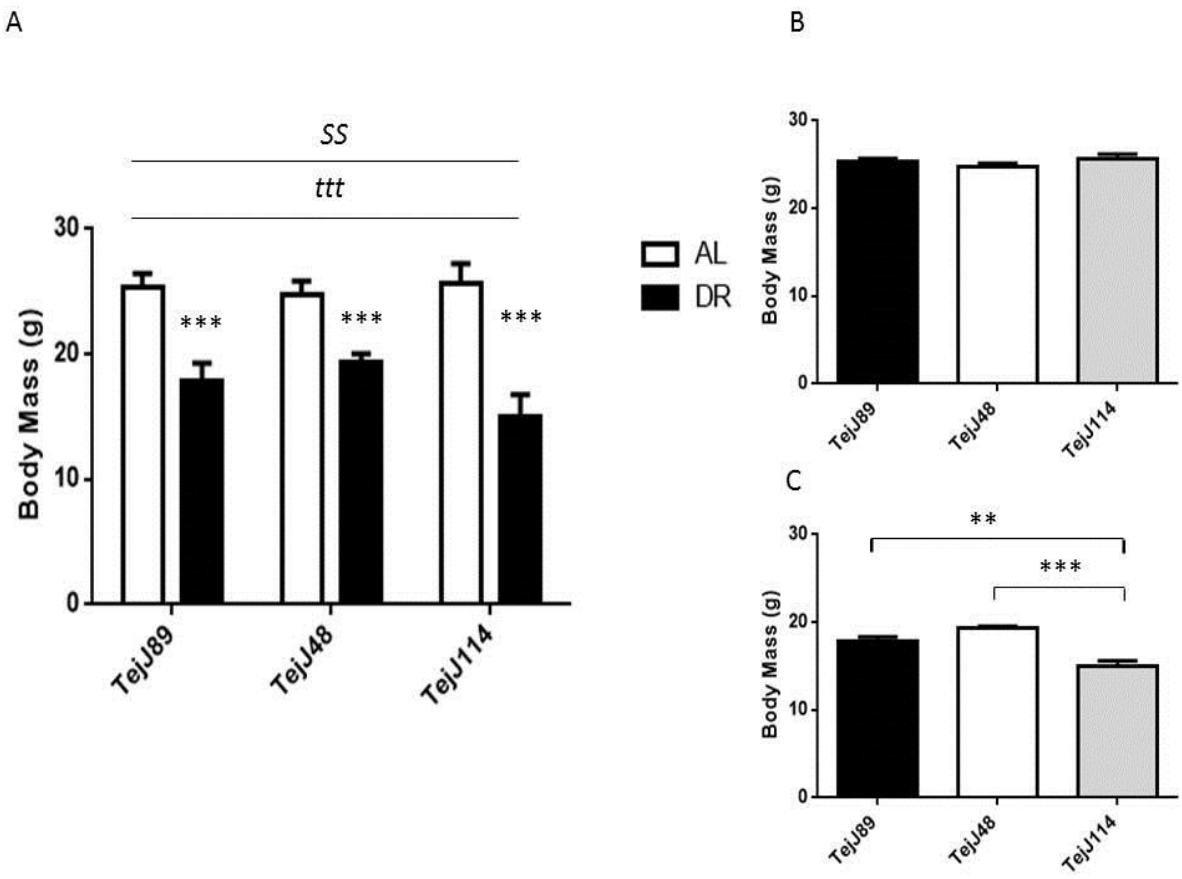

Figure 3.15: Body mass (BM) of female TejJ89 (A), TejJ48 (B) and TejJ114 (C) ILSXISS mice fed an AL diet or 40% DR over a 10 month period (equivalent to 13 months of age). Treatment had a significant effect on BM in all strains, with DR mice having reduced BM compared to AL controls (A). No strain effect was detected on BM in the AL mice (B). Within the DR mice (C) strain was found to have a significant effect on BM. Values are expressed as mean ± SEM, with n = 8 per group. ** denotes $p<0.01$, ***$p<0.0001$. t= treatment effect; ttt denotes $p<0.001$. S= strain effect; SS denotes $p<0.001$.

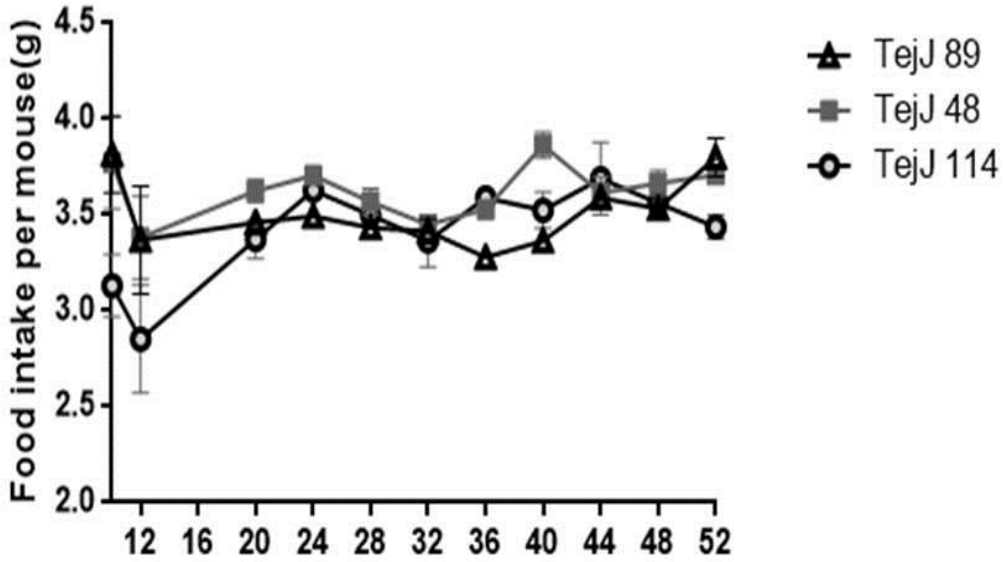

Figure 3.16: Food intake per mouse (g) of AL female ILSXISS mice from 12 weeks of age until 52 weeks of age. No strain-specific differences in food intake were observed. Values are expressed as mean ± SEM, with n = 8 per group.

3.4.2 (B) White Adipose Tissue

WAT data was corrected for BM and all analysis performed on corrected data. A significant treatment ($F=21.25$, $p<0.001$) and strain ($F=6.078$, $p=0.004$) effect on gonadal WAT was detected, with a highly significant reduction in WAT mass (expressed as a percentage of BM) following long-term DR (Figure 3.17 A). However, strain TejJ114 was the only strain to show a significant reduction in WAT when compared to its AL control ($p<0.01$). When considered as percentage loss, strain TejJ114 had the greatest reduction of WAT (60.3%) relative to AL WAT levels, withTejJ89 and TejJ48 mice having a lesser reduction compared to AL counterparts (48.6% and 43.9% respectively). Strain-specific differences were detected within the AL mice ($F= 4.301$, $p=0.022$), (Figure 3.17B), with strain TejJ114 having greater gonadal WAT mass relative to strain TejJ48 ($p<0.05$). No strain-specific differences were seen in the DR mice (Figure 3.17 C).

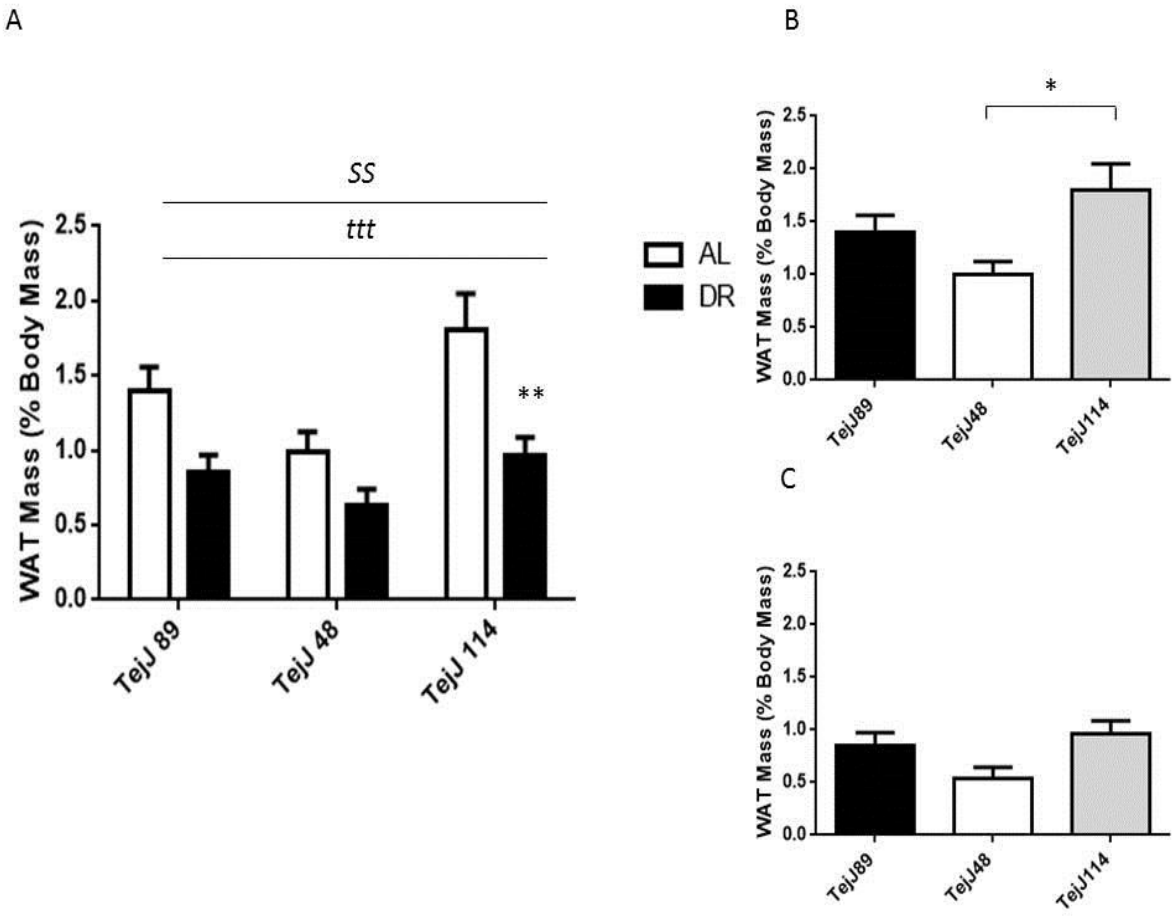

Figure 3.17: Gonadal white adipose tissue (WAT) ILSXISS mice fed an AL diet or 40% DR over a 10 month period (equivalent to 13 months of age.) A treatment effect was observed with long-term DR in all strains (A). Strain specific differences were observed within AL mice (B) unlike the DR mice (C). Values are expressed as mean ± SEM, with n = 8 per group. * denotes $p < 0.05$, **$p<0.005$. t= treatment effect; ttt denotes $p<0.001$. S= strain effect; SS denotes $p<0.01$.

3.4.2 (C) Brown Adipose Tissue

BAT mass (expressed as percentage of BM) was significantly increased in DR mice ($F = 14.47$, $p < 0.001$). Following post hoc analysis, this DR effect was found to be significant only in strain TejJ89 mice (Figure 3.18 A). Within both the AL (Figure 3.18B) and the DR mice (Figure 3.18 C), no strain-specific effects on BAT mass were detected.

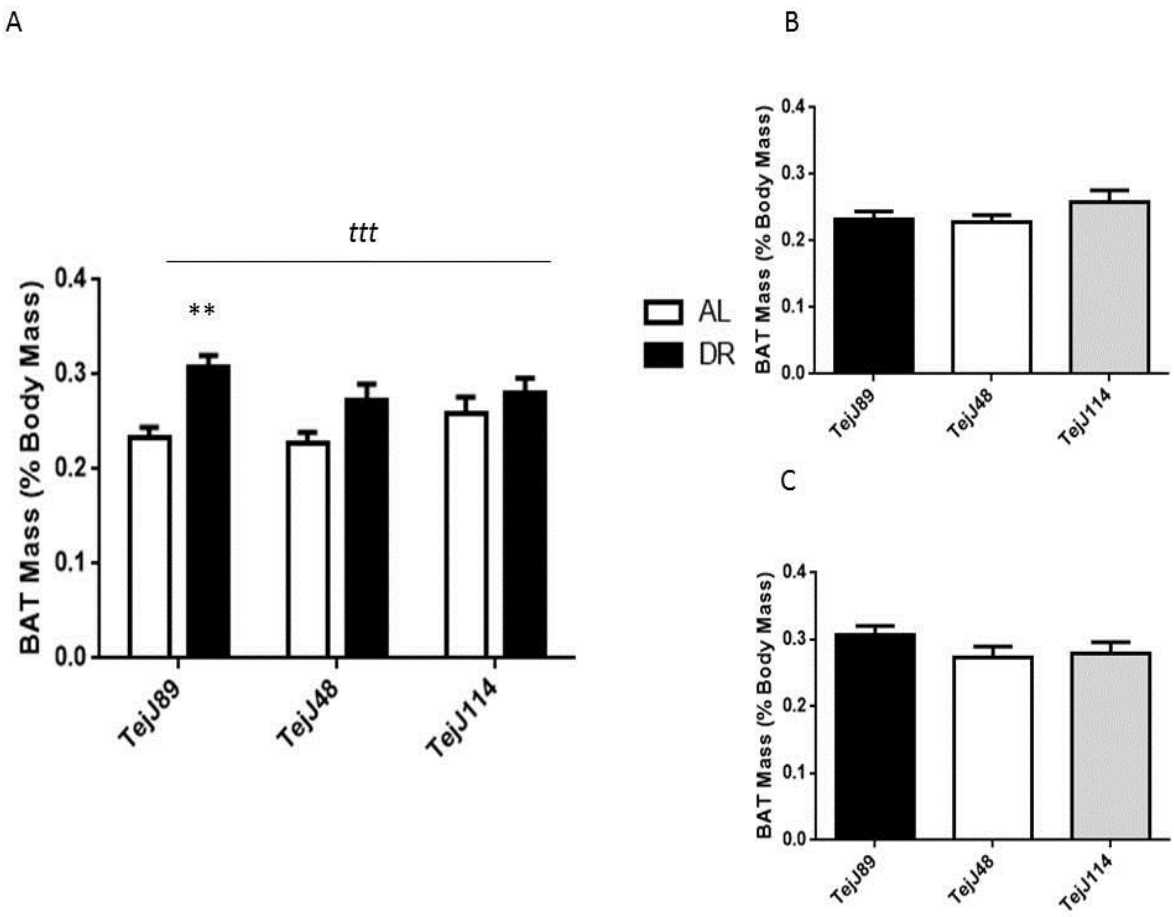

Figure 3.18: Brown adipose tissue (BAT) mass in female ILSXISS mice fed an AL diet or 40% DR over a 10 month period (equivalent to 13 months of age). BAT was increased with DR in strain TejJ89 relative to AL controls (A). No detectable strain-effect was reported in the AL (B) or DR mice (C). Values are expressed as mean ± SEM, with n = 8 per group. ** denotes p $p<0.005$, t= treatment effect; ttt denotes $p<0.001$.

3.4.2 (D) UCP-1

UCP-1 protein levels in BAT were unaffected by treatment and strain (Figure 3.19 A, B and C).

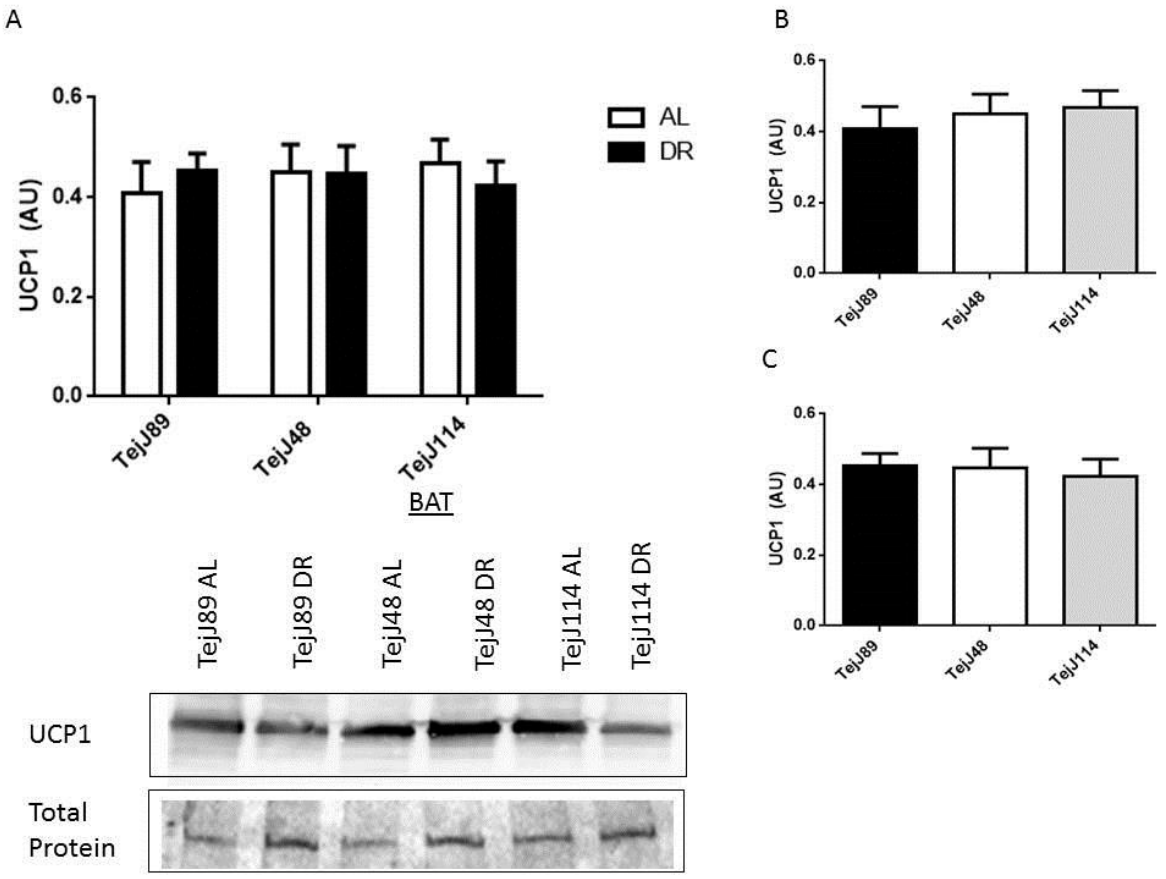

Figure 3.19 : UCP-1 protein levels in brown adipose tissue in female ILSXISS mice fed an AL diet or 40% DR over a 10 month period (equivalent to 13 months of age)(A). No detectable treatment or strain effect was reported (DR mice (C). Values are expressed as arbitrary units (AU) relative to total protein (determined by Ponceau staining) and as mean ± SEM, with n = 8 per group.

3.4.2 (D) Fasting blood glucose

Fasting blood glucose levels were significantly affected by both treatment ($F = 38.03$, $p < 0.001$) and strain ($F = 14.67$, $p < 0.001$; Figure 3.20A). Long-term DR increased fasting blood glucose levels relative to AL controls in strain TejJ89 ($p<0.001$) and TejJ48 ($p<0.05$). Within the AL mice, a significant strain-specific effect existed ($F=7.635$, $p=0.002$) with elevated fasting blood glucose in strain TejJ48 relative to both TejJ89 ($p<0.01$) and TejJ114 ($p<0.01$) (Figure 3.20 B). Similarly within the DR mice a significant strain effect was reported ($F=9.397$, $p=0.004$), but with reduced levels of fasting blood glucose in strain TejJ114 compared to both TejJ89 ($p<0.01$) and TejJ48 ($p<0.001$) (Figure 3.20C).

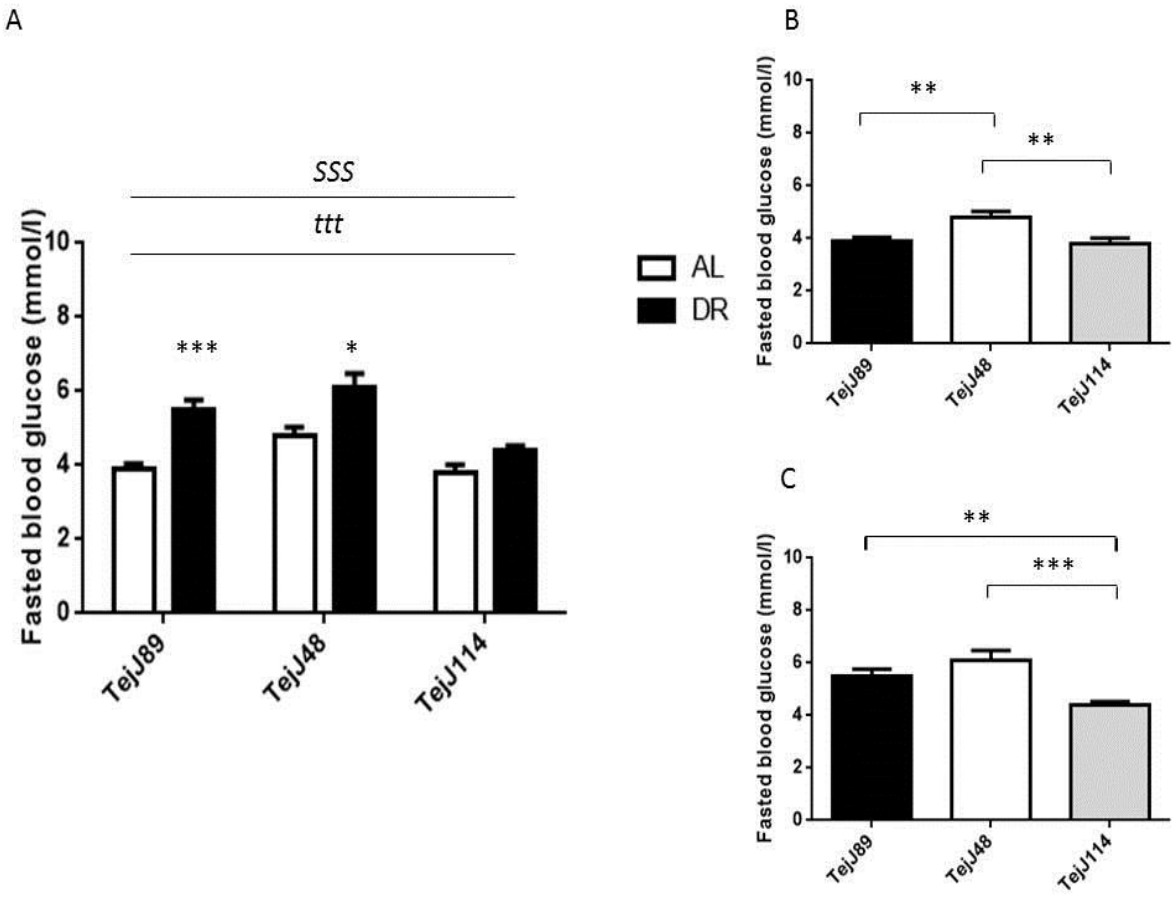

Figure 3.20: Fasted blood glucose levels in female ILSXISS mice fed an AL diet or 40% DR over a 10 month period (equivalent to 13 months of age). Fasting blood glucose levels were increased overall by treatment (A). Strain effect apparent in both AL (B) and DR (C) mice. Values are expressed as mean ± SEM, with n = 8 per group. * denotes $p < 0.05$, **$p<0.005$, ***$p<0.0001$. , t= treatment effect; ttt denotes $p<0.001$, S= strain effect; SS denotes $p<0.01$.

3.4.2 (F) Fed blood glucose

Fed blood glucose levels were significantly affected by treatment ($F=49.86$, $p<0.001$), strain ($F=9.364$, $p<0.001$), with a significant treatment*strain interaction observed ($F=4.887$, $p=0.011$) (Figure 3.21 A). DR decreased fed blood glucose levels relative to AL controls in strains TejJ48 ($p<0.001$) and TejJ114 ($p<0.001$). Within the AL mice, a significant strain-specific effect existed ($F=4.226$, $p=0.023$) with strain TejJ114 having higher fed blood glucose levels relative to strain TejJ89 ($p<0.05$) (Figure 3.21 B). Similarly within the DR mice a significant strain effect was identified ($F=10.28$, $p=0.004$) with lower fasting blood glucose observed in strain TejJ48 compared to both TejJ89 ($p<0.01$) and TejJ114 ($p<0.01$) (Figure 3.21C).

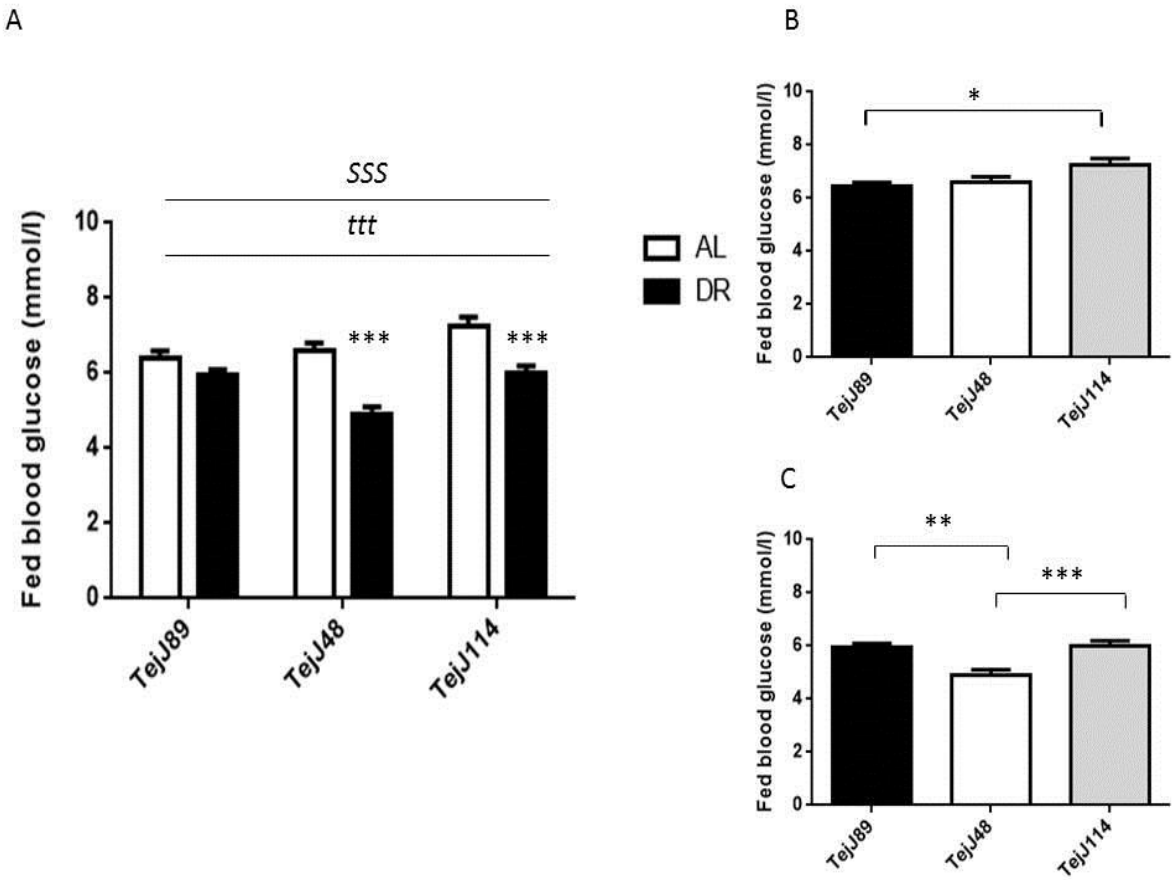

Figure 3.21: Fed blood glucose levels in female ILSXISS mice fed an AL diet or 40% DR over a 10 month period (equivalent to 13 months of age). Fed blood glucose was reduced by treatment (A). Strain differences were detected in both the AL (B), DR mice (C). Values are expressed as mean ± SEM, with n = 8 per group. * denotes $p < 0.05$, **$p<0.005$, ***$p<0.0001$. t= treatment effect; ttt denotes $p<0.001$, S= strain effect; SSS denotes $p<0.001$.

3.4.2 (G) Glucose Tolerance

Glucose tolerance was significantly affected by treatment, being reduced overall in DR mice ($F=49.86$, $p<0.001$; Figure 3.22A), however glucose tolerance was not improved in DR mice of any strain relative to AL controls. While no strain-specific effect was identified in AL mice (Figure 3.252B), a significant strain-specific effect was seen under DR (F-3.561, $p =0.038$); strain TejJ89 had poorer glucose tolerance relative to strain TejJ114 ($p<0.05$) (Figure 3.22 C). Glucose tolerance responses are plotted in Figure 3.23.

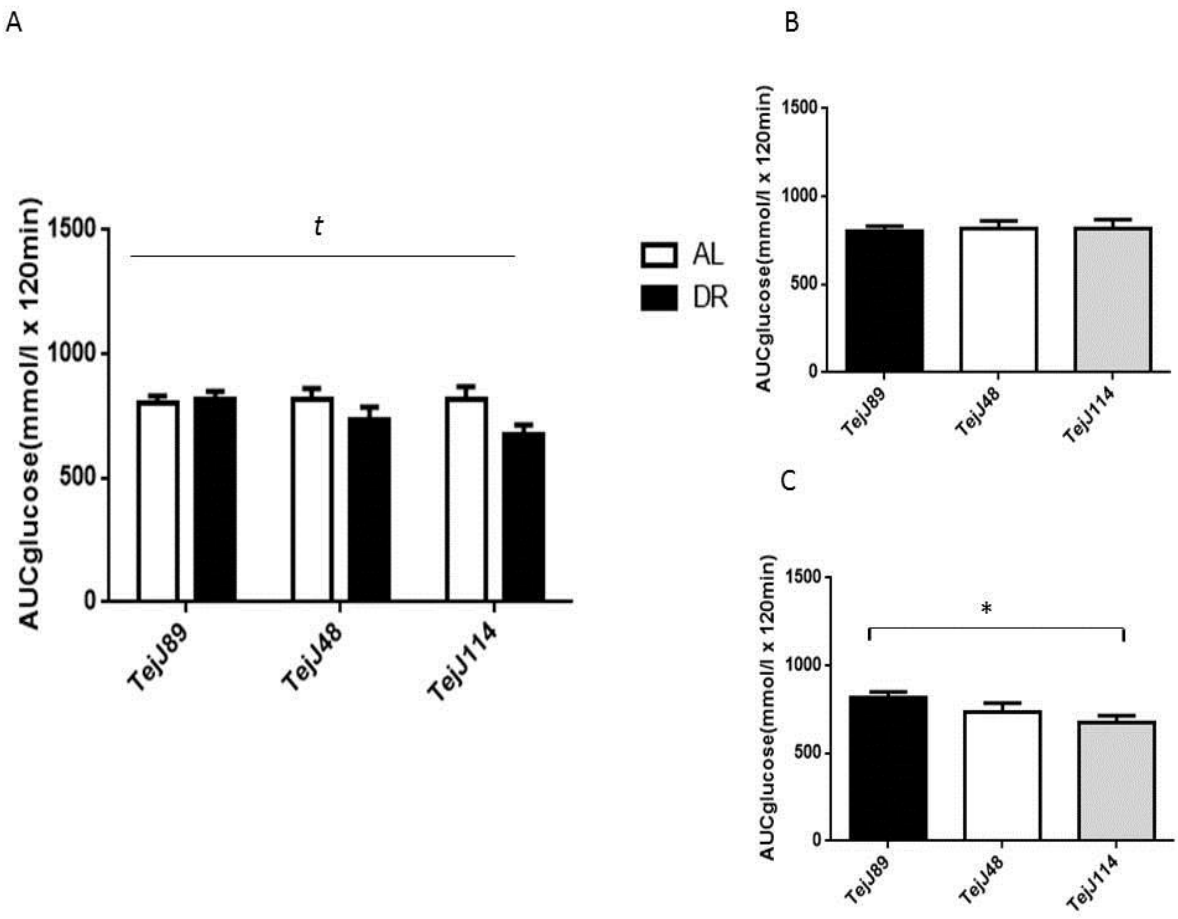

Figure 3.22: Glucose tolerance (denoted by area under the curve (AUC)) following an IP injection of 20% glucose (2g kg^{-1}) in female ILSXISS mice fed an AL diet or 40% DR diet over a 10 month period (equivalent to 13 months of age). Treatment was found to have a significant effect on glucose tolerance (A). No strain specific differences were observed within the AL (B) or DR (C) mice. Values are expressed as mean ± SEM, with n = 8 per group. * denotes $p < 0.05$. t= treatment effect; t denotes $p<0.05$.

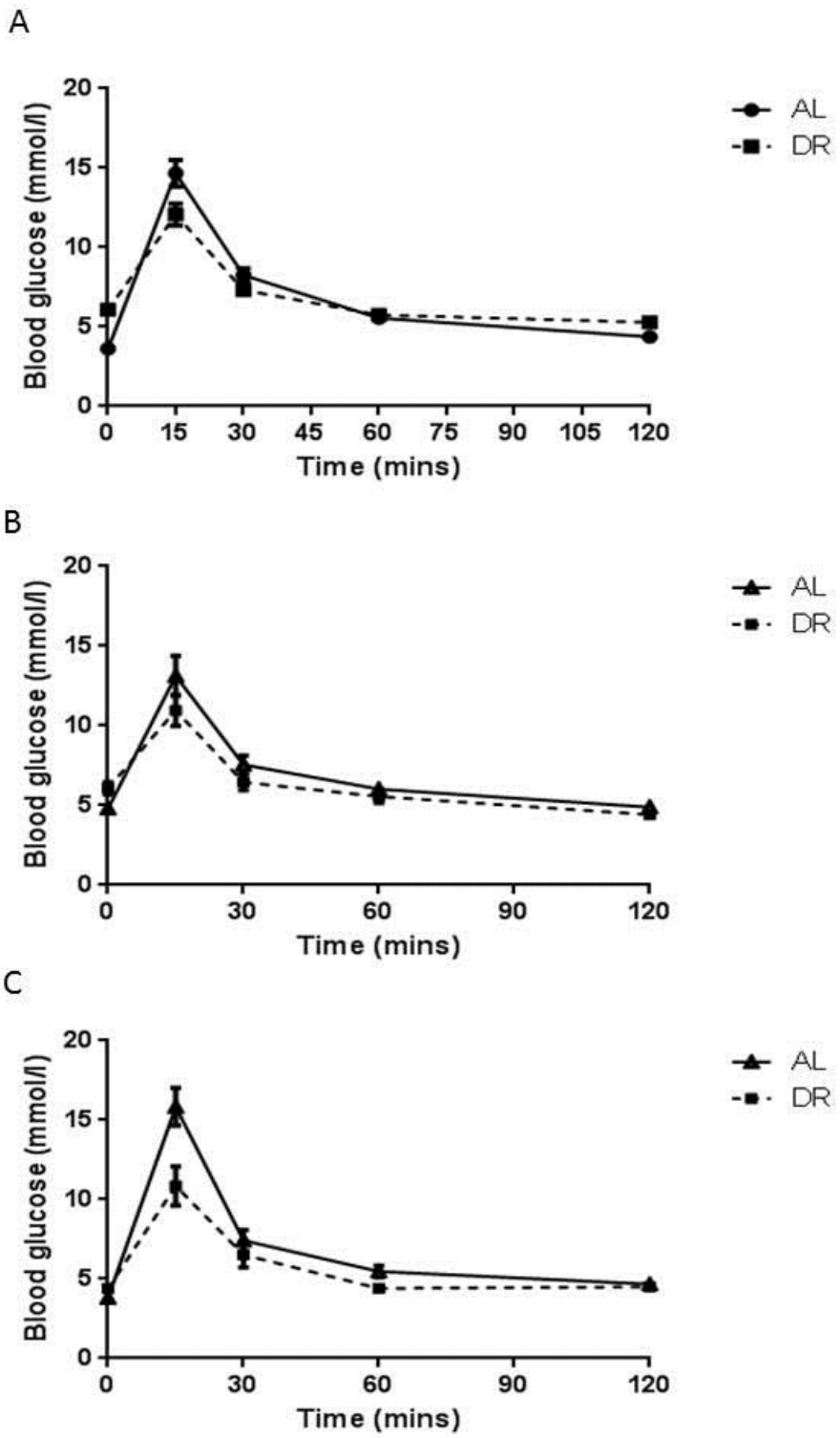

Figure 3.23: Glucose tolerance curves for strain TejJ89 (A), TejJ48 (B) and TejJ114 (C) in female ILSXISS mice fed an AL diet or 40% DR over a 10 month period (equivalent to 13 months of age, following an IP injection of 20% glucose (2g kg^{-1}). Values are expressed as mean ± SEM, with n = 8 per group.

3.4.2 (H) Fasting plasma insulin

Fasting plasma insulin levels were unaffected by treatment (Figure 3.24 A). However, a significant strain-effect was detected ($F = 4.349$, $P = 0.021$). While no strain-specific differences were observed within AL mice (Figure 3.24 B), a significant strain-specific effect was observed within the DR group ($F=4.526$, $p=0.028$), with strain TejJ89 ($p<0.05$) hyperinsulinaemic relative to strain TejJ48 (Figure 3.24 C).

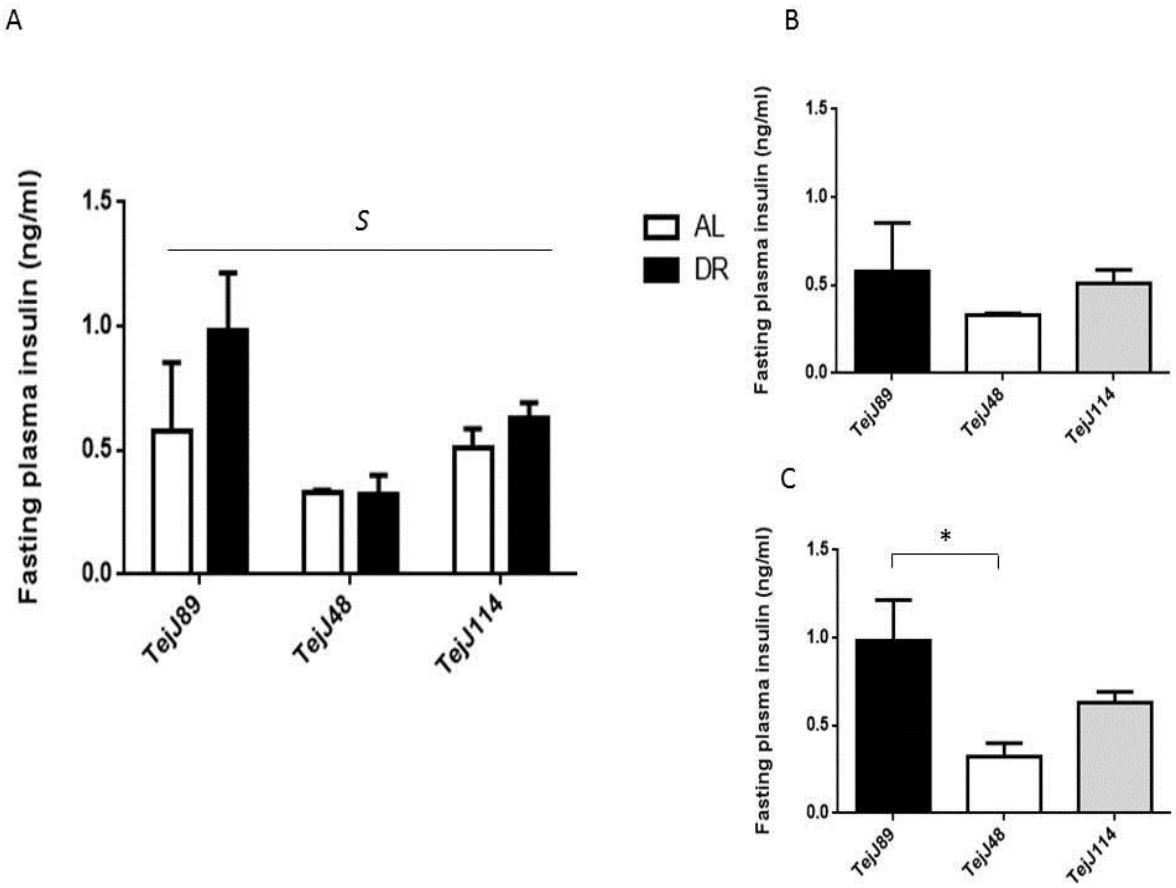

Figure 3.24: Fasted plasma insulin levels in female ILSXISS mice fed an AL or 40% DR over a 10 month period (equivalent to 13 months of age). No treatment effect was apparent following long-term DR on fasting plasma insulin levels (A). Representative of fasting plasma insulin in AL (B) and DR (C) mice. Values are expressed as mean ± SEM, with n = 8 per group. * denotes $p < 0.05$. S= strain effect; S denotes $p<0.05$.

3.4.2 (I) Insulin resistance - HOMA IR

Insulin resistance, as assessed using the homeostatic model assessment of insulin (HOMA2), was affected by both treatment ($F = 6.898$, $P = 0.013$) and strain ($F= 3.480$, $p = 0.044$) (Figure 3.25 A). Long-term DR surprisingly increased insulin resistance relative to AL controls in strain TejJ89 ($p<0.01$). Within the AL mice (Figure 3.25B) a significant strain-specific effect existed ($F=5.200$, $p=0.018$), with strain TejJ114 being more insulin resistant than either TejJ89 ($p<0.05$) or TejJ48 ($p<0.05$). Within DR mice a significant strain-specific effect was seen ($F=4.152$, $p=0.037$), with strain TejJ89 ($p<0.05$) having increased insulin resistance when compared to TejJ48 (Figure 3.25 C).

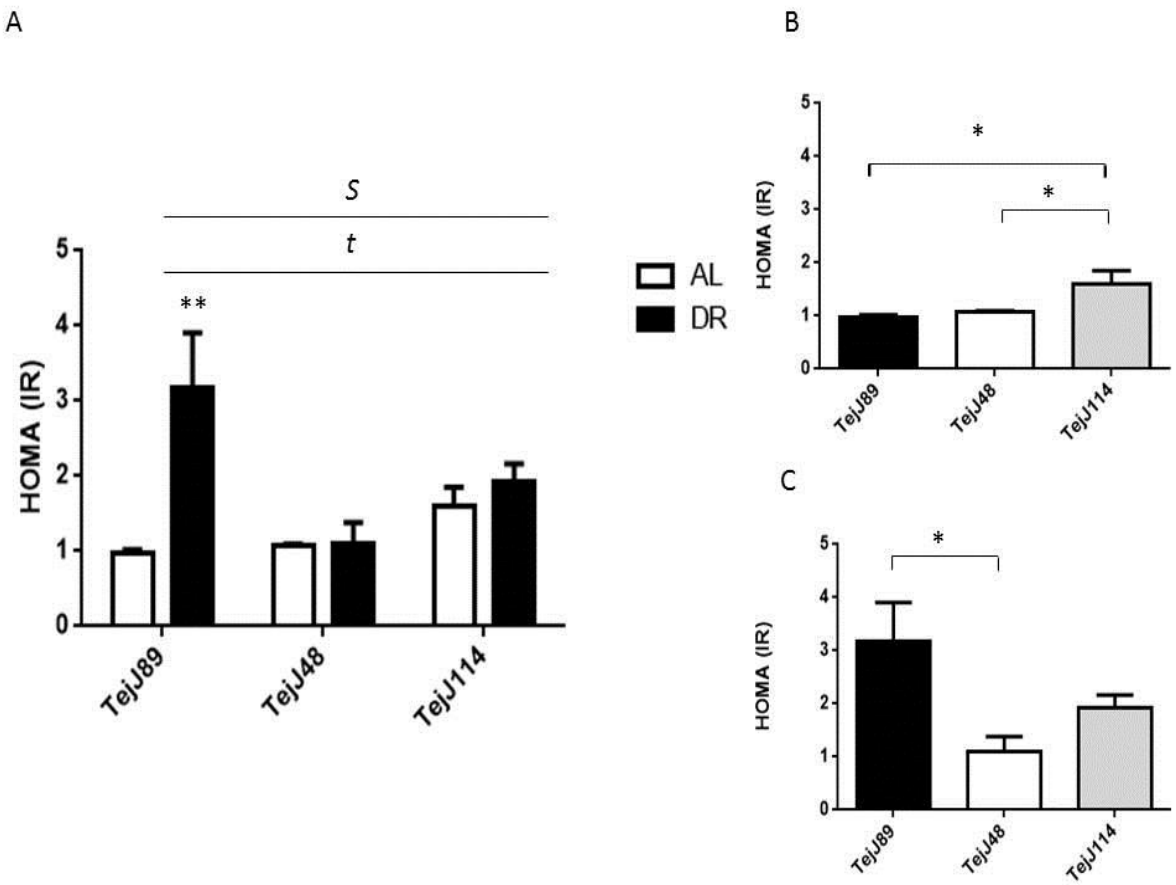

Figure 3.25: Homeostatic Model of Assessment (HOMA) of insulin resistance (IR) in female ILSXISS mice fed an AL diet or 40% DR over a 10 month period (equivalent to 13 months of age)(A). HOMA IR was found to be strain-specific in the AL (B) and DR mice (C). Values are expressed as mean ± SEM, with n = 8 per group. * denotes $p < 0.05$, **$p<0.005$.

3.4.2 (J) Fasting plasma IGF-1

Fasting plasma IGF-1 levels were found to be unaltered by treatment or strain following long-term DR (Figure 3.26 A). However, when assessed independent of treatment, i.e. to assess strain effects within AL or DR groups no strain-specific differences were found within the AL treatment group (Figure 3.26 B).A significant strain effect was observed however in DR mice (Figure 3.26 C), with strain TejJ89 appearing to have the lowest levels of fasting plasma IGF-1, although the results were not significantly different following post-hoc analysis.

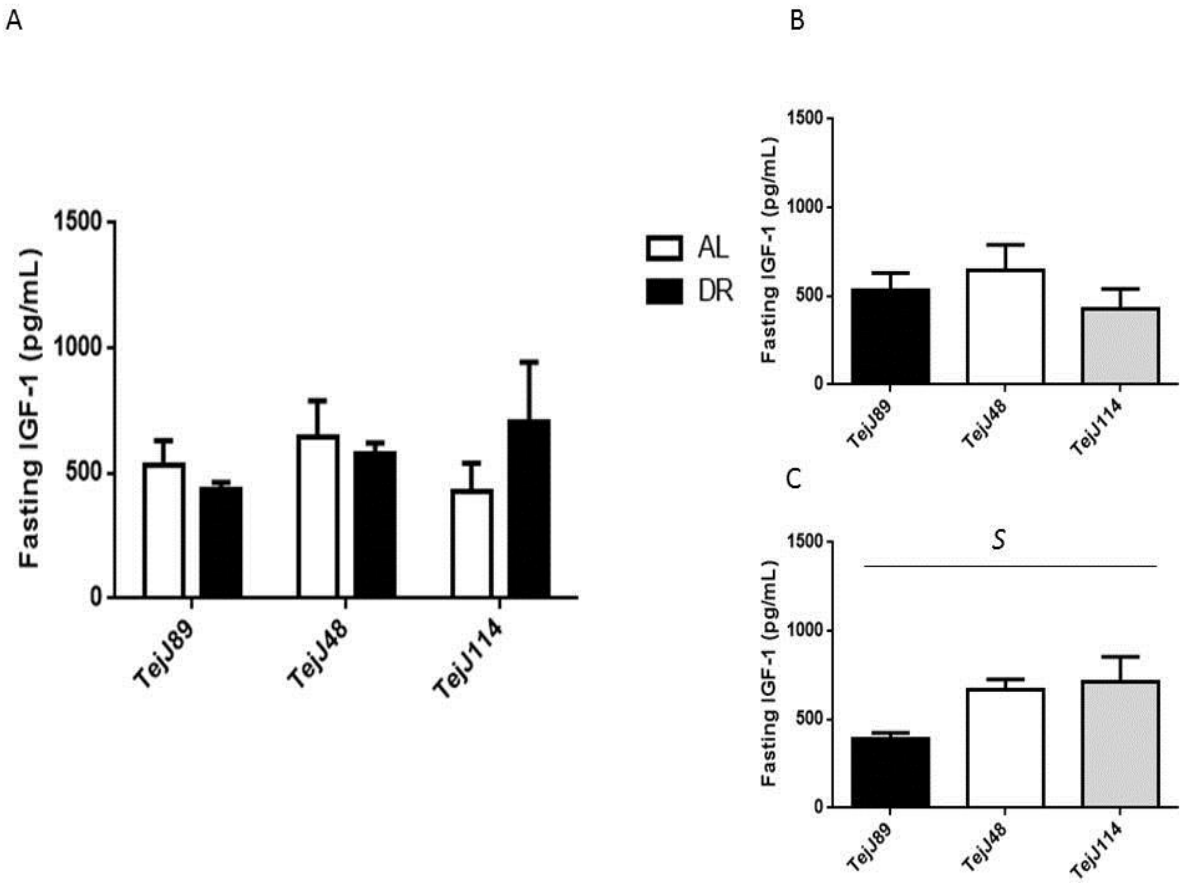

Figure 3.26: Fasting plasma IGF-1 levels in female ILSXISS mice fed an AL diet or 40% DR over a 10 month period (equivalent to 13 months of age). Plasma IGF-1 was unaltered by treatment (A). IGF-1 levels in AL (B) and DR (C) mice. Values are expressed as mean ± SEM, with n = 8 per group. * denotes $p < 0.05$, **$p<0.005$.

3.5 Discussion

The pursuit of effective strategies and therapeutics for improved health and survival has long relied on DR for determining the mechanistic processes of ageing. However, emerging evidence calls into question the universality of the effects of DR in extending lifespan, with genotype appearing to dictate both the magnitude and direction of lifespan response. In this study we employed a comparative approach to address the effects of 40% DR on numerous key physiological and metabolic hallmarks of DR response (BM, adiposity, glucose homeostasis), in three heterogeneous strains of ILSXISS RI mice, and to investigate these hallmarks as proposed candidate mechanisms underlying lifespan extension and slowed ageing. Our results indicate that genetic background appears relevant to the physiological response of mice to DR, with changes in body composition, specifically in body and fat mass following long-term DR found to correspond with the reported lifespan response to DR in these strains.

3.5.1 DR and Body Mass

Reductions in BM are characteristic of DR in mammals (Mattison et al. 2017; Mitchell et al. 2016), and female ILXISS mice of each strain weighed less than AL controls following both short and long-term 40% DR. However, interestingly strain TejJ114, which exhibits lifespan shortening under 40% DR (Rikke et al. 2010; Liao et al. 2010), lost significantly more BM under both short-term (2 months) and long-term (10 months) DR relative to their appropriate AL controls. Whilst BM loss is a universal feature of DR in rodents (Weindruch & Walford 1988), my data shows that strain TejJ114 lost over 50% of BM under DR which may help explain the negative effect or DR on lifespan in this strain. Indeed it has been shown that adenylyl cyclase type 5 knockout mice (AC5 KO) that are long lived under AL conditions, show lifespan shortening under DR that is associated with a significant reduction in BM (Yan et al. 2012). Potentially 40% DR is too severe a protocol in TejJ114, as evidenced by the >50% loss in total BM in this strain. Organisms typically display a tent-shaped lifespan response to DR (Clancy et al. 2002; Fontana & Partridge 2015), in that there is a dietary regime that maximises lifespan. In mice, different genotypes have different optimal DR conditions for longevity. For example, lifespan in DBA/2 mouse is maximal under 20% DR but maximal in C57BL/6 mice under 40% DR (Mitchell et al. 2016). Similarly in flies, the long-lived *chico* genotype are

found to have similar lifespan peaks to control flies following DR, but at different levels of nutrient restriction (Clancy et al. 2002).

Mice preferentially utilise WAT as an energy source under DR, in order to meet essential energy requirements in a time of reduced food intake (Mitchell et al. 2015a). In addition, losses in visceral adipose tissue have been associated with the beneficial metabolic effects of DR (Berg & Simms 1960; Barzilai et al. 1998; Gabriely et al. 2002). Despite TejJ114 showing a clear reduction in BM during short-term DR, surprisingly I observed an increase in gonadal WAT suggesting that other WAT pads and/or lean mass were preferentially lost in this strain. Reductions in specific organs have reported in rodents under DR, including hearts, livers, kidney (Bevilacqua et al. 2005), prostate, spleen, and skeletal muscle mass (Mitchell et al. 2015b; R Weindruch & Sohal 1997; Selman et al. 2005). It has been suggested that a selective reduction of different fat depots and the redistribution of fat mass to other sites may play a role in lifespan extension (Muzumdar et al. 2008), and in support of this C57BL/6 female mice under DR reportedly undergo redistribution of fat stores from visceral to subcutaneous depots (Varady et al. 2010). Increases of WAT mass at several fat depots including inguinal, gonadal, subcutaneous retroperitoneal, and mesenteric white adipose tissue, has also been reported following short-term mild (5%) DR in female C57BL/6 mice (Li, Cope, Johnson, D. L. J. Smith, et al. 2010). One limitation of my study was that no other fat depots, such as the mesenteric or omental, were measured.

In contrast, under long-term DR strain TejJ114 lost >50% of BM relative to AL controls and also lost the greatest percentage gonadal WAT. Previous work has shown that ILSXISS strains with greater capacity for fat preservation under 40% DR showed the greatest increase in lifespan under DR, whereas conversely larger losses of fat mass were associated with lifespan shortening under DR (Liao et al. 2011), with my data showing this relationship for TejJ114. While this association has come under some criticism, with Speakman *et al* (2011) highlighting that if positive responders are analysed irrespective of non- and negative-responders, no association between fat maintenance and longevity with DR exists. Contrary to this argument, a study of DBA/2 and C57BL/6 mice under different levels of DR, reported preservation of fat mass to be associated with increased lifespan, suggesting that a limit to adipose loss is in fact crucial to show lifespan benefits under DR (Mitchell et al. 2016).

BAT mass tends to increase under DR in rodents (Valle et al. 2008; Fabbiano, Suá Rez-Zamorano, et al. 2016; Ghosh et al. 2014), and higher levels of BAT has been shown to afford protection against metabolic dysfunction (Lowell et al. 1993) and obesity (Yoneshiro et al. 2013). Short-term DR had no impact on BAT mass in any ILSXISS strain, with the reasons for this unclear. However, it has recently been proposed that increased BAT mass following DR is directly linked to alterations in WAT (Fabbiano, Suá Rez-Zamorano, et al. 2016). We observe no changes in WAT in any strain under short-term DR, which may help explain the lack of effect in BAT. In most rodent DR studies, including my own, DR animals are maintained at 22^0 C, i.e. below the lower limit of the thermoneutral temperature zone (Speakman & Keijer 2012), thus DR mice are subject to thermoregulatory stress. Following implementation of DR animals must employ a number of compensatory strategies in order to conserve energy and preserve fat mass (Waterlow 1986). Following long-term DR, we observed BAT hypertrophy in strain TejJ89 only, the strains that shown lifespan extension under 40% DR. This may suggest that the metabolic efficiency and/ or plasticity of this strain is important to lifespan extension, with enhanced thermoregulation through non-shivering thermogenesis perhaps involved in the beneficial effect of DR on lifespan. Indeed transgenic over-expression of UCP1 extends lifespan in mice (Gates et al. 2007), and BAT, which is responsible for non-shivering thermogenesis, is increased with DR in rodents (Valle et al. 2008; Fabbiano, Suá Rez-Zamorano, et al. 2016) . Conversely, we propose that the inability of strain TejJ114 to defend against loss of WAT, combined with the inability to increase BAT mass during a time of thermoregulatory stress, may indicate that this strain are metabolically constrained under 40% DR. In agreement, ILSXISS strains with the greatest reductions in body temperature following DR were those same strains which were less responsive to the lifespan effects of DR (Rikke & Johnson 2007).

3.5.2 Glucose Homeostasis

The responses identified in relation to aspects of metabolism between the ILSXISS mice collectively suggest that no link exists between improved glucose homeostasis and longevity under 40% DR. This is perhaps surprising, given that improvements in glucose homeostasis are thought to be key components of extended lifespan (Bartke, 2008; Bartke & Brown-Borg, 2004). Glucose tolerance was not improved in DR mice under either long or short term DR, unlike findings previously reported in C57BL/6 or DBA/2 mice (Hempenstall et al. 2010; Mitchell et

al. 2016; Mitchell et al. 2015b). This suggests that certain strains are more responsive to DR than others, and may perhaps explain the observed lack of effect in glucose tolerance in the ILSXISS mice. Indeed C57BL/6 mice under DR have been shown to be more glucose intolerant than DBA/2 mice (Hempenstall et al. 2010). We similarly saw no clear association between fasting plasma insulin or IGF-1 levels or insulin sensitivity under DR and reported lifespan response between strains, despite the widespread support for such a link to longevity following DR in other strains (Hempenstall et al. 2010; Mitchell et al. 2015b). However, clear strain-specific differences were observed in line with comparative studies of DBA/2 mice and C57BL/6 mice (Hempenstall et al. 2010; Berglund et al. 2008; Goren et al. 2004).

The reasons for differences between this study and those which report reduced insulin/IGF-1 levels and insulin sensitivity following DR is unclear but may be due to differences in magnitude or duration of DR, whether animals were fed or fasted at time of sampling, and/or the lack of a graded reduction in food intake between studies. Indeed the protocol in this study is similar to that of Hempenstall *et al*, who also report no improvements in insulin with DR (Hempenstall et al. 2010). They too employ a stepwise reduction in food intake to introduce DR, and restrict DR mice on a daily basis, unlike some studies which feed animals double or triple rations on certain days. Moreover, such a discrepancy in protocol exists between the Liao *et al* and Rikke *et al* study which independently describe the lifespan effects of the ILSXISS mice (Liao et al. 2010; Rikke et al. 2010) and the current one. In these studies (Liao et al. 2010; Rikke et al. 2010) mice were essentially under intermittent fasting (IF), and it would be interesting to assess if the lifespan response in the strains would be upheld if carried out with 40% DR as employed in this study. Moreover, it would be useful to determine measures of glucose homeostasis under the IF protocol used in Liao *et al* and Rikke *et al*, to investigate if they correlated well with direction of reported lifespan response.

Previous reports of gender-specific effects on murine lifespan have been reported (Holzenberger et al. 2003; Selman et al. 2008), and the importance of gender in DR response is becoming more apparent (Mitchell et al. 2016). Male mice are known to be more susceptible to conditions which are associated with insulin resistance and impaired glucose homeostasis (Merry et al. 2017). Furthermore, lifelong 20% and 40% DR in female C57BL/6 and DBA/2 mice had no effect on fasting plasma insulin levels (Mitchell et al. 2016), unlike male counterparts. If

fasting plasma insulin response is dictated by gender, it would indicate that improved insulin sensitivity is not a universal driver of DR. It would be interesting to investigate the metabolic phenotype in the corresponding male ILSXISS strains under DR and AL conditions, to determine if improved insulin sensitivity with DR is in fact a health benefit only associated with males. Recently questions have been raised about the translatability of mouse research, the majority of which has been carried out on the C57BL/6 strain, to a genetically heterogeneous population, such as humans (Miller 2016). Moreover, the majority of DR studies have been largely investigating responses in male animals, with the NIH seeking to address this problem and include females in research (Clayton & Collins 2014). The lack of research on female animals makes comparing results across studies difficult. Moreover, studying the glucose homeostatic response to DR in male animals of a single genetic background may not produce definitive results from which deductions can be made for female ILSXISS strains. It is becoming more apparent that both gender and genotype interact to dictate the DR response (Mitchell et al. 2016; Valle et al. 2005), therefore exactly how DR would impact IGF-1 is not known in female ILSXISS mice, and may explain the apparent lack of beneficial effects with DR.

3.6 General conclusion

In summary, loss of WAT with long-term DR was associated with reduced lifespan, indicating that fat maintenance is important to the beneficial effects of DR. Moreover, BAT hypertrophy was associated with longevity, suggesting that cooperation between these two fat types following DR may be a key component of slowed ageing. These data suggests that that DR-induced lifespan extension in ILSXISS mice is not linked with improved glucose tolerance, enhanced insulin sensitivity or decreased IGF-1. My findings do however highlight the complex relationship between DR, genotype and lifespan extension. Most likely improved glucose homeostasis is one branch of an overarching mechanistic process underlying DR (see Anderson & Weindruch 2010) and it will be important to assess glucose homeostasis under less restrictive feeding conditions, in order to determine if a strain-specific optimal level of restriction will elicit improvements associated with DR in these strains. Furthermore it is not known how genotype impacts metabolic signatures commonly associated with DR. Disentangling the effects of genotype on classic hallmarks of DR will be crucial in understanding the mechanisms involved in lifespan extension and the shared processes of mammalian ageing.

Chapter 4: Disentangling the effect of dietary restriction on mitochondrial function using recombinant inbred mice

4.1 Abstract

Dietary restriction (DR) extends lifespan and healthspan in many species, but precisely how it elicits its beneficial effects is unclear. We investigated the impact of DR on mitochondrial function within liver and skeletal muscle of female ILSXISS mice that exhibit strain-specific variation in lifespan under 40% DR. Strains TejJ89 (lifespan increased under DR), TejJ48 (lifespan unaffected by DR) and TejJ114 (lifespan decreased under DR) were studied following 10 months of 40% DR (13 months of age). Oxygen consumption rates (OCR) within isolated liver mitochondria were unaffected by DR in TejJ89 and TejJ48, but decreased by DR in TejJ114. DR had no effect on hepatic protein levels of PGC-1a, TFAM, and OXPHOS complexes I-V. Mitonuclear protein imbalance (nDNA:mtDNA ratio) was unaffected by DR, but HSP90 protein levels were reduced in TejJ114 under DR. Surprisingly hepatic mitochondrial hydrogen peroxide (H_2O_2) production was elevated by DR in TejJ89, with total superoxide dismutase activity and protein carbonyls increased by DR in both TejJ89 and TejJ114. In skeletal muscle, DR had no effect on mitochondrial OCR, OXPHOS complexes or mitonuclear protein imbalance, but H_2O_2 production was decreased in TejJ114 and nuclear PGC-1a increased in TejJ89 under DR. Our findings indicate that hepatic mitochondrial dysfunction associated with reduced lifespan of TejJ114 mice under 40% DR, but similar dysfunction was not apparent in skeletal muscle mitochondria. We highlight tissue-specific differences in the mitochondrial response in ILSXISS mice to DR, and underline the importance and challenges of exploiting genetic heterogeneity to help understand mechanisms of ageing.

4.2 Introduction

Dietary restriction (DR), in its most general sense; defined here as reductions in energy intake, reductions in specific macro or micronutrients or as intermittent fasting, is the most extensively applied experimental intervention employed to manipulate ageing and longevity (Selman 2014b; Mair & Dillin 2008). Since the first study demonstrating that DR extended the reproductive period and lifespan of female rats almost one century ago (Osborne et al. 1917), an extensive body of research has studied the effects of DR in a wide number of organisms (Selman 2014b; Mair & Dillin 2008; Fontana & Partridge 2015; Shimokawa & Trindade 2010; Weindruch & Walford 1988). In addition to its effects on lifespan, DR also attenuates and/or postpones a broad-spectrum of age-associated pathologies, including obesity, insulin resistance, cognitive decline, immune dysfunction, stem cell ageing, sarcopaenia and cataracts (Selman 2014b; Mair & Dillin 2008; Fontana & Partridge 2015; Shimokawa & Trindade 2010). DR in rodents confers protection against a number of spontaneous and experimentally-induced cancers (Weindruch & Walford 1988), and delays several age-associated pathologies, including metabolic and cardiovascular disease, cancer and brain atrophy in non-human primates (Colman et al. 2009; Colman et al. 2014; Mattison et al. 2012) . Similarly, DR elicits numerous beneficial metabolic effects in humans including weight loss, lower visceral and intramuscular adiposity, insulin sensitivity and lowers several risk factors linked to cancer and cardiovascular disease (Fontana et al. 2010; Murphy et al. 2011).

However, contrary to the belief that the effect of DR on longevity is universal, several studies have reported a lack of, or even a detrimental effect of, DR on lifespan (Mattison et al. 2012; Harrison & Archer 1987; Carey et al. 2002; Forster et al. 2003; Rikke et al. 2010; Schleit et al. 2013; reviewed in Mulvey et al. 2014). In Rhesus macaques (*Macaca mulatta*), DR extended lifespan in a study conducted by the National Primate Research Centre at the University of Wisconsin (Colman et al. 2014), but did not extend lifespan in a study undertaken by the National Institute of Health (Mattison et al. 2012). The precise reasons for the differing outcomes between these studies appears complex but may reflect inter-study differences in diet, animal husbandry and geographical origin (Selman 2014b; Colman et al. 2014; Partridge 2012). In addition, a potentially critical factor that may help explain the unresponsiveness of particular organisms to DR-induced longevity is genetic background (Selman 2014b; Colman et al. 2014; Partridge 2012; Swindell 2012). For example, the effect of DR on survival in DBA/2 mice has been a source of debate

for many years, with DR reported to extend (Turturro et al. 1999; Lipman 2002), have no effect (Fernandes et al. 1976), or shorten lifespan (Forster et al. 2003). However, a recent study examining lifespan in male and female DBA/2 and C57BL/6 mice under 20% and 40% DR revealed that DBA/2 mice are indeed responsive to DR, although the impact of sex, strain and the magnitude of DR on survival outcome appears important (Mitchell et al. 2016). In two independent studies undertaken by the Universities of Texas (Liao et al. 2010) and Colorado (Rikke et al. 2010), survival was determined in multiple strains of heterogeneous ILSXISS recombinant inbred mice maintained on 40% DR, with distinct strain-specific effects on survival observed following 40% DR. The first study (Liao et al. 2010) reported that across 39 female and 41 male strains studied, only 21% of female strains and 5% of male strains showed life extension under DR. Surprisingly, a greater number of strains (27% and 26% for females and males respectively) showed reduced lifespan under DR. The latter study (Rikke et al. 2010), which assayed 42 female ILSXISS strains, similarly reported a significant strain-specific response to DR, with only 21% of strains showing life extension and 19% showing life shortening effects of DR.

Despite DR being the primary experimental intervention used to study ageing, it is still unclear as to precisely how DR acts mechanistically to induce its effects, although a multitude of mechanisms have been proposed (Fontana & Partridge 2015; Shimokawa & Trindade 2010; Masoro 2005; Hine et al. 2015; Anderson & Weindruch 2010). Mitochondrial dysfunction is a key hallmark of ageing and disease (Lopez-Otin et al. 2013), with ageing associated with altered mitochondrial morphology, reduced mitochondrial oxidative capacity and ATP production, increased mitochondrial derived reactive oxygen species (ROS) generation and greater oxidative damage (Wang & Hekimi 2015). Consequently, significant research effort has investigated whether DR can induce beneficial effects on the mitochondrial phenotype, such as maintaining mitochondrial function during ageing, reducing ROS production and attenuating oxidative damage. While it is generally assumed that DR reduces ROS production, a recent meta-analysis involving 157 rodent DR studies in which ROS levels (primarily hydrogen peroxide) were assayed, highlighted that 62% of studies actually reported no change in ROS levels relative to ad libitum (AL) fed controls (Walsh et al. 2014). Ambiguity also exists regarding the effect of DR on mitochondrial respiration in rodents, with DR reported to increase (Hempenstall et al. 2012; A. J. Lambert et al. 2004; Nisoli et al. 2005; Lanza et al. 2012), decrease (Sohal et al. 1994), or have no effect relative to

AL controls (Gredilla et al. 2001). Similarly, the impact of DR on various antioxidants and markers of oxidative damage appears fairly inconclusive, although as with all these parameters tissue-specific effects, the duration and intensity of DR, the sex and the age of the animals at the point of study may affect experimental outcomes (Walsh et al. 2014). The concept that DR induces mitochondrial biogenesis, that is the production of new mitochondrial proteins, has been proposed as a critical mechanism underlying the beneficial effects of DR (Civitarese et al. 2007), with DR reported to induce mitochondrial biogenesis in a number of tissues including liver (Nisoli et al. 2005). Peroxisome proliferator activated receptor gamma coactivator 1-alpha (PGC-1α is described as the master regulator of mitochondrial biogenesis (Puigserver et al. 1998). DR slows age-related declines in Pgc-1a expression in rat skeletal muscle and heart, and it is proposed that mitochondrial function adapts to DR through PGC-1α regulation (Nisoli et al. 2005; Anderson et al. 2008; López-Lluch et al. 2006). However, there is considerable debate in the literature as to how best to quantify biogenesis. Indeed, several studies suggest that DR may increase mitochondrial efficiency in order to maintain an 'optimally efficient' electron transport system, potentially driven by the nuclear localisation of PGC-1α (Anderson et al. 2008; Finley et al. 2012) without any increase in mitochondrial number per se (Hempenstall et al. 2012; Lanza et al. 2012; Hancock et al. 2011). Hancock *et al.* (2011) examined a range of tissues, including liver and skeletal muscle, in rats and suggested that rather than altering rate of protein synthesis in the mitochondria that DR affords protection to mitochondria through defending against DNA damage. Similarly, Lanza *et al*. (2012) reported that DR did not stimulate the synthesis of new mitochondrial proteins in mouse skeletal muscle, but rather minimised damage to existing cellular components, through decreased mitochondrial oxidant emission and upregulated antioxidant defences. Indeed, mitochondrial protein synthesis within liver, muscle and heart of mice was unaffected by DR, although cellular proliferation was decreased (Miller et al. 2012), with a recent proteomic approach reporting that mitochondrial biogenesis may actually be reduced within liver of DR mice (John C Price et al. 2012). Consequently, such findings question the concept that DR increases mitochondrial biogenesis, and further challenge the somewhat counterintuitive idea of expending energy on protein synthesis at a time of energy and/or nutrient restriction (Lanza et al. 2012).

Recently, the role of mitonuclear protein imbalance, that is a stoichiometric imbalance between OXPHOS subunits encoded by nuclear DNA (nDNA) and

mitochondrial DNA (mtDNA) which activates the cytoprotective mitochondrial unfolded protein response (UPR^{mt}), in longevity control has gained significant coverage (Houtkooper et al. 2013; Mouchiroud et al. 2013; Baqri et al. 2014; Hill & Van Remmen 2014b). Both rapamycin and resveratrol induced mitonuclear protein imbalance and UPR^{mt} in mouse hepatocytes in vitro (Houtkooper et al. 2013). UPR^{mt} induction in *C. elegans* also appeared necessary for longevity in developing worms exposed to high glucose, but shortened lifespan when induced in adulthood (Tauffenberger et al. 2016). Longevity in BXD mice is associated with reduced mitochondrial translation as determined by reduced expression of mitochondrial protein 5 (Mrps-5); Mrps-5 expression in skeletal muscle decreases with age and this is attenuated by DR (Houtkooper et al. 2013). Similarly, skeletal muscle from long-lived Surf1/ mice display evidence of UPR^{mt} (Pulliam et al. 2014). However, whether mitonuclear imbalance and UPR^{mt} are important in DR-induced longevity in mice remains to be elucidated.

Given the ongoing quest to identify the mechanistic drivers of DR, it has been suggested that employing a comparative-type approach which takes advantage of the variability in the DR response reported in certain rodent strains may help delineate the mechanisms underpinning DR (Mulvey et al. 2014; Swindell 2012). Indeed, several groups have already undertaken such approaches using DBA/2 mice (Rebrin et al. 2011; Ferguson et al. 2007; Sohal et al. 2009), showing for example that this strain are hyperinsulinaemic and insulin resistant compared to C57BL/6 mice (Hempenstall et al. 2010). In the present study we investigated the potential linkage between DR-induced longevity and mitochondrial function within both liver and skeletal muscle by exploiting the highly variable effect of DR on lifespan in ILSXISS mice. To this end we compared females mice from three ILSXISS strains showing repeatable responses to 40% DR across two independent studies (Rikke et al. 2010; Liao et al. 2010); TejJ89 (lifespan extended under DR relative to AL controls), TejJ48 (lifespan unaffected by DR), and TejJ114 (lifespan shortened under DR). We predicted that DR would positively impact on a number of parameters associated with mitochondrial function in strain TejJ89, that DR would have no impact on these parameters in strain TejJ48, and that DR would induce mitochondrial dysfunction in the negative responding TejJ114 (see Fig 4.1 for schematic outlining of our original predictions).

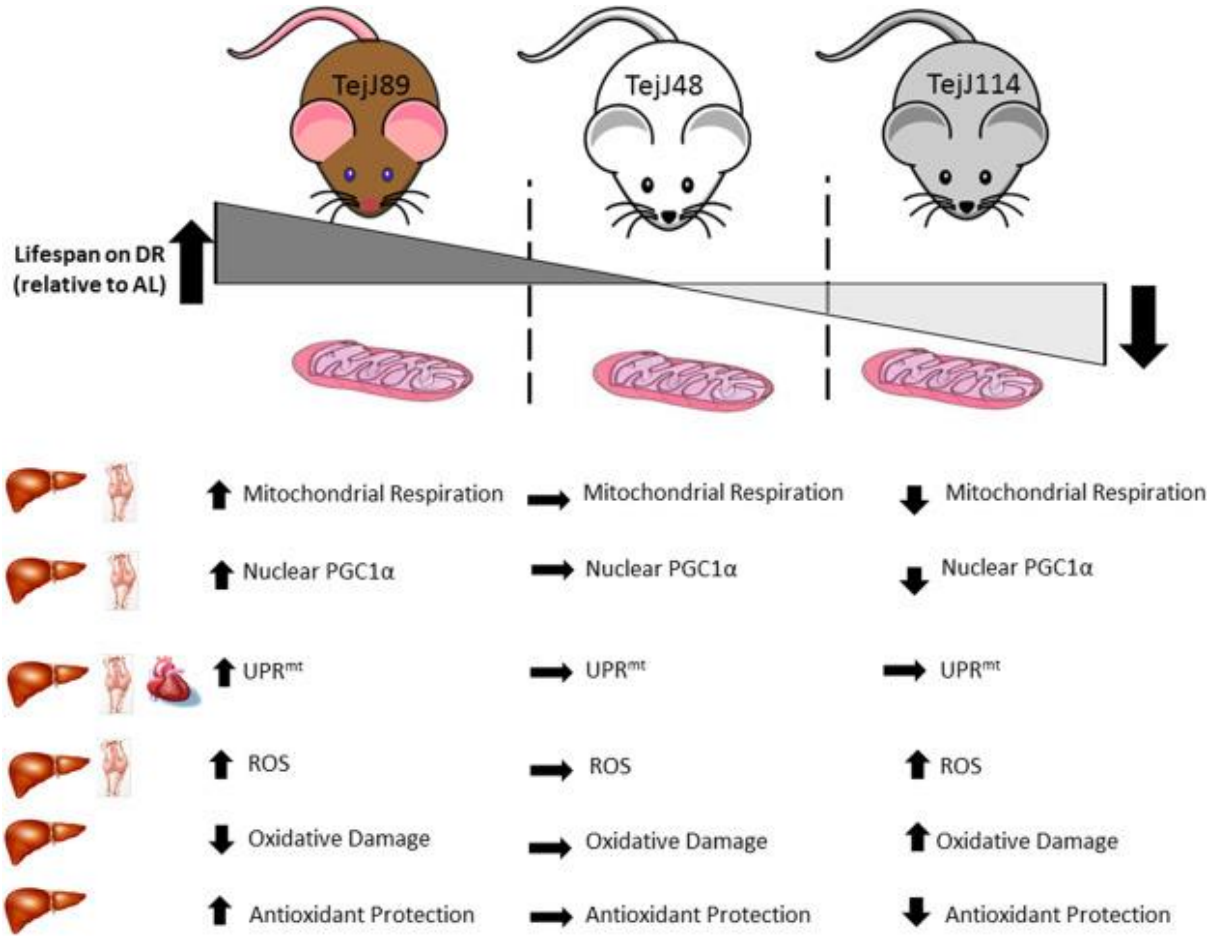

Fig. 4.1: Schematic showing the predicted mitochondrial functional response to 10 months of 40% dietary restriction (DR) in three strains of female ILSXISS mice that show a differential response of DR on longevity (**TejJ89 lifespan extension; TejJ48 no change in lifespan; TejJ114 lifespan shortening**).

4.2. Materials and methods

4.2.1. Animals

ILSXISS recombinant inbred (RI) mouse strains are derived from a cross between inbred long sleep (ILS) and inbred short sleep (ISS) mice (Williams et al. 2004). Mice from three strains; TejJ89, TejJ48 and TejJ114 were purchased from a commercial breeder (The Jackson Laboratory, Bar Harbour, Maine, URL: http://www.informatics.jax.org). The rationale for studying these particular strains was that in addition to repeatable effect of DR on lifespan across two independent studies (Rikke et al. 2010; Liao et al. 2010), no strain-specific differences in median lifespan were observed upon ad libitum (AL) feeding. Mice were maintained in groups of 4 post-weaning in shoebox cages (48 cm × 15 cm × 13 cm), with AL access to water and standard chow (CRM(P), Research Diets Services, LBS Biotech, UK; Atwater Fuel Energy-protein 22%, carbohydrate 69%, fat 9%) and maintained on a 12L/12D cycle (lights on 0700–1900h) at 22 ± 2 °C. At 9 weeks of age, cages were assigned to either an AL or DR group, with no difference in body mass observed between treatment groups at this time (TejJ89 AL vs. DR $t = 0.056$, $p = 0.583$, TejJ48 AL vs. DR $t = 0.677$, $p = 0.509$, TejJ114 AL vs. DR $t = 0.289$, $p = 0.777$). Mice were introduced to DR in a graded fashion; at 10 weeks of age mice were exposed to 10% DR (90% of AL feeding), at 11 weeks this was increased to 20% DR, and from 12 weeks of age until the termination of the experiment mice were exposed to 40% DR, relative to their appropriate strain-specific AL controls. Total food intake of AL mice from each strain was measured weekly (±0.01 g) and food intake of the DR cohort calculated from the average AL intake per mouse over the preceding week (Hempenstall et al. 2010). DR mice were fed daily at 1800 hrs and fed directly into the cage. Following 10 months of 40% DR (equivalent to 13 months of age), mice were fasted overnight and then culled the following morning by cervical dislocation. One lobe of liver, one gastrocnemius muscle and the heart were dissected and immediately snap-frozen in liquid nitrogen and stored at −80 °C until use. The remaining liver tissue and gastrocnemius muscle were subsequently used for the mitochondrial functional studies. A total of 4 mice per day were culled, with the time between dissection, mitochondrial isolation and mitochondrial analysis kept as uniformed as possible, with the particular tissue (liver or skeletal muscle) processed and analysed alternated each day. All experiments were carried out under a licence from the UK Home Office (Project Licence 60/4504) and followed the “principles of laboratory animal care” (NIH Publication No. 86-23, revised 1985).

4.2.2. Mitochondrial respiration

4.2.2.1. Isolation of mouse liver and skeletal muscle mitochondria

Liver mitochondria were isolated using previously published protocols (Brand & Nicholls 2011; Rogers et al. 2011). Briefly the liver was weighed and washed in MSHE + BSA buffer (210 mM mannitol, 70 mM sucrose, 5 mM HEPES, 1 mM EGTA and 0.5% (w/v) fatty acid free bovine serum albumin (pH 7.2)). The liver was then rapidly minced with scissors in 10 vol of MSHE + BSA buffer before homogenisation (2–3 strokes) using a glass-glass homogeniser (Fisher Scientific, Loughborough, UK). As with the liver, gastrocnemius muscle was harvested, weighed, washed and then minced in ice-cold isolation buffer (100 mM sucrose, 100 mM KCL, 50 mM Tris HCl, 1 mM KH_2PO_4,0.1 mM EGTA, 0.2% BSA (pH 7.4)), as previously described (Garcia-Cazarin et al. 2011). The muscle was subsequently rinsed three times in 1 ml of fresh isolation buffer, and then 1 ml of 2% Proteinase Type XXIV (Sigma Aldrich, Dorset, UK) was added and the sample vortexed for 1 min^{-1} at room temperature, followed by 1 min^{-1} incubation on ice. Samples were subsequently added to a glass homogeniser and 4 ml of isolation buffer added before homogenisation (10 strokes). Using differential centrifugation for both liver (Brand & Nicholls 2011; Rogers et al. 2011) and muscle (Garcia-Cazarin et al. 2011) a mitochondrial pellet was isolated and subsequently re-suspended (liver; MSHE buffer with no BSA, skeletal muscle; suspension buffer (225 mM Mannitol, 75 mM sucrose, 10 mM Tris, 0.1 mM EDTA (pH 7.4)). Total liver and skeletal muscle mitochondrial protein (mg/ml) were determined using the Bradford assay (Sigma Aldrich, Dorset, UK).

4.2.2.2. XF assay – plate preparation

Isolated mitochondria were diluted 10X in mitochondrial assay solution (MAS; 70 mM sucrose, 220 mM mannitol, 10 mM KH_2PO_4, 5 mM $MgCl_2$, 2 mM HEPES, 1.0 mM EGTA and 0.2% (w/v) fatty acid-free BSA, pH 7.2) containing substrate (10 mM pyruvate, 2 mM malate), and subsequently diluted to produce a 10 µg mitochondrial suspension. Mitochondria were added to a Seahorse XF assay plate (Agilent Technologies, CA, USA) at a concentration of 10 µg per well. The plate was centrifuged at 2000g for 20 min at 4 °C. A XF cartridge (Agilent Technologies) was then prepared as described by Brand et al. (Brand & Nicholls 2011). The plate was then transferred to a XF24 Analyser (Agilent Technologies) and the experiment initiated as previously described (Rogers et al. 2011). Basal Oxygen consumption

rate (OCR) was measured in substrate (10 mM pyruvate, 2 mM malate). Following this OCR was sequentially recorded for state 3 (addition of ADP (4 mM)), state 4 (addition of oligomycin (2.5 µg/ml)), state 3u (FCCP (4 µM Carbonyl cyanide 4-(trifluoromethoxy) phenylhydrazone)), and finally in the presence of Antimycin A and rotenone (4 µM), inhibitors of Complex III and I respectively, to determine non-mitochondrial respiratory capacity (Rogers et al. 2011). Analysis was carried out using Seahorse XF software (www.seahorsebio.com). Respiratory control ratio, expressed as the ratio between state 3u (FCCP-induced maximal uncoupled-stimulated respiration) and state 4° (respiration in the absence of ADP) did not differ by treatment within a strain or between strains for either liver or muscle mitochondria (Figure S1A&B).

4.2.3. Protein extraction

Liver, skeletal muscle and heart tissue were suspended in 1 ml of ice cold RIPA buffer (Radio Immuno Precipitation Assay buffer, 150 mM sodium chloride, 1.0% NP-40 or Triton X-100, 0.5% sodium deoxycholate, 0.1% SDS (sodium dodecyl sulphate), 50 mM Tris, pH 8.0) containing protease inhibitors (Halt™ Protease and Phosphatase Inhibitor Cocktail, Thermo Fisher Scientific, UK). The liver and heart were rapidly minced on ice with scissors and homogenised. A stainless steel bead (Catalogue # 69989, QIAGEN, Manchester, UK) was added to the eppendorf containing the skeletal muscle tissue and RIPA buffer, and then the muscle was homogenised at maximum speed (30 Hz) for 4 min^{-1} on the RETSCH MM 400 mixer mill (Catalogue# 10573034, Fisher Scientific). Following homogenisation all lysates were incubated on ice for 40-60 min^{-1} before being centrifuged at 16,000 *g* for 10 min^{-1} at 4 °C, and total protein levels subsequently determined using the BCA protein assay (G Biosciences, MO, USA). Nuclear and cytoplasmic fractionation of liver and skeletal muscle was undertaken using the ReadyPrep™ Protein Extraction (Cytoplasmic/Nuclear) Kit (Catalogue #163-2089, Bio-Rad, UK). Briefly, ~50 mg of tissue was homogenised together with 0.75 ml of cold cytoplasmic protein extraction buffer containing protease inhibitors (Halt™ Protease and Phosphatase Inhibitor Cocktail) using a chilled Wheaton Dounce tissue homogeniser (Catalogue #62400-595, VWR, West Sussex, UK), with protein concentration of each fraction determined using the BCA protein assay.

4.2.4. Western blot analysis

Equal volumes of tissue protein extract (50 µg) in Laemmli sample buffer were loaded onto 4–12% Bis-Tris pre-cast polyacrylamide gels (Life Technologies, Paisley, UK). Following this, proteins were transferred to polyvinylidene difluoride membranes (BioRad). Ponceau staining was used to ensure equal loading of protein and for normalisation purposes. Membranes were incubated in Tris-buffered saline Tween (1X TBST) containing 5% BSA for 1 h^{-1}. Blots were then washed in TBST (5 × 5min), incubated with primary antibody for 24 h^{-1} (4 °C), washed again (TBST) and incubated with secondary antibody for 1 h^{-1} at room temperature. Blots were visualised using Clarity™ Western ECL Substrate (BioRad) and a ChemiDoc™XRS system (BioRad). Antibodies for peroxisome proliferator-activated receptor-gamma co-activator 1 alpha (PGC-1α) and the oxidative phosphorylation complex antibody (OXPHOS cocktail; CI subunit NDUFB8, CII-30kDa (SDH), CIII-Core protein 2 (UQCRC2), CIV subunit I (MTCO1) and CV alpha subunit (ATP5A) were from Abcam, Cambridge, UK, mitochondrial transcription factor A (TFAM) and secondary (anti-rabbit) antibodies from Santa Cruz Biotechnology Inc. (Santa Cruz, CA, USA), and HSP60 and HSP90 from BD Biosciences (BD Biosciences, Oxford, UK. Mitonuclear protein imbalance (nDNA:mtDNA ratio) was determined by the ratio of nuclear encoded SDHB (Complex II) to mitochondrial-encoded MTCO1 (Complex IV) as described previously (Houtkooper et al. 2013).

4.2.5. Mitochondrial ROS production

Fresh respiratory medium (MAS; 70 mM sucrose, 220 mM mannitol, 10 mM KH_2PO_4, 5 mM $MgCl_2$, 2 mM HEPES, 1.0 mM EGTA and 0.2% (w/v) fatty acid-free BSA, pH 7.2) was supplemented with 1U/ml horseradish peroxidase and 10 µM Amplex® Red reagent (ThermoFisher Scientific, UK) as previously described (Zhou et al. 1997). 90 µl of this medium was then added to each well of a standard 96 well plate (Costar®, Sigma Aldrich, UK) and heated for 2 min^{-1} at 37 °C. Fluorescence was then measured at 15 s intervals for 2–3 min using a spectrophotometer (Clariostar microplate reader, BMG Labtech) at excitation and emission wavelength of 563 and 587 nm respectively. A sequential protocol was then run simultaneously for each sample in triplicate and completed within 15 min^{-1}. First the baseline fluorescence was measured by adding 10 µl of mitochondrial suspension, and then mitochondrial hydrogen peroxide production from all complexes was determined by adding a saturating concentration of succinate (10 mM), and then rotenone added

(0.5 µM; an inhibitor of complex I). The fluorescence signal was calibrated using 176 nM of hydrogen peroxide, and then hydrogen peroxide production was calculated following background correction.

4.2.6. Oxidative damage and antioxidant levels

Protein carbonyl (PC), total glutathione (GSH) and total superoxide dismutase (SOD) activity were measured in liver samples using commercially available kits and following the manufacturer's protocols (Catalogue#10005020 Carbonyl assay kit, #706002 Total SOD activity assay kit, #703002 Glutathione assay kit, Cayman Chemical Company, Estonia). Hepatic 4-Hydroxynonenal (HNE)-protein adduct levels were determined using an anti-HNE-His mouse IgG protein binding plate (Catalogue#STA-838, Cell Biolabs Inc., CA, USA). All assays were read on a plate reader (BMG Labtech, UK).

4.2.7. Statistical analysis

All statistical analyses were performed using R and figures were produced using GraphPad Prism (GraphPad Inc., La Jolla, CA, USA, version 5) software. Data were checked for normality using the Shapiro–Wilks test and a logarithmic transformation was undertaken if data not normally distributed. Data was analysed using linear modelling (LM) with treatment (AL or DR) and strain (TejJ89, TejJ48 and TejJ114) introduced as fixed factors. Following transformation, if the data was not normally distributed an appropriate non-parametric test was applied. Results are reported as mean ± standard error of the mean (SEM), with $p < 0.05$ regarded as statistically significant.

4.3. Results

Mitochondrial oxygen consumption rates (OCR) within isolated liver mitochondria under all conditions studied (Figure 4. 2 A) were unaffected by 10 months of 40% DR in strain TejJ89 relative to AL controls. A similar lack of a DR effect on hepatic respiratory capacities was observed in strain TejJ48 (Figure 4.2 B). In contrast, DR in strain TejJ114 (Figure 4. 2 C) significantly reduced State 3 ($t = 2.860$, $p = 0.006$) and State 3u ($t = 2.950$, $p = 0.006$) mitochondrial OCR relative to AL controls. While no differences in mitochondrial OCR were observed across ILSXISS strains under AL feeding (Figure 4.2 D), State 3 OCR in TejJ89 was significantly increased ($t = 2.24$, $p = 0.039$) relative to the other two strains under DR (Figure 4.2 E).

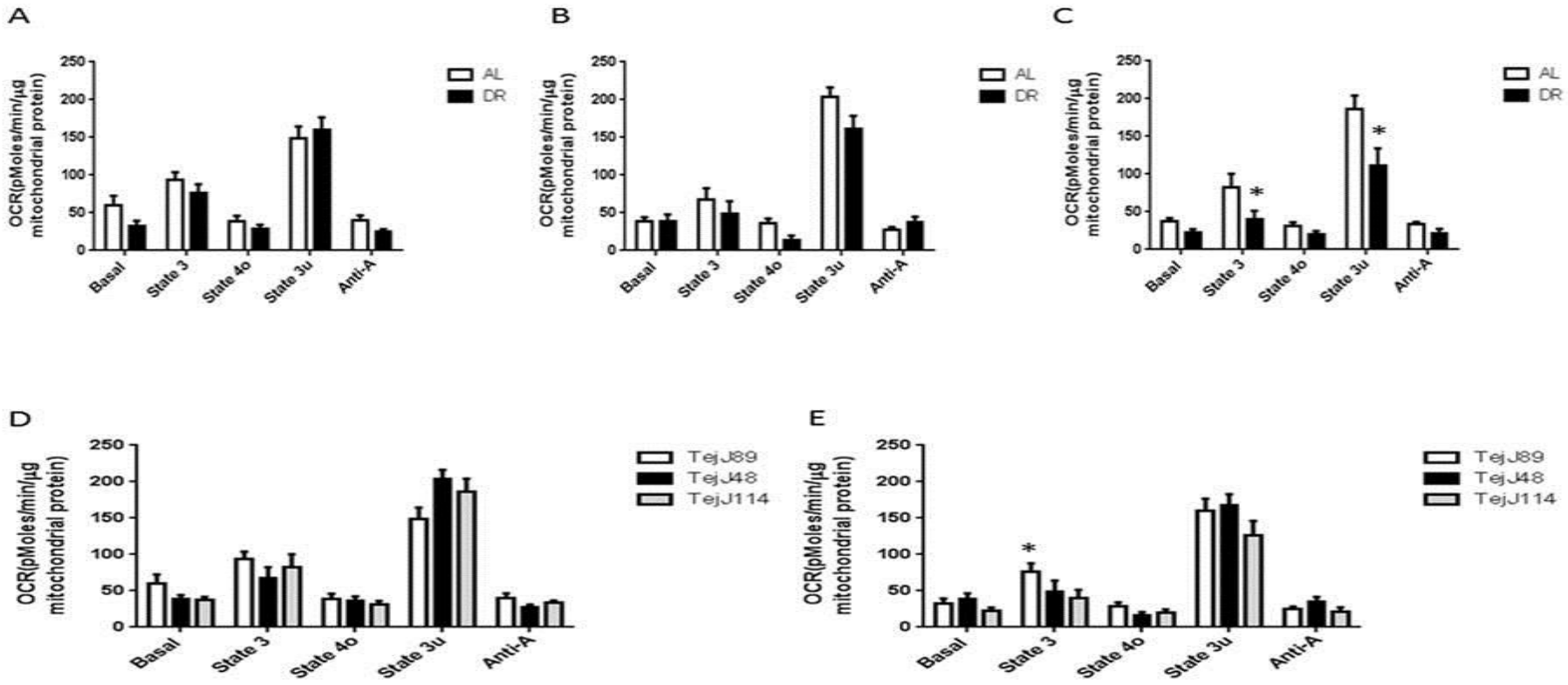

Figure 4.2: Mitochondrial respiration (Oxygen consumption rate, OCR) was unaltered by 10 months of 40% DR in isolated liver mitochondria from strains TejJ89 (A) and TejJ48 (B). In strain TejJ114 (C), a treatment effect was observed, with State 3 and State 3u OCR significantly reduced under DR relative to AL mice. No strain differences on mitochondrial functional was observed in AL mice (D). (E) State 3 respiratory capacity was significantly increased in strain TejJ89 under DR when compared with the other strains under DR. Values are expressed as mean ± SEM, with n = 8 per group. * denotes $p < 0.05$.

Mitochondrial hydrogen peroxide (H_2O_2) production within liver was increased significantly ($t = 3.555$, $p = 0.002$) by DR in strain TejJ89 relative to its appropriate control, but DR had no effect on H_2O_2 production in strains TejJ48 and TejJ114 (Figure 4.3 A). While no difference between strains in H_2O_2 production was observed under AL feeding (Figure 4.3 B), strain TejJ89 had significantly higher ROS levels compared to TejJ48 and TejJ114 under DR, and TejJ48 had significantly higher ROS levels ($t = 2.339$, $p = 0.039$) compared to TejJ114 (Figure 4.3 C). Total hepatic SOD activity was increased by DR treatment in strains TejJ89 ($t = 3.776$, $p = 0.004$) and TejJ114 ($t = 2.845$, $p = 0.010$) relative to their respective AL controls (Figure 4.3 A), but no strain-specific effect on SOD activity was observed under either AL or DR feeding (Figure S2A & B). Liver total glutathione (Figure 4.4 B; Figure S2C and D) and 4-HNE (Figure 4.4 C; Figure S2E & F) were unaffected by either treatment or strain. However, hepatic protein carbonyl (PC) levels (Figure 4 4 D) were significantly increased in strains TejJ89 ($t = 2.420$, $p = 0.037$) and TejJ114 ($t = 2.440$, $p = 0.040$) under DR when compared to their respective AL controls. In addition, while PC levels were not different between strains under AL feeding (Figure S2G), hepatic PC levels were significantly lower in TejJ48 compared to both TejJ89 ($t = 6.860$, $p < 0.001$) and TejJ114 ($t = 3.220$, $p = 0.010$) under DR (Figure S2H). Total hepatic protein levels of PGC-1α (Figure 4.5 A), a key transcriptional co-activator linked to mitochondrial metabolism and biogenesis, was unaltered by treatment or strain, with both nuclear (Figure 4.5 B) and cytoplasmic (Figure 4.5 C) PGC-1α levels likewise unaffected. Similarly, mitochondrial transcription factor A (TFAM), a key activator of mitochondrial transcription, was unaffected by DR or strain (Figure 4.5 D). We then examined various OXPHOS complexes within liver, but again observed no treatment effect or observed any differences between strains under AL or DR feeding (Figure S3A-C). Given the evidence of mitochondrial dysfunction in TejJ114, we then went on to investigate whether DR induced mitonuclear protein imbalance and UPR^{mt} by firstly calculating the ratio of nuclear encoded SDHB to mitochondrially encoded MTCO1 as previously described (Houtkooper et al. 2013). We observed no effect of either treatment or strain on mitochondrial nuclear imbalance (Figure 4.6 A–C). No differences were observed between either treatment groups or strains in the mitochondrial chaperone HSP60 (Figure 4.6 D), but a significant reduction in hepatic HSP90 (Figure 4.6 E) was observed in strain TejJ114 under DR ($t = 2.267$, $p = 0.045$) relative to AL controls.

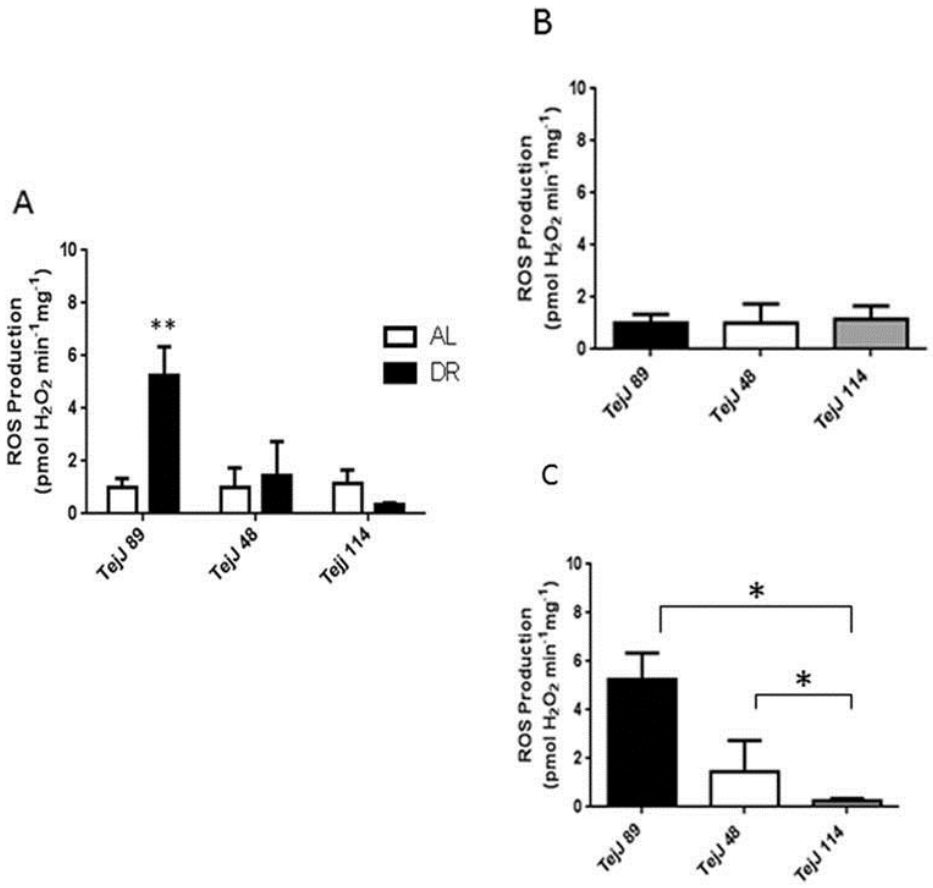

Figure 4.3: Hydrogen peroxide (H_2O_2) production within isolated liver mitochondria, expressed as fold change relative to respective AL controls. (A) H_2O_2 production was increased by DR in strain TejJ89. H_2O_2 production was unaltered between strains under AL feeding (B), but under DR (C) H_2O_2 production was elevated in strain TejJ89 relative to both TejJ48 and TejJ114, and strain TejJ48 produced more H_2O_2 than TejJ114. Values are expressed as mean ± SEM, with n = 6 per group. **$p < 0.001$, *$p < 0.05$.

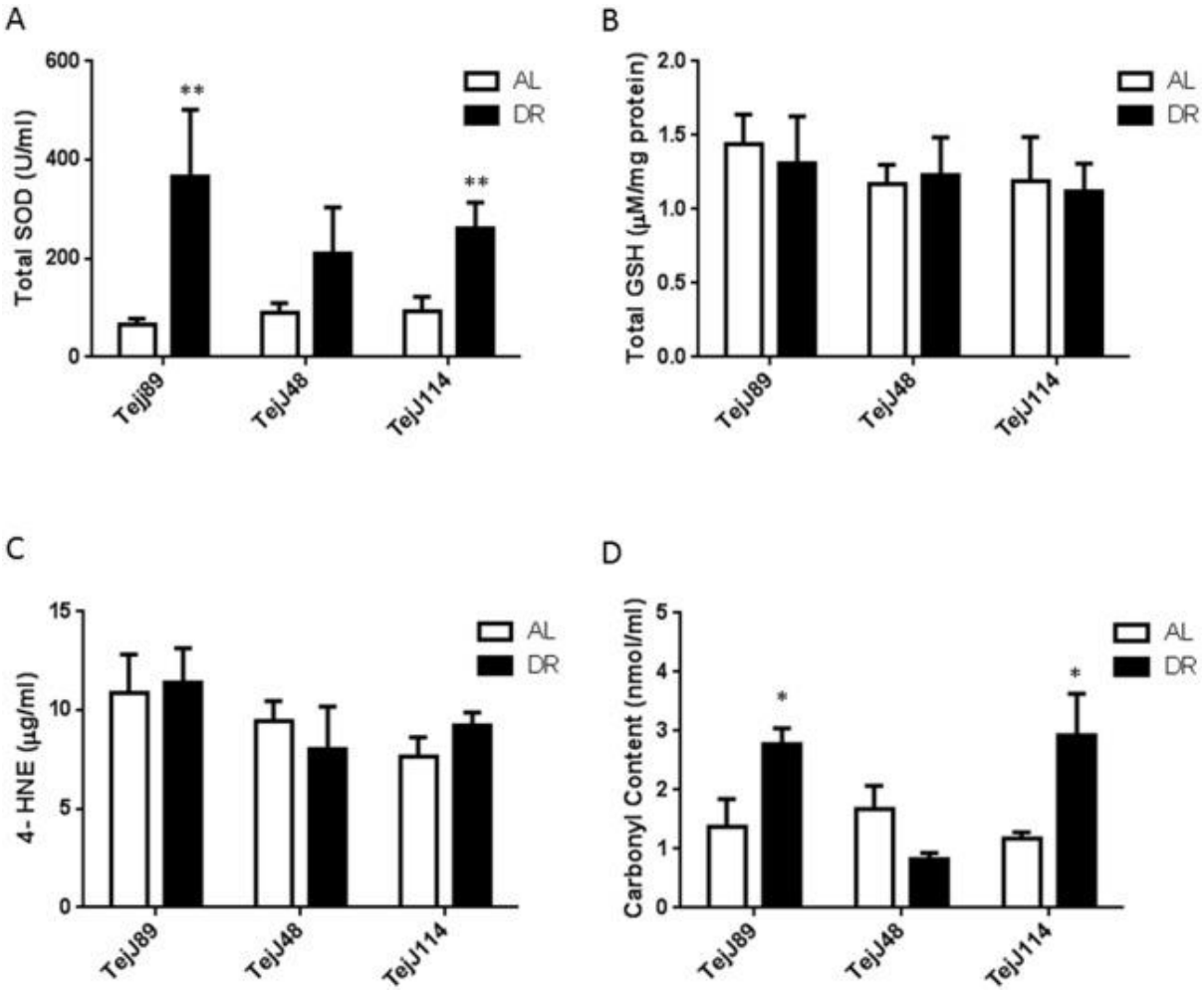

Figure 4.4: Hepatic antioxidant defence and oxidative damage markers. (A) Total SOD activity was significantly increased by DR in strains TejJ89 and TejJ114 relative to their respective AL controls. (B) Total glutathione (GSH) and (C) 4-Hydroxynonenal (HNE) levels were unaffected by treatment or strain. (D) Protein carbonyl (PC) levels were significantly increased by DR in strains TejJ89 and TejJ114 relative to AL controls. Values are expressed as mean ± SEM, where n = 6 per group. **$p < 0.001$, *$p < 0.05$.

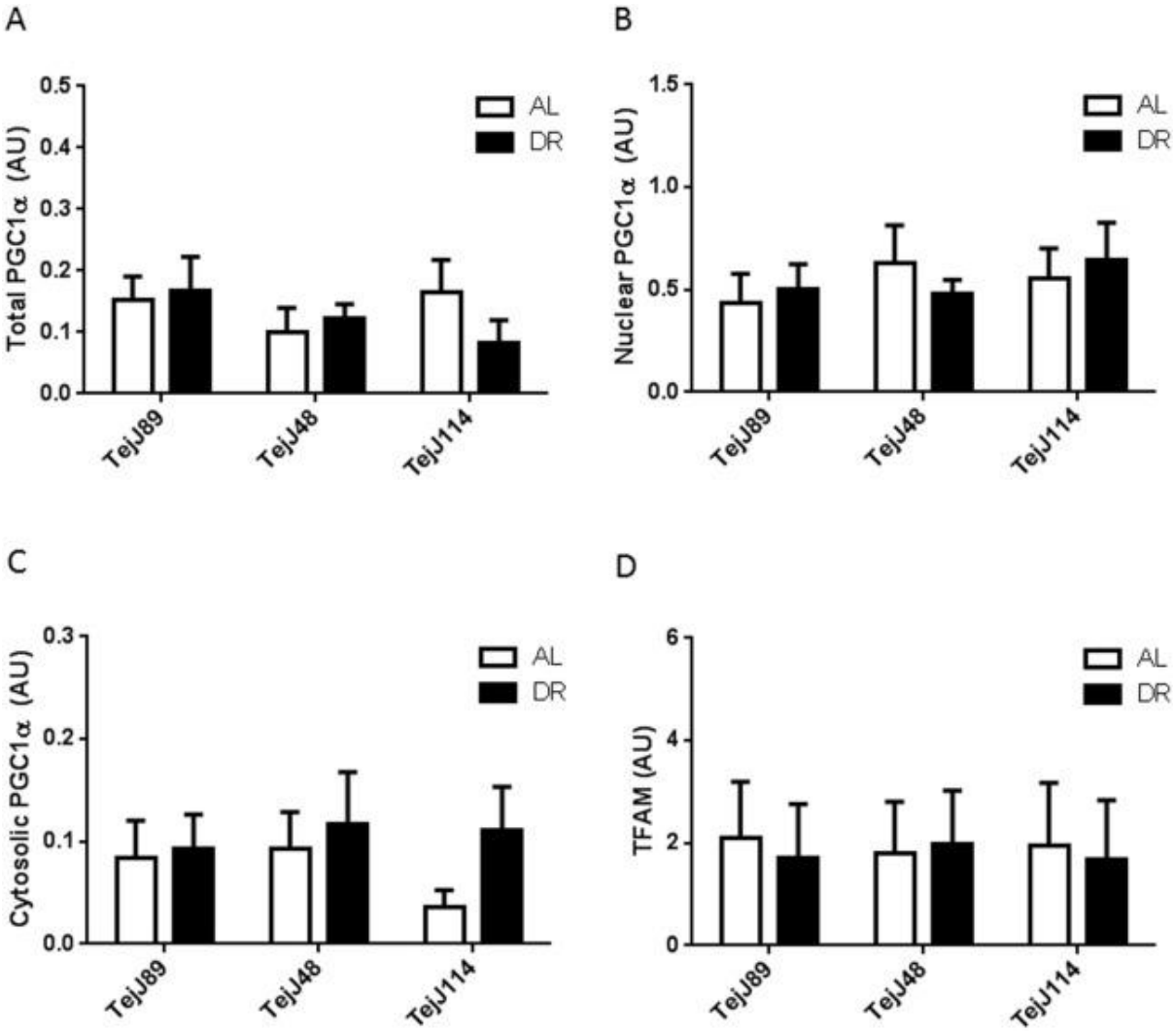

Figure 4.5: Total (A), nuclear (B), and cytosolic (C) hepatic PGC-1α protein levels. No treatment or strain differences in hepatic PGC-1α protein levels were observed (D). DR and strain similarly had no effect on hepatic TFAM levels. Values are expressed as arbitrary units (AU) relative to total protein (determined by Ponceau staining). All values are expressed as means ± SEM, where n = 6 per group.

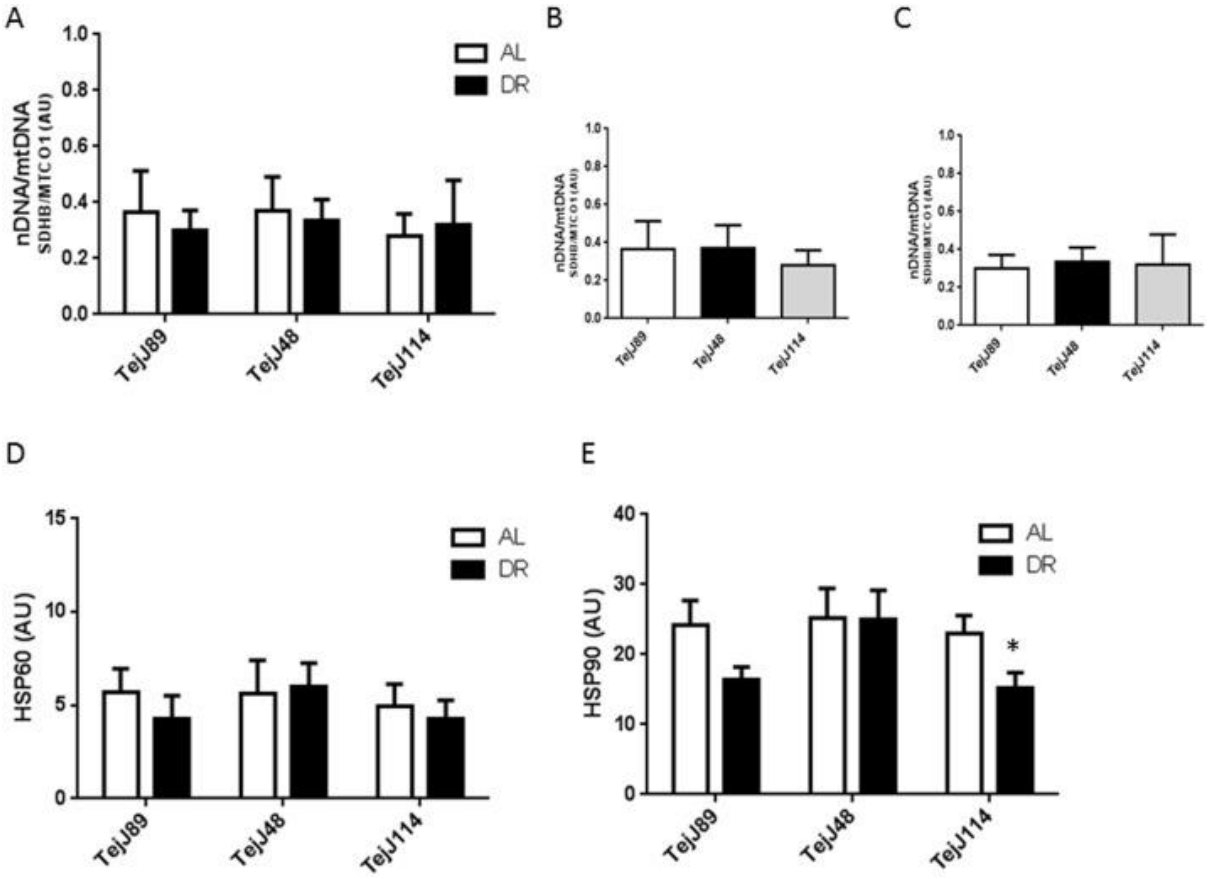

Figure 4.6: Hepatic mitonuclear protein imbalance, expressed as the ratio between the nuclear DNA (SDHB) relative to mitochondrial DNA (MTCO1). (A–C) Mitochondrial protein imbalance was unaffected by treatment or strain. No treatment or strain effects were detected in HSP60 levels (D), however hepatic HSP90 was significantly reduced by DR in strain TejJ114 compared to its AL counterpart (E). No differences in HSP90 levels were observed between strains within the AL or DR treatment groups. Values are expressed as arbitrary units (AU) relative to total protein (determined by Ponceau staining). All values are expressed as means ± SEM, where n = 6 per group. *$p < 0.05$.

In order to determine whether mitochondrial dysfunction in strain TejJ114 was specific to liver, we also examined a number of mitochondrial parameters in isolated skeletal muscle from these same mice. No treatment or strain-specific differences in mitochondrial OCR were observed (Figure 4.7A–E). Similar to liver, total and cytosolic PGC-1α levels in muscle (Figure 4.8 A and C) were unaffected by DR in all strains, although nuclear PGC-1α levels (Figure 4.8 B) were increased by DR in TejJ89 ($t = 3.174$, $p = 0.034$). Skeletal muscle mitochondrial H_2O_2 production was significantly reduced under DR in strain TejJ114 (Mann Whitney $p = 0.009$) (Figure 4.9 A) compared to AL controls, but unaffected by DR in the other two strains. No differences in mitochondrial H_2O_2 production was observed between strains under AL feeding (Figure 4.9 B), but was significantly reduced in TejJ114 under DR relative to TejJ89 ($t = 2.903$, $p = 0.044$) and TejJ48 (Mann Whitney $p = 0.009$; Figure 4.9 C). Protein levels of various OXPHOS complexes and mitonuclear protein imbalance within skeletal muscle were unaffected by treatment and strain (Fig. S3D-F; Figure 4.10A), with similar findings observed in heart (Figure S3G-I; Figure 4.10 B).

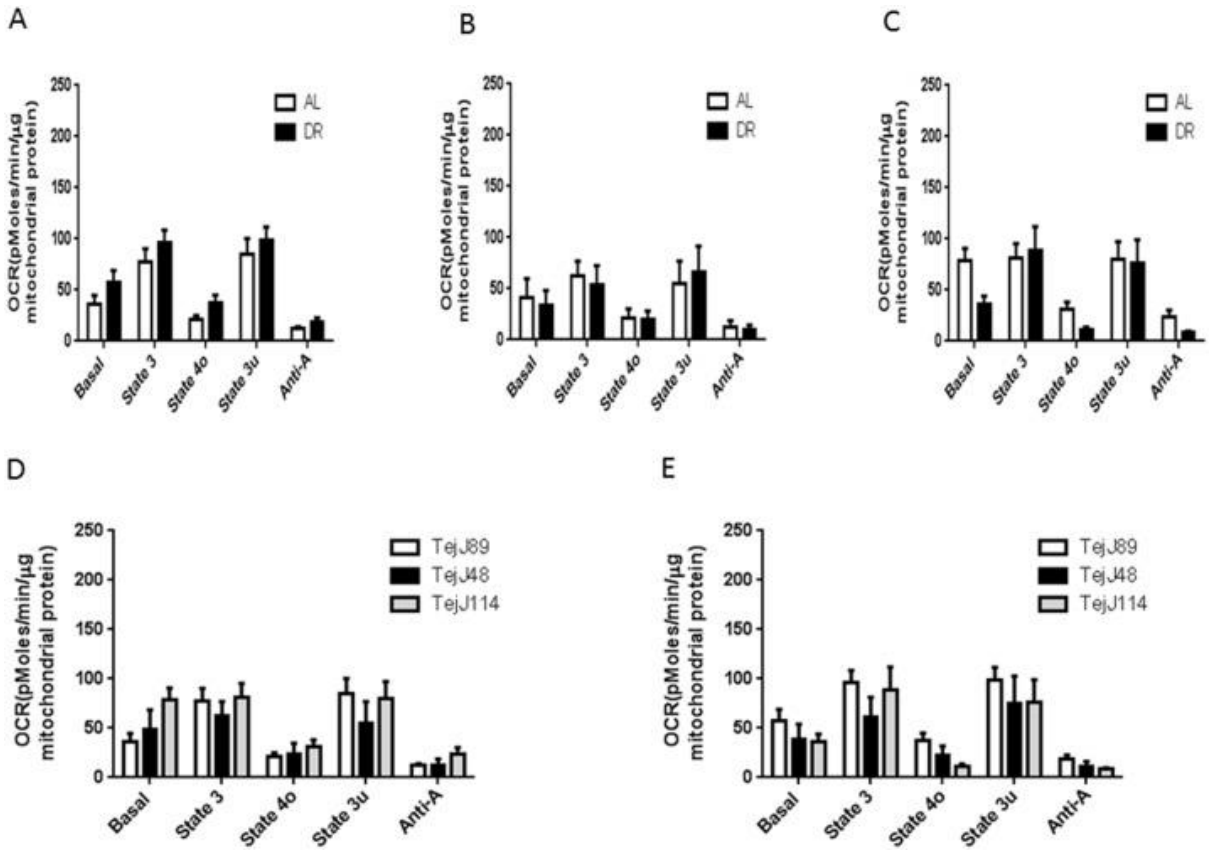

Figure 4.7: Mitochondrial respiration (Oxygen consumption rate, OCR) in isolated skeletal muscle mitochondria was unaltered by 10 months of 40% DR in all strains (A–C). Similarly no differences were observed between strains within the AL (D) or DR groups (E). Values are expressed as mean ± SEM, with n = 8 per group.

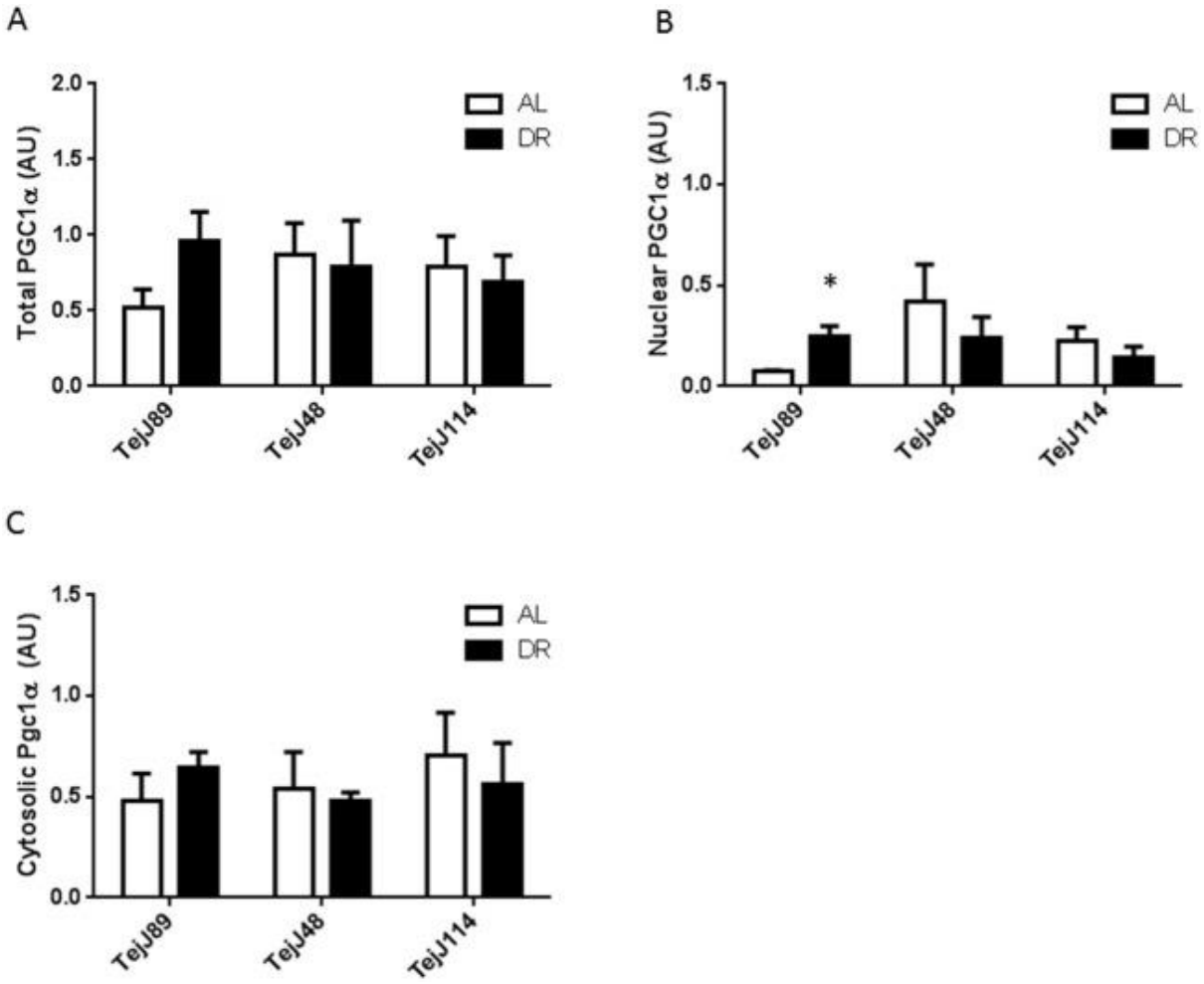

Figure 4.8: Total (A), nuclear (B), and cytosolic (C) PGC-1α protein levels in skeletal muscle. No differences in PGC-1α protein levels were observed by treatment in total (A) or cytosolic (C) skeletal muscle fractions. An increase in PGC-1α was observed in nuclear PGC-1α protein fraction with DR (B). Strain was not found to alter PGC-1α levels in total, nuclear or cytosolic proteins within either the AL or DR treatment group. Values are expressed as arbitrary units (AU) relative to total protein (determined by Ponceau staining). All values are expressed as means ± SEM, where n = 6 per group.

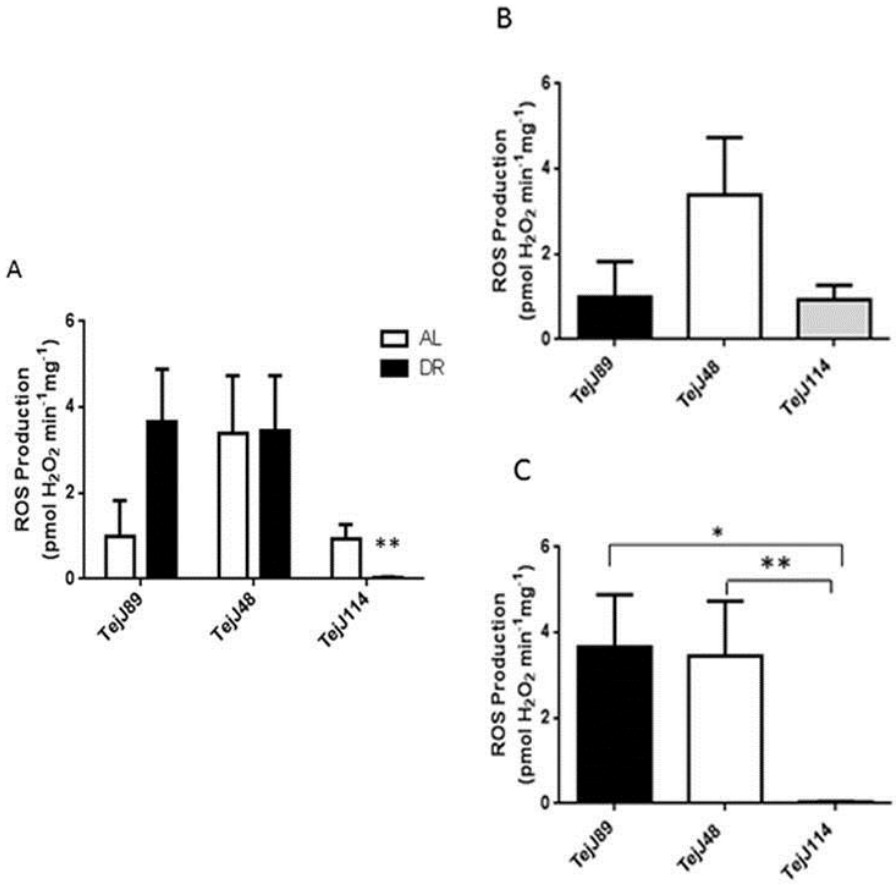

Figure 4.9: Skeletal muscle mitochondrial hydrogen peroxide (H_2O_2 production, expressed as fold change relative to respective AL controls. (A) H_2O_2 production was significantly decreased by DR in strain TejJ114. H_2O_2 production was unaltered between strains under AL feeding (B), but under DR feeding H_2O_2 production was reduced in strain TejJ114 relative to the other two strains (C). Values are expressed as mean ± SEM, with n = 6 per group. **p < 0.001, *p < 0.05.

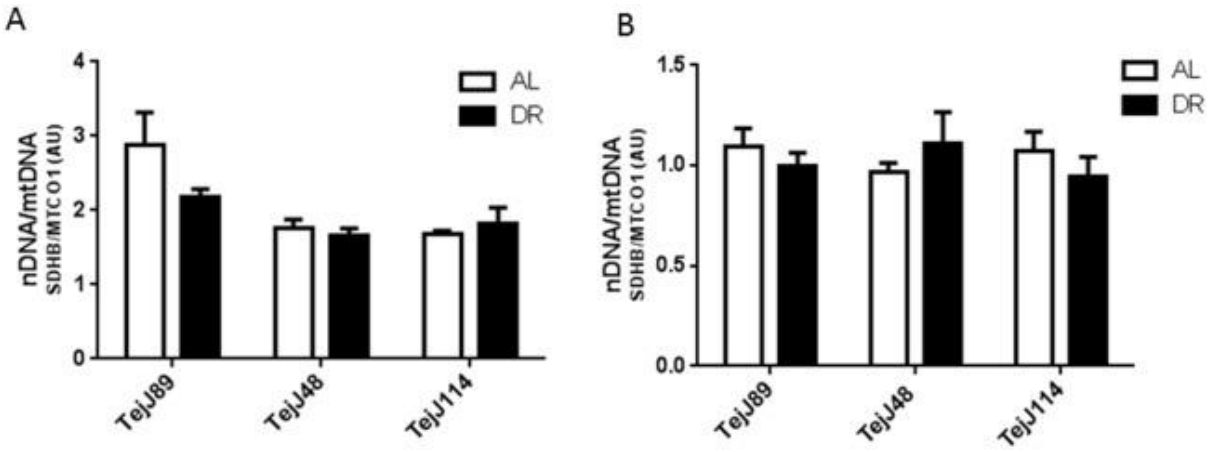

Figure 4.10: Mitonuclear protein imbalance in gastrocnemius (A) and heart (B), expressed as the ratio between the nuclear DNA (SDHB) relative to mitochondrial DNA (MTCO1). No treatment or strains effects were detected. Values are expressed as arbitrary units (AU) relative to total protein (determined by Ponceau staining). All values are expressed as means ± SEM, where n = 6 per group.

4.4 Discussion

The phenotypic plasticity of the mitochondria is crucial to allow energetic demands to be met and in order to sustain bioenergetic efficiency (Hancock et al. 2011; Brand 2005). Consequently impairments in this dynamic system can lead to profound health consequences, with mitochondrial dysfunction widely proposed as a hallmark of ageing (Finley & Haigis 2009; Hunt et al. 2006). As discussed earlier, enhanced mitochondrial function has been put forward as a candidate mechanism underlying the beneficial effects of DR on lifespan and healthspan (Ruetenik & Barrientos 2015; Gouspillou & Hepple 2013). Here we sought to investigate mitochondrial function in using a comparative approach in ILSXISS mice which are known to show significant strain-specific variation in lifespan under 40% DR (Rikke et al. 2010; Liao et al. 2010).

Contrary to our initial predictions, 40% DR did not alter hepatic mitochondrial respiratory capacity in strain TejJ89, which is reported to show lifespan extension under DR. While several studies have reported that DR increases mitochondrial respiratory capacity in rodents (Hempenstall et al. 2012; A. J. Lambert et al. 2004; Nisoli et al. 2005; Lanza et al. 2012), other studies have reported a DR-induced decrease (Bevilacqua et al. 2004; Sohal et al. 1994; Weindruch et al. 1980), or no effect of DR on mitochondrial respiratory capacity (Gredilla et al. 2001; Adrian J. Lambert et al. 2004) relative to AL controls. The precise reasons for this ambiguity appear complex but the tissue studied, the preparation used (isolated mitochondria vs. permeabilised tissue vs. tissue homogenate), the duration, age of onset and level of DR imposed, and the sex, age and the genetic background of the animal may all be important (Hempenstall et al. 2012; Gouspillou & Hepple 2013; Maynard S, Hejl AM, Dinh TS, Keijzers G, Hansen ÅM, Desler C, Moreno-Villanueva M, Bürkle A, Rasmussen LJ, Waldemar G 2015; Lauritzen et al. 2015). Strain TejJ48 under DR, as predicted, displayed essentially no mitochondrial phenotype relative to its AL control. However, in strain TejJ114, mitochondrial respiratory capacity associated with State 3 and State 3u (maximal uncoupled oxygen consumption rates) were significantly reduced under DR. Both ageing and many pathologies associated with ageing reduce mitochondrial respiratory capacities in a range of tissues (Porter et al. 2015; Lee et al. 2016), and the apparent DR-induced hepatic mitochondrial dysfunction may offer new insights as to why DR truncates lifespan in this particular ILSXISS strain. To determine whether the hepatic mitochondrial dysfunction in TejJ114 was liver-specific, we determined mitochondrial respiratory

capacity in isolated skeletal muscle mitochondria in these same ILSXISS mice under AL and DR feeding. While DR is known to preserve mitochondrial function during ageing in certain mouse strains, such as C57BL/6 and male B6D2F1 (Hempenstall et al. 2012; Lanza et al. 2012), we saw no effect of DR on skeletal muscle mitochondrial respiratory capacity in any strain. In view of the well-defined role of PGC-1α in modulating mitochondrial function, and given that mitochondrial adaptations to DR may be driven through a PGC-1α -induced transcriptional program (Anderson et al. 2008; Finley et al. 2012; Gouspillou & Hepple 2013; Corton & Brown-Borg 2005), we investigated protein levels of PGC-1α within liver in each strain under AL and DR. In line with the absence of any effect of DR on mitochondrial respiratory capacity, we observed no increase in hepatic PGC-1α (total, cytosolic, nuclear) or in mitochondrial transcription factor A (TFAM) protein levels of strain TejJ89 under DR. Similarly, PGC-1α and TFAM levels were unaffected by DR in strains TejJ48 or TejJ114. However, a tissue-specific response was observed with 40% DR significantly increasing nuclear PGC-1α within skeletal muscle of strain TejJ89, in line with what has been reported in other studies (For review see Gouspillou & Hepple 2013).

We then employed an immunoblot approach to examine respiratory chain complexes I, II, III, IV and V, and we again observed no treatment effect in any strains for liver, skeletal muscle or in heart. Indeed, it has been reported that DR-induced attenuation of ageing-associated declines in mitochondrial function within skeletal muscle appears to be independent of any effect on mitochondrial respiratory chain protein levels (Lanza et al. 2012) However, this approach enabled us to examine mitonuclear protein imbalance; that is the ratio of nuclear encoded SDHB to mitochondrially encoded MTCO1. An increase in this ratio is associated with an induction in the cytoprotective mitochondrial unfolded protein response (UPR^{mt}), a recently proposed conserved lifespan determinant (Houtkooper et al. 2013). We found no evidence that DR increased mitonuclear protein imbalance within the liver, skeletal muscle or heart of ILSXISS mice under DR feeding. The UPR^{mt} invokes a transcriptional program in response to a number of processes, including mitochondrial dysfunction, resulting in the induction of various chaperones and proteases that help facilitate mitochondrial proteostasis (Schulz & Haynes 2015). We therefore, then examined the molecular chaperones HSP60 and HSP90, and similarly showed a lack of any treatment effect across our strains, except for a significant reduction in HSP90 levels within liver of TejJ114 mice under DR. HSP90

engages with a large number of ‘client’ proteins through co-chaperones, plays a major role in signal transduction, protects the 20S proteasome against oxidative inactivation and may actively regulate mitochondrial metabolism (Castro et al. 2014; Pearl 2016; Franco et al. 2015). Whilst it is difficult to disentangle cause and effect here, our data indicates that in strain TejJ114 40% DR leads to hepatic mitochondrial dysfunction and that this is correlated with reduced HSP90 levels.

It is evident that both ageing and several disease states are associated with greater ROS-induced oxidative damage, but it is equivocal as to whether ROS-induced oxidative damage is the mechanism underpinning ageing and disease (Walsh et al. 2014; Speakman & Selman 2011; Perez et al. 2009). A large number of studies have investigated whether DR can reduce ROS, induce various antioxidants and attenuate oxidative damage in model organisms. In an excellent recent meta-analysis, the Van Remmen laboratory (Walsh et al. 2014) examined several hundred studies that have investigated the effect of DR in rodents on ROS production, various antioxidants and on oxidative damage. Their approach found that DR had remarkably little impact on ROS production or antioxidant activity overall, but 53% of studies reported that DR reduced oxidative damage. Perhaps surprisingly we found that DR in strain TejJ89, which shows lifespan extension under 40% DR, had significantly higher hepatic mitochondrial H_2O_2 production, alongside greater hepatic total SOD activity and higher protein carbonyl levels relative to its appropriate AL control. In addition, TejJ89 had significantly higher hepatic mitochondrial H_2O_2 production relative to the other two strains under DR feeding. Strain TejJ114 had increased hepatic total SOD activity and protein carbonyl levels relative to its AL controls, but mitochondrial ROS levels were not significantly altered. Similarly, the hepatic protein carbonyl levels in line TejJ114 under DR could not be explained by differences in hepatic NADPH oxidase levels (Figure S4). The mitochondrial ROS profile in skeletal muscle was similar in skeletal muscle but H_2O_2 production was significantly reduced by DR in TejJ114 compared to its appropriate control and when compared to the other two strains under DR. Consequently, our findings further question the precise role of ROS-induced oxidative damage being the mechanism underpinning ageing. We can speculate that the increased ROS under DR in strain TejJ89 elicited a beneficial mitohormesis-like effect (Ristow & Schmeisser 2011) resulting in DR-induced longevity, although this remains to be determined and does not appear to involve the UPR^{mt}. As a small aside, it is particularly sobering to note that in the comprehensive meta-analysis on

DR and oxidative stress in rodents undertaken by Walsh *et al.* (Walsh et al. 2014), 96% of all observations were made in male rodents, with the remaining 4% undertaken using females alone or mixed sex populations.

In conclusion, our findings do not completely support our initial predictions (Figure 4.1), in which we forecast a clear continuum from the stimulatory and beneficial effects of DR on the mitochondrial phenotype in positive responding strain TejJ89 through to predicted mitochondrial dysfunction in strain TejJ114 under DR. In the positive responding strain TejJ89 we saw no evidence of a DR-induced increase in mitochondrial respiratory capacity in liver and muscle mitochondria or in PGC-1α levels within liver, although nuclear PGC-1α levels were induced in muscle. Paradoxically, TejJ89 had increased hepatic mitochondrial ROS production, greater SOD activity and higher hepatic protein carbonyl levels under DR, further highlighting the complexity between mitochondrial respiratory capacity, mitochondrial ROS and oxidative damage (Salin et al. 2015). While strain TejJ114 under DR did show evidence of mitochondrial dysfunction within liver relative to AL controls, this effect was tissue-specific as was not observed in skeletal muscle. What is clear is that it will now be important to investigate whether the liver-specific mitochondrial dysfunction observed in strain TejJ114 under 40% DR is evident under less restrictive feedings conditions, i.e. 10–30% DR, as for all these strains we do not currently know where exactly the optimal longevity 'sweet-spot' under DR sits. Our data raises the possibility that DR-induced longevity in ILSXISS mice does not appear to involve mitonuclear imbalance and UPR^{mt}, which appears to be the case in worm DR (eat-2) mutants (Durieux et al. 2011). What is also clear is that almost all we know about the potential mechanisms underlying DR in rodents is based almost exclusively on C57BL/6 mice (Swindell 2012). Consequently, there is a need for more studies using mouse strains in addition to C57BL/6 mice, e.g. ILSXISS, DBA/2, UM-HET3, as these models may help provide new insights in to ageing mechanisms that are public, i.e. shared, across all mouse strains rather than mechanisms that are private, i.e. specific to C57BL/6 mice.

Chapter 5: Enhanced proteostasis as a mechanism underlying DR-induced lifespan– an investigation using ILSXISS recombinant inbred mice

5. 1 Abstract

Enhanced protein synthesis rate is proposed as underlying the pro-longevity effect of dietary restriction (DR). However, debate exists as to whether DR should increase protein synthesis, an energetically costly process, in a time of nutrient scarcity. Alternatively maintenance of proteomic homeostasis (or proteostasis) has been implicated as a shared characteristic of slowed ageing. I hypothesised that proteostatic mechanisms would be increased in mice known to undergo lifespan extension with DR, as is seen in models of slowed ageing, and conversely reduced in mice known to experience lifespan truncation following restriction. In order to investigate the effect of DR on protein synthesis rates I examined the impact of 2 months of 40% DR on protein synthesis rates in female ILSXISS mice that have been shown to exhibit strain-specific variation in lifespan under DR. Using an isotopically labelled marker, deuterium oxide (D_2O), I simultaneously assessed protein synthesis in multiple subcellular fractions along with DNA synthesis in the myofibrillar, mitochondrial and cytoplasmic proteins in skeletal muscle, heart, and liver tissue over 2 weeks in order to gain insight into proteostatic mechanisms. As assessed by the ^{new}protein/^{new}DNA ratio protein synthesis was found to be increased in cytoplasmic, mitochondrial and mixed proteins in the skeletal muscle of all strains following short-term DR. Increases in cytoplasmic proteins in strain TejJ89 were reported suggesting a correlation with DR-induced longevity. However, results were tissue specific, and no evidence of increased synthesis was found in any protein fraction in the heart. Collectively these results did not entirely support my initial predictions, as reduced protein synthesis was not found to be associated with lifespan shortening, and increases in the skeletal muscle in both mitochondrial and myofibrillar proteins were not strain-specific. With the exception of the increase in cytoplasmic proteins in strain TejJ89 skeletal muscle, these results suggest that increased synthesis is not associated the anti-ageing effects of DR, at least following short-term restriction.

5.2 Introduction

Protein homeostasis, or proteostasis, is the ability of an organism to maintain the proteome through a number of intricate networks, and the loss of which is associated with the ageing process (Lopez-Otin et al. 2013). Maintenance of a healthy proteome, involves a number of cellular pathways, collectively referred to as the proteostasis network. (See Figure 5.1) This network involves the coordination of protein synthesis, folding, modification, assembly, breakdown and clearance of damaged proteins (Wolff et al. 2014). These networks act to detect and repair upsets to the proteome, thus restoring a state of homeostasis (Vilchez et al. 2014). Changes to the proteome namely arise through changes in the rate of protein synthesis, the making of new proteins *de novo*, (Alvarez-Castelao et al. 2012), and the ability to alter rate of protein synthesis adaptively is crucial in regulating proteostasis (Alvarez-Castelao et al. 2012; Cajigas et al. 2010). It has been shown that a number of proteostatic mechanisms are enhanced in long-lived animals (Pride et al. 2015), with the these species having the most stable proteomes (Treaster et al. 2014). Furthermore, interventions which enhance components of these proteostatic networks extend lifespan in invertebrate and in mammals (Tonoki et al. 2009; Olsen et al. 2006; Satoh et al. 2013; Labbadia & Morimoto 2015). It has been proposed that the beneficial effects of dietary restriction (DR) are at least partially mediated through improved proteostasis, particularly through increased rate of protein synthesis, and indeed increased protein synthesis has been extensively reported in rodents following DR (Lambert & Merry 2000; Goldspink & Kelly 1984; Jazwinski 2000; Ward & Richardson 1991; de Cabo et al. 2015). However reports of reduced protein synthesis with DR (Henderson et al. 2010), has led to debate over the relevance of increased protein synthesis as an important proteostatic mechanism in the anti-ageing effects of DR.

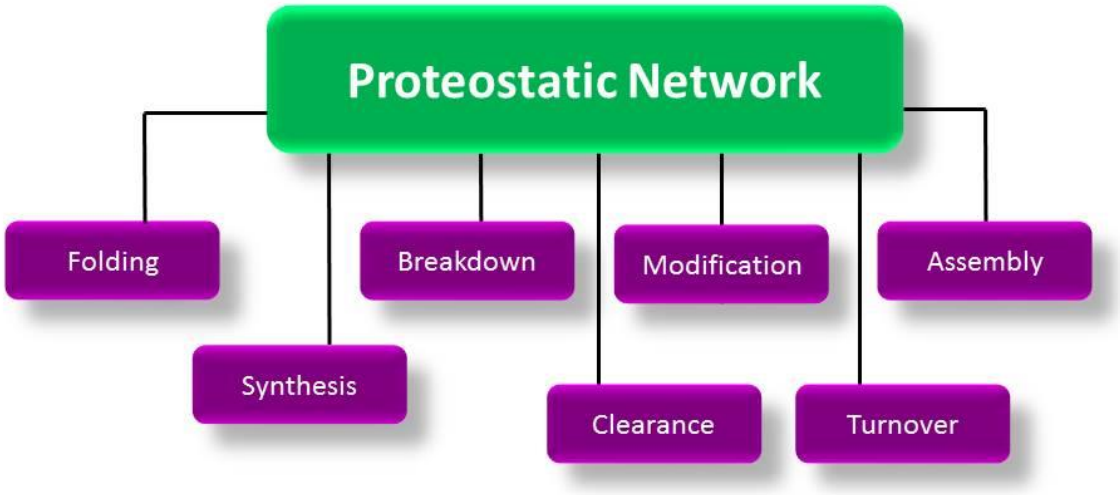

Figure 5.1: The cellular pathways involved in maintaining the proteome.

5.2.1 DR and Protein Synthesis

Two apparently contradictory mechanisms relating to protein synthesis have been proposed as mediating the life-extending effects of DR. Researchers have postulated that increased protein synthesis following DR results in more efficient replacement of damaged proteins, thus leading to lower levels of oxidative damage, through efficient clearing and repairing of damaged proteins (Tavernarakis & Driscoll 2002; Morimoto & Cuervo 2014). Indeed in rodents enhanced protein synthesis has been reported on numerous occasions (Holehan & Merry 1986; Jazwinski 2000; Lambert & Merry 2000; Lewis et al. 1985; Ward & Richardson 1991). Long-term DR (28 months), including in 30 month old male C57BL/6 mice, increased hepatic protein turnover following DR (Hagopian et al. 2003). In monkeys (*Macaca mulatta*) DR reportedly protected against the age-related decline in protein synthesis, but also increased protein synthesis relative to AL controls (Colman et al. 2009), and in human diploid fibroblasts serum from DR animals is known to delay senescence and increase protein synthesis in cultured cells (de Cabo et al. 2015). On the other

hand, DR has been proposed to decrease protein synthesis, with higher rate of protein breakdown, due to lower demand for protein replacement. In keeping with this theory, male C57BL/6 mice following long-term DR, reportedly have reduced rates of protein synthesis in the hepatic tissue (John C Price et al. 2012), and also following long-term DR in the skeletal muscle and heart of male B6D2F1 mice (Miller et al. 2013).

However upon reanalysis, using a new method of assessment, Miller and colleagues came to the opposite conclusion of how DR alters protein synthesis in the male B6D2F1 mouse. Initially no alterations in rates of mitochondrial protein synthesis (Miller et al. 2012), cytoplasmic or myofibrillar (mixed) proteins in heart or liver tissue were reported following DR (Miller et al. 2013; Miller et al. 2012). Within any given tissue, protein content will reflect a dynamic turnover between protein degradation and synthesis (Poortmans et al. 2012), such that large increases in protein breakdown are likely to be matched by an increased rate of protein synthesis, in order to ensure the proteome remains in a state of homeostasis. Consequently measurement of synthesis rates in isolation could be perceived as unchanged, and increases in protein synthesis may go undetected (Miller et al. 2014). To circumvent this Miller *et al* propose instead to compare quantity of protein synthesised in relation to the rate of cellular proliferation (measured as synthesis of DNA). Thus the ratio between new protein synthesis to new DNA synthesis (^{new}protein/^{new}DNA) gives a reflective measure of the ongoing synthesis and breakdown of proteins and thus a more accurate representation of changes in proteostasis. When determined by the ^{new}protein/^{new}DNA ratio, short (1 week) and long-term (6 weeks) 40% DR is found to increase protein synthesis in all subcellular fractions assessed, including cytoplasmic, myofibrillar and mitochondrial proteins, in both the heart and skeletal muscle of male B6D2F1 mice (Miller et al. 2013; Drake et al. 2015). Moreover, following treatment with rapamycin, a DR mimetic associated with lifespan extension (Drake et al. 2013), and in the Snell long-lived mouse model (Drake et al. 2015) heart and skeletal muscle were also found to have increased rates of protein synthesis, suggesting enhanced proteostatic mechanisms to be a shared feature of slowed-ageing.

Mitochondrial dysfunction is a hallmark of ageing (Lopez-Otin et al. 2013) and may be related to the decrease in synthesis rates of mitochondrial proteins observed by middle age in humans (Rooyackers et al. 1996). Synthesis of mitochondrial proteins however, termed mitochondrial biogenesis, is poorly defined and debate

has arisen as to how best to quantify mitochondrial biogenesis (Miller & Hamilton 2012; Miller et al. 2016; Hancock et al. 2011) (See Table 5.1 for list of different methods of mitochondrial biogenesis quantification in DR studies) For example, mitochondrial biogenesis is often determined through quantification of mRNA or mtDNA (Nisoli et al. 2005; Civitarese et al. 2007), however increases in mRNA content does not equate to increased protein abundance (Mootha et al. 2003), nor do changes in signalling proteins necessarily mean a change in biogenesis (see Miller & Hamilton 2012 for full discussion). Mitochondrial biogenesis is the generation of new mitochondrial proteins (Ryan & Hoogenraad 2007), increases to which are proposed as underlying the beneficial lifespan effects of DR. However ambiguity exists regarding the effect of DR on mitochondrial biogenesis with DR reported to increase (López-Lluch et al. 2006; Nisoli et al. 2005; Civitarese et al. 2007), or have no effect (Lanza et al. 2012; Hancock et al. 2011) in comparison to AL controls. The ^{new}protein/^{new}DNA ratio however may be one means to more accurately determine changes in synthesis.

Table5.1 Summary of DR on markers of mitochondrial biogenesis

Author	Genotype	Sex	DR	Duration	Tissue	Method	Result
Lanza et al 2012	B6D2F1 Mouse	♂	40% Onset 24months of age	10 days	Sk. M	mtDNA Protein content Stable isotope labelling	↓
Hancock et al 2011	Wistar Rat	♂	30%	14 weeks	Sk. M Heart Brain Liver Adipose tissue	mRNA analysis of mito proteins	No change
Nisoli et al 2005	C57BL/6 eNOS(-/-) mouse	♂	40%	3 or 12 months	WAT	mtDNA abundance mRNA expression of mito genes	↑
Hempenstall et al 2012	C57BL/6 mouse	♂	30%	1, 9 or 18 months	Sk.M	Protein Content; PGC1a, mRNA expression mito genes	No change
Miller et al 2012	B6D2F1 Mouse	♂	40%	4 Hours or 6 weeks	Sk.M Liver Heart	D2O	↑*
Miller et al 2012	B6D2F1 Mouse	♂	40% @ 6/12/24 months of age	6 weeks	Sk.M Liver Heart	D2O	↑*
Mulvey et al 2016	ILSXISS TejJ89, TejJ48, TejJ114 mice	♀	40% @ 12 weeks of age	10 months	Sk. M Liver Heart	Protein content; PGC1-α	↑ Sk. M –nuclear proteins only* Liver ns Heart ns
Civitarese et al 2007	Humans	♂ & ♀	25% Mix of CR and increased exercise	6 Months	Sk.M	mRNA expression of mito genes	↑

↓= Reduced mitochondrial biogenesis with DR

No change= No effect of DR on mitochondrial biogenesis

↑= increased mitochondrial biogenesis with DR**↑*=Increased mitochondrial biogenesis as assessed by the new protein to DNA synthesis ratio**

5.2.2 Deuterium Oxide as a means of assessing proteostasis

Increased protein synthesis following DR has often been reported following flooding doses of an essential amino acid such as phenylalanine, valine or leucine (Goldspink & Kelly 1984; Lewis et al. 1985; el Haj et al. 1986; Merry et al. 1987; Zangarelli et al. 2006; Dai et al. 2014). However, this method may stimulate a feeding response and thus may reflect an acute response to AA flooding, rather than long-term synthesis rates. An alternative method to measure synthesis involves using a labelled precursor, such as isotopically labelled water, deuterium oxide (D_2O). D_2O has free access to all body pools and equilibrates throughout all tissues rapidly (Busch et al. 2006; Neese et al. 2002; Hellerstein & Murphy 2004). Body water is enriched over an extended period of time, typically 2 weeks, and therefore offers a long-term labelling design, which is beneficial for study changes which occur with DR. D_2O is an ideal precursor as hydrogen from water is associated with most biosynthetic processes, and the equilibrated water is therefore incorporated into a variety of tissues and proteins.

5.2.3 ILSXISS mice

Whilst DR was once considered a ubiquitous means of extending lifespan, recent evidence suggests that this may not always be the case. DR fails to extend longevity in some animals (Cooper et al. 2004; Kirk 2001) and mouse strains (Fernandes et al. 1976; Forster et al. 2003; Goodrick et al. 1990; Harper et al. 2006; Harrison & Archer 1987). Indeed, genotype has emerged as a potentially important determinant of both the extent and direction of the DR longevity effect (Rikke et al. 2010; Liao et al. 2010; Mitchell et al. 2016). In two independent lifespan analysis of genetically heterogeneous recombinant inbred (RI) mouse strains, it was found that the strains exhibit extensive genetic variation in the lifespan response to DR (Liao et al. 2010; Rikke et al. 2010), ranging from lifespan lengthening to lifespan shortening. The strain-specific lifespan variation of the ILSXISS RI lines allows lines to be classified according to DR response (see Swindell 2012; Mulvey et al. 2014 for discussion). To this end, we employed a comparative approach with three strains of female ILSXISS, shown to have a repeatable lifespan response in two independent DR studies (Rikke et al. 2010; Liao et al. 2010). One line of positive responders; TejJ89 (undergo lifespan extension with DR), non-responders; TejJ48 (no lifespan effect with DR), and a line of negative responders; TejJ114 (truncation of lifespan with DR) were used comparatively assess proteostasis as a mechanism

involved in DR-induced lifespan extension. The examination of subcellular fractions; mitochondrial, cytoplasmic and myofibrillar, synthesis rates in skeletal muscle, heart and liver allows a comparison of tissues representative of post-mitotic, semi-mitotic and mitotic to more fully evaluate the effect of DR on proteostatic mechanisms (Miller et al. 2014; Miller et al. 2012). As the impact of DR on increased proteostasis is ambiguous we sought to investigate the association between DR and increased lifespan and to provide insight into the role of proteostasis as a candidate mechanism of lifespan extension with DR.

5.3 Methods

5.3.1 Animals and Experimental Design

Female mice from three strains of ILSXISS RI mice with established lifespan responses to 40% DR (Rikke et al. 2010; Liao et al. 2010) were used; TejJ89 (lifespan extension with 40% DR), TejJ48 (no change to lifespan) and TejJ114 (lifespan reduction) and were maintained as described in detail in Chapter 2 section 2.1.2. Briefly, at 9 weeks of age eight animals from each strain were assigned to an AL or DR feeding regime within each strain. DR was introduced in a graded fashion, as described in Chapter 2, with full restriction of 40% implemented at 12 weeks of age, based on the AL counterparts intake from the previous week. Mice were maintained on an AL or DR feeding regime for a period of 2 months, equivalent to 5 months of age.

At 5 months of age AL and DR mice (n=8 per group) were fasted overnight, in a fresh cage, with AL access to normal drinking water. DR mice were given an initial intraperitoneal injection (IP) of 99% $^{2}H_2O$ to rapidly enrich the pool of body water pool (assumed 60% of body weight) to 5% deuterium, and then enrichment was then maintained by *ad libitum* access to drinking water enriched with 8% $^{2}H_2O$ for a 2-week labelling period (Miller et al. 2012; Neese et al. 2002). Following the 2-week enrichment period, the mice were fasted overnight and then culled under Home Office regulations following CO_2 inhalation. Plasma via blood from cardiac puncture blood was collected and spun down (as described in Chapter 2; 2.1.2) and the resultant plasma stored at −80°C. The heart, liver and the gastrocnemius muscles were collected snap frozen in liquid nitrogen and subsequently stored at −80°C. Bone marrow was collected, and used to calculate synthesis rates over the 2 week labelling period by comparing bone marrow, essentially representing a fully turned over population of cells and therefore a precursor to the enrichment, with tissue from the same animal (Miller et al. 2012; Miller et al. 2013). Bone marrow from the femur was collected by removing both ends of the bone shaft with scissors, leaving the femur cavity exposed. The femur was held over fresh Eppendorf and the cavity was flushed with 1 ml of phosphate buffered saline using a 3cc syringe with a 25 gauge needle. The resultant material collected in the Eppendorf was immediately stored at -20°C. Samples were subsequently shipped on dry ice to the Translational Research on Aging and Chronic Disease Laboratory at Colorado State University for analysis (See Figure 5.1 for experimental design).

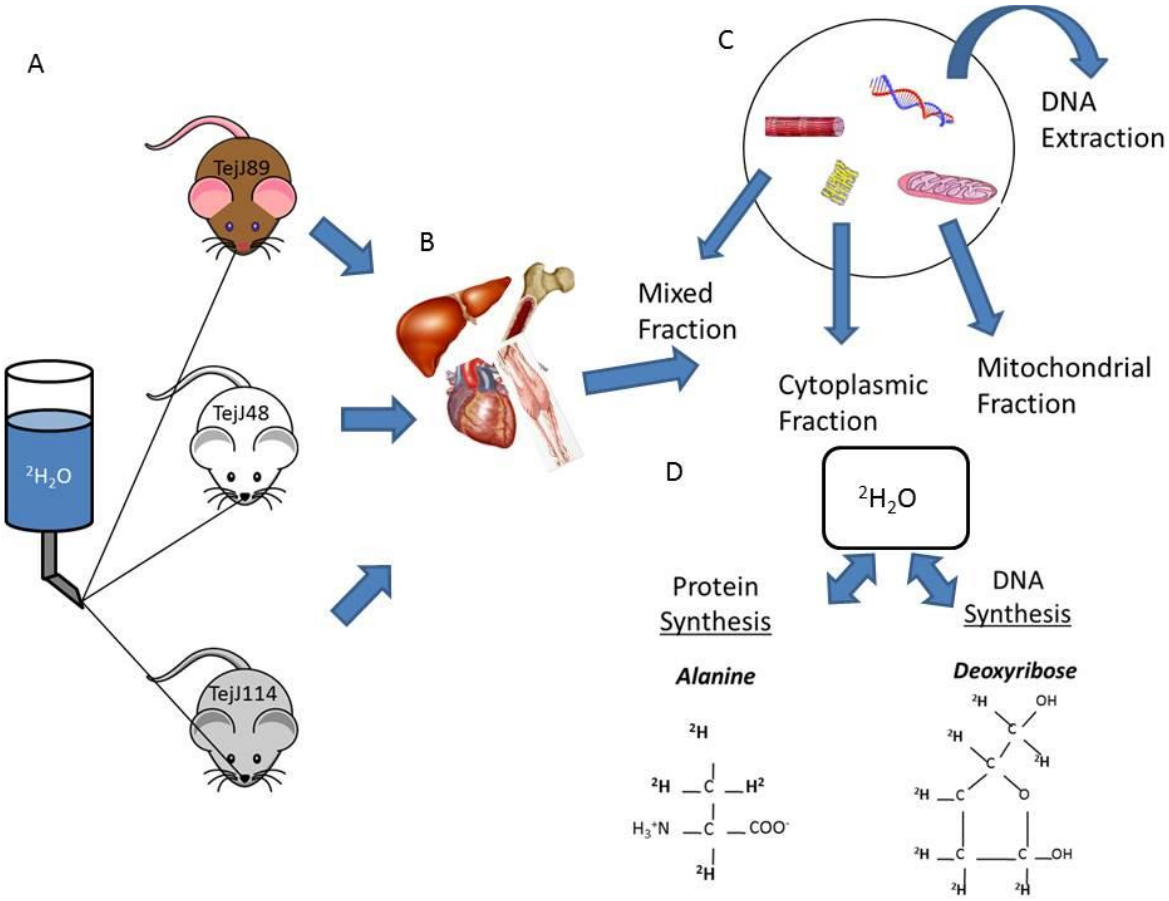

Figure 5.2: Schematic of experimental design used to determine the synthesis of DNA and protein at 5 months of age (following 2 months of ad libitum (AL) or 40% dietary restricted (DR) feeding). (A) (^2H_2O) was administered through AL access to drinking water for 2 weeks following IP injection. (B) Liver, heart, gastrocnemius and bone marrow were collected and (C) through a series of differential centrifugation steps and DNA extraction procedure, DNA was extracted and tissue separated into the mixed (myofibrillar; consisting of primarily of contractile proteins in the heart and skeletal muscle), cytoplasmic and mitochondrial protein fractions. (D) It was possible to measure the rates of newly synthesised proteins and DNA, assessed through the incorporation of deuterium from body water (Adapted from Miller and Hamilton 2014).

5.3.2 Protein isolation

Fractionation of heart, liver and skeletal muscle tissue was carried out according to a series of differential centrifugation steps, as described in previously published protocols (Robinson et al. 2010; Miller et al. 2012). All steps were taken under the supervision of, and with the assistance of collaborators at Colorado State University (CSU), CO, USA. Tissues were powdered using a pestle and mortar, under liquid nitrogen. Tissue was weighed out (50-70mg) and homogenised, using a bead homogenizer (Next Advance Inc., Averill Park NY), 1:10 in isolation buffer (100 mM KCl, 40 mM Tris HCl, 10 mM Tris Base, 5 mM MgCl2, 1mM EDTA, 1mM ATP, pH=7.5) with phosphatase and protease inhibitors (HALT, Thermo Scientific). Subcellular fractions of mixed (Mixed; consisting of nuclei, plasma and of essential contractile proteins (heart and skeletal muscle)), cytosolic (Cyto; other cytosolic organelles with the exception of mitochondria and nuclei) and mitochondrial (Mito) proteins were isolated following homogenisation as previously described (Miller et al. 2012; Drake et al. 2015; Busch et al. 2006).

5.3.3 DNA isolation

For DNA, ~8 µg of total DNA was extracted following the manufacturer's protocol (MiniDNA kit, Qiagen) from approximately 30 mg tissue. This process involved leaving the tissue overnight in lysis buffer at 37°C to access DNA in the nucleus. The sample was prepared, loaded to a spin column, and centrifuged, through a series of purification steps. The DNA was eluted, to ensure the removal of nuclei from the spin column, into 200µl TE buffer (10 mM Tris, 1 mM EDTA, pH 8.0) and stored at -20°C until preparation for analysis via GC/MS. Bone marrow suspension was centrifuged for 10 minutes at 2,000 x g. The pellet was treated using the same protocol employed for tissue DNA isolation.

5.3.4 Sample preparation and analysis via Gas chromatography–mass spectrometry

5.3.4 (A) Protein

To hydrolyse the protein samples, 3ml (Cyto and Mix) or 750 µl (Mito) of 6N HCL was added to 13X100 glass tubes, followed by incubation for 24 h at 120°C.

All subsequent steps described for this protocol were carried out by collaborators at CSU.

The hydrolysates were ion exchanged, dried under vacuum and resuspended in 1 ml molecular biology grade H_2O. Derivation of 500 µl of suspended samples (500 µl acetonitrile, 50µl 1M K2HPO4 (pH 11), and 20 µl of pentafluorobenzyl bromide (Pierce Scientific, Rockford, IL)) was carried out, samples were sealed and left to incubate for 1h at 100°C. Ethyl acetate was used to extract derivatives. Through drying by N_2 and subsequent vacuum centrifugation, the organic layer was removed, and samples were reconstituted in 1 ml of ethyl acetate prior to GC/MS analysis and then analysed as previously described.

5.3.4 (B) Body Water

To determine body water enrichment, 125 µl of plasma was placed into the inner well of o-ring screw on cap and placed inverted on heating block overnight. Next, 2 µl of 10 M NaOH and 20 µl of acetone were added to all samples and 20 µl 0%–20% D_2O standards and capped immediately. Samples were vortexed at low speed and kept overnight at room temperature. Samples were extracted with addition of 200 µl hexane, and the organic layer was transferred through anhydrous Na_2SO_4 into gas chromatography vials and analysed via EI mode using a DB-17MS column.

5.3.4 (C) DNA synthesis measurement

Determination of ^2H incorporation into purine deoxyribose (dR) of DNA was performed, as previously described (Drake et al. 2015; Neese et al. 2002; Miller et al. 2013). Briefly, nuclease S1 and potato acid phosphatase was used to hydrolyse DNA isolated from whole tissue at 37°C overnight. Pentafluorobenzyl hydroxylamine and acetic acid were reacted with hydrolysates and then acetylated with acetic anhydride and 1-methylimidazole. Dichloromethane extracts were dried, resuspended in ethyl acetate, and analysed by GC/MS as previously described (Miller et al. 2014; Neese et al. 2002; Miller et al. 2013). The fractional synthesis rate (f) was calculated by using DNA from bone marrow since this pool is essentially fully turned over population and indicative of the true precursor enrichment (Miller & Hamilton 2012; Miller et al. 2013).

5.3.5 New protein to new DNA synthesis ratio

From the synthesis rates of protein and DNA, a protein synthesis to DNA synthesis ratio was calculated as this has been suggested to be indicative of

changes in proteostasis. This ratio illustrates how much new protein is made in relation to the rate of cellular proliferation (new DNA) during the labelling period (Miller et al. 2014; Drake et al. 2015).

5.3.6 Statistical Analysis

Statistical analysis was performed using PRISM. Differences between treatment (AL and DR) and Strain (TejJ89, TejJ48 and TejJ114) were compared using a two-way analysis of variance (ANOVA), but checked by linear model for consistency with analysis in previous chapters. When a significant difference was detected, post hoc analysis was performed with a Tukey multiple comparison test. Significance was set at $p<0.05$ and data are presented as means ±SEM.

5.4 Results

Protein Synthesis

5.4 (A) DR and protein synthesis in Skeletal Muscle

A significant treatment effect on protein synthesis rates in skeletal muscle (whole gastrocnemius homogenate) was observed, with reductions detected, in all subcellular fractions following short-term DR (Figure 5.2 (A) Mito: $F = 19.00$, $p < 0.001$, Figure 5.3 (A) Cyto= $F = 8.426$, $p = 0.005$ and Figure 5.4 (A) Myo: $F = 21.22$, $p< 0.001$). Strain TejJ89 was found to have reduced protein synthesis relative to AL controls in both the Mito ($p<0.01$) and Myo ($p<0.01$) protein fractions (Figure 5.2 A and 5.4 A). Strain was also found to have a significant effect on protein synthesis rate in both the Mito ($F = 4.918$, $p= 0.011$) and the Myo ($F= 4.712$, $p= 0.013$) subcellular fractions, with no detectable strain effect observed in the Cyto fraction. A one-way ANOVA was carried out, independent of treatment, both within the AL and DR mice in the Mito and Myo fractions, in order to determine direction of strain-effect. No strain-effect was observed within the AL mice for either the Mito (Figure 5.2 B) or Myo fraction (Figure 5.4 B). Strain was found to have a significant effect however, within the DR mice in both the Mito ($F= 3.782$, $p= 0.036$) and the Myo ($F=5.890$, $p=0.007$). In the Mito fraction (Figure 5.2 C) strain TejJ89 had significantly lower rates of protein synthesis compared to TejJ48 following short-term DR. In the Myo fraction (Figure 5.4 C) synthesis was significantly reduced in strain TejJ89 compared with both TejJ48 ($p<0.01$) and TejJ114 ($p<0.05$).

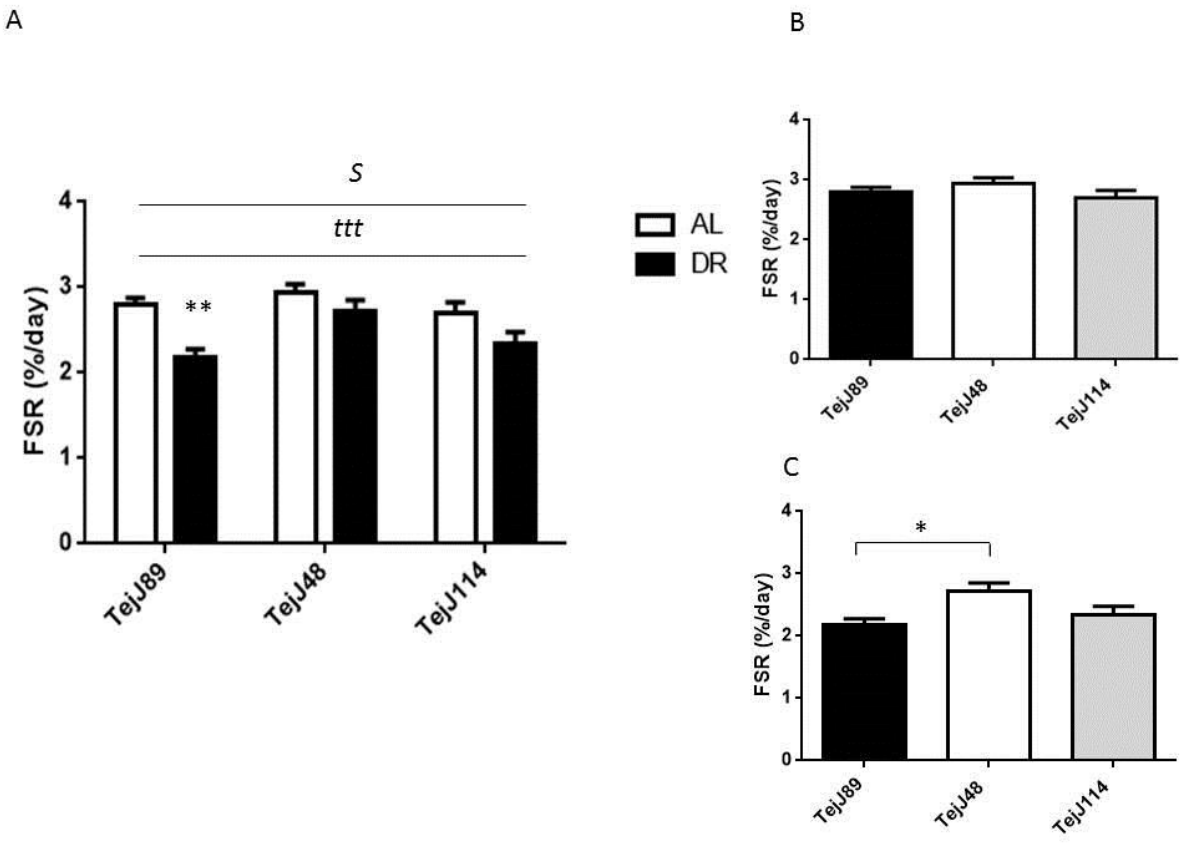

Figure 5.3: Protein fractional synthesis rates (FSR) in the Mito subcellular fraction of skeletal muscle in three strains of female ILSXISS mice maintained on 40% DR or AL feeding for 2 months. (A) Significant effect of treatment and strain on FSR was observed on mitochondrial protein synthesis. (B) No strain effect was detected within the AL mice. Within the DR TejJ89 had reduced protein synthesis relative to TejJ48 (C). Values are means ± SEM, n = 8 per group (both AL and DR), *= AL vs DR p<0.05*, p<0.01**, *t*= treatment effect; $p<0.001^{ttt}$, *S*= strain effect; $p<0.05^{S}$

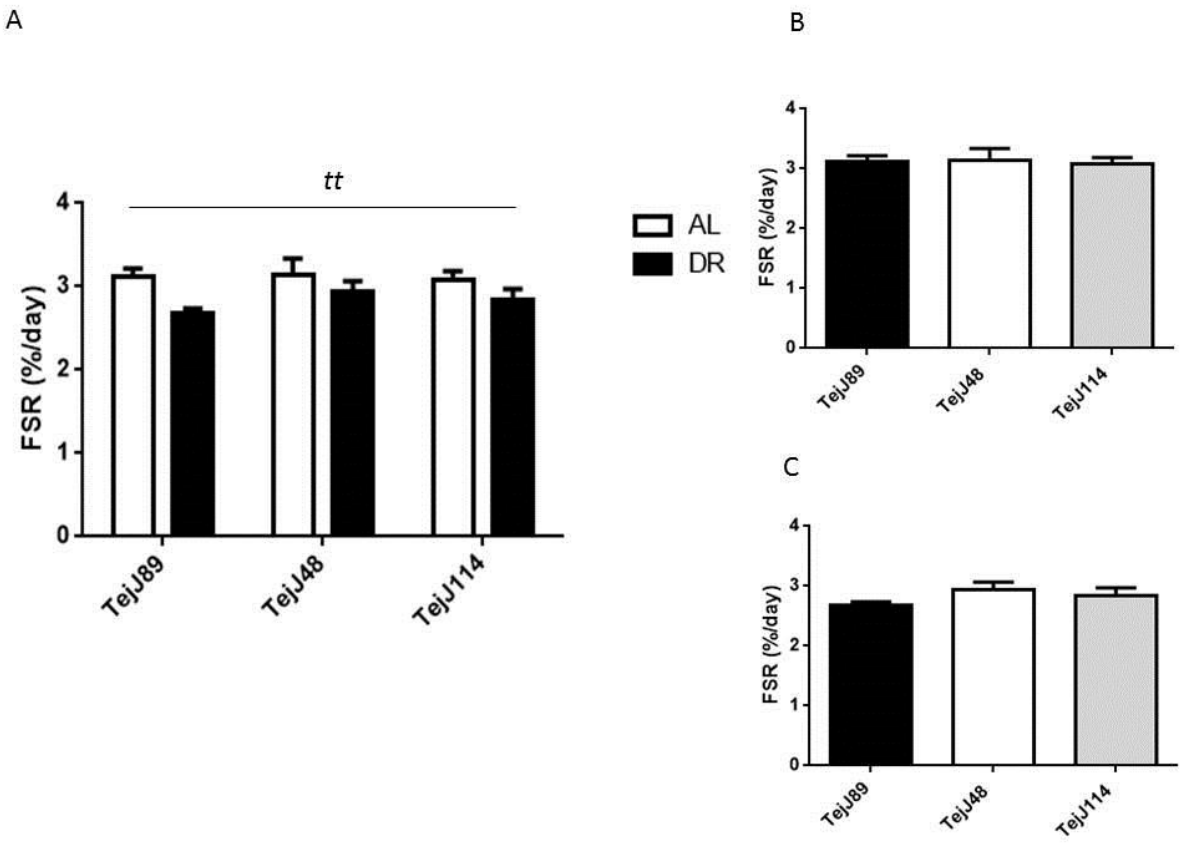

Figure 5.4: Protein fractional synthesis rates (FSR) in the Cyto subcellular fraction of skeletal muscle in three strains of female ILSXISS mice maintained on 40% DR or AL feeding for 2 months. (A)Treatment was found to have a significant effect on FSR in the Cyto fraction in skeletal muscle, with no strain effect detected in either AL (B) or DR (C) mice. Values are means ± SEM, n = 8 per group (both AL and DR), *t*= treatment effect; $p<0.01^{tt}$.

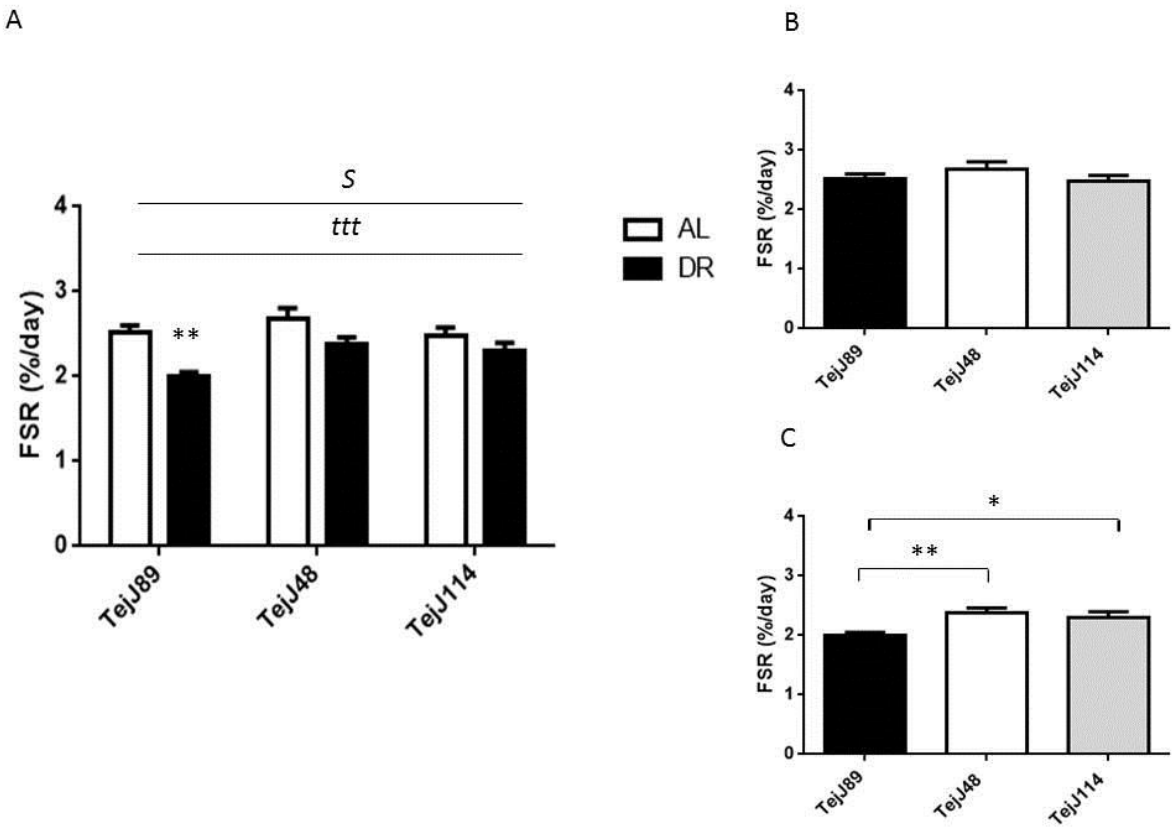

Figure 5.5: Protein fractional synthesis rates (FSR) in the Myo subcellular fraction of the skeletal muscle in three strains of female ILSXISS mice maintained on 40% DR or AL feeding for 2 months (A) A significant treatment and strain effect was observed in the Myo FSR, with reduced rates of protein synthesis in TejJ89 with DR, relative to AL controls. (B) No strain effect was apparent within the AL mice of the Myo fraction, however a significant effect of strain was detected within the DR mice (C), with reduced synthesis in TejJ89. Values are means ± SEM, n = 8 per group (both AL and DR),* denotes p<0.05*, p<0.01**, *t*= treatment effect; $p<0.001^{ttt}$, *S*= strain effect; $p<0.05^{S}$.

5.4 (B) DR and protein synthesis in Heart

In the heart there were no detectable treatment effects on any subcellular fraction (Mito; Figure 5.5 A, Cyto; Figure 5.6 A, Myo; Figure 5.7 A). No significant strain-effect was observed in either the Mito or Myo fractions. However, significant strain- effect was observed in the cytoplasmic fraction ($F = 5.448$, $p= 0.006$). Independent of treatment, no strain effect was apparent within the AL mice in any of the subcellular fractions (Mito; Figure 5.5 B, Cyto; Figure 5.6 B, Myo; Figure 5.7 B). Within the DR mice a strain effect was detected in the Cyto ($F=5.448$, $p=0.006$), with strain TejJ48 having increased synthesis rates relative to strain TejJ114 (Figure 5.6 C).

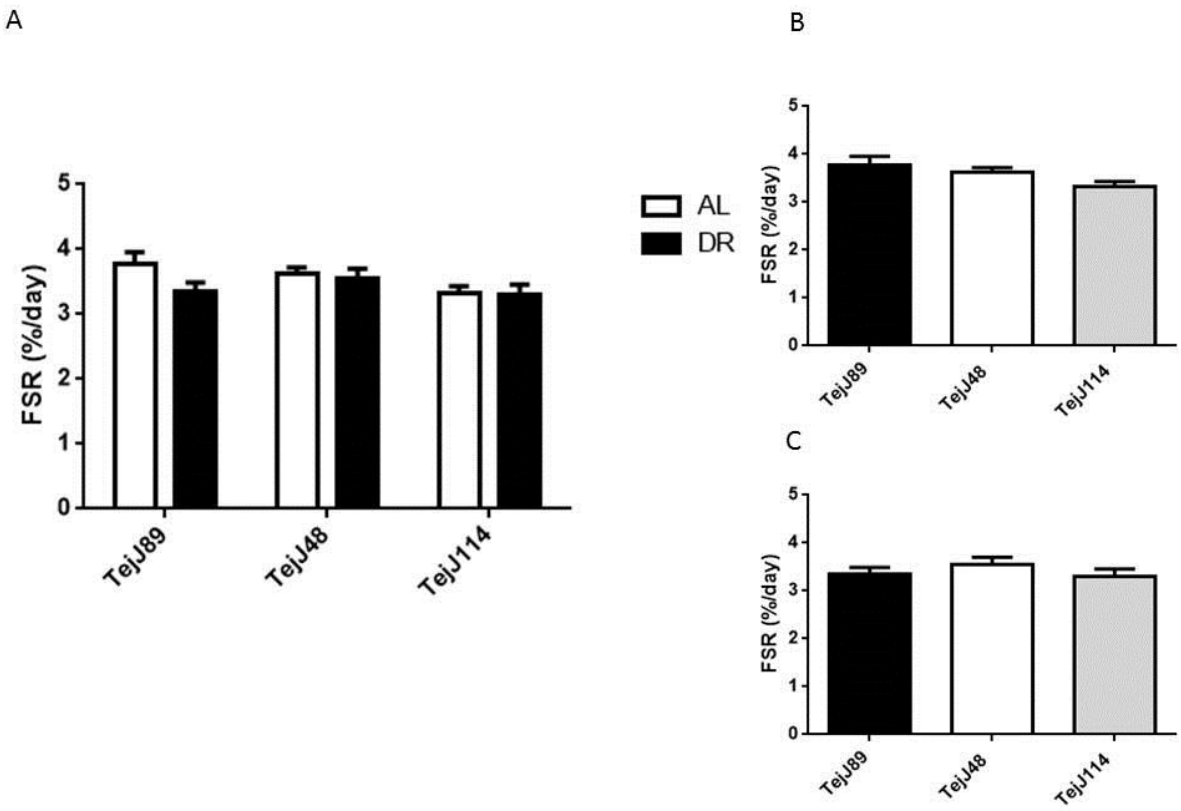

Figure 5.6: Protein fractional synthesis rates (FSR) in the Mito subcellular fraction of the heart tissue in three strains of female ILSXISS mice maintained on 40% DR or AL feeding for 2 months (A) No treatment or strain effect was observed in the protein turnover. (B) No strain effect was apparent within the AL mice (B) or DR mice (C). Values are means ± SEM, n = 8 per group (both AL and DR).

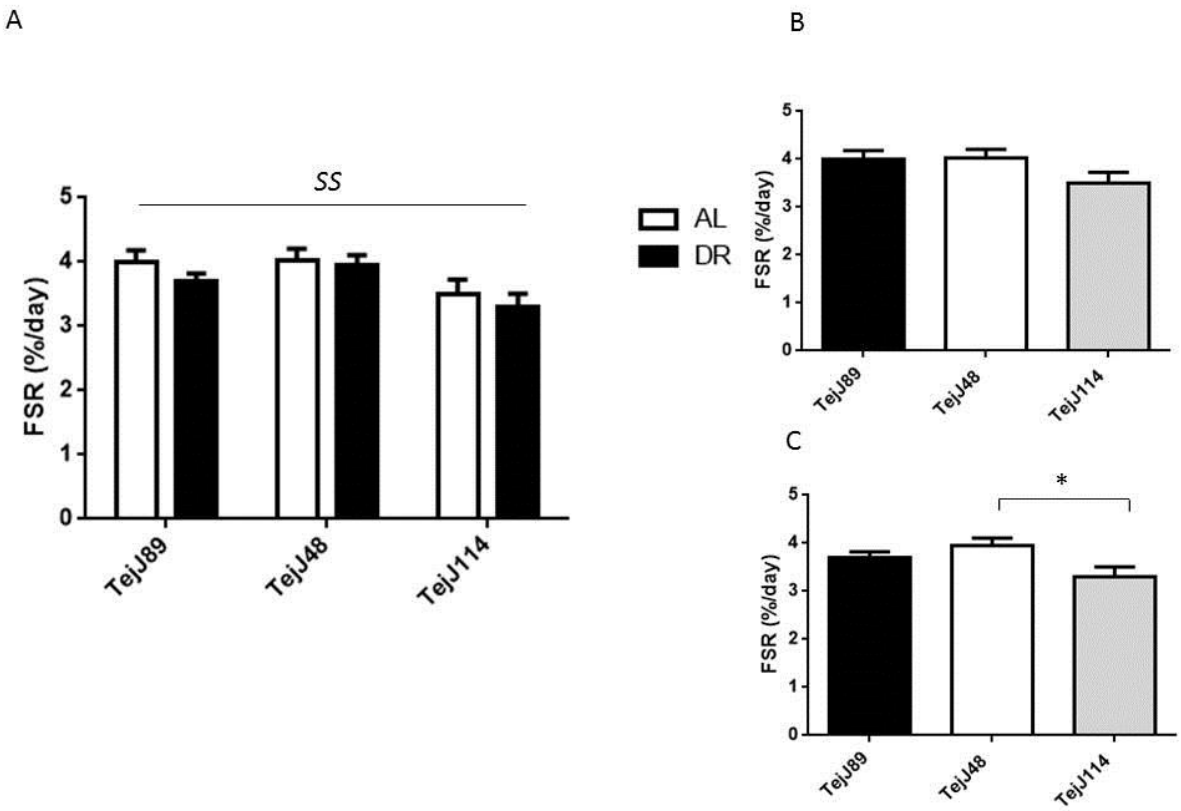

Figure 5.7: Protein fractional synthesis rates (FSR) in the Cyto subcellular fraction of the heart tissue in three strains of female ILSXISS mice maintained on 40% DR or AL feeding for 2 months (A). A significant strain effect was observed in the protein turnover. (B) No strain effect was apparent within the AL mice (B) or DR mice (C). Values are means ± SEM, n = 8 per group (both AL and DR).),* denotes $p<0.05$, *S*= strain effect; $p<0.01^{SS}$.

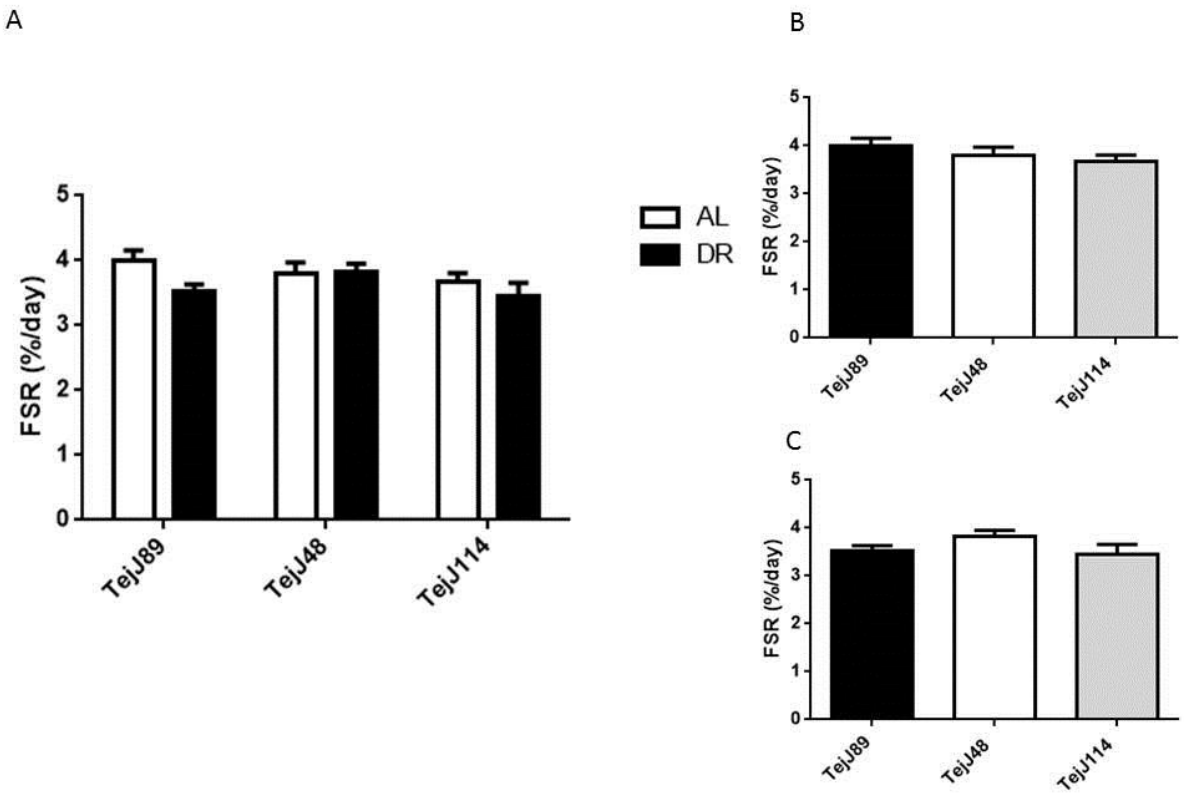

Figure 5.8: Protein fractional synthesis rates (FSR) in the Myo subcellular fraction of the heart tissue in three strains of female ILSXISS mice maintained on 40% DR or AL feeding for 2 months (A) No treatment or strain effect was observed in the protein turnover. (B) No strain effect was apparent within the AL mice (B) or DR mice (C).Values are means ± SEM, n = 8 per group (both AL and DR).

5.4 (C) DR and protein synthesis Liver

No treatment effect was observed in Mito (Figure 5.8), Cyto (Figure 5.9) or Myo (Figure 5.10) protein synthesis rates in liver tissue in any strain. Similarly no strain effect was observed within AL or DR mice in any liver fraction. It is important to note that it is not possible to detect differences when the protein pool is fully turned over in each case, which was found to be the case for liver in this study.

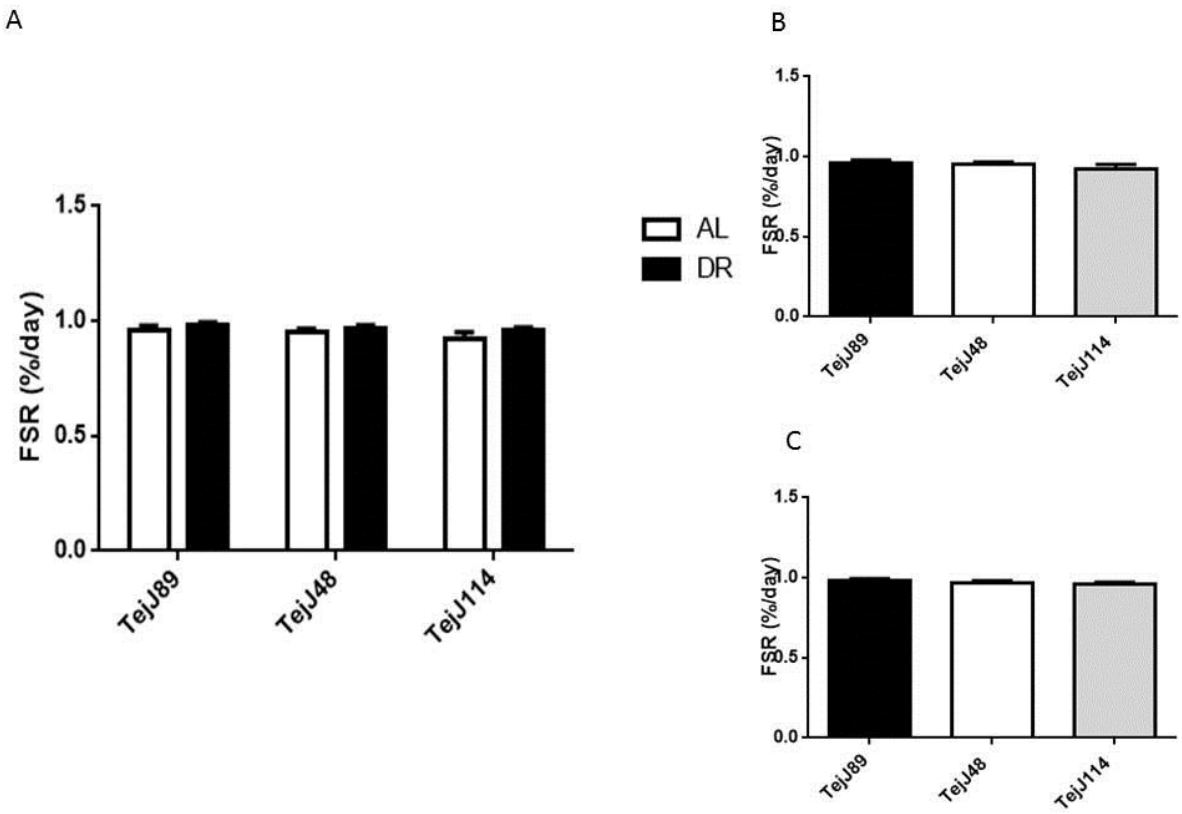

Figure 5.9: Protein fractional synthesis rates (FSR) in the Mito subcellular fraction of the liver tissue in three strains of female ILSXISS mice maintained on 40% DR or AL feeding for 2 months (A) No treatment or strain effect was observed in the protein turnover. (B) No strain effect was apparent within the AL mice (B) or DR mice (C). Values are means ± SEM, n = 8 per group (both AL and DR).

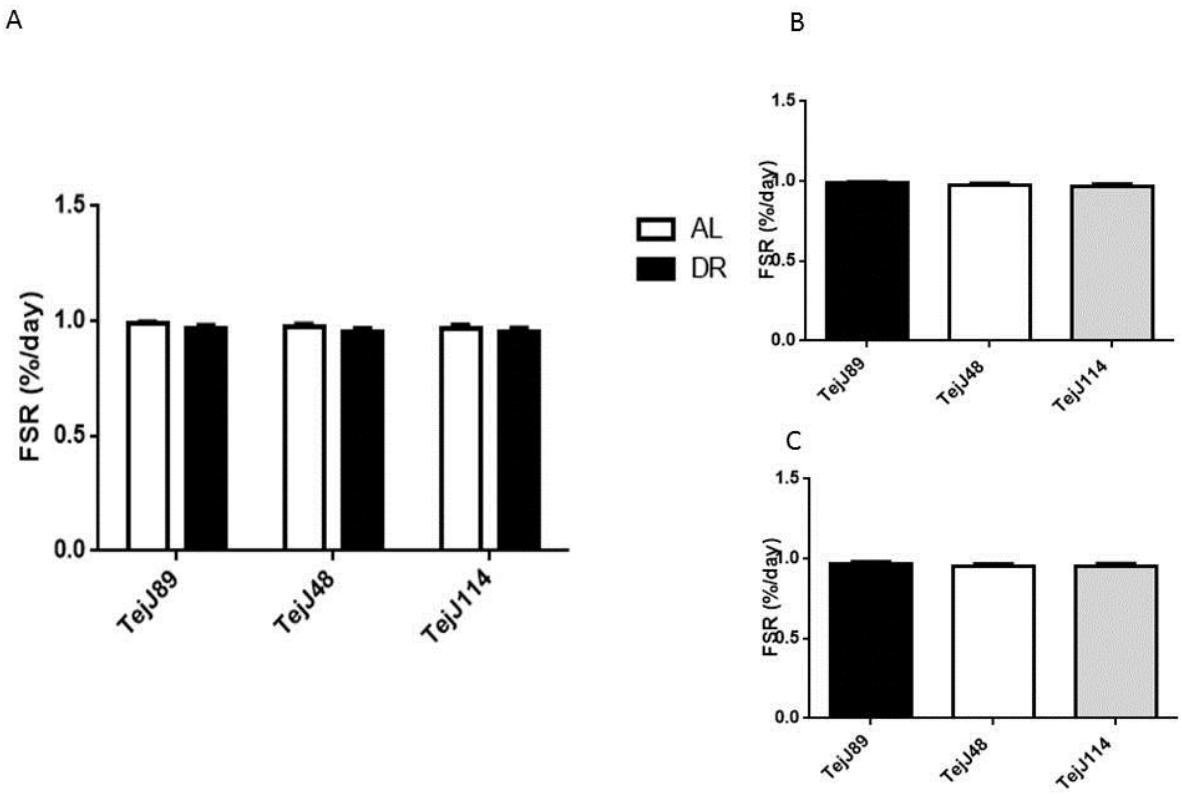

Figure 5.10: Protein fractional synthesis rates (FSR) in the Cyto subcellular fraction of the liver tissue in three strains of female ILSXISS mice maintained on 40% DR or AL feeding for 2 months (A) No treatment or strain effect was observed in the protein turnover. (B) No strain effect was apparent within the AL mice (B) or DR mice (C). Values are means ± SEM, n = 8 per group (both AL and DR).

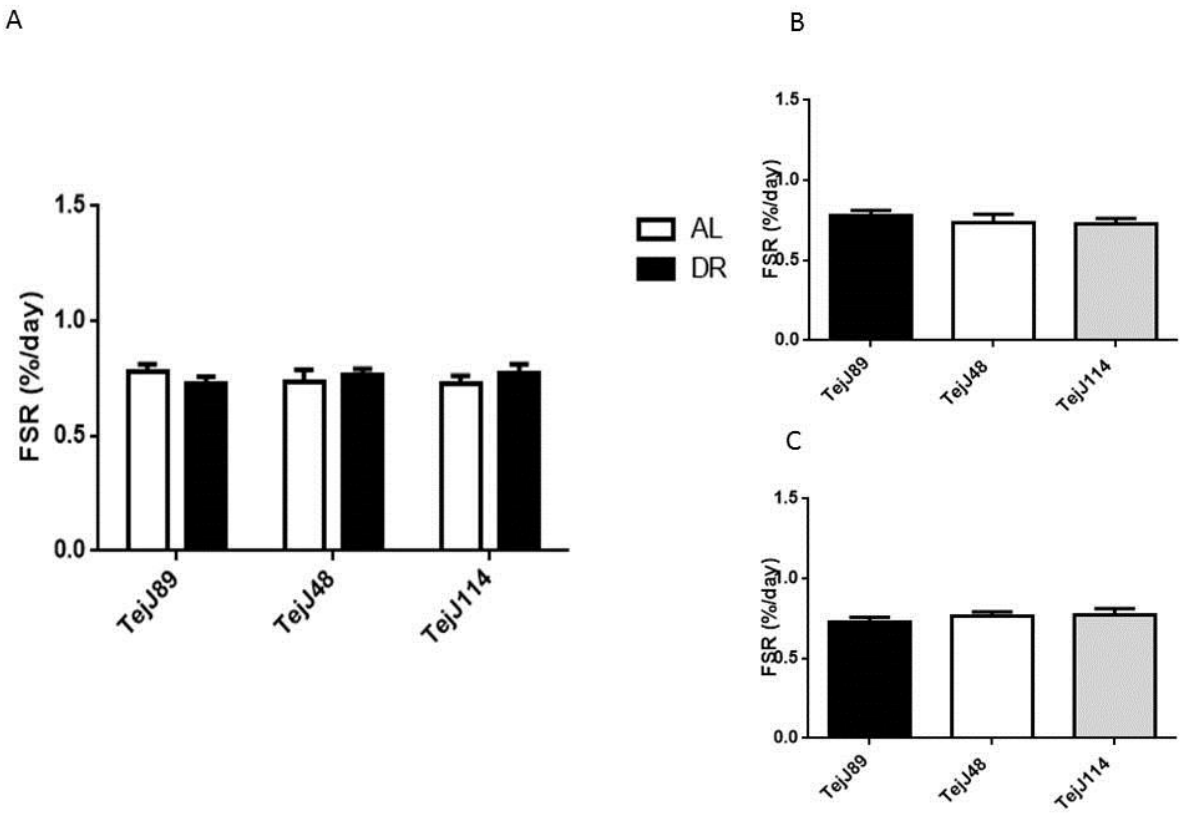

Figure 5.11: Protein fractional synthesis rates (FSR) in the Myo subcellular fraction of the liver tissue in three strains of female ILSXISS mice maintained on 40% DR or AL feeding for 2 months (A) No treatment or strain effect was observed in the protein turnover. (B) No strain effect was apparent within the AL mice (B) or DR mice (C). Values are means ± SEM, n = 8 per group (both AL and DR).

5.4 (D) DR and DNA Synthesis

A significant treatment effect was apparent in skeletal muscle DNA synthesis rate ($F= 14.84$, $p< 0.001$), with strain TejJ89 having significantly lower synthesis rate relative to its AL control (Figure 5.11). No strain effects were apparent on DNA synthesis in the skeletal muscle. Within the heart tissue, no treatment or strain-effect was observed on DNA synthesis rate (Figure 5.12). Rate of DNA synthesis was not altered by treatment in liver tissue (Figure 5.13), however strain was found to have an effect ($F= 5.317$, $p= 0.008$). When examined independent of treatment no strain differences were observed within the AL mice. Strain effects were however detected within the DR mice ($F=5.634$, $p=0.010$) with lower synthesis rates found in TejJ89 when compared with both TejJ48 and TejJ114 (Figure 5.13 C).

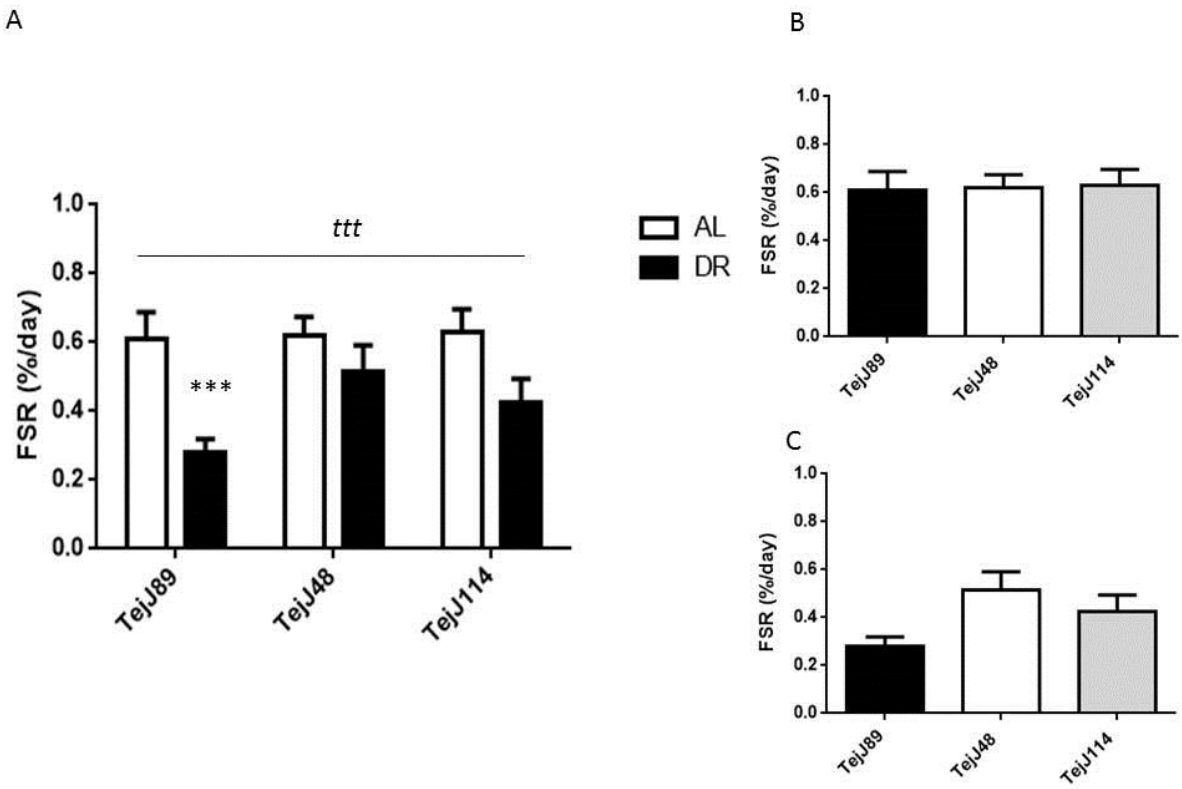

Figure 5.12: DNA fractional synthesis rate (FSR) in the skeletal muscle in three strains of female ILSXISS mice maintained on 40% DR or AL feeding for 2 months. (A) A significant effect of treatment was detected in DNA FSR. No strain effects were detected in the AL (B) or DR (C) mice. Values are means ± SEM, n = 8 per group (both AL and DR).

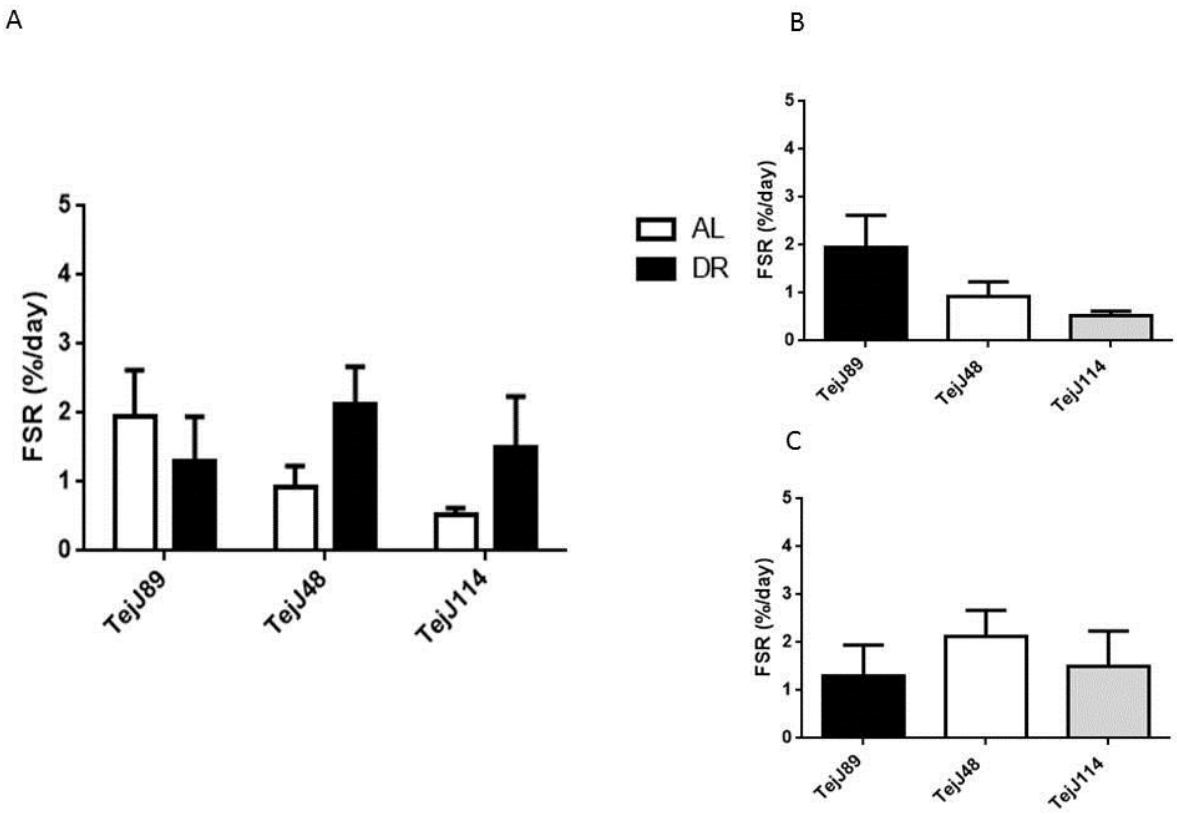

Figure 5.13: DNA fractional synthesis rate (FSR) in the heart in three strains of female ILSXISS mice maintained on 40% DR or AL feeding for 2 months. (A) No effect of were apparent following short-term DR (A). Furthermore, no strain-effects were detected in the AL (B) or DR (C) mice. Values are means ± SEM, n = 8 per group (both AL and DR).

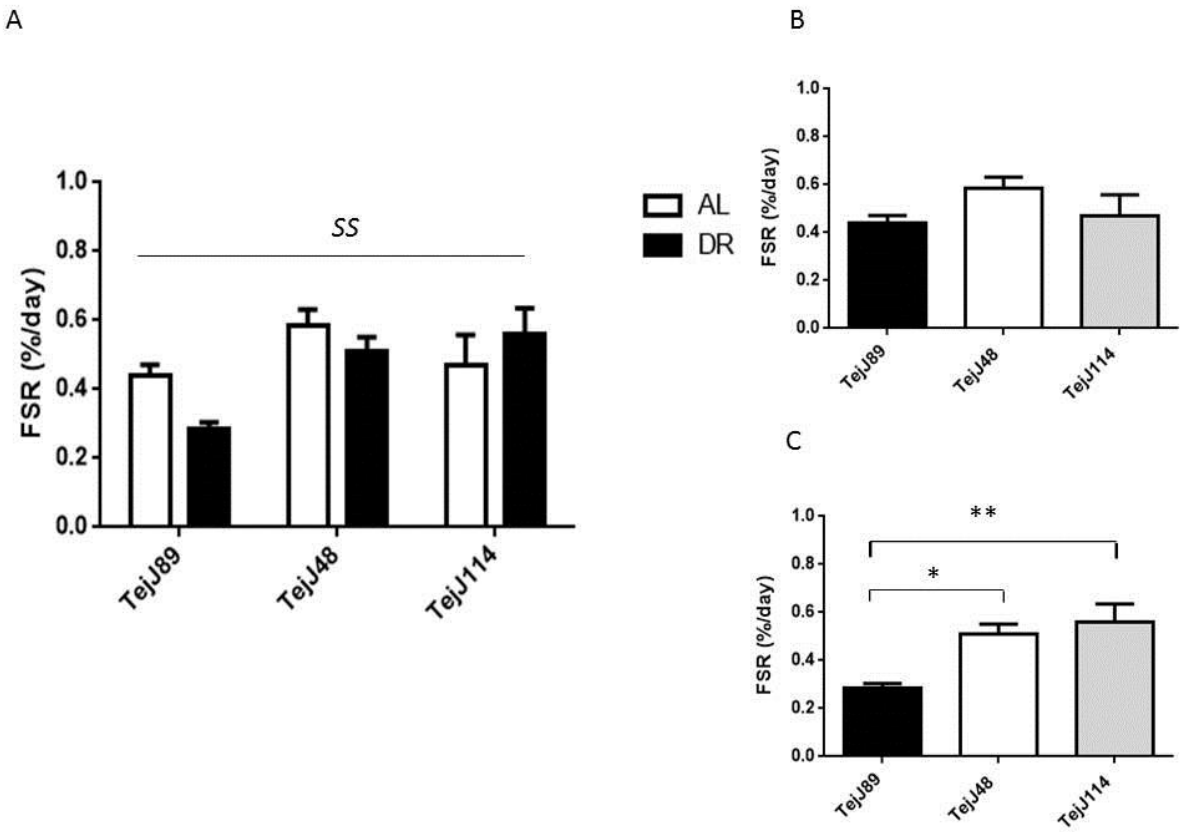

Figure 5.14: DNA fractional synthesis rate (FSR) in the liver in three strains of female ILSXISS mice maintained on 40% DR or AL feeding for 2 months. (A) No effect of treatment was apparent following short-term DR (A). No strain-effects were detected in the AL (B) mice, however in the DR mice, strain TejJ89 was found to have significantly reduced DNA synthesis compared to both other strains (C). Values are means ± SEM, n = 8 per group (both AL and DR), *denotes p<0.05*, p<0.01**, *S*= strain effect; $p<0.01^{SS.}$.

5.4 **(E) DR and Protein:DNA synthesis (^{new}protein/^{new}DNA).**

In the skeletal muscle, treatment was found to have a significant effect on the new protein to DNA synthesis ratio in all subcellular fractions being elevated in DR mice (Figure 5.14 (A) Mito: $F = 10.48$, $p = 0.002$, Figure 5.15 (A) Cyto: $F = 14.38$, $p < 0.001$ and Figure5.16 (A) Myo: $F = 12.26$, $p=0.001$). Cytoplasmic synthesis rates were increased by DR in strain TejJ89, compared to AL counterparts (Figure 5.15 A). No strain effect was apparent in the new protein to new DNA synthesis ratio of any protein fraction in either AL or DR mice No treatment or strain differences in this ratio was observed in either the heart (Figure 5.16) or liver (Figure 5.17).

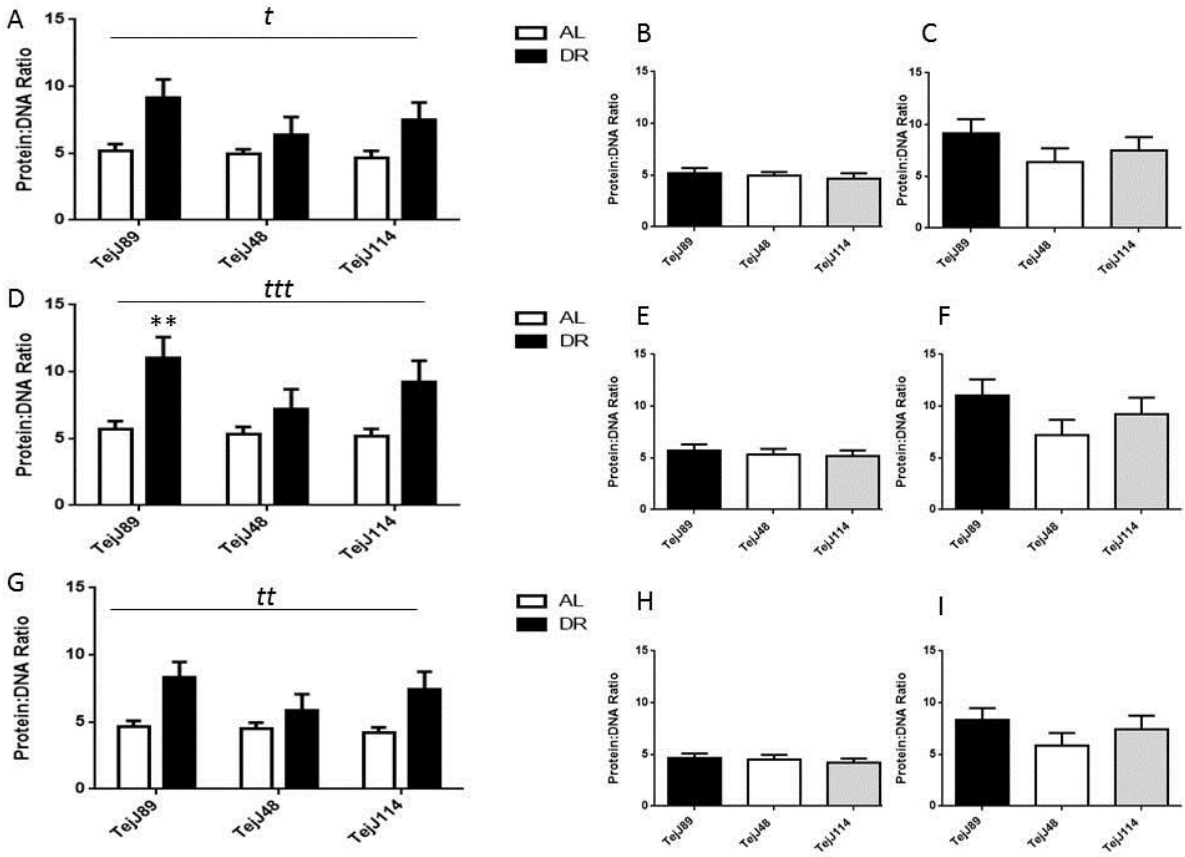

Figure 5.15: New Protein to DNA synthesis ratio in three strains of female ILSXISS mice maintained on 40% DR or AL feeding for 2 months in the Mito (A), Cyto (D) and Myo (G) fraction of skeletal muscle tissue. Synthesis ratios were found to be increased in all fractions following short-term DR. However no strain effects were apparent in the AL (B) or (C) DR mice of the Mito fraction. Similarly in the AL (E) or DR (F) rates of the Cyto, or the AL (H) or DR (I) of the Myo fraction, no strain specific differences were apparent. Values are means ± SEM, n = 8 per group (both AL and DR), ** denotes $p<0.01$, t= treatment effect; $p<0.05^{t}$, $p<0.01^{tt}$, $p<0.001^{ttt.}$

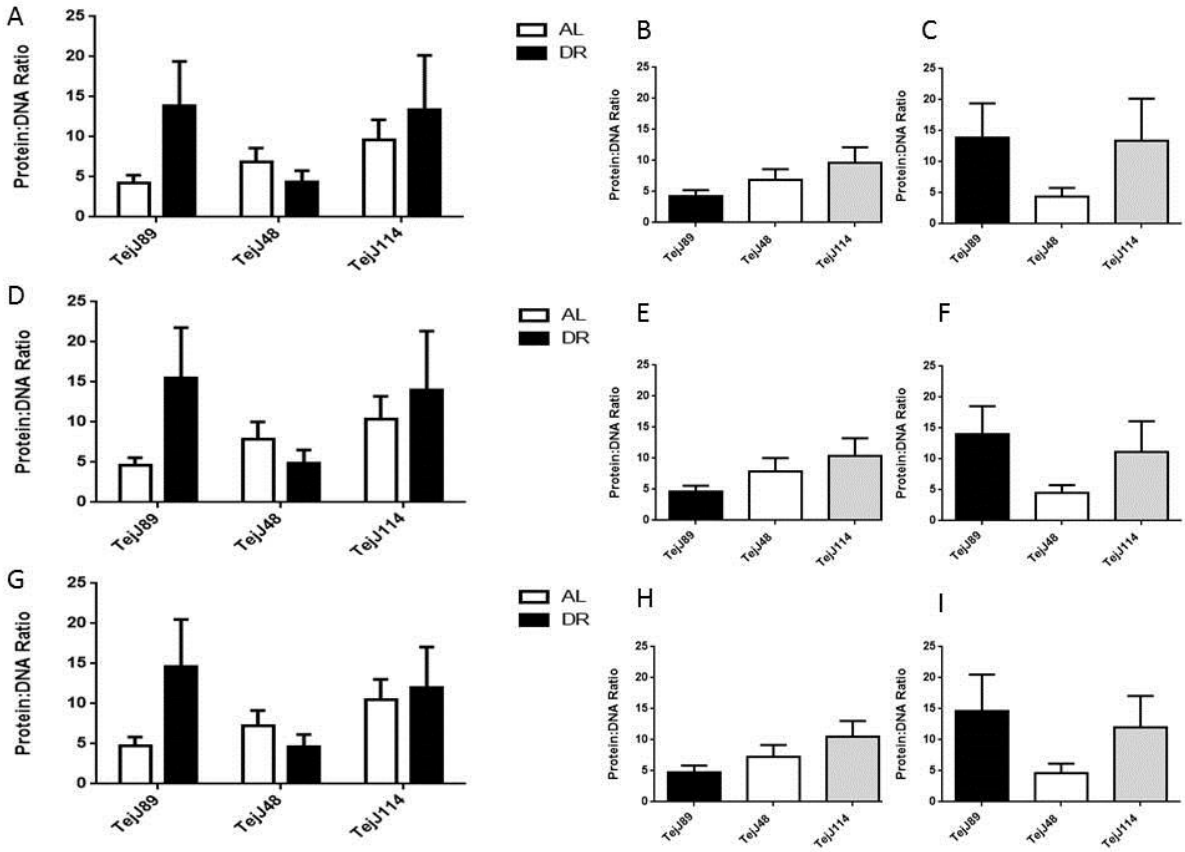

Figure 5.16: Protein to DNA synthesis ratio in three strains of female ILSXISS mice maintained on 40% DR or AL feeding for 2 months in the Mito (A-C), Cyto (D-F) and Myo (G-I) fraction of heart tissue. No treatment or strain effects were observed within any subcellular fraction. Values are means ± SEM, n = 8 per group (both AL and DR).

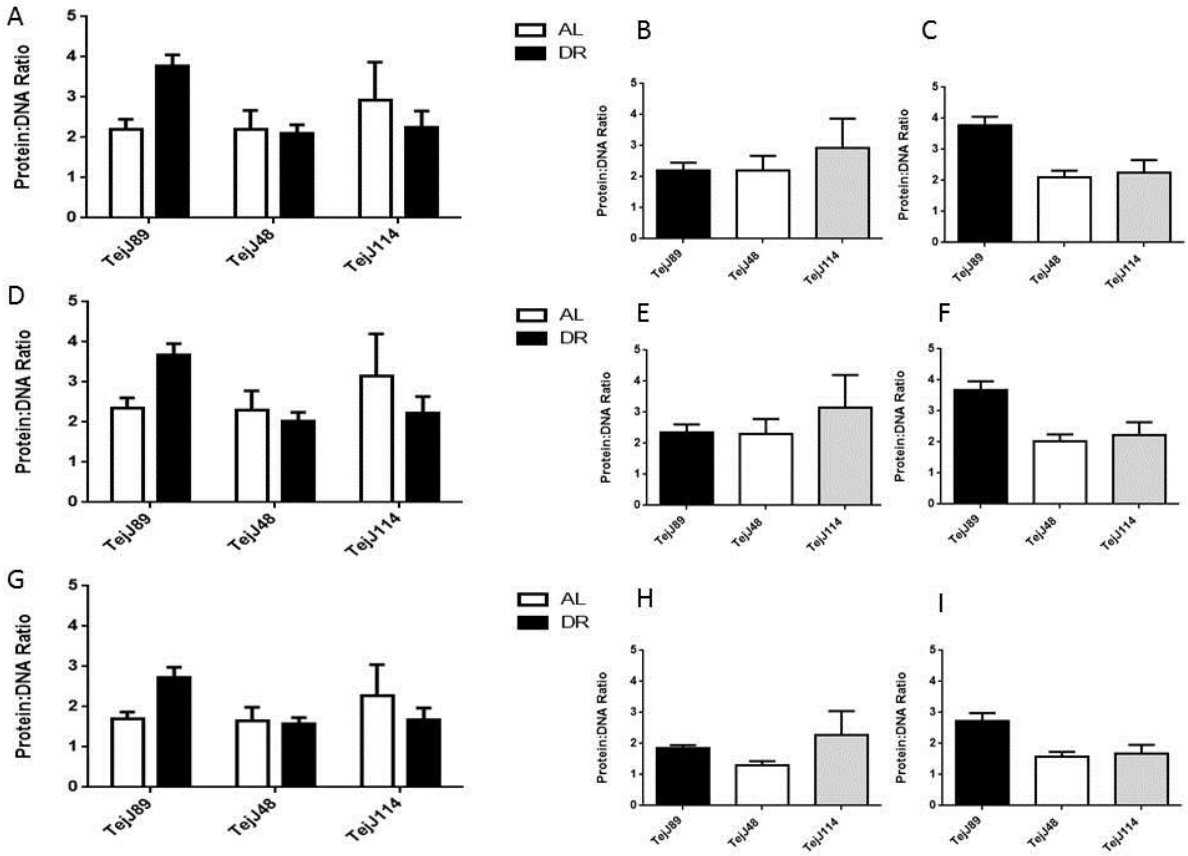

Figure 5.17: Protein to DNA synthesis ratio in three strains of female ILSXISS mice maintained on 40% DR or AL feeding for 2 months in the Mito (A-C), Cyto (D-F) and Myo (G-I) fraction of liver tissue. No treatment or strain effects were observed within any subcellular fraction. Values are means ± SEM, n = 8 per group (both AL and DR).

5.3 Discussion

Loss of proteostasis is associated with ageing (Lopez-Otin et al. 2013) and a number of age-related pathologies (Labbadia & Morimoto 2015; Morimoto & Cuervo 2014). As discussed earlier (section 5.2.1), enhanced proteostasis is proposed as a candidate mechanism underlying the anti-ageing effects of DR (Tavernarakis & Driscoll 2002). One component of proteostasis is protein synthesis, and it has been shown repeatedly that DR increases the rate of protein synthesis in rodents (Lambert & Merry 2000; Goldspink & Kelly 1984; Jazwinski 2000; Ward & Richardson 1991; de Cabo et al. 2015), although see also (Henderson et al. 2010), and DR slows age-related declines in hepatic protein synthesis and degradation rates (Lambert & Merry 2000). Similarly, there has been widespread support for the premise that mitochondrial biogenesis increases in rodents (Nisoli et al. 2005) and humans (Civitarese et al. 2007) under DR. However, more recently several studies have suggested that DR does not increase production of new mitochondria (biogenesis), but rather maintains energetically efficient mitochondria (Hempenstall et al. 2012; Lanza et al. 2012; Hancock et al. 2011). Indeed short-term 30% DR in C57BL/6 mice did not increase mitochondrial biogenesis in skeletal muscle, yet increased PGC1-α (Hempenstall et al. 2012), key regulator of mitochondrial biogenesis (Puigserver et al. 1998). These findings led the authors to suggest that rather than mitochondrial biogenesis being critical to DR-induced longevity it was more a case that a functionally efficient mitochondrial electron transport chain was critical, a finding that has now been reported in other model systems (Lanza et al. 2012; Hempenstall et al. 2012; Mittal et al. 2009). That under DR, newly synthesised proteins are allocated to cellular somatic maintenance rather than growth (Hamilton & Miller 2017) perhaps makes energetic sense, in line with the disposable soma idea of Kirkwood (Kirkwood & Holliday 1979).

While historically it has been impossible to disentangle how newly synthesised proteins are apportioned within the cell, I utilised a novel deuterated isotopic label. This enabled the ssimultaneous determination of protein and DNA synthesis rates within cytoplasmic, mitochondrial and myofibrillar subcellular protein fractions within the liver, heart and skeletal muscle tissue of female ILSXISS mice following short-term (2 months) 40% DR (Liao et al. 2010; Rikke et al. 2010). This approach helps provide mechanistic insight about how newly synthesised proteins are apportioned to newly proliferating cells versus those apportioned to somatic

maintenance through calculating the ^{new}protein/^{new}DNA ratio between. ^{new}protein/^{new}DNA ratio, whereby proliferating cells should show a ratio ~1 (↑ protein synthesis: ↑ DNA synthesis) and cellular maintenance should show a ratio >1 (↑ protein synthesis: ↔DNA synthesis) (Hamilton & Miller 2017).

In skeletal muscle, short-term DR increased the ^{new}protein/^{new}DNA ratio in all subcellular protein fractions when compared to the ratio in AL mice. These findings are in agreement to previous reports in DR mice (Miller et al. 2012; Miller et al. 2013; Miller et al. 2014) and in a number of long-lived mouse models (Drake et al. 2013; Drake et al. 2014; Drake et al. 2015). In particular, DNA synthesis rates were reduced in strain 89 under DR, a phenotype reported in a number of long-lived mouse strains and perhaps suggests that this line has greater metabolic flexibility to reduce cell proliferation rates under DR. Similarly while there was a general DR-wide increase in the ^{new}protein/^{new}DNA ratio in all strains, the effects were generally more apparent in line 89. Indeed, an increased ^{new}protein/^{new}DNA ratio in the cytoplasmic fraction was only significant between AL and DR mice from line 89 within skeletal muscle. Interestingly, the synthesis of proteins from RNA in the cytoplasm is a known modulator of ageing and lifespan in yeast (Delaney et al. 2013; Borbolis & Syntichaki 2015). Consequently, the increase in the ratio in line 89 may be somehow relevant to DR-induced longevity, although this obviously requires further investigation. Importantly, my work showed that mitochondrial biogenesis in skeletal muscle, as determined by the ^{new}protein/^{new}DNA ratio, was increased under DR across all three strains, suggesting that DR does not increase production of new mitochondria, but rather maintains energetically efficient mitochondria in line with previous studies (Hempenstall et al. 2012; Lanza et al. 2012; Hancock et al. 2011), and that this may not be important to DR-induced longevity.

In the heart, the ^{new}protein/^{new}DNA ratio in cytoplasmic, mitochondrial or myofibrillar was unaffected by DR in all ILXISS strains. The result is perhaps surprising given that ^{new}protein/^{new}DNA ratio has been reportedly increased in all subcellular protein fractions in heart following long-term DR (Miller et al. 2012; Miller et al. 2013). Moreover, this ratio in heart was also observed in long-lived Snell (Drake et al. 2013; Drake et al. 2015) and rapamycin treated mice (Drake et al. 2014). What is clear from my data is that there was a trend for a DR-induced increase in the ratio in strain 89 but that this did not reach significance, potentially highlighting a lack of power in my study (n=8). In a reanalysis of their data (Miller et al. 2012; Miller et al. 2013), using the ^{new}protein/^{new}DNA ratio, Miller *et al* (Miller et

al. 2014) reported that DR increased the ratio in skeletal muscle and heart although it is unclear which age-cohort of male B6D2F1 mice were presented. The mice in my study were 5 months of age, and thus still relatively young, and it may be possible that DR-induced changes in this ratio might only be detectable in the context of ageing, as multiple components of the proteostatic network are known to become impaired during ageing (Taylor & Dillin 2011; Kaushik & Cuervo 2015). Following the 2 week labelling period utilised in this study, I found that all liver fractions were fully turned over, as reported previously in other D_2O studies (Miller et al. 2012; Miller et al. 2013; Drake et al. 2013) leading to the introduction of a new, time-course approach that was introduced by Miller and Hamilton after the collections of our samples. Consequently, this meant that it was not possible to determine the ^{new}protein/^{new}DNA ratio in this tissue. However, the DNA fractional synthesis rate was significantly reduced in line 89 under DR when compared to the other 2 lines under DR, suggesting that cellular proliferation was significantly reduced in this tissue, again indicating a tissue maintenance phenotype in this line. Long-term DR has been shown to reduce both protein synthesis and breakdown in mice, suggesting that the beneficial effect of DR on cellular fitness may work instead through reduced protein synthesis (J. C. Price et al. 2012). Interestingly, cellular proliferations is associated with various cancers (Lopez-Saez et al. 1998), and while we do not know what the various ILXISS line die of under DR it would be interesting to determine whether this line retains reduced hepatic cellular proliferation in older ages and indeed whether this is associated with a reduced incidence of hepatic carcinomas. However, unfortunately I was not able to repeat this study in a longer-term DR protocol due to time limitations and the tissue requirements of the mitochondrial studies (Chapter 4).

Chapter 6: General Discussion

6.1 General Overview

Identifying the mechanisms underlying the ageing process remains one of the greatest challenges, not only to biological research, but also to society in regards to the increased social and economic burden caused by the co-morbidities of ageing. As described in Chapters 1and 2 of this thesis, I utilised the inherent strain-specific lifespan response to dietary restriction (DR) of ILSXISS recombinant inbred (RI) mice, categorised previously as “positive” (strain TejJ89), “non” (strain TejJ48) or “negative” (strain TejJ114) responders, in terms of DR-induced longevity (Rikke et al. 2010; Liao et al. 2010). I employed this intrinsic variability in the DR response in order to probe putative mechanisms underlying slowed ageing and longevity. I sought to determine the impact of short- (2 months of 40% DR, equivalent to 5 months of age) and long-term DR (10 months of 40%, equivalent to 13 months of age) on candidate hallmarks of ageing, including numerous physiological and metabolic parameters (Chapter 3), hepatic and skeletal muscle mitochondrial function (Chapter 4*)* and protein synthesis within liver, skeletal muscle and heart (Chapter 5)*.*

Overall, my findings from the experiments described in Chapters 3, 4 and 5 highlight firstly that genotype appears important to the DR response in terms of the parameters I measured, with strain-specific differences widely observed. Secondly, metabolic flexibility, i.e. the ability for adaptive metabolism in a time of nutrient scarcity, appears to be an important process underlying DR-induced lifespan extension (Chapter 3 & 4). My findings indicate that the maintenance of gonadal white adipose tissue (WAT) and simultaneous hypertrophy of brown adipose tissue (BAT) may be important correlates of longevity under DR; both seen in strain TejJ89 following long-term 40% DR, and neither observed in either the negative responding strain TejJ114 or non-respondingTejJ48. Long-term DR did not enhance hepatic or skeletal muscle mitochondrial function in contrast to a number of previous studies in mice (López-Lluch et al. 2006; Nisoli et al. 2005; Hempenstall et al. 2012; Lanza et al. 2012), but interestingly hepatic mitochondrial dysfunction was observed in the negative responding TejJ114 under long-term 40% DR. My research also showed that enhanced glucose homeostasis, including increased glucose tolerance and insulin sensitivity, proposed as being a conserved response to DR in mice, was not seen in ILSXISS strains following short- or long-term DR. In this chapter I will synthesise and review my main findings, suggest potential explanations for the

observed results, and highlight some limitations and propose some future research avenues that may help provide additional insights.

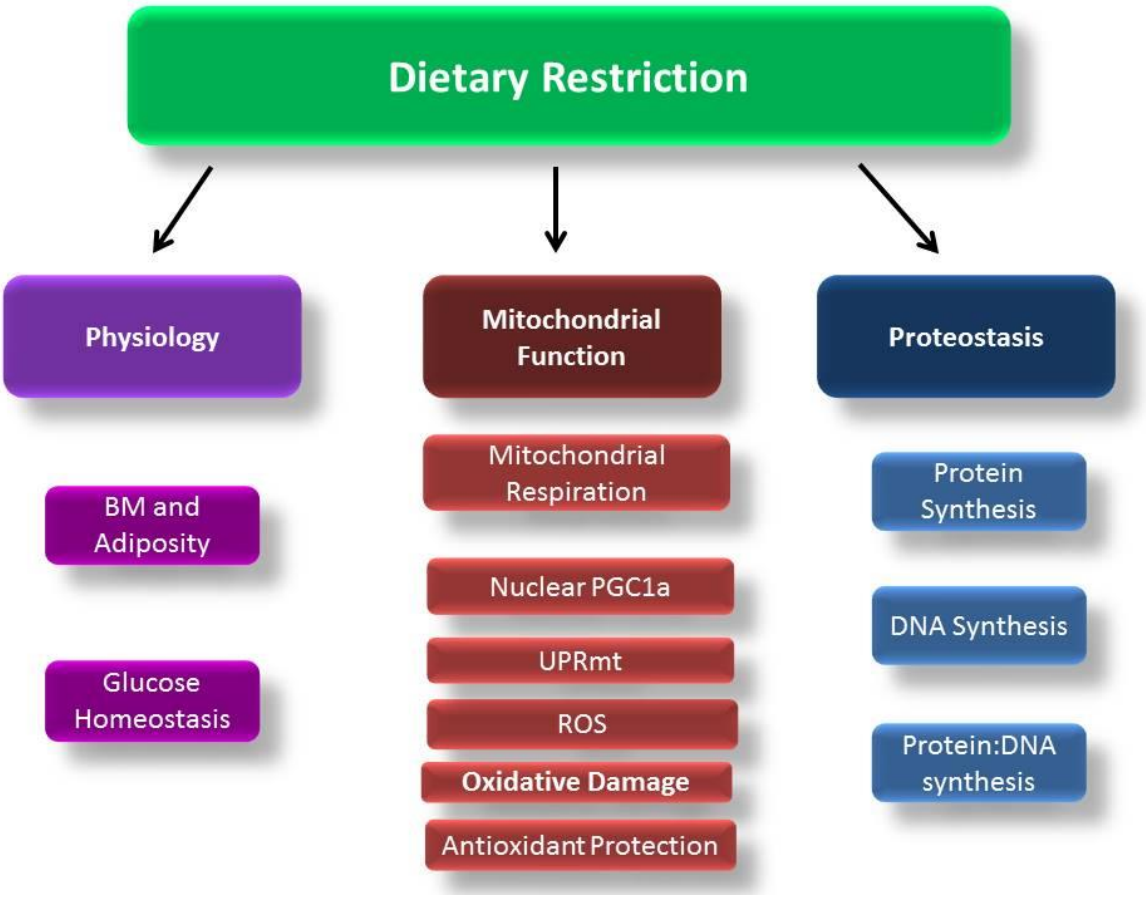

Figure 6.1: Summary of original Aims; investigate the impact of 40% DR on three well characterised hallmarks of ageing in female ILSXISS mice.

6.2 40% DR differentially affects body mass and fat mass in ILSXISS mice dependent of duration

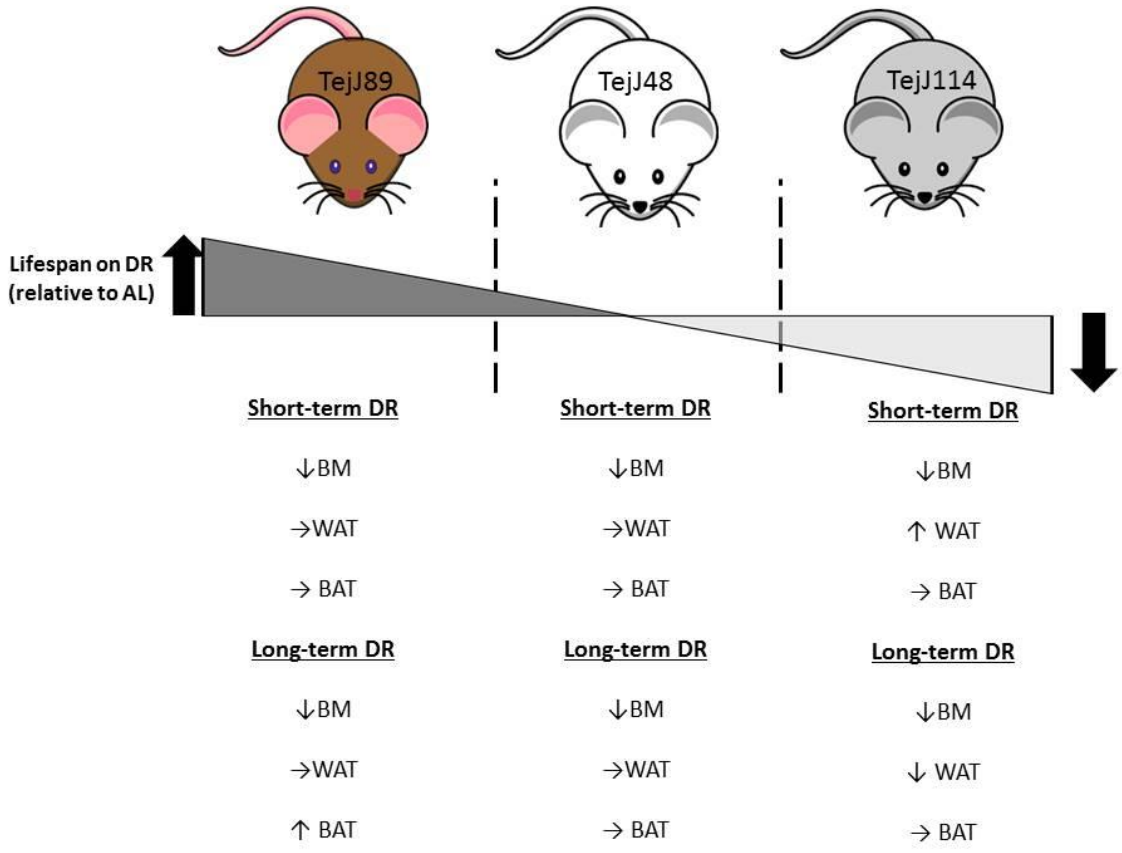

Figure 6.2: Impact of short- (2 months) and long-term (10 months) 40% DR on body mass, gonadal white adipose tissue (WAT) mass and brown adipose tissue BAT) mass in female ILSXISS mice.

Body mass (BM) was significantly reduced in all strains under short-term and DR, although neither the mass of gonadal WAT or BAT was decreased, suggesting that the losses in BM observed were due to decreases in other WAT depots or in lean mass. TejJ114 actually showed an increase in gonadal WAT (corrected for BM changes) under short-term DR, with similar results been reported following short-term (3 weeks) of 5% DR female C57BL/6J mice (Li, Cope, Johnson, D. L. Smith, et al. 2010). The reason for the increase in gonadal WAT in TejJ114 is unclear, however physiological adaptations in behaviour, such as irregular eating patterns or binge eating under DR may impact on the accumulation in fat (Dietz 1995; Chaput et al. 2007) and perhaps TejJ114 was more prone to these behaviours, although this is purely conjecture as I did not look at this in my study. Female C57BL/6J mice under 5% DR showed “gorging behaviour” following implementation of restriction (Li, Cope, Johnson, D. L. Smith, et al. 2010), and the authors suggested that condensing food intake into a narrower time frame results in a more effective storage of triglycerides within the gonadal WAT depot, and also in inguinal, retroperitoneal and mesenteric WAT. Reductions in lean mass and organ mass have been shown following 3 months of DR in mice (Faulks et al. 2006; Mitchell et al. 2015a)

Under long-term DR, strain TejJ114 was found to have lost a much greater amount of mass (52.3%), relative to its appropriate AL control, than either TejJ89 (34.5 %) or Tej48 (24.6 %). Strain TejJ89 had proportionally similar gonadal WAT mass as AL controls, but BAT mass increased significantly within the DR group; UCP1 protein levels were unaffected. Conversely TejJ114 mice under long-term DR had significantly smaller mass-corrected gonadal WAT compared to AL mice, but BAT was unaffected. Maintenance of WAT has been described previously as a mediator of DR response in ILSXISS mice, with strains with the least reduction in fat more likely to show life extension, and those with the greatest reductions more likely to have shortened lifespan (Liao et al. 2011). Moreover, significant loss of fat under DR in long-lived adenylyl cyclase type 5 knockout mice has been linked to DR-induced metabolic deterioration and death (Yan et al. 2012). Increases in BAT are reported in mice and rats under DR (Fabbiano, Suarez-Zamorano, et al. 2016; Valle et al. 2005; Okita et al. 2012; Valle et al. 2008), and my findings indicate a link between WAT maintenance and BAT hypertrophy and DR-induced longevity in TejJ89. Mice under DR are known to be thermoregulatory stressed (Speakman & Keijer 2012), and so the significant loss in gonadal WAT mass, with no increases in

BAT mass, in strain TejJ114 following long-term DR may indicate that this strain is more reliant on shivering thermogenesis to maintain body temperature under DR, using gonadal WAT as an energy source. Mice lacking uncoupling protein 1 (UCP-1 KO), which are unable to generate heat production through non-shivering thermogenesis within BAT, are found to switch to fatty acid metabolism and appear to be more reliant on shivering thermogenesis (Shabalina et al. 2010). Moreover, depletion of reactive oxygen species (ROS) results in hypothermia upon cold exposure in male C57BL/6J, and inhibits UCP1-dependent increases in whole body energy expenditure, and authors propose increased ROS in BAT as a mechanism that drives UCP1-dependent thermogenesis (Chouchani et al. 2016). Although ROS was not measured in BAT in this study, I observed reduced levels of ROS within skeletal muscle of strain TejJ114 under long-term DR (Chapter 4). The idea of the rate of living theory was first proposed by Pearl in 1928 (Pearl 1928), and the reduction in body temperature (T_b) has been proposed as being critical to DR-induced longevity (Duffy et al. 1989; Lane et al. 1995; Vaanholt et al. 2012; Turturro & Hart 1991). However, in ILSXISS mice, greater reductions in T_b following DR were associated with shortened lifespan under DR (Rikke et al. 2003; Rikke & Johnson 2007), and my findings suggest that a lack of BAT hypertrophy, and in the case of TejJ114 the resulting loss of WAT, may be important.

6.3 Enhanced glucose homeostasis is not essential to longevity with DR

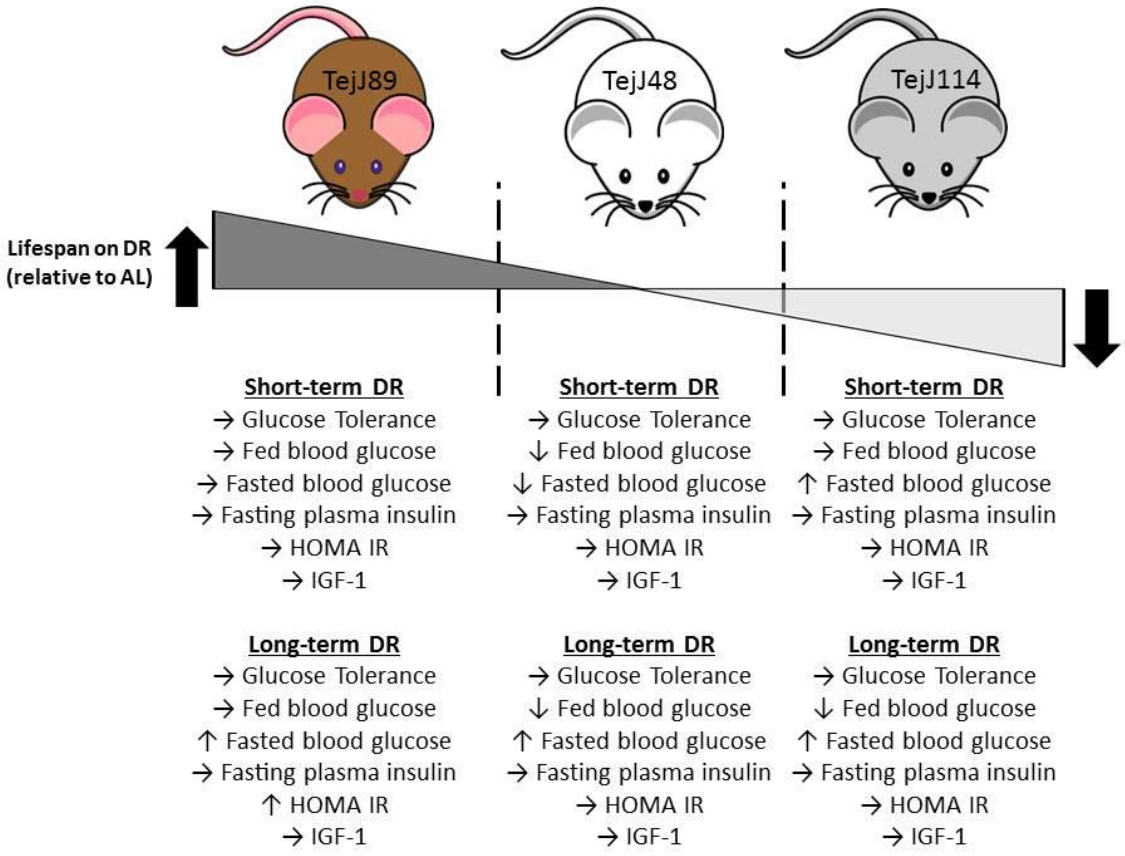

Figure 6.3: Impact of short- (2 months) and long-term (10 months) 40% DR on glucose homeostasis in female ILSXISS mice.

Enhanced glucose homeostasis, including improved glucose tolerance, insulin sensitivity and decreased plasma levels of insulin and insulin-like growth factor-1 (IGF-1), has been reported following short and long-term DR in mice (Hempenstall et al. 2010; Argentino et al. 2005; Mitchell et al. 2016) and is also characteristic of longevity in some (Bartke et al. 2007; Blüher et al. 2003), but not all (Selman et al. 2008) long-lived mice. However, I found no evidence that differences in glucose tolerance, insulin resistance or IGF-1 were associated with DR-induced longevity in female ILSXISS mice, or indeed that impaired glucose homeostasis was associated with lifespan shortening under DR. While my findings do not support the premise of alterations in glucose and insulin to underlie the beneficial effects of DR, strain-specific difference in glucose homeostasis are well established under both AL and DR conditions. For instance, male C57BL/6 and DBA/2 mice following short-term DR are not found to have reduced fasting plasma insulin, and DBA/2 mice are hyperinsulinaemic relative to C57BL/6 mice under both AL and DR conditions (Hempenstall et al. 2010). I employed the Homeostatic Model of Assessment for insulin resistance (HOMA IR), a simple and time-efficient proxy for the determination of insulin resistance. However, while this has been shown to be a good proxy for insulin resistance in mice (Selman et al. 2009; Hempenstall et al. 2010) it has failed to adequately predict IR in a number of human studies (Ferrara & Goldberg 2001; Anderson et al. 1995; Yeni-Komshian et al. 2000). Surprisingly IGF-1, which has been shown to be decreased in DR mice (Hempenstall et al. 2010; Mitchell et al. 2016) was unaffected by DR in ILSXISS mice, irrespective of the DR duration. Humans unlike rodents, are not found to have reduced IGF-1 following long-term DR (Fontana et al. 2008), and long-lived Klotho mice have increased insulin resistance and IGF-1 (Bartke 2006). Moreover, mice with reduced levels of IGF-1 have an increase in maximum but not median lifespan, indicating that a reduction in IGF-1 alone is insufficient to increase both mean and maximal life span in mice (Lorenzini et al. 2014).

6.4 Mitochondrial dysfunction was associated with lifespan shortening with DR

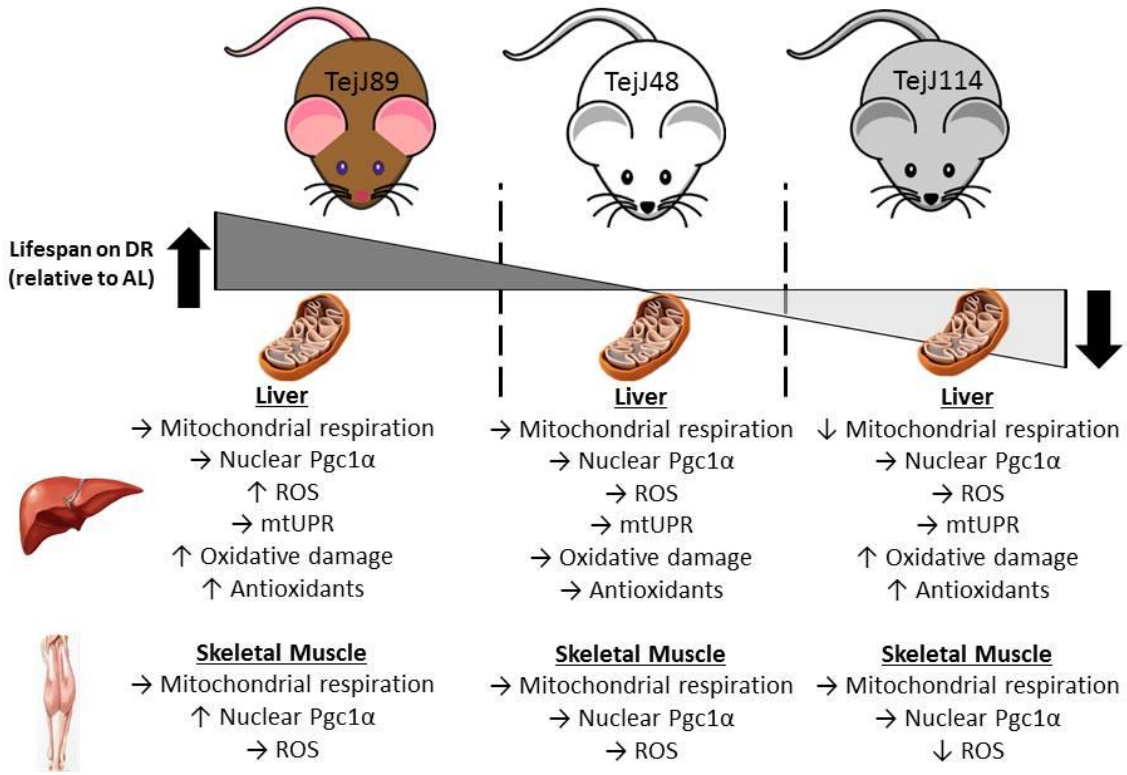

Figure 6.4: Impact of long-term (10 months) 40% DR on mitochondrial function, ROS and oxidative damage in female ILSXISS mice.

Mitochondrial dysfunction is proposed as being a key hallmark of ageing and disease (Lopez-Otin et al. 2013), and reports in model systems suggest improvements in mitochondrial function correlate closely with DR-induced longevity (Ruetenik & Barrientos 2015; Feuers 1998; Zid et al. 2009). However, I observed in strain TejJ114 that long-term 40% DR induced hepatic mitochondrial dysfunction; mitochondrial function was unaffected by long-term DR in strains TejJ89 and TejJ48. While I originally predicted that mitochondrial dysfunction would be associated with a shortening of lifespan in TejJ114 under DR, the absence of any beneficial effect of DR on mitochondrial function in TeJJ89, unlike those reported in both skeletal muscle and liver under DR (Hempenstall et al. 2012; Lanza et al. 2012; Weindruch et al. 1980), suggest that, in ILXISS mice at least, enhanced mitochondrial respiration does not underlie DR-induced longevity. Although it should be noted that differences in mitochondrial protocols exist between my study and those of Lanza (2012) and Hempenstall (2012). I also found that TejJ89 under long-term DR had greater production of hepatic reactive oxygen species (Hydrogen peroxide; H_2O_2) relative to AL controls, whilst lower ROS was seen in TejJ114. Recently debate has arisen over the precise role of oxidative damage in causing ageing (Speakman & Selman 2011; Gems & Doonan 2009), and my findings conflict with the widely held belief that DR acts through reductions in ROS-induced oxidative damage (Lambert & Merry 2004; López-Lluch et al. 2006). However, accumulating evidence suggests that ROS, including superoxide, hydrogen peroxide, and multiple others, are not the cause of oxidative damage, but instead act as important signalling molecules that protect against disease, thus consequently increases lifespan (Ristow & Zarse 2010; Ristow & Schmeisser 2014), and may explain the DR-induced longevity and increased hepatic ROS in TejJ89. Increased hepatic oxidative damage was reported in strain TejJ114 under DR, but H_2O_2 levels were unaffected. Thus, it is feasible that an alternative ROS source, such as superoxide or the hydroxyl radical may be responsible for the increase in oxidative damage seen, perhaps related to the mitochondrial dysfunction observed in this same strain under DR. Indeed, while H_2O_2 is the most widely used measure of ROS production, it was recently reported in a meta-analysis that H_2O_2 is largely unchanged in rodents subject to DR (Walsh et al. 2014).

6.5 Increased cytoplasmic protein synthesis in the skeletal muscle is important to longevity with DR

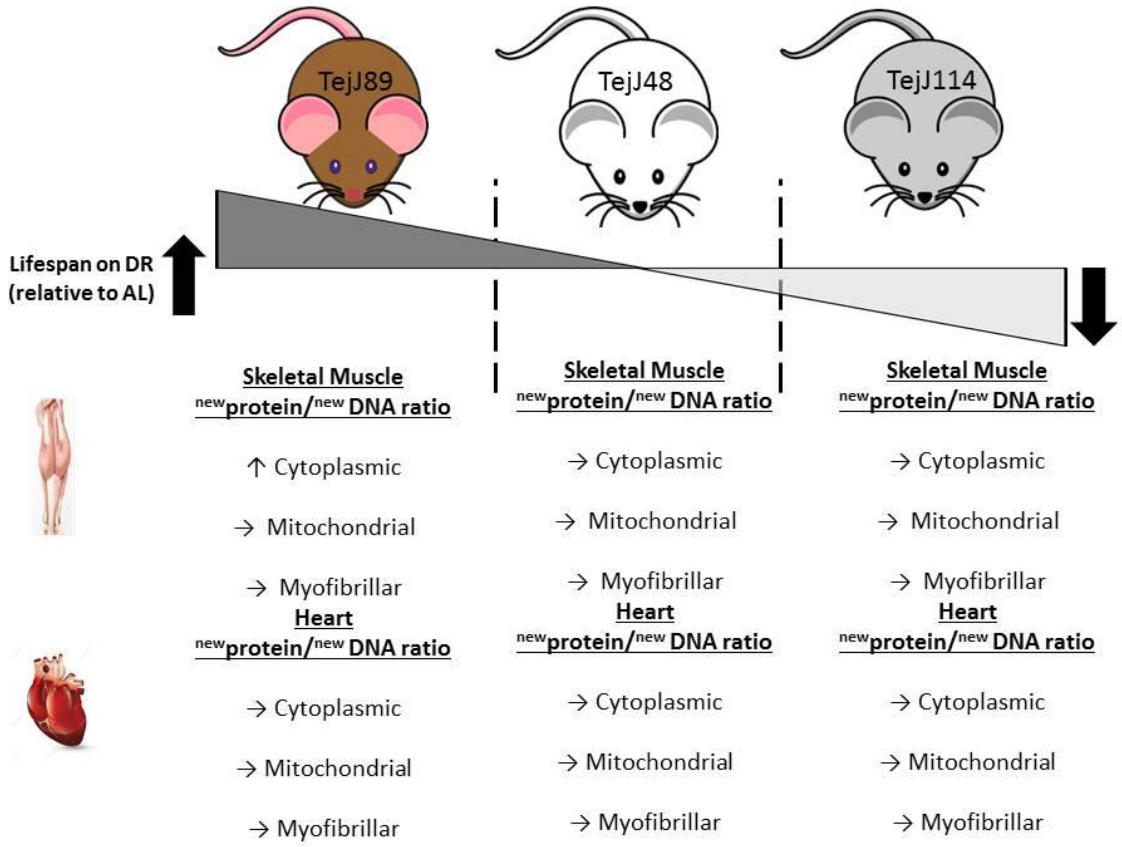

Figure 6.5: Impact of long-term (10 months) 40% DR on ^{new}protein/^{new}DNA ratio in three strains of female ILSXISS mice.

Loss of proteostasis is associated with ageing (Lopez-Otin et al. 2013), while the ability to maintain a healthy proteome through protein homeostasis, or proteostasis, is associated with enhanced longevity (Morimoto & Cuervo 2014; Treaster et al. 2014; Kaushik & Cuervo 2015). Here, through the use of a novel technique; ^{new}protein/^{new}DNA ratio, which gives mechanistic insight about how newly synthesised proteins are apportioned to newly proliferating cells versus those apportioned to somatic maintenance (Miller et al. 2014), I investigated the role of proteostasis as a candidate mechanism underlying lifespan extension in ILSXISS mice. Protein synthesis rates in three subcellular protein fractions; cytoplasmic, myofibrillar and mitochondrial proteins, in skeletal muscle, heart and liver were determined under short-term 40% DR. In muscle increases in cytoplasmic, myofibrillar and mitochondrial were reported. I only observed an increase in the ^{new}protein/^{new}DNA ratio in the cytoplasmic protein fraction in strain TejJ89 under DR. The absence of any increase in this ratio in either the mitochondrial or myofibrillar proteins in skeletal muscle in any ILSXISS strain is perhaps surprising, given the increases in both fractions previously reported in male B6D2F1 skeletal muscle following DR reported by Miller *et al* (2012; 2013), who ultimately concluded that increased proteostasis is a shared feature of DR (Miller et al. 2014; Hamilton & Miller 2017). Increased mitochondrial biogenesis has been proposed as a candidate mechanism underlying lifespan extension following DR (Lopez-Lluch et al. 2008; López-Lluch et al. 2006; Civitarese et al. 2007; Nisoli et al. 2005), although debate has existed on what is the best way to determine biogenesis (Miller et al. 2014; Miller et al. 2016). My results, which utilise the ^{new}protein/^{new}DNA ratio (Miller et al. 2014; Drake et al. 2015; Hamilton & Miller 2017) suggest that DR favours the maintenance of existing mitochondria, preserving mitochondrial efficiency, rather than inducing mitochondrial biogenesis, in line with other studies in skeletal muscle of mice under DR (Hempenstall et al. 2012; Lanza et al. 2012; Hancock et al. 2011). Moreover, I saw no changes in any protein fractions within the heart, unlike the increases reported in male B6D2F1 following short-term DR (Miller et al. 2012; Miller et al. 2013). It is possible that due to only examining ^{new}protein/^{new}DNA ratio following short-term DR (5 months of age), it may be that no age-related impairments to the proteostatic systems existed and hence this may explain the absence of effects.

6.6 Limitations and future directions

One limitation of this study is that our measurements were taken relatively early in the *ad libitum* lifespan (Liao et al. 2010; Rikke et al. 2010) of these mice, at 5 and 13 months of age. The reason these particular time-points were chosen was that strain TejJ114 has a median lifespan of approximately 800 days under AL feeding, compared to median lifespan of 400 days under DR (Liao et al. 2010; Rikke et al. 2010). Although these strains were sampled at the same age, their biological age was likely to be different. The degree of inter-individual variation in biological age, rather than chronological (i.e. time since birth), is known to be substantial in humans (Shiels & Ritzau-Reid 2015; Belsky et al. 2015). Strain TejJ114 appear to have accelerated ageing with DR, and the identification of appropriate biomarkers of biological age will be key to understanding the mechanisms of DR induced slowed ageing (Shiels et al. 2017; Shiels & Ritzau-Reid 2015).

Following DR, model organisms typically display a tent-shaped lifespan response (Clancy et al. 2002; discussed in Fontana & Partridge 2015). For example, in *Drosophila*, long-lived *Chico* mutants have optimal longevity on a different level of nutrient restriction compared to wild-type controls (Clancy et al. 2002). Similarly both male and female DBA/2 and C57BL/6 mice are known to have both strain and sex-specific differences in the level of DR known to maximise lifespan (Mitchell et al. 2016). Consequently, it is possible that 40% DR was too stringent a DR regime for strain TejJ114 and hence resulted in shortening of lifespan, but that it was optimal for longevity in stain TejJ89 (See Figure 6.7). Consequently, it would be interesting to undertake further lifespan studies in ILSXISS strains under different levels of DR. Indeed, a group in the US is currently exposing nine different ILSXISS female lines known to exhibit strain-specific lifespan responses to DR to 10%, 20% and 40% DR.

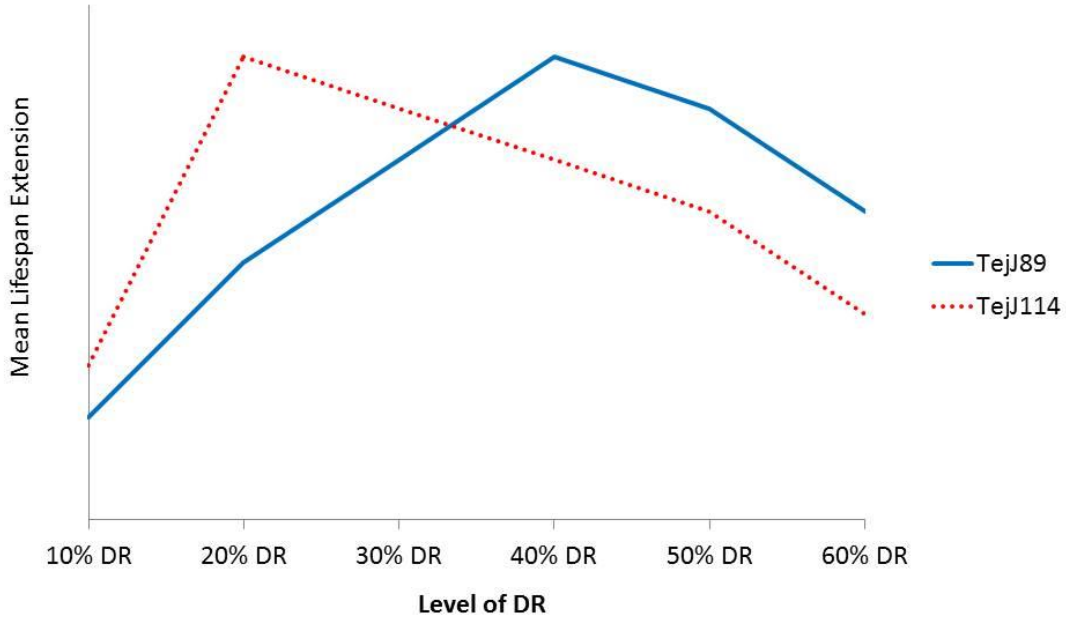

Figure 6.6: Proposed strain-specific differences in the levels of DR required to induce maximal longevity effects in ILSXISS strains TejJ89 (positive) and TejJ114 (negative).

As most research to date has been conducted on male C57BL/6 mice it is difficult to ascertain whether the proposed mechanisms, currently described as hallmarks of DR, are in fact universal modulators of slowed ageing, as there is little basis for comparison in other strains or indeed in female mice. Furthermore, while we found maintenance of WAT mass and increase in BAT to be associated with longevity under DR, we did not measure browning, the conversion of white adipocytes into brown adipocytes (Giralt & Villarroya 2013). Previous DR studies report browning of WAT in male mice, and suggest this being important to longevity under DR (Fabbiano, Suarez-Zamorano, et al. 2016). Moreover an investigation into the role of fibroblast growth factor 21 (FGF21) would be interesting, as it is associated with enhanced thermogenic activity in BAT by using UCP-1 to dissipate energy as heat, and FGF21 and UCP-1 appear to work synergistically under fasted conditions (Chapnik et al. 2017). Moreover, FGF21 is activated by non-shivering

thermogenesis and can induce browning of WAT (Hondares et al. 2011; Fisher et al. 2012).

Another avenue which may be worth pursuing is the repetition of this study under the same experimental protocols used by Liao *et al* and Rikke *et al* (Liao et al. 2010; Rikke et al. 2010). While the authors state that mice were under 40% DR, they were actually fed every other day. This method of feeding is more similar to intermittent fasting, rather than typical DR, as mice are not in a fasted state on days of feeding, and as discussed earlier (section 6.2) gorging behaviour may have an impact on physiological response (Dietz 1995). Therefore it would be interesting to investigate the lifespan response of TejJ89, TejJ48 and TejJ114 following the daily 40% DR protocol as used in this study, to determine if lifespan responses are the same under both restriction protocols.

6.7 Concluding remarks

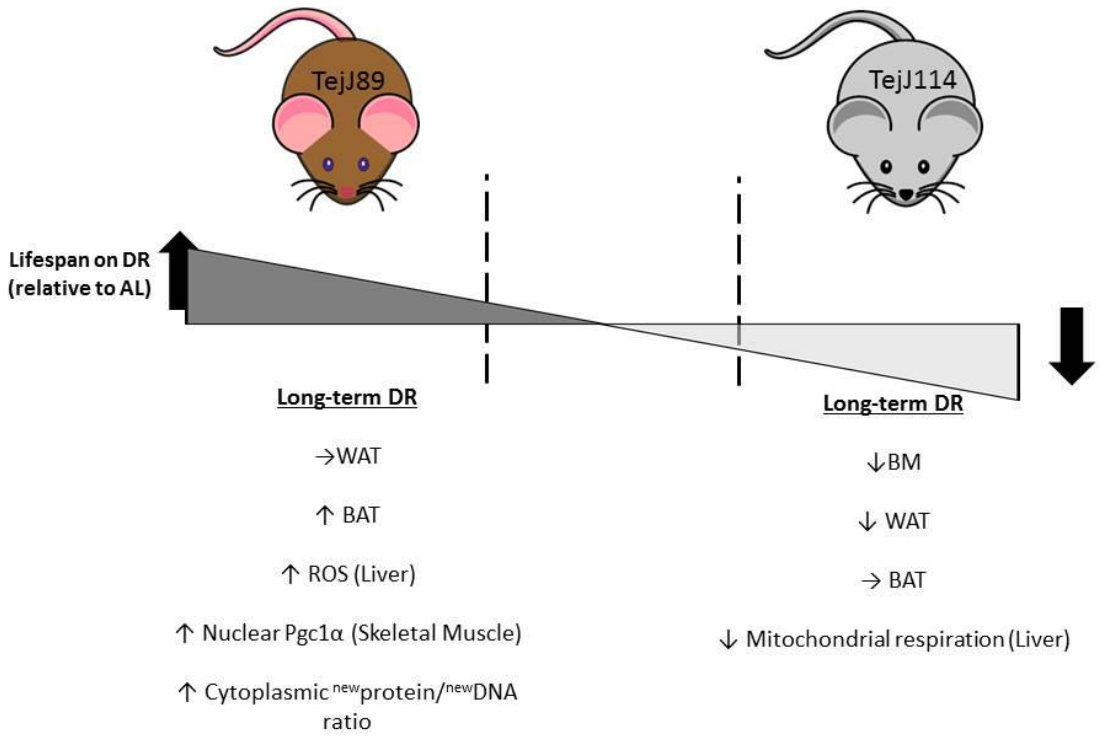

Figure 6.7: Summary figure of responses associated with lifespan extension in strain TejJ89 and lifespan shortening in TejJ114 following 10 months of 40% DR.

The results of this thesis have furthered our knowledge of the mechanisms underlying the DR response and helped to expand our understanding the importance of genotype in DR research. Collectively my data suggests a role for adaptive metabolism as being crucial to longevity with DR, with maintenance of mitochondrial efficiency, found to be more important to lifespan than enhanced function. Conversely, mitochondrial dysfunction, and metabolic inflexibility suggest that negative responders were metabolically constrained resulting in lifespan shortening. Strain TejJ48 as predicted was found unresponsive in most respects. Phenotypic plasticity of the mitochondria is essential to sustain both efficient mitochondria, but also to adapt to energetic demands (Hancock et al. 2011; Brand 2005). Here I find that flexibility relating to adaptive metabolism, in terms of managing fat stores, and maintaining functionally efficient mitochondria, as crucial to longevity with DR, and it appears that the inability of strain TejJ114 to adapt to DR in times of nutritional deficit is detrimental to lifespan response. Perhaps surprisingly enhanced glucose homeostasis was not found to be a prerequisite to lifespan extension. Understanding the impact of genotype on metabolism is critical for transferability of DR research to implementing effective strategies for humans, and for the development of safe and efficacious DR pharmaceutical drug targets. It is clear that the dramatic rise in the proportion of elderly individuals making up our population is going to have significant ramifications. Consequently understanding the fundamental processes that drive ageing and increase the susceptibility to develop disease is undoubtedly one of the greatest current challenges in biomedical research. Future research efforts should take greater advantage of the inherent differences in longevity and pathology at death seen across different mouse strains (Storer 1966) to further understand how specific interventions, including DR, genetic inactivation of IIS/mTOR and rapamycin treatment, act to modulate lifespan and health in the background of increasing genetic heterogeneity.

Appendix I

Supplementary data

The following are the supplementary data related to Chapter 4:

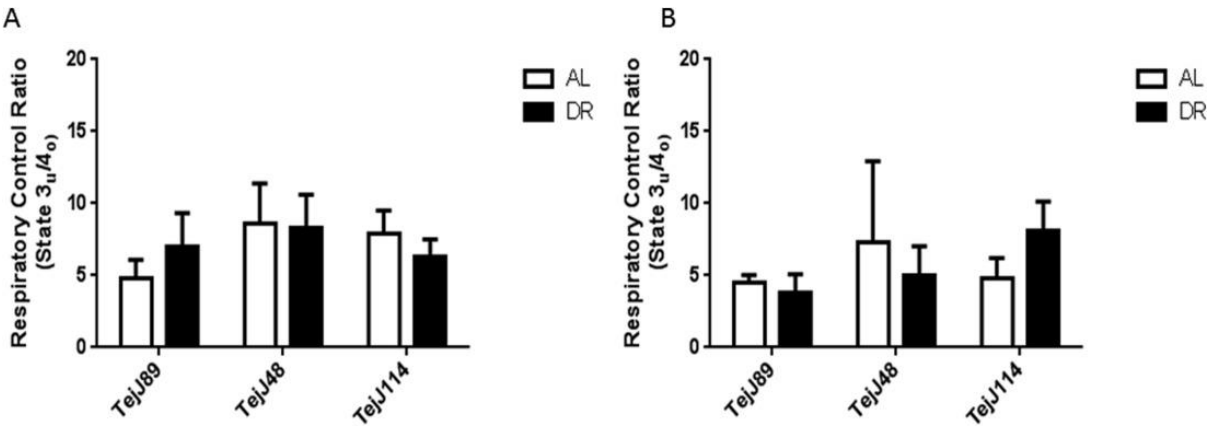

FigureS1: Respiratory control ratio, expressed as the ratio between state 3u (FCCP-induced maximal uncoupled-stimulated respiration) and state 4o (respiration in the absence of ADP) in isolated liver (A) and skeletal muscle (B) mitochondria. No differences were observed by treatment within a strain or between strains.

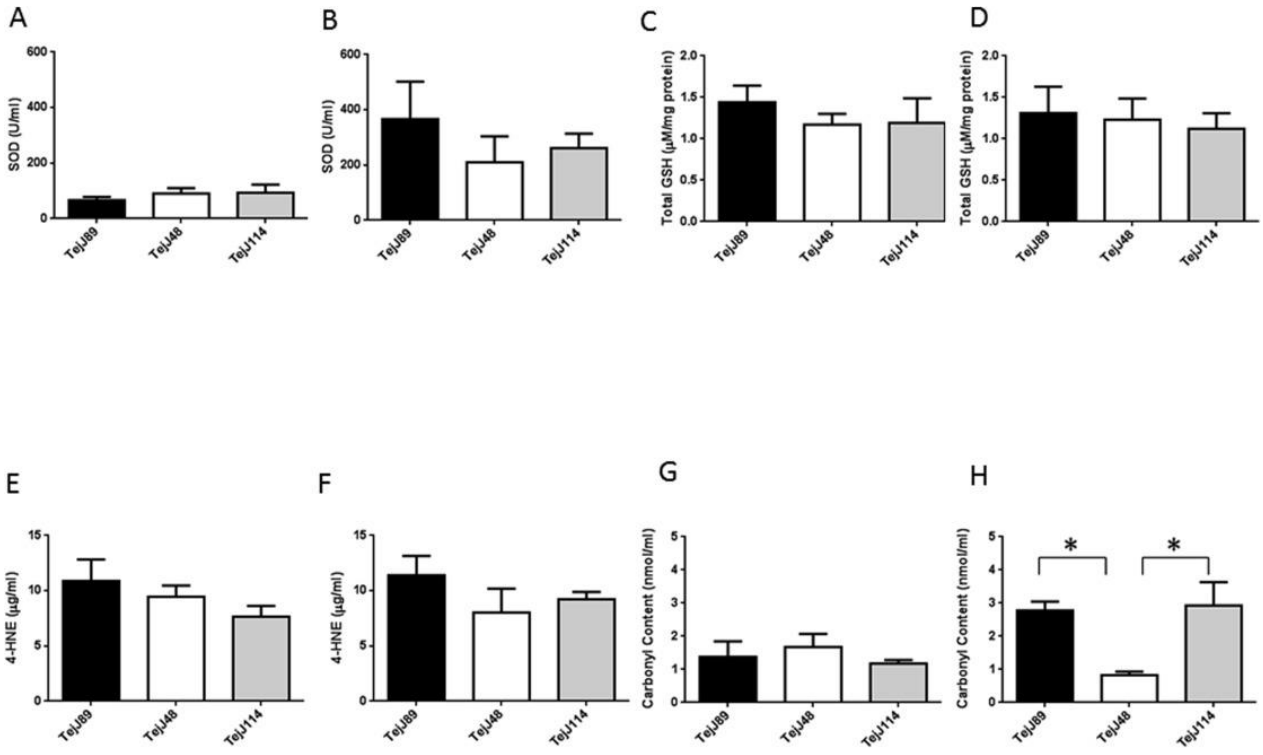

Figure S2: Hepatic antioxidant defence and oxidative damage markers. Total SOD activity was unaltered between strains in either AL (A) or DR (B) mice. Total GSH levels were similarly unaffected by strain under AL (C) or DR feeding (D). 4-HNE levels were unaffected by treatment (E) or by strain (F). Protein carbonyl levels in AL mice (G) were unaffected by strain, but protein carbonyl levels were significantly reduced in strain TejJ48 compared to both strain TejJ89 and TejJ114 under DR (H). Values are expressed as mean ± SEM, where n= 6 per group. * $p<0.05$.

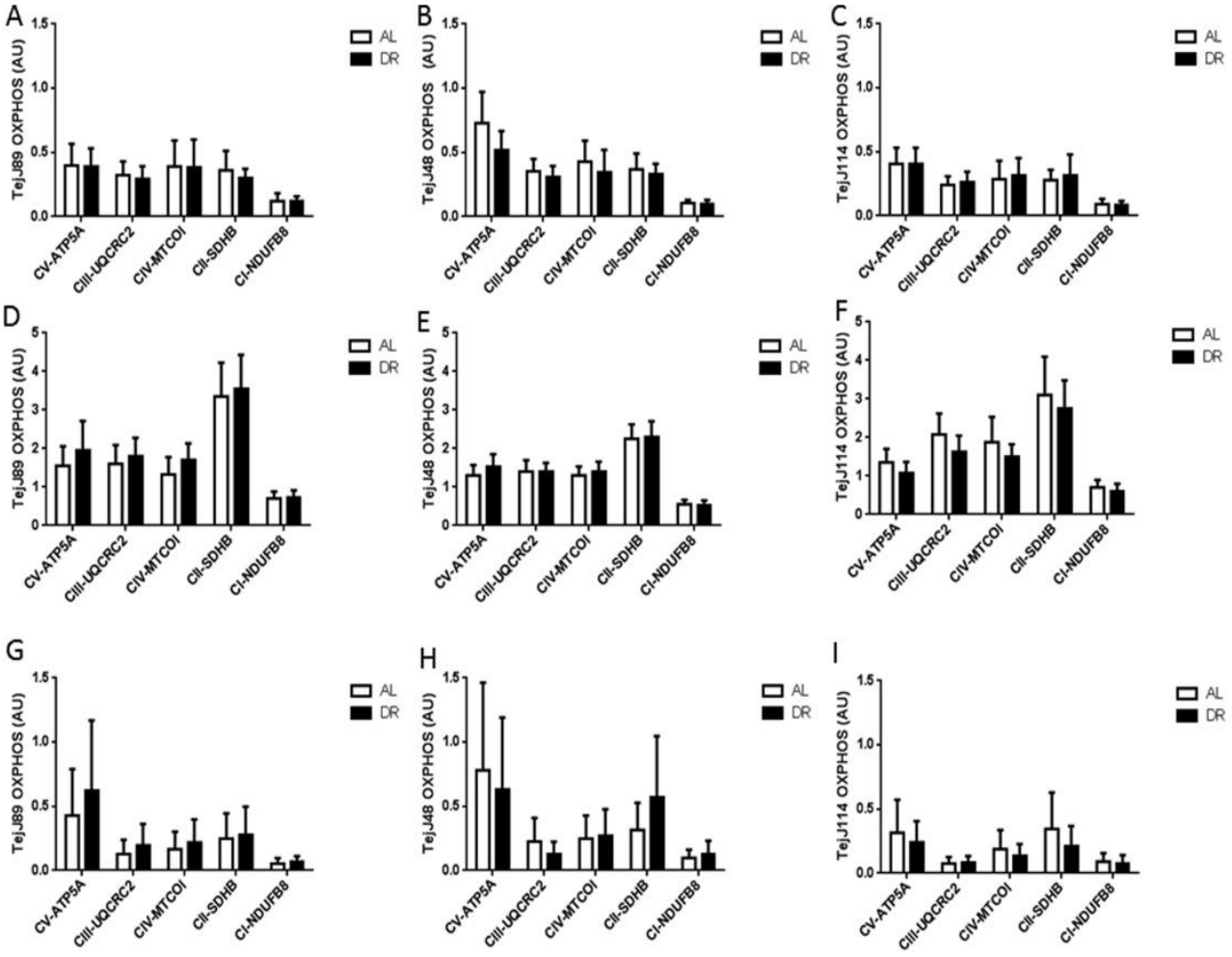

Figure S3: Protein levels of the OXPHOS proteins CI subunit (NDUFB8), CII-30kDa (SDH), CIII-Core protein 2 (UQCRC2), CIV subunit I (MTCO1) and CV alpha subunit (ATP5A) in AL and DR mice from each of the mouse strains. OXPHOS proteins were unaffected by treatment in liver (A-C), skeletal muscle (D-F) and heart (G-I). Values for A–E are arbitrary units (AU) expressed relative to total protein (Ponceau staining). Values are expressed as mean ± SEM, where n= 6 per group.

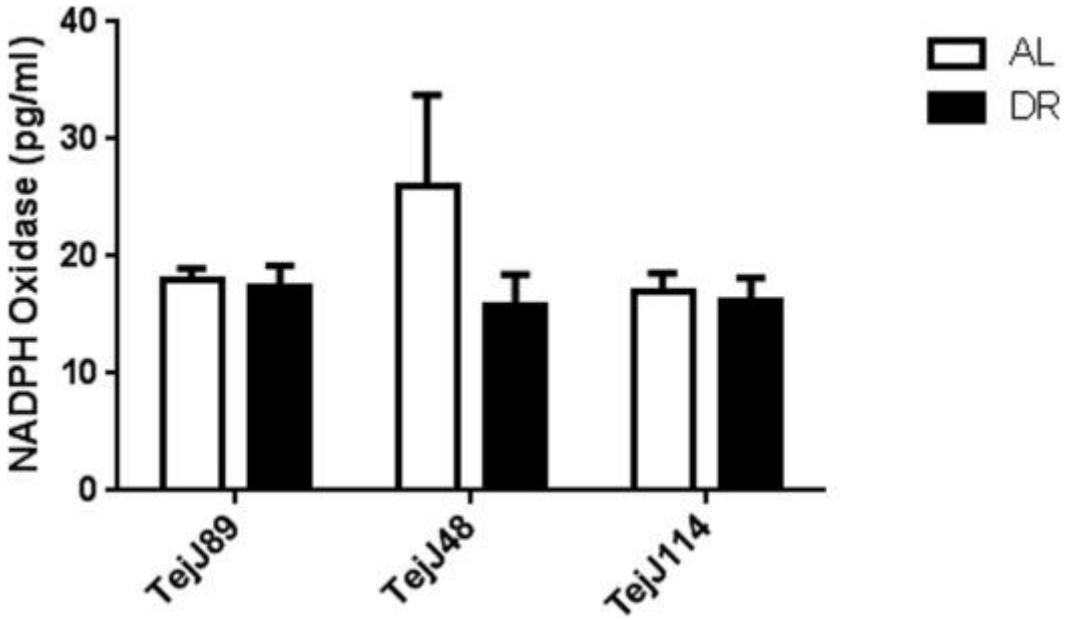

Figure S4: Hepatic NADPH oxidase levels. No differences were observed with treatment or between strains. Values are expressed as mean ± SEM, where n= 6 per group.

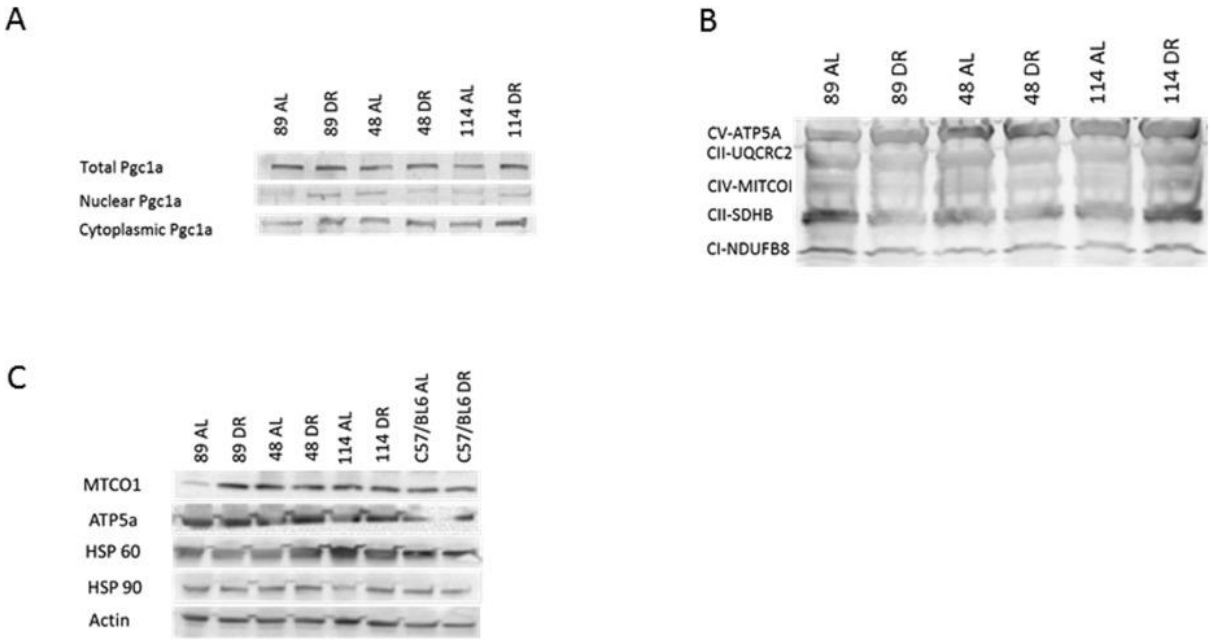

Figure S5: Representative blots for total, cytoplasmic and nuclear PGC-1α (A), OXPHOS (B) and HSP60/90 (C) proteins in liver.

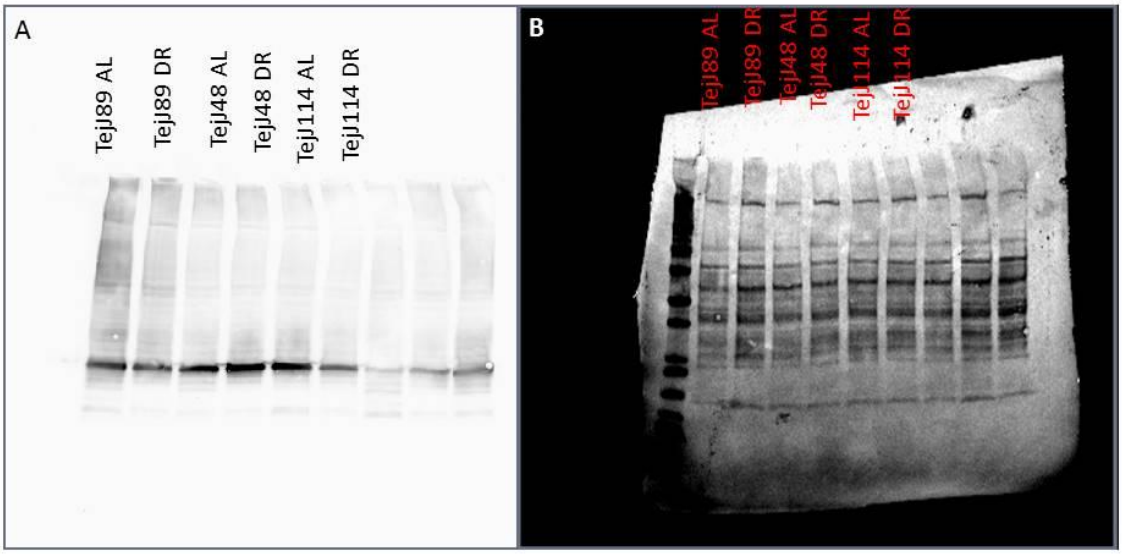

Figure S6: Representative blots for UCP-1 (A) and Total Protein (B) in BAT of mice following 10 months DR.

Bibliography

Agarwal, S. & Sohal, R.S., 1994. DNA oxidative damage and life expectancy in houseflies. *Proceedings of the National Academy of Sciences of the United States of America*, 91(25), pp.12332–5. Available at: http://www.pubmedcentral.nih.gov/articlerender.fcgi?artid=45431&tool=pmcentrez&rendertype=abstract.

Ahima, R.S. & Flier, J.S., 2000. Adipose tissue as an endocrine organ. *Trends in endocrinology and metabolism: TEM*, 11(8), pp.327–332.

Alvarez-Castelao, B., Ruiz-Rivas, C. & Castano, J.G., 2012. A critical appraisal of quantitative studies of protein degradation in the framework of cellular proteostasis. *Biochemistry research international*, 2012, p.823597.

Anderson, R.L. et al., 1995. Exploration of simple insulin sensitivity measures derived from frequently sampled intravenous glucose tolerance (FSIGT) tests. The Insulin Resistance Atherosclerosis Study. *American journal of epidemiology*, 142(7), pp.724–732.

Anderson, R.M. et al., 2008. Dynamic regulation of PGC-1?? localization and turnover implicates mitochondrial adaptation in calorie restriction and the stress response. *Aging Cell*, 7(1), pp.101–111.

Anderson, R.M. & Weindruch, R., 2010. Metabolic reprogramming, caloric restriction and aging. *Trends in endocrinology and metabolism: TEM*, 21(3), pp.134–41. Available at: http://www.sciencedirect.com/science/article/pii/S1043276009001945 [Accessed March 31, 2016].

Andrikopoulos, S. et al., 2005. Differential effect of inbred mouse strain (C57BL/6, DBA/2, 129T2) on insulin secretory function in response to a high fat diet. *Journal of Endocrinology*, 187(1), pp.45–53.

Anisimov, V.N. et al., 2008. Metformin slows down aging and extends life span of female SHR mice. *Cell cycle (Georgetown, Tex.)*, 7(17), pp.2769–2773.

Anson, R.M. et al., 2003. Intermittent fasting dissociates beneficial effects of dietary restriction on glucose metabolism and neuronal resistance to injury from calorie intake. *Proceedings of the National Academy of Sciences of the*

United States of America, 100(10), pp.6216–20. Available at: http://www.pubmedcentral.nih.gov/articlerender.fcgi?artid=156352&tool=pmcentrez&rendertype=abstract.

Anson, R.M., Jones, B. & de Cabod, R., 2005. The diet restriction paradigm: a brief review of the effects of every-other-day feeding. *Age (Dordrecht, Netherlands)*, 27(1), pp.17–25.

Argentino, D.P. et al., 2005. Effects of Long-Term Caloric Restriction on Early Steps of the Insulin-Signaling System in Mouse Skeletal Muscle. , 60(1), pp.28–34.

Asher, G. & Sassone-Corsi, P., 2015. Time for food: the intimate interplay between nutrition, metabolism, and the circadian clock. *Cell*, 161(1), pp.84–92.

Austad, S.N., 2010. Cats, “rats,” and bats: the comparative biology of aging in the 21st century. *Integrative and comparative biology*, 50(5), pp.783–792.

Austad, S.N. & Bartke, A., 2015. Sex Differences in Longevity and in Responses to Anti-Aging Interventions: A Mini-Review. *Gerontology*, 62(1), pp.40–46.

Ayala, V. et al., 2007. Dietary protein restriction decreases oxidative protein damage, peroxidizability index, and mitochondrial complex I content in rat liver. *The journals of gerontology. Series A, Biological sciences and medical sciences*, 62(4), pp.352–360.

Balcombe, N.R. & Sinclair, A., 2001. Ageing: definitions, mechanisms and the magnitude of the problem. *Best practice & research. Clinical gastroenterology*, 15(6), pp.835–849.

Baqri, R.M. et al., 2014. Mitochondrial chaperone TRAP1 activates the mitochondrial UPR and extends healthspan in Drosophila. *Mechanisms of ageing and development*, 141–142, pp.35–45.

Bartels, S.J. & Naslund, J.A., 2013. The underside of the silver tsunami--older adults and mental health care. *The New England journal of medicine*, 368(6), pp.493–496.

Bartke, A. et al., 2007. Effects of Dietary Restriction on the Expression of Insulin-Signaling-Related Genes in Long-Lived Mutant Mice. *Interdiscip Top Gerontol.*, 35, pp.69–82.

Bartke, A., 2008. Insulin and aging. *Cell Cycle*, 7(21), pp.3338–3343.

Bartke, A., 2006. Long-lived Klotho mice: new insights into the roles of IGF-1 and insulin in aging. *Trends in endocrinology and metabolism: TEM*, 17(2), pp.33–35.

Bartke, A. et al., 2001. Prolonged longevity of hypopituitary dwarf mice. *Experimental gerontology*, 36(1), pp.21–28.

Bartke, A. & Brown-Borg, H., 2004. Life Extension in the Dwarf Mouse. *Current Topics in Developmental Biology*, 63, pp.189–225.

Barusch, A.S., 2013. The aging tsunami: time for a new metaphor? *Journal of gerontological social work*, 56(3), pp.181–184.

Barzilai, N. et al., 1998. Caloric restriction reverses hepatic insulin resistance in aging rats by decreasing visceral fat. *The Journal of clinical investigation*, 101(7), pp.1353–1361.

Barzilai, N. et al., 2012. The critical role of metabolic pathways in aging. *Diabetes*, 61(6), pp.1315–22.

Barzilai, N. & Gupta, G., 1999a. Interaction between aging and syndrome X: new insights on the pathophysiology of fat distribution. *Annals of the New York Academy of Sciences*, 892(718), pp.58–72.

Barzilai, N. & Gupta, G., 1999b. Revisiting the role of fat mass in the life extension induced by caloric restriction. *The journals of gerontology. Series A, Biological sciences and medical sciences*, 54(3), pp.B89–B96.

Belsky, D.W. et al., 2015. Quantification of biological aging in young adults. *Proceedings of the National Academy of Sciences of the United States of America*, 112(30), pp.E4104-10.

Berg, B.N. & Simms, H.S., 1960. Nutrition and longevity in the rat. II. Longevity and the onset of disease with different levels of intake. *J. Nutr.*, 71, pp.255–63.

Berglund, E.D. et al., 2008. Glucose metabolism in vivo in four commonly used inbred mouse strains. *Diabetes*, 57, pp.1790–1799. Available at: http://www.pubmedcentral.nih.gov/articlerender.fcgi?artid=2972983&tool=pmc

entrez&rendertype=abstract%5Cnhttp://diabetes.diabetesjournals.org/content/57/7/1790.short.

Berryman, D.E. et al., 2008. Role of the GH/IGF-1 axis in lifespan and healthspan: lessons from animal models. *Growth hormone & IGF research : official journal of the Growth Hormone Research Society and the International IGF Research Society*, 18(6), pp.455–471.

Bertrand, H. a et al., 1980. Changes in adipose mass and cellularity through the adult life of rats fed ad libitum or a life-prolonging restricted diet. *Journal of gerontology*, 35(6), pp.827–835.

Bevilacqua, L. et al., 2004. Effects of short- and medium-term calorie restriction on muscle mitochondrial proton leak and reactive oxygen species production. *American journal of physiology. Endocrinology and metabolism*, 286(5), pp.E852–E861.

Bevilacqua, L. et al., 2005. Long-term caloric restriction increases UCP3 content but decreases proton leak and reactive oxygen species production in rat skeletal muscle mitochondria. *Am J Physiol Endocrinol Metab*, 289(3), pp.E429-38. Available at: http://www.ncbi.nlm.nih.gov/pubmed/15886224.

Bhattacharya, A. et al., 2012. Dietary restriction but not rapamycin extends disease onset and survival of the H46R/H48Q mouse model of ALS. *Neurobiology of aging*, 33(8), pp.1829–1832.

Bjedov, I. & Partridge, L., 2011. A longer and healthier life with TOR down-regulation: genetics and drugs. *Biochemical Society transactions*, 39(2), pp.460–465.

Blüher, M., Kahn, B.B. & Kahn, C.R., 2003. Extended longevity in mice lacking the insulin receptor in adipose tissue. *Science (New York, N.Y.)*, 299(5606), pp.572–4. Available at: http://www.sciencemag.org/cgi/doi/10.1126/science.1078223%5Cnhttp://www.ncbi.nlm.nih.gov/pubmed/12543978.

Borbolis, F. & Syntichaki, P., 2015. Cytoplasmic mRNA turnover and ageing. *Mechanisms of ageing and development*, 152, pp.32–42.

Le Bourg, E., 2010. Predicting whether dietary restriction would increase longevity

in species not tested so far. *Ageing research reviews*, 9(3), pp.289–297.

Le Bourg, E. & Rattan, S.I.S., 2006. Can dietary restriction increase longevity in all species, particularly in human beings? Introduction to a debate among experts. *Biogerontology*, 7(3), pp.123–125.

Bradford, M.M., 1976. A rapid and sensitive method for the quantitation of microgram quantities of protein utilizing the principle of protein-dye binding. *Analytical biochemistry*, 72, pp.248–254.

Braeckman, B.P., Demetrius, L. & Vanfleteren, J.R., 2006. The dietary restriction effect in C. elegans and humans: is the worm a one-millimeter human? *Biogerontology*, 7(3), pp.127–133.

Brand, M.D., 2005. The efficiency and plasticity of mitochondrial energy transduction. *Biochem Soc Trans*, 33(Pt 5), pp.897–904.

Brand, M.D.D. & Nicholls, D.G.G., 2011. Assessing mitochondrial dysfunction in cells. *Biochemical Journal*, 435(2), pp.297–312. Available at: http://biochemj.org/lookup/doi/10.1042/BJ20110162%5Cnhttp://www.pubmedcentral.nih.gov/articlerender.fcgi?artid=3076726&tool=pmcentrez&rendertype=abstract.

Brown-Borg, H. et al., 1996. Dwarf mice and the ageing process. *Nature*, 384, pp.33–33.

Bruss, M.D. et al., 2010. Calorie restriction increases fatty acid synthesis and whole body fat oxidation rates. *American journal of physiology. Endocrinology and metabolism*, 298(1), pp.E108-16.

Busch, R. et al., 2006. Measurement of protein turnover rates by heavy water labeling of nonessential amino acids. *Biochimica et biophysica acta*, 1760(5), pp.730–744.

de Cabo, R. et al., 2015. Serum from calorie-restricted animals delays senescence and extends the lifespan of normal human fibroblasts in vitro. *Aging*, 7(3), pp.152–166.

Cajigas, I.J., Will, T. & Schuman, E.M., 2010. Protein homeostasis and synaptic plasticity. *The EMBO journal*, 29(16), pp.2746–2752.

Cantley, J. et al., 2009. Deletion of the von Hippel-Lindau gene in pancreatic beta cells impairs glucose homeostasis in mice. *The Journal of clinical investigation*, 119(1), pp.125–135.

Carey, J.R. et al., 2002. Life history response of Mediterranean fruit flies to dietary restriction. *Dietary restriction of Mediterranean fruit flies, J. R. Carey et al.*, 1(2), pp.140–148. Available at: http://doi.wiley.com/10.1046/j.1474-9728.2002.00019.x%5Cnpapers3://publication/doi/10.1046/j.1474-9728.2002.00019.x.

Carey, J.R., 2002. Longevity minimalists: life table studies of two species of northern Michigan adult mayflies. *Experimental gerontology*, 37(4), pp.567–570.

Carey, V.J. et al., 1997. Body fat distribution and risk of non-insulin-dependent diabetes mellitus in women. The Nurses' Health Study. *American journal of epidemiology*, 145(7), pp.614–619.

Carrillo, A.E. & Flouris, A.D., 2011. Caloric restriction and longevity: effects of reduced body temperature. *Ageing research reviews*, 10(1), pp.153–162.

Castro, J.P. et al., 2017. 4-Hydroxynonenal (HNE) modified proteins in metabolic diseases. *Free radical biology & medicine*, 111, pp.309–315.

Castro, J.P. et al., 2014. HSP90 cleavage associates with oxidized proteins accumulation after oxidative stress. *Free Radical Biology and Medicine*, 75, pp.S24–S25.

Cava, E. & Fontana, L., 2013. Will calorie restriction work in humans? *Aging*, 5(7), pp.507–514.

Chaix, A. et al., 2014. Time-restricted feeding is a preventative and therapeutic intervention against diverse nutritional challenges. *Cell metabolism*, 20(6), pp.991–1005.

Chapnik, N., Genzer, Y. & Froy, O., 2017. Relationship between FGF21 and UCP1 levels under time-restricted feeding and high-fat diet. *The Journal of nutritional biochemistry*, 40, pp.116–121.

Chaput, J.-P., Gilbert, J.-A. & Tremblay, A., 2007. Relationship between food insecurity and body composition in Ugandans living in urban Kampala.

Journal of the American Dietetic Association, 107(11), pp.1978–1982.

Chatterjee, S. et al., 2016. Type 2 Diabetes as a Risk Factor for Dementia in Women Compared With Men: A Pooled Analysis of 2.3 Million People Comprising More Than 100,000 Cases of Dementia. *Diabetes care*, 39(2), pp.300–307.

Cheney, K.E. et al., 1980. Survival and disease patterns in C57BL/6J mice subjected to undernutrition. *Experimental gerontology*, 15(4), pp.237–258.

Chevion, M., Berenshtein, E. & Stadtman, E.R., 2000. Human studies related to protein oxidation: protein carbonyl content as a marker of damage. *Free radical research*, 33 Suppl, pp.S99-108.

Chouchani, E.T. et al., 2016. Mitochondrial ROS regulate thermogenic energy expenditure and sulfenylation of UCP1. *Nature*, 532(7597), pp.112–116.

Civitarese, A.E. et al., 2007. Calorie restriction increases muscle mitochondrial biogenesis in healthy humans. *PLoS Medicine*, 4(3), pp.485–494.

Clancy, D.J. et al., 2002. Dietary restriction in long-lived dwarf flies. *Science (New York, N.Y.)*, 296(5566), p.319.

Clayton, J. & Collins, F., 2014. Policy: NIH to balance sex in cell and animal studies. *Nature*, 509, pp.282–283. Available at: https://www.ncbi.nlm.nih.gov/pmc/articles/PMC5101948/.

Cohen, H.Y. et al., 2004. Calorie restriction promotes mammalian cell survival by inducing the SIRT1 deacetylase. *Science (New York, N.Y.)*, 305(5682), pp.390–392.

Colman, R.J. et al., 2009. Caloric Restriction Delays Disease Onset and Mortality in Rhesus Monkeys. *Science*, 325(10 July), pp.201–204.

Colman, R.J. et al., 2014. Caloric restriction reduces age-related and all-cause mortality in rhesus monkeys. *Nature communications*, 5, p.3557. Available at: http://www.mendeley.com/research/caloric-restriction-reduces-agerelated-allcause-mortality-rhesus-monkeys/.

Cooper, T. et al., 2004. Effect of caloric restriction on life span of the housefly, Musca domestica. *FASEB Journal*, 13, pp.1–13. Available at:

http://www.fasebj.org/content/18/13/1591.short.

Corton, J.C. & Brown-Borg, H.M., 2005. Peroxisome Proliferator-Activated Receptor γ Coactivator 1 in Caloric Restriction and Other Models of Longevity. *The Journals of Gerontology Series A: Biological Sciences and Medical Sciences* , 60(12), pp.1494–1509. Available at: http://biomedgerontology.oxfordjournals.org/content/60/12/1494.abstract.

Coschigano, K.T. et al., 2000. Assessment of growth parameters and life span of GHR/BP gene-disrupted mice. *Endocrinology*, 141(7), pp.2608–2613.

Cuervo, A.M., 2008. Autophagy and aging: keeping that old broom working. *Trends in genetics : TIG*, 24(12), pp.604–612.

Dai, D.-F. et al., 2014. Altered proteome turnover and remodeling by short-term caloric restriction or rapamycin rejuvenate the aging heart. *Aging cell*, 13(3), pp.529–539.

Das, M., Gabriely, I. & Barzilai, N., 2004. Caloric restriction, body fat and ageing in experimental models. *Obesity Reviews*, 5(1), pp.13–19.

DeFronzo, R.A., 1981. Glucose intolerance and aging. *Diabetes care*, 4(4), pp.493–501.

Delaney, J.R. et al., 2013. Stress profiling of longevity mutants identifies Afg3 as a mitochondrial determinant of cytoplasmic mRNA translation and aging. *Aging cell*, 12(1), pp.156–166.

Després, J. & Lemieux, I., 2006. Abdominal obesity and metabolic syndrome. *Nature*, 444, pp.881–887.

Dhahbi, J. et al., 2004. Temporal linkage between the phenotypic and genomic responses to caloric restriction. *Proc Natl Acad Sci U S A.*, 101(15), pp.5524–9.

Dietz, W.H., 1995. Does hunger cause obesity? *Pediatrics*, 95(5), pp.766–767.

Dietz, W.H. et al., 2015. Management of obesity: improvement of health-care training and systems for prevention and care. *Lancet (London, England)*, 385(9986), pp.2521–2533.

Dionne, D.A. et al., 2016. Caloric restriction paradoxically increases adiposity in

mice with genetically reduced insulin. *Endocrinology*, 157(7), pp.2724–2734.

Drake, J.C. et al., 2013. Assessment of mitochondrial biogenesis and mTORC1 signaling during chronic rapamycin feeding in male and female mice. *The journals of gerontology. Series A, Biological sciences and medical sciences*, 68(12), pp.1493–1501.

Drake, J.C. et al., 2014. Long-lived crowded-litter mice have an age-dependent increase in protein synthesis to DNA synthesis ratio and mTORC1 substrate phosphorylation. *American journal of physiology. Endocrinology and metabolism*, 307(9), pp.E813-21.

Drake, J.C. et al., 2015. Long-lived Snell dwarf mice display increased proteostatic mechanisms that are not dependent on decreased mTORC1 activity. *Aging cell*, 14(3), pp.474–482.

Duan, W. & Mattson, M.P., 1999. Dietary restriction and 2-deoxyglucose administration improve behavioral outcome and reduce degeneration of dopaminergic neurons in models of Parkinson's disease. *Journal of neuroscience research*, 57(2), pp.195–206.

Duffy, P.H. et al., 1989. Effect of chronic caloric restriction on physiological variables related to energy metabolism in the male Fischer 344 rat. *Mechanisms of ageing and development*, 48(2), pp.117–133.

Durieux, J., Wolff, S. & Dillin, A., 2011. The Cell-Non-Autonomous Nature of Electron Transport Chain-Mediated Longevity. *Cell*, 144(1), pp.79–91.

Eden, E. et al., 2011. Proteome half-life dynamics in living human cells. *Science (New York, N.Y.)*, 331(6018), pp.764–768.

Edwards, C. et al., 2015. Mechanisms of amino acid-mediated lifespan extension in Caenorhabditis elegans. *BMC genetics*, 16, p.8.

Fabbiano, S., Suá Rez-Zamorano, N., et al., 2016. Caloric Restriction Leads to Browning of White Adipose Tissue through Type 2 Immune Signaling. *Cell Metabolism*, 24(October), pp.1–13. Available at: http://dx.doi.org/10.1016/j.cmet.2016.07.023.

Fabbiano, S., Suarez-Zamorano, N., et al., 2016. Caloric Restriction Leads to Browning of White Adipose Tissue through Type 2 Immune Signaling. *Cell*

metabolism, 24(3), pp.434–446.

Fabrizio, P. & Longo, V.D., 2003. The chronological life span of Saccharomyces cerevisiae. *Aging cell*, 2(2), pp.73–81.

Fanara, P. et al., 2004. In vivo measurement of microtubule dynamics using stable isotope labeling with heavy water. Effect of taxanes. *The Journal of biological chemistry*, 279(48), pp.49940–49947.

Faulks, S.C. et al., 2006. Calorie restriction in mice: effects on body composition, daily activity, metabolic rate, mitochondrial reactive oxygen species production, and membrane fatty acid composition. *The journals of gerontology. Series A, Biological sciences and medical sciences*, 61(8), pp.781–794.

Ferguson, M. et al., 2007. Effect of long-term caloric restriction on oxygen consumption and body temperature in two different strains of mice. *Mechanisms of Ageing and Development*, 128(10), pp.539–545.

Fernandes, G., Yunis, E.J. & Good, R.A., 1976. Influence of diet on survival of mice. *Proceedings of the National Academy of Sciences of the United States of America*, 73(4), pp.1279–83. Available at: http://www.pubmedcentral.nih.gov/articlerender.fcgi?artid=430247&tool=pmcentrez&rendertype=abstract.

Ferrara, C.M. & Goldberg, A.P., 2001. Limited value of the homeostasis model assessment to predict insulin resistance in older men with impaired glucose tolerance. *Diabetes care*, 24(2), pp.245–249.

Feuers, R.J., 1998. The effects of dietary restriction on mitochondrial dysfunction in aging. *Annals of the New York Academy of Sciences*, 854, pp.192–201.

Finley, L.W.S. et al., 2012. Skeletal muscle transcriptional coactivator PGC-1α mediates mitochondrial, but not metabolic, changes during calorie restriction. *Proceedings of the National Academy of Sciences of the United States of America*, 109(8), pp.2931–6. Available at: http://www.pubmedcentral.nih.gov/articlerender.fcgi?artid=3286952&tool=pmcentrez&rendertype=abstract.

Finley, L.W.S. & Haigis, M.C., 2009. The coordination of nuclear and mitochondrial

communication during aging and calorie restriction. *Ageing research reviews*, 8(3), pp.173–88. Available at: http://www.sciencedirect.com/science/article/pii/S1568163709000166 [Accessed March 24, 2016].

Fisher, F.M. et al., 2012. FGF21 regulates PGC-1alpha and browning of white adipose tissues in adaptive thermogenesis. *Genes & development*, 26(3), pp.271–281.

Flurkey, K. et al., 2001. Lifespan extension and delayed immune and collagen aging in mutant mice with defects in growth hormone production. *Proceedings of the National Academy of Sciences of the United States of America*, 98(12), pp.6736–6741.

Fok, W.C. et al., 2014. Combined treatment of rapamycin and dietary restriction has a larger effect on the transcriptome and metabolome of liver. *Aging Cell*.

Fontaine, K.R. et al., 2003. Years of life lost due to obesity. *JAMA, January*, 289(2), pp.187–193. Available at: http://www.ncbi.nlm.nih.gov/pubmed/12517229.

Fontana, L. et al., 2007. Calorie restriction or exercise: effects on coronary heart disease risk factors. A randomized, controlled trial. *American journal of physiology. Endocrinology and metabolism*, 293, pp.E197–E202.

Fontana, L. et al., 2013. Dietary protein restriction inhibits tumor growth in human xenograft models. *Oncotarget*, 4(12), pp.2451–2461.

Fontana, L. et al., 2016. Effects of 2-year calorie restriction on circulating levels of IGF-1, IGF-binding proteins and cortisol in nonobese men and women: A randomized clinical trial. *Aging Cell*, 15(1), pp.22–27.

Fontana, L. et al., 2004. Long-term calorie restriction is highly effective in reducing the risk for atherosclerosis in humans. *Proceedings of the National Academy of Sciences of the United States of America*, 101(7), pp.6659–6663.

Fontana, L. et al., 2008. Long-term effects of calorie or protein restriction on serum IGF-1 and IGFBP-3 concentration in humans. *Aging cell*, 7(5), pp.681–687. Available at: http://onlinelibrary.wiley.com/doi/10.1111/j.1474-9726.2008.00417.x/full.

Fontana, L., Klein, S. & Holloszy, J.O., 2010. Effects of long-term calorie restriction and endurance exercise on glucose tolerance, insulin action, and adipokine production. *AGE*, 32(1), pp.97–108. Available at: http://dx.doi.org/10.1007/s11357-009-9118-z.

Fontana, L. & Partridge, L., 2015. Promoting health and longevity through diet: From model organisms to humans. *Cell*, 161(1), pp.106–118. Available at: http://dx.doi.org/10.1016/j.cell.2015.02.020.

Forster, M.J., Morris, P. & Sohal, R.S., 2003. Genotype and age influence the effect of caloric intake on mortality in mice Mortality in Mice. *The FASEB Journal*, (Apr;17(6)), pp.690–2. Available at: Epub 2003 Feb 5.

Franco, M.C. et al., 2015. Nitration of Hsp90 on Tyrosine 33 regulates mitochondrial metabolism. *Journal of Biological Chemistry*, 290(31), pp.19055–19066.

Funkat, A. et al., 2004. Metabolic adaptations of three inbred strains of mice (C57BL/6, DBA/2, and 129T2) in response to a high-fat diet. *The Journal of nutrition*, 134(12), pp.3264–3269.

Gabriely, I. et al., 2002. Removal of visceral fat prevents insulin resistance and glucose intolerance of aging: an adipokine-mediated process? *Diabetes*, 51(10), pp.2951–2958.

Garcia-Cazarin, M.L., Snider, N.N. & Andrade, F.H., 2011. Mitochondrial Isolation from Skeletal Muscle. *Journal of Visualized Experiments : JoVE.*, 49(2452), p.doi:10.3791/2452. Available at: http://www.jove.com/video/2452.

Gariani, K. et al., 2016. Eliciting the mitochondrial unfolded protein response by nicotinamide adenine dinucleotide repletion reverses fatty liver disease in mice. *Hepatology (Baltimore, Md.)*, 63(4), pp.1190–1204.

Gates, A.C. et al., 2007. Respiratory uncoupling in skeletal muscle delays death and diminishes age-related disease. *Cell metabolism*, 6(6), pp.497–505.

Gems, D. & Doonan, R., 2009. Antioxidant defense and aging in C. elegans: Is the oxidative damage theory of aging wrong? *Cell Cycle*, 8(11), pp.1681–1687.

Gems, D. & Partridge, L., 2013. Genetics of longevity in model organisms: debates and paradigm shifts. *Annual review of physiology*, 75, pp.621–644.

Ghosh, S. et al., 2014. A systems biology analysis of the unique and overlapping transcriptional responses to caloric restriction and dietary methionine restriction in rats. *FASEB journal : official publication of the Federation of American Societies for Experimental Biology*, 28(6), pp.2577–2590.

Giralt, M. & Villarroya, F., 2013. White, brown, beige/brite: different adipose cells for different functions? *Endocrinology*, 154(9), pp.2992–3000.

Giroud, S. et al., 2010. The grey mouse lemur uses season-dependent fat or protein sparing strategies to face chronic food restriction. *PLoS ONE*, 5(1).

Goldspink, D.F. et al., 1987. The influence of chronic dietary intervention on protein turnover and growth of the diaphragm and extensor digitorum longus muscles of the rat. *Experimental gerontology*, 22(1), pp.67–78.

Goldspink, D.F. & Kelly, F.J., 1984. Protein turnover and growth in the whole body, liver and kidney of the rat from the foetus to senility. *The Biochemical journal*, 217(2), pp.507–516.

Goodrick, C.L. et al., 1990. Effects of intermittent feeding upon body weight and lifespan in inbred mice: interaction of genotype and age. *Mechanisms of Ageing and Development*, 55(1), pp.69–87.

Goren, H.J., Kulkarni, R.N. & Kahn, C.R., 2004. Glucose homeostasis and tissue transcript content of insulin signaling intermediates in four inbred strains of mice: C57BL/6, C57BLKS/6, DBA/2, and 129X1. *Endocrinology*, 145(7), pp.3307–3323.

Gouspillou, G. & Hepple, R.T., 2013. Facts and controversies in our understanding of how caloric restriction impacts the mitochondrion. *Experimental gerontology*, 48(10), pp.1075–84. Available at: http://www.sciencedirect.com/science/article/pii/S0531556513000818 [Accessed March 31, 2016].

Grandison, R.C., Piper, M.D.W. & Partridge, L., 2009. Amino-acid imbalance explains extension of lifespan by dietary restriction in Drosophila. *Nature*, 462(7276), pp.1061–1064.

Gredilla, R. et al., 2001. Caloric restriction decreases mitochondrial free radical generation at complex I and lowers oxidative damage to mitochondrial DNA in

the rat heart. *The FASEB journal : official publication of the Federation of American Societies for Experimental Biology*, 15(7), pp.1589–1591.

Greer, E.L. & Brunet, A., 2009. Different dietary restriction regimens extend lifespan by both independent and overlapping genetic pathways in C. elegans. *Aging cell*, 8(2), pp.113–127.

Gross, L. & Dreyfuss, Y., 1984. Reduction in the incidence of radiation-induced tumors in rats after restriction of food intake. *Proceedings of the National Academy of Sciences of the United States of America*, 81(23), pp.7596–7598.

Hagopian, K., Ramsey, J.J. & Weindruch, R., 2003. Caloric restriction increases gluconeogenic and transaminase enzyme activities in mouse liver. *Experimental gerontology*, 38(3), pp.267–278.

el Haj, A.J. et al., 1986. The effect of chronic and acute dietary restriction on the growth and protein turnover of fast and slow types of rat skeletal muscle. *Comparative biochemistry and physiology. A, Comparative physiology*, 85(2), pp.281–287.

Halagappa, V.K.M. et al., 2007. Intermittent fasting and caloric restriction ameliorate age-related behavioral deficits in the triple-transgenic mouse model of Alzheimer's disease. *Neurobiology of disease*, 26(1), pp.212–220.

Hamilton, K.L. & Miller, B.F., 2017. Mitochondrial proteostasis as a shared characteristic of slowed aging: the importance of considering cell proliferation. *The Journal of physiology*.

Hancock, C.R. et al., 2011. Does calorie restriction induce mitochondrial biogenesis? A reevaluation. *The FASEB journal : official publication of the Federation of American Societies for Experimental Biology*, 25, pp.785–791.

Harper, J.M., 2008. Wild-derived mouse stocks: an underappreciated tool for aging research. *Age (Dordrecht, Netherlands)*, 30(2–3), pp.135–145.

Harper, J.M., Leathers, C.W. & Austad, S.N., 2006. Does caloric restriction extend life in wild mice? *Aging Cell*, 5(6), pp.441–449.

Harrison, D.E. et al., 2009. Rapamycin fed late in life extends lifespan in genetically heterogeneous mice. *Nature*, 460(7253), pp.392–395.

Harrison, D.E. & Archer, J.R., 1987. Genetic differences in effects of food restriction on aging in mice. *The Journal of nutrition*, 117(2), pp.376–382.

Harrison, D.E., Archer, J.R. & Astle, C.M., 1984. Effects of food restriction on aging: separation of food intake and adiposity. *Proceedings of the National Academy of Sciences of the United States of America*, 81(6), pp.1835–8.

Hayflick, L., 2010. Dietary Restriction: Theory Fails to Satiate. *Science*, 329(5995), pp.1014–1015.

Hellerstein, M.K. & Murphy, E., 2004. Stable isotope-mass spectrometric measurements of molecular fluxes in vivo: emerging applications in drug development. *Current opinion in molecular therapeutics*, 6(3), pp.249–264.

Hellerstein, M.K. & Neese, R.A., 1999. Mass isotopomer distribution analysis at eight years: theoretical, analytic, and experimental considerations. *The American journal of physiology*, 276(6 Pt 1), pp.E1146-70.

Hempenstall, S. et al., 2012. Dietary restriction increases skeletal muscle mitochondrial respiration but not mitochondrial content in C57BL/6 mice. *Mechanisms of Ageing and Development*, 133(1), pp.37–45.

Hempenstall, S. et al., 2010. The impact of acute caloric restriction on the metabolic phenotype in male C57BL/6 and DBA/2 mice. *Mechanisms of Ageing and Development*, 131(2), pp.111–118. Available at: http://dx.doi.org/10.1016/j.mad.2009.12.008.

Henderson, G.C. et al., 2010. Effects of adiposity and 30 days of caloric restriction upon protein metabolism in moderately vs. severely obese women. *Obesity (Silver Spring, Md.)*, 18(6), pp.1135–1142. Available at: http://dx.doi.org/10.1038/oby.2009.505.

Hepple, R.T. et al., 2005. Long-term caloric restriction abrogates the age-related decline in skeletal muscle aerobic function. *The FASEB Journal express article*, 25(4), pp.1–25.

Hill, S. & Van Remmen, H., 2014a. Mitochondrial stress signaling in longevity: A new role for mitochondrial function in aging. *Redox Biology*, 2, pp.936–944. Available at: http://www.sciencedirect.com/science/article/pii/S2213231714000883

[Accessed September 30, 2015].

Hill, S. & Van Remmen, H., 2014b. Mitochondrial stress signaling in longevity: A new role for mitochondrial function in aging. *Redox Biology*, 2, pp.936–944.

Himms-Hagen, J., 1985. Food restriction increases torpor and improves brown adipose tissue thermogenesis in ob/ob mice. *The American journal of physiology*, 248(5 Pt 1), pp.E531-9.

Hine, C. et al., 2015. Endogenous hydrogen sulfide production is essential for dietary restriction benefits. *Cell*, 160(1–2), pp.132–44. Available at: http://www.sciencedirect.com/science/article/pii/S0092867414015256 [Accessed November 7, 2015].

Holehan, A.M. & Merry, B.J., 1986. The experimental manipulation of ageing by diet. *Biological reviews of the Cambridge Philosophical Society*, 61(4), pp.329–368.

Holzenberger, M. et al., 2003. IGF-1 receptor regulates lifespan and resistance to oxidative stress in mice. *Nature*, 421(6919), pp.182–187.

Hondares, E. et al., 2011. Thermogenic activation induces FGF21 expression and release in brown adipose tissue. *The Journal of biological chemistry*, 286(15), pp.12983–12990.

Houtkooper, R.H. et al., 2013. Mitonuclear protein imbalance as a conserved longevity mechanism. *Nature*, 497(7450), pp.451–7. Available at: http://www.pubmedcentral.nih.gov/articlerender.fcgi?artid=3663447&tool=pmcentrez&rendertype=abstract.

Huffman, D.M. & Barzilai, N., 2009. Role of Visceral Adipose Tissue in Aging. *Biochimica et biophysica acta*, 1790(10), pp.1117–1123.

Hunt, N.D. et al., 2006. Bioenergetics of aging and calorie restriction. *Ageing research reviews*, 5(2), pp.125–43. Available at: http://www.sciencedirect.com/science/article/pii/S1568163706000286 [Accessed March 24, 2016].

Jazwinski, S.M., 2000. Metabolic control and ageing. *Trends in genetics : TIG*, 16(11), pp.506–511.

Jin, Y.H. & Koizumi, A., 1994. Decreased cellular proliferation by energy restriction is recovered by increasing housing temperature in rats. *Mechanisms of ageing and development*, 75(1), pp.59–67.

Kanda, T. et al., 2007. Reduced-energy diet improves survival of obese KKAy mice with viral myocarditis: induction of cardiac adiponectin expression. *International journal of cardiology*, 119(3), pp.310–318.

Kaushik, S. & Cuervo, A.M., 2015. Proteostasis and aging. *Nature medicine*, 21(12), pp.1406–1415.

Keenan, K.P. et al., 1996. The effects of diet, ad libitum overfeeding, and moderate dietary restriction on the rodent bioassay: the uncontrolled variable in safety assessment. *Toxicologic pathology*, 24(6), pp.757–768.

Keenan, K.P. et al., 1997. The effects of diet, overfeeding and moderate dietary restriction on Sprague-Dawley rat survival, disease and toxicology. *The Journal of nutrition*, 127(5 Suppl), p.851S–856S.

Kemnitz, J.W. et al., 1994. Dietary restriction increases insulin sensitivity and lowers blood glucose in rhesus monkeys. *The American journal of physiology*, 266(4 Pt 1), pp.E540-7.

Kenyon, C., 2005. The plasticity of aging: insights from long-lived mutants. *Cell*, 120(4), pp.449–460.

Kim, J.-H. et al., 2008. Lifelong exercise and mild (8%) caloric restriction attenuate age-induced alterations in plantaris muscle morphology, oxidative stress and IGF-1 in the Fischer-344 rat. *Experimental gerontology*, 43(4), pp.317–329.

Kirk, K.L., 2001. Dietary restriction and aging: comparative tests of evolutionary hypotheses. *The journals of gerontology. Series A, Biological sciences and medical sciences*, 56(3), pp.B123–B129.

Kirkwood, T.B. & Holliday, R., 1979. The evolution of ageing and longevity. *Proceedings of the Royal Society of London. Series B, Biological sciences*, 205(1161), pp.531–546.

Kirkwood, T.B.L., 2008. Understanding ageing from an evolutionary perspective. *Journal of internal medicine*, 263(2), pp.117–127.

Kirkwood, T.B.L., 2005. Understanding the odd science of aging. *Cell*, 120(4), pp.437–447.

Klein, S., Wadden, T. & Sugerman, H.J., 2002. AGA technical review on obesity. *Gastroenterology*, 123(3), pp.882–932.

Kooptiwut, S. et al., 2002. Comparison of insulin secretory function in two mouse models with different susceptibility to beta-cell failure. *Endocrinology*, 143(6), pp.2085–2092.

Kritchevsky, D., 2002. Caloric restriction and experimental carcinogenesis. *Hybridoma and hybridomics*, 21(2), pp.147–151.

Labbadia, J. & Morimoto, R.I., 2015. The biology of proteostasis in aging and disease. *Annual review of biochemistry*, 84, pp.435–464.

Ladiges, W. et al., 2009. Lifespan extension in genetically modified mice. *Aging cell*, 8(4), pp.346–352.

Lambert, A.J. et al., 2004. Effect of ageing and caloric restriction on specific markers of protein oxidative damage and membrane peroxidizability in rat liver mitochondria. *Mechanisms of Ageing and Development*, 125(8), pp.529–538.

Lambert, A.J. et al., 2004. The effect of aging and caloric restriction on mitochondrial protein density and oxygen consumption. *Experimental Gerontology*, 39(3), pp.289–295.

Lambert, A.J. & Merry, B.J., 2004. Effect of caloric restriction on mitochondrial reactive oxygen species production and bioenergetics: reversal by insulin. *American journal of physiology. Regulatory, integrative and comparative physiology*, 286(1), pp.R71-9.

Lambert, A.J. & Merry, B.J., 2000. Use of primary cultures of rat hepatocytes for the study of ageing and caloric restriction. *Experimental gerontology*, 35(5), pp.583–594.

Lane, M.A. et al., 1995. Diet restriction in rhesus monkeys lowers fasting and glucose-stimulated glucoregulatory end points. *The American journal of physiology*, 268(5 Pt 1), pp.E941-8.

Lane, R.K., Hilsabeck, T. & Rea, S.L., 2015. The role of mitochondrial dysfunction in age-related diseases. *Biochimica et biophysica acta*, 1847(11), pp.1387–1400.

Lanza-Jacoby, S. et al., 2013. Calorie restriction delays the progression of lesions to pancreatic cancer in the LSL-KrasG12D; Pdx-1/Cre mouse model of pancreatic cancer. *Experimental biology and medicine (Maywood, N.J.)*, 238(7), pp.787–797.

Lanza, I.R. et al., 2012. Chronic caloric restriction preserves mitochondrial function in senescence without increasing mitochondrial biogenesis. *Cell Metabolism*, 16(6), pp.777–788. Available at: http://dx.doi.org/10.1016/j.cmet.2012.11.003.

Lauritzen, K.H. et al., 2015. Impaired dynamics and function of mitochondria caused by mtDNA toxicity leads to heart failure. *American Journal of Physiology - Heart and Circulatory Physiology*, 309(3), pp.H434–H449. Available at: http://ajpheart.physiology.org/content/309/3/H434.abstract.

Lawler, D.F. et al., 2008. Diet restriction and ageing in the dog: major observations over two decades. *The British journal of nutrition*, 99(4), pp.793–805.

Lee, C.K. et al., 1999. Gene expression profile of aging and its retardation by caloric restriction. *Science (New York, N.Y.)*, 285(5432), pp.1390–1393.

Lee, H.-Y. et al., 2016. Targeted Expression of Catalase to Mitochondria Prevents Age-Associated Reductions in Mitochondrial Function and Insulin Resistance. *Cell Metabolism*, 12(6), pp.668–674. Available at: http://dx.doi.org/10.1016/j.cmet.2010.11.004.

Lees, E.K. et al., 2015. Effects of hepatic protein tyrosine phosphatase 1B and methionine restriction on hepatic and whole-body glucose and lipid metabolism in mice. *Metabolism: clinical and experimental*, 64(2), pp.305–314.

Lees, E.K. et al., 2014. Methionine restriction restores a younger metabolic phenotype in adult mice with alterations in fibroblast growth factor 21. *Aging cell*, 13(5), pp.817–27. Available at: http://www.pubmedcentral.nih.gov/articlerender.fcgi?artid=4331744&tool=pmcentrez&rendertype=abstract [Accessed February 13, 2017].

Lenaz, G. et al., 2000. Mitochondrial bioenergetics in aging. *Biochimica et Biophysica Acta (BBA) - Bioenergetics*, 1459(2–3), pp.397–404. Available at: http://www.sciencedirect.com/science/article/pii/S0005272800001778 [Accessed March 28, 2016].

Levine, M.E. et al., 2014. Low protein intake is associated with a major reduction in IGF-1, cancer, and overall mortality in the 65 and younger but not older population. *Cell metabolism*, 19(3), pp.407–417.

Lewis, S.E. et al., 1985. The effects of aging and chronic dietary restriction on whole body growth and protein turnover in the rat. *Experimental gerontology*, 20(5), pp.253–263.

Li, X., Cope, M.B., Johnson, M.S., Smith, D.L.J., et al., 2010. Mild calorie restriction induces fat accumulation in female C57BL/6J mice. *Obesity (Silver Spring, Md.)*, 18(3), pp.456–462.

Li, X., Cope, M.B., Johnson, M.S., Smith, D.L., et al., 2010. Mild calorie restriction induces fat accumulation in female C57BL/6J mice. *Obesity (Silver Spring, Md.)*, 18(3), pp.456–462. Available at: http://dx.doi.org/10.1038/oby.2009.312.

Liao, C.-Y., Johnson, T.E. & Nelson, J.F., 2013. Genetic Variation in Responses to Dietary Restriction – An Unbiased Tool for Hypothesis Testing. *Exp Gerontol*, 48(10): 10, pp.1025–1029.

Liao, C.Y. et al., 2011. Fat maintenance is a predictor of the murine lifespan response to dietary restriction. *Aging Cell*, 10(4), pp.629–639.

Liao, C.Y. et al., 2010. Genetic variation in the murine lifespan response to dietary restriction: From life extension to life shortening. *Aging Cell*, 9(1), pp.92–95.

Lin, S.-J. et al., 2002. Calorie restriction extends Saccharomyces cerevisiae lifespan by increasing respiration. *Nature*, 418(6895), pp.344–348.

Lipman, R. et al., 1995. Is late-life caloric restriction beneficial? *Aging (Milano)*, 7, p.136–139.

Lipman, R.D., 2002. Effect of calorie restriction on mortality kinetics in inbred strains of mice following 7,12-dimethylbenz[a]anthracene treatment. *The journals of gerontology. Series A, Biological sciences and medical sciences*, 57(4), pp.B153-7. Available at:

http://biomedgerontology.oxfordjournals.org/content/57/4/B153.short%5Cnhttp://biomedgerontology.oxfordjournals.org/cgi/doi/10.1093/gerona/57.4.B153%5Cnhttp://www.ncbi.nlm.nih.gov/pubmed/11909880.

Lopez-Lluch, G. et al., 2008. Mitochondrial biogenesis and healthy aging. *Experimental gerontology*, 43(9), pp.813–819.

López-Lluch, G. et al., 2006. Calorie restriction induces mitochondrial biogenesis and bioenergetic efficiency. *Proceedings of the National Academy of Sciences of the United States of America*, 103(6), pp.1768–73. Available at: http://www.pubmedcentral.nih.gov/articlerender.fcgi?artid=1413655&tool=pmcentrez&rendertype=abstract.

López-Lluch, G. et al., 2008. Mitochondrial biogenesis and healthy aging. *Experimental gerontology*, 43(9), pp.813–9. Available at: http://www.sciencedirect.com/science/article/pii/S0531556508001757 [Accessed February 14, 2016].

Lopez-Otin, C. et al., 2013. The hallmarks of aging. *Cell*, 153(6).

Lopez-Saez, J.F. et al., 1998. Cell proliferation and cancer. *Histology and histopathology*, 13(4), pp.1197–1214.

Lopez-Torres, M. et al., 2002. Influence of aging and long-term caloric restriction on oxygen radical generation and oxidative DNA damage in rat liver mitochondria. *Free Radic Biol Med*, 32(9), pp.882–889. Available at: http://www.ncbi.nlm.nih.gov/entrez/query.fcgi?cmd=Retrieve&db=PubMed&dopt=Citation&list_uids=11978489.

Lorenzini, A. et al., 2014. Mice producing reduced levels of insulin-like growth factor type 1 display an increase in maximum, but not mean, life span. *The journals of gerontology. Series A, Biological sciences and medical sciences*, 69(4), pp.410–419.

Lowell, B.B. et al., 1993. Development of obesity in transgenic mice after genetic ablation of brown adipose tissue. *Nature*, 366(6457), pp.740–742.

Macotela, Y. et al., 2009. Sex and depot differences in adipocyte insulin sensitivity and glucose metabolism. *Diabetes*, 58(4), pp.803–812.

Madeo, F. et al., 2015. Essential role for autophagy in life span extension. *The*

Journal of clinical investigation, 125(1), pp.85–93.

Mair, W. & Dillin, A., 2008. Aging and survival: the genetics of life span extension by dietary restriction. *Annual review of biochemistry*, 77, pp.727–754.

Makrides, S.C., 1983. Protein synthesis and degradation during aging and senescence. *Biological reviews of the Cambridge Philosophical Society*, 58(3), pp.343–422.

Masoro, E.J., 2009. Caloric restriction-induced life extension of rats and mice: A critique of proposed mechanisms. *Biochimica et Biophysica Acta - General Subjects*, 1790(10), pp.1040–1048. Available at: http://dx.doi.org/10.1016/j.bbagen.2009.02.011.

Masoro, E.J., 2000. Caloric restriction and aging: An update. *Experimental Gerontology*, 35(3), pp.299–305.

Masoro, E.J., 1999. Commentary on “Revisiting the Role of Fat Mass in the Life Extension Induced by Caloric Restrietion.” *Journal ofGerontology: BIOLOGICAL SCIENCES*, 54A(3), p.B97.

Masoro, E.J. et al., 1992. Dietary restriction alters characteristics of glucose fuel use. *Journal of gerontology*, 47(6), pp.B202-8.

Masoro, E.J., 2005. Overview of caloric restriction and ageing. *Mechanisms of Ageing and Development*, 126(9 SPEC. ISS.), pp.913–922.

Masternak, M.M. et al., 2004. Divergent effects of caloric restriction on gene expression in normal and long-lived mice. *The journals of gerontology. Series A, Biological sciences and medical sciences*, 59(8), pp.784–788.

Matthews, D. et al., 1985. Homeostasis model assessment: insulin resistance and beta-cell function from fasting plasma glucose and insulin concentrations in man. *Diabetologia*, 28, pp.412–9.

Mattison, J.A. et al., 2017. Caloric restriction improves health and survival of rhesus monkeys. *Nature communications*, 8, p.14063.

Mattison, J. a. et al., 2012. Impact of caloric restriction on health and survival in rhesus monkeys from the NIA study. *Nature*, 489(7415), pp.318–321. Available at: http://dx.doi.org/10.1038/nature11432.

Mattson, M.P. et al., 2014. Meal frequency and timing in health and disease. *Proceedings of the National Academy of Sciences of the United States of America*, 111(47), pp.16647–16653.

Mattson, M.P., 2010. Perspective: Does brown fat protect against diseases of aging? *Ageing Research Reviews*, 9, pp.69–76.

Maynard S, Hejl AM, Dinh TS, Keijzers G, Hansen ÅM, Desler C, Moreno-Villanueva M, Bürkle A, Rasmussen LJ, Waldemar G, B.V., 2015. Defective mitochondrial respiration, altered dNTP pools and reduced AP endonuclease 1 activity in peripheral blood mononuclear cells of Alzheimer's disease patients. *Aging (Albany NY)*, 7(10), pp.793–815.

McCay, C.M. et al., 1939. Retarded growth, life span, ultimate body size and age changes in the albino rat after feeding diets restricted in calories. *J. Nutr.*, 18, pp.1–13.

McCay, C.M., Crowell, M.F. & Maynard, L.A., 1935. The effect of retarded growth upon the length of life span and upon the ultimate body size. 1935. *Nutrition (Burbank, Los Angeles County, Calif.)*, 5(3), p.155–71; discussion 172.

McKiernan, S.H. et al., 2004. Early-onset calorie restriction conserves fiber number in aging rat skeletal muscle. *FASEB journal : official publication of the Federation of American Societies for Experimental Biology*, 18(3), pp.580–581.

Merry, B.J. et al., 1987. The effects of ageing and chronic dietary restriction on in vivo hepatic protein synthesis in the rat. *Mechanisms of ageing and development*, 39(2), pp.189–199.

Merry, T.L. et al., 2017. Impairment of insulin signalling in peripheral tissue fails to extend murine lifespan. *Aging cell*.

Meyer, T.E. et al., 2006. Long-term caloric restriction ameliorates the decline in diastolic function in humans. *Journal of the American College of Cardiology*, 47(2), pp.398–402. Available at: http://dx.doi.org/10.1016/j.jacc.2005.08.069.

Miller, B.F. et al., 2012. A comprehensive assessment of mitochondrial protein synthesis and cellular proliferation with age and caloric restriction. *Aging Cell*, 11(1), pp.150–161.

Miller, B.F. et al., 2013. Calorie restriction does not increase short-term or long-term protein synthesis. *The journals of gerontology. Series A, Biological sciences and medical sciences*, 68(5), pp.530–538.

Miller, B.F. et al., 2014. The measurement of protein synthesis for assessing proteostasis in studies of slowed aging. *Ageing research reviews*, 18, pp.106–111.

Miller, B.F. & Hamilton, K.L., 2012. A perspective on the determination of mitochondrial biogenesis. *American journal of physiology. Endocrinology and metabolism*, 302(5), pp.E496-9.

Miller, B.F., Konopka, A.R. & Hamilton, K.L., 2016. The rigorous study of exercise adaptations: why mRNA might not be enough. *Journal of applied physiology (Bethesda, Md. : 1985)*, 121(2), pp.594–596.

Miller, R.A. et al., 2005. Methionine-deficient diet extends mouse lifespan, slows immune and lens aging, alters glucose, T4, IGF-I and insulin levels, and increases hepatocyte MIF levels and stress resistance. *Aging cell*, 4(3), pp.119–125.

Miller, R.A., 2016. Not Your Father's, or Mother's, Rodent: Moving Beyond B6. *Neuron*, 91(6), pp.1185–1186.

Mitchell et al., 2015a. The effects of graded levels of calorie restriction: I. impact of short term calorie and protein restriction on body composition in the C57BL/6 mouse. *Oncotarget*, 6(18).

Mitchell et al., 2015b. The effects of graded levels of calorie restriction: II. impact of short term calorie and protein restriction on body composition in the C57BL/6 mouse. *Oncotarget*, 6(18), pp.15902–15930.

Mitchell, G.W., 2014. The silver tsunami. *Physician executive*, 40(4), pp.34–38.

Mitchell, S.J. et al., 2016. Effects of Sex, Strain, and Energy Intake on Hallmarks of Aging in Mice. *Cell Metabolism*, 23(6), pp.1093–1112.

Mittal, N., Babu, M.M. & Roy, N., 2009. The efficiency of mitochondrial electron transport chain is increased in the long-lived mrg19 Saccharomyces cerevisiae. *Aging cell*, 8(6), pp.643–653.

Mootha, V.K. et al., 2003. Integrated analysis of protein composition, tissue diversity, and gene regulation in mouse mitochondria. *Cell*, 115(5), pp.629–640.

Morimoto, R.I. & Cuervo, A.M., 2014. Proteostasis and the aging proteome in health and disease. *The journals of gerontology. Series A, Biological sciences and medical sciences*, 69 Suppl 1, pp.S33-8.

Mouchiroud, L. et al., 2013. The NAD(+)/Sirtuin Pathway Modulates Longevity through Activation of Mitochondrial UPR and FOXO Signaling. *Cell*, 154(2), pp.430–441.

Mulvey, L., Sinclair, A. & Selman, C., 2014. Lifespan Modulation in Mice and the Confounding Effects of Genetic Background. *Journal of Genetics and Genomics*, 41(9), pp.497–503.

Munch, D., Amdam, G. V & Wolschin, F., 2008. Ageing in a eusocial insect: molecular and physiological characteristics of life span plasticity in the honey bee. *Functional ecology*, 22(3), pp.407–421.

Murphy, J.C. et al., 2011. Preferential reductions in intermuscular and visceral adipose tissue with exercise-induced weight loss compared with calorie restriction. *Journal of Applied Physiology*, 112(1), pp.79–85. Available at: http://jap.physiology.org/content/112/1/79.abstract.

Muzumdar, R. et al., 2008. Visceral adipose tissue modulates mammalian longevity. *Aging Cell*, 7(3), pp.438–440.

Nakagawa, S. et al., 2012. Comparative and meta-analytic insights into life extension via dietary restriction. *Aging Cell*, 11(3), pp.401–409.

Neese, R.A. et al., 2002. Measurement in vivo of proliferation rates of slow turnover cells by 2H2O labeling of the deoxyribose moiety of DNA. *Proceedings of the National Academy of Sciences of the United States of America*, 99(24), pp.15345–15350.

Nicholls, D.G., 2004. Mitochondrial membrane potential and aging. *Aging Cell*, 3(1), pp.35–40.

Nicklas, B.J. et al., 2006. Abdominal obesity is an independent risk factor for chronic heart failure in older people. *Journal of the American Geriatrics*

Society, 54(3), pp.413–420.

Nielsen, J. et al., 2016. Eye lens radiocarbon reveals centuries of longevity in the Greenland shark (Somniosus microcephalus). *Science (New York, N.Y.)*, 353(6300), pp.702–704.

Nisoli, E. et al., 2005. Calorie restriction promotes mitochondrial biogenesis by inducing the expression of eNOS. *Science (New York, N.Y.)*, 310(5746), pp.314–317.

Okita, N. et al., 2012. Differential responses of white adipose tissue and brown adipose tissue to caloric restriction in rats. *Mechanisms of ageing and development*, 133(5), pp.255–266.

Olsen, A., Vantipalli, M.C. & Lithgow, G.J., 2006. Lifespan extension of Caenorhabditis elegans following repeated mild hormetic heat treatments. *Biogerontology*, 7(4), pp.221–230.

Omodei, D. & Fontana, L., 2011. Calorie restriction and prevention of age-associated chronic disease. *FEBS letters*, 585(11), pp.1537–1542.

Orentreich, N. et al., 1993. Low methionine ingestion by rats extends life span. *The Journal of nutrition*, 123(2), pp.269–274.

Osborne, T.B., Mendel, L.B. & Ferry, E.L., 1917. The Effect of Retardation of Growth Upon the Breeding Period and Duration of Life of Rats. *Science*, 45, pp.294–295.

Palmer, B.F. & Clegg, D.J., 2015. The sexual dimorphism of obesity. *Molecular and cellular endocrinology*, 402, pp.113–119.

Pamplona, R. & Barja, G., 2006. Mitochondrial oxidative stress, aging and caloric restriction: the protein and methionine connection. *Biochimica et biophysica acta*, 1757(5–6), pp.496–508.

Partridge, L., 2012. Diet and Healthy Aging — NEJM. , pp.26–27. Available at: http://www.nejm.org/doi/full/10.1056/NEJMcibr1210447.

Partridge, L. & Gems, D., 2002. Mechanisms of ageing: public or private? *Nature reviews. Genetics*, 3(3), pp.165–175.

Partridge, L., Piper, M.D.W. & Mair, W., 2005. Dietary restriction in Drosophila.

Mechanisms of Ageing and Development, 126(9 SPEC. ISS.), pp.938–950.

Payne, B.A.I. & Chinnery, P.F., 2015. Mitochondrial dysfunction in aging: Much progress but many unresolved questions. *Biochimica et biophysica acta*, 1847(11), pp.1347–1353.

Pearl, L.H., 2016. The HSP90 molecular chaperone - an enigmatic ATPase. *Biopolymers*, 105(8). Available at: http://www.ncbi.nlm.nih.gov/pubmed/26991466.

Pearl, R., 1928. *The Rate of Living*, Knopf, New York.

Perez, V.I. et al., 2009. Is the oxidative stress theory of aging dead? *Biochim Biophys Acta*, 1790(10), pp.1005–1014.

Picard, M. et al., 2010. Mitochondrial functional impairment with aging is exaggerated in isolated mitochondria compared to permeabilized myofibers. *Aging cell*, 9(6), pp.1032–1046.

Picard, M. et al., 2011. Mitochondrial structure and function are disrupted by standard isolation methods. *PloS one*, 6(3), p.e18317.

Pinney, D.O., Stephens, D.F. & Pope, L.S., 1972. Lifetime effects of winter supplemental feed level and age at first parturition on range beef cows. *Journal of animal science*, 34(6), pp.1067–1074.

Poortmans, J.R. et al., 2012. Protein turnover, amino acid requirements and recommendations for athletes and active populations. *Brazilian journal of medical and biological research = Revista brasileira de pesquisas medicas e biologicas*, 45(10), pp.875–890.

Porter, C. et al., 2015. Mitochondrial respiratory capacity and coupling control decline with age in human skeletal muscle. *American Journal of Physiology - Endocrinology and Metabolism*, 309(3), pp.E224–E232. Available at: http://ajpendo.physiology.org/content/309/3/E224.abstract.

Price, J.C. et al., 2012. The effect of long term calorie restriction on in vivo hepatic proteostatis: a novel combination of dynamic and quantitative proteomics. *Molecular & Cellular Proteomics*, pp.1801–1814.

Price, J.C. et al., 2012. The effect of long term calorie restriction on in vivo hepatic

proteostatis: a novel combination of dynamic and quantitative proteomics. *Molecular & cellular proteomics : MCP*, 11(12), pp.1801–1814.

Pride, H. et al., 2015. Long-lived species have improved proteostasis compared to phylogenetically-related shorter-lived species. *Biochemical and biophysical research communications*, 457(4), pp.669–675.

Puigserver, P. et al., 1998. A Cold-Inducible Coactivator of Nuclear Receptors Linked to Adaptive Thermogenesis. *Cell*, 92(6), pp.829–839. Available at: http://www.sciencedirect.com/science/article/pii/S0092867400814105 [Accessed October 21, 2015].

Pulliam, D.A. et al., 2014. Complex IV Deficient Surf1(−/−) Mice Initiate Mitochondrial Stress Responses. *The Biochemical journal*, 462(2), pp.359–371. Available at: http://www.ncbi.nlm.nih.gov/pmc/articles/PMC4145821/.

Racette, S.B. et al., 2006. One year of caloric restriction in humans: feasibility and effects on body composition and abdominal adipose tissue. *The journals of gerontology. Series A, Biological sciences and medical sciences*, 61(9), pp.943–950.

Ramsey J., J. et al., 2000. Restriction of energy intake, energy expenditure, and aging. *Free Radical Biology and Medicine*, 29(10), pp.946–968. Available at: http://linkinghub.elsevier.com/retrieve/pii/S0891584900004172.

Rattan, S.I., 1996. Synthesis, modifications, and turnover of proteins during aging. *Experimental gerontology*, 31(1–2), pp.33–47.

Rebrin, I., Forster, M.J. & Sohal, R.S., 2011. Association between life-span extension by caloric restriction and thiol redox state in two different strains of mice. *Free radical biology & medicine*, 51(1), pp.225–233.

Richie, J.P.J. et al., 1994. Methionine restriction increases blood glutathione and longevity in F344 rats. *FASEB journal : official publication of the Federation of American Societies for Experimental Biology*, 8(15), pp.1302–1307.

Riera, C.E. et al., 2016. Signaling Networks Determining Life Span. *Annual review of biochemistry*, 85, pp.35–64.

Rikke, B.A. et al., 2010. Genetic dissection of dietary restriction in mice supports the metabolic efficiency model of life extension. *Experimental Gerontology*,

45(9), pp.691–701. Available at: http://dx.doi.org/10.1016/j.exger.2010.04.008.

Rikke, B.A. et al., 2003. Strain variation in the response of body temperature to dietary restriction. *Mechanisms of ageing and development*, 124(5), pp.663–678.

Rikke, B.A. & Johnson, T.E., 2007. Physiological genetics of dietary restriction: uncoupling the body temperature and body weight responses. *American journal of physiology. Regulatory, integrative and comparative physiology*, 293(4), pp.R1522-7. Available at: http://ajpregu.physiology.org/content/293/4/R1522.abstract.

Rincon, M., Rudin, E. & Barzilai, N., 2005. The insulin/IGF-1 signaling in mammals and its relevance to human longevity. *Experimental Gerontology*, 40(11), pp.873–877.

Ristow, M. & Schmeisser, K., 2014. Mitohormesis: Promoting Health and Lifespan by Increased Levels of Reactive Oxygen Species (ROS). *Dose-response : a publication of International Hormesis Society*, 12(2), pp.288–341. Available at: http://www.pubmedcentral.nih.gov/articlerender.fcgi?artid=4036400&tool=pmcentrez&rendertype=abstract.

Ristow, M. & Schmeisser, S., 2011. Extending life span by increasing oxidative stress. *Free Radical Biology and Medicine*, 51(2), pp.327–336.

Ristow, M. & Zarse, K., 2010. How increased oxidative stress promotes longevity and metabolic health: The concept of mitochondrial hormesis (mitohormesis). *Experimental Gerontology*, 45(6), pp.410–418.

Robinson, M.M. et al., 2010. Acute {beta}-adrenergic stimulation does not alter mitochondrial protein synthesis or markers of mitochondrial biogenesis in adult men. *American journal of physiology. Regulatory, integrative and comparative physiology*, 298(1), pp.R25-33.

Robinson, M.M. et al., 2011. Long-term synthesis rates of skeletal muscle DNA and protein are higher during aerobic training in older humans than in sedentary young subjects but are not altered by protein supplementation. *FASEB journal : official publication of the Federation of American Societies for Experimental Biology*, 25(9), pp.3240–3249.

Rogers, G.W. et al., 2011. High throughput microplate respiratory measurements using minimal quantities of isolated mitochondria. *PLoS ONE*, 6(7).

Rogers, N.H. et al., 2012. Aging Leads to a Programmed Loss of Brown Adipocytes in Murine Subcutaneous White Adipose Tissue. *Aging Cell*, 11(6), pp.1–18.

Rooyackers, O.E. et al., 1996. Effect of age on in vivo rates of mitochondrial protein synthesis in human skeletal muscle. *Proceedings of the National Academy of Sciences of the United States of America*, 93(26), pp.15364–15369.

Ross, R. et al., 2008. Does the relationship between waist circumference, morbidity and mortality depend on measurement protocol for waist circumference? *Obesity reviews : an official journal of the International Association for the Study of Obesity*, 9(4), pp.312–325.

Ruetenik, A. & Barrientos, A., 2015. Dietary restriction, mitochondrial function and aging: From yeast to humans. *Biochimica et Biophysica Acta - Bioenergetics*, 1847(11), pp.1434–1447. Available at: http://dx.doi.org/10.1016/j.bbabio.2015.05.005.

Ryan, B.J. et al., 2015. Mitochondrial dysfunction and mitophagy in Parkinson's: from familial to sporadic disease. *Trends in biochemical sciences*, 40(4), pp.200–210.

Ryan, M.T. & Hoogenraad, N.J., 2007. Mitochondrial-nuclear communications. *Annual review of biochemistry*, 76, pp.701–722.

Saely, C.H., Geiger, K. & Drexel, H., 2011. Brown versus white adipose tissue: A mini-review. *Gerontology*, 58(1), pp.15–23.

Saito, M. et al., 2009. High incidence of metabolically active brown adipose tissue in healthy adult humans: effects of cold exposure and adiposity. *Diabetes*, 58(7), pp.1526–1531.

Salin, K. et al., 2015. Individuals with higher metabolic rates have lower levels of reactive oxygen species in vivo. *Biology Letters*, pp.4–7.

Salvioli, S. et al., 2001. Mitochondria, aging and longevity - A new perspective. *FEBS Letters*, 492(1–2), pp.9–13.

Sanz, A. et al., 2006. Effect of lipid restriction on mitochondrial free radical production and oxidative DNA damage. *Annals of the New York Academy of Sciences*, 1067, pp.200–209.

Sanz, A., Caro, P. & Barja, G., 2004. Protein restriction without strong caloric restriction decreases mitochondrial oxygen radical production and oxidative DNA damage in rat liver. *Journal of bioenergetics and biomembranes*, 36(6), pp.545–552.

Satoh, A. et al., 2013. Sirt1 extends life span and delays aging in mice through the regulation of Nk2 homeobox 1 in the DMH and LH. *Cell metabolism*, 18(3), pp.416–430.

Schleit, J. et al., 2013. Molecular mechanisms underlying genotype-dependent responses to dietary restriction. *Aging Cell*, 12(6), pp.1050–1061.

Schulz, A.M. & Haynes, C.M., 2015. UPR(mt)-mediated cytoprotection and organismal aging. *Biochimica et biophysica acta*, 1847(11), pp.1448–56. Available at: http://www.sciencedirect.com/science/article/pii/S0005272815000584 [Accessed May 1, 2016].

Selman, C., 2014a. Dietary restriction and the pursuit of effective mimetics. *Proceedings of the Nutrition Society*, 73(JANUARY 2014), p.260–270. DOI: 10.1017/S0029665113003832. Available at: http://www.ncbi.nlm.nih.gov/pubmed/24411076.

Selman, C., 2014b. Dietary restriction and the pursuit of effective mimetics. *The Proceedings of the Nutrition Society*, 73(2), pp.260–270.

Selman, C. et al., 2005. Energy expenditure of calorically restricted rats is higher than predicted from their altered body composition. *Mechanisms of Ageing and Development*, 126(6–7), pp.783–793.

Selman, C. et al., 2008. Evidence for lifespan extension and delayed age-related biomarkers in insulin receptor substrate 1 null mice. *The FASEB journal : official publication of the Federation of American Societies for Experimental Biology*, 22(3), pp.807–818.

Selman, C. et al., 2009. Ribosomal protein S6 kinase 1 signaling regulates

mammalian life span. *Science (New York, N.Y.)*, 326(5949), pp.140–144.

Serra, V. et al., 2003. Extracellular superoxide dismutase is a major antioxidant in human fibroblasts and slows telomere shortening. *The Journal of biological chemistry*, 278(9), pp.6824–6830.

Shabalina, I.G. et al., 2010. Cold tolerance of UCP1-ablated mice: a skeletal muscle mitochondria switch toward lipid oxidation with marked UCP3 up-regulation not associated with increased basal, fatty acid- or ROS-induced uncoupling or enhanced GDP effects. *Biochimica et biophysica acta*, 1797(6–7), pp.968–980.

Sheldon, W.G., Bucci, T.J., et al., 1995. Age-related neoplasia in a lifetime study of ad libitum-fed and food-restricted B6C3F1 mice. *Toxicologic pathology*, 23(4), pp.458–476.

Sheldon, W.G., Warbritton, A.R., et al., 1995. Glaucoma in food-restricted and ad libitum-fed DBA/2NNia mice. *Laboratory animal science*, 45(5), pp.508–518.

Shi, H. et al., 2007. Sexually dimorphic responses to fat loss after caloric restriction or surgical lipectomy. *American journal of physiology. Endocrinology and metabolism*, 293(1), pp.E316-26.

Shiels, P.G. et al., 2017. The role of epigenetics in renal ageing. *Nature reviews. Nephrology*, 13(8), pp.471–482.

Shiels, P.G. & Ritzau-Reid, K., 2015. Biological Ageing, Inflammation and Nutrition: How Might They Impact on Systemic Sclerosis? *Current aging science*, 8(2), pp.123–130.

Shimokawa, I. & Trindade, L.S., 2010. Dietary restriction and aging in rodents: a current view on its molecular mechanisms. *Aging and disease*, 1(2), pp.89–107. Available at: http://www.pubmedcentral.nih.gov/articlerender.fcgi?artid=3295025&tool=pmcentrez&rendertype=abstract.

Singh, R.J., 2002. Glutathione: a marker and antioxidant for aging. *The Journal of laboratory and clinical medicine*, 140(6), pp.380–381.

Sittig, L.J. et al., 2016. Genetic Background Limits Generalizability of Genotype-Phenotype Relationships. *Neuron*, 91(6), pp.1253–1259.

Soare, A. et al., 2011. Long-term calorie restriction, but not endurance exercise, lowers core body temperature in humans. *Aging*, 3(4), pp.374–379.

Sohal, R., Svensson, I. & Brunk, U., 1990. Hydrogen peroxide production by liver mitochondria in different species. *Mechanisms of ageing and …*, 53, pp.209–215. Available at: http://ukpmc.ac.uk/abstract/MED/2115947.

Sohal, R.S. et al., 2009. Life span extension in mice by food restriction depends on an energy imbalance. *The Journal of nutrition*, 139(3), pp.533–9. Available at: http://www.pubmedcentral.nih.gov/articlerender.fcgi?artid=2646218&tool=pmcentrez&rendertype=abstract.

Sohal, R.S. et al., 1994. Oxidative damage, mitochondrial oxidant generation and antioxidant defenses during aging and in response to food restriction in the mouse. *Mechanisms of Ageing and Development*, 74(1–2), pp.121–133.

Sohal, R.S. & Weindruch, R., 1996. Oxidative stress, caloric restriction, and aging. *Science (New York, N.Y.)*, 273(5271), pp.59–63.

Solon-Biet, S. et al., 2015. Dietary Protein to Carbohydrate Ratio and Caloric Restriction: Comparing Metabolic Outcomes in Mice. *Cell Reports*, 11(10), pp.1529–1534.

Speakman, J.R. & Keijer, J., 2012. Not so hot: Optimal housing temperatures for mice to mimic the thermal environment of humans. *Molecular metabolism*, 2(1), pp.5–9.

Speakman, J.R. & Mitchell, S.E., 2011. Caloric restriction. *Molecular Aspects of Medicine*, 32(3), pp.159–221. Available at: http://dx.doi.org/10.1016/j.mam.2011.07.001.

Speakman, J.R. & Selman, C., 2011. The free-radical damage theory: Accumulating evidence against a simple link of oxidative stress to ageing and lifespan. *BioEssays*, 33(4), pp.255–259.

Stadtman, E.R., 1992. Protein oxidation and aging. *Science (New York, N.Y.)*, 257(5074), pp.1220–1224.

Stanford, K.I. et al., 2013. Brown adipose tissue regulates glucose homeostasis and insulin sensitivity. *The Journal of clinical investigation*, 123(1), pp.215–223.

Stein, P.K. et al., 2012. Caloric restriction may reverse age-related autonomic decline in humans. *Aging cell*, 11(4), pp.644–650.

Storer, J.B., 1966. Longevity and gross pathology at death in 22 inbred mouse strains. *Journal of gerontology*, 21(3), pp.404–409.

Stout, R.W., 1994. Glucose tolerance and ageing. *Journal of the Royal Society of Medicine*, 87(10), pp.608–609.

Sun, L. et al., 2009. Life-span extension in mice by preweaning food restriction and by methionine restriction in middle age. *The journals of gerontology. Series A, Biological sciences and medical sciences*, 64(7), pp.711–722.

Suzman, R. et al., 2015. Health in an ageing world--what do we know? *Lancet (London, England)*, 385(9967), pp.484–486.

Swindell, W.R., 2012. Dietary restriction in rats and mice: a meta-analysis and review of the evidence for genotype-dependent effects on lifespan. *Ageing research reviews*, 11(2), pp.254–70. Available at: http://www.sciencedirect.com/science/article/pii/S156816371100078X [Accessed March 31, 2016].

Tannenbaum, A., 1940. The initiation and growth of tumors. Introduction. I. Effects of underfeeding. *Am. J. Cancer*, 38(3), p.335–350. Available at: https://www.scopus.com/record/display.uri?eid=2-s2.0-0001728228&origin=inward&txGid=21AAA69847EFFFBD53292D2FAA90D770.wsnAw8kcdt7IPYLO0V48gA%3A2.

Tauffenberger, A., Vaccaro, A. & Parker, J.A., 2016. Fragile lifespan expansion by dietary mitohormesis in C. elegans. *Aging*, 8(1), pp.1–12.

Tavernarakis, N. & Driscoll, M., 2002. Caloric restriction and lifespan: a role for protein turnover? *Mechanisms of ageing and development*, 123(2–3), pp.215–229.

Taylor, R.C. & Dillin, A., 2011. Aging as an event of proteostasis collapse. *Cold Spring Harbor perspectives in biology*, 3(5).

Tonoki, A. et al., 2009. Genetic evidence linking age-dependent attenuation of the 26S proteasome with the aging process. *Molecular and cellular biology*, 29(4), pp.1095–1106.

Treaster, S.B. et al., 2014. Superior proteome stability in the longest lived animal. *Age (Dordrecht, Netherlands)*, 36(3), p.9597.

Turturro, A. & Hart, R.W., 1991. Longevity-assurance mechanisms and caloric restriction. *Annals of the New York Academy of Sciences*, 621, pp.363–372.

Turturro, a et al., 1999. Growth curves and survival characteristics of the animals used in the Biomarkers of Aging Program. *The journals of gerontology. Series A, Biological sciences and medical sciences*, 54(11), pp.B492–B501.

Vaanholt, L.M., Magee, V. & Speakman, J.R., 2012. Factors predicting individual variability in diet-induced weight loss in MF1 mice. *Obesity (Silver Spring, Md.)*, 20(2), pp.285–294.

Vague, J., 1947. [Not Available]. *La Presse medicale*, 55(30), p.339.

Valle, A. et al., 2008. Caloric restriction retards the age-related decline in mitochondrial function of brown adipose tissue. *Rejuvenation research*, 11(3), pp.597–604.

Valle, A. et al., 2005. Sex-related differences in energy balance in response to caloric restriction. *American journal of physiology. Endocrinology and metabolism*, 289(1), pp.E15-22.

Varady, K.A. et al., 2010. Improvements in body fat distribution and circulating adiponectin by alternate-day fasting versus calorie restriction. *The Journal of nutritional biochemistry*, 21(3), pp.188–195.

Vilchez, D., Saez, I. & Dillin, A., 2014. The role of protein clearance mechanisms in organismal ageing and age-related diseases. *Nature communications*, 5, p.5659.

Wallace, D.C., 2012. Mitochondria and cancer. *Nature reviews. Cancer*, 12(10), pp.685–698.

Wallace, T.M., Levy, J.C. & Matthews, D.R., 2004. Use and abuse of HOMA modeling. *Diabetes Care*, 27(6), pp.1487–1495.

Walsh, M.E., Shi, Y. & Van Remmen, H., 2014. The effects of dietary restriction on oxidative stress in rodents. *Free radical biology & medicine*, 66, pp.88–99.

Wang, Y. et al., 2005. Comparison of abdominal adiposity and overall obesity in

predicting risk of type 2 diabetes among men. *The American journal of clinical nutrition*, 81(3), pp.555–563.

Wang, Y. & Hekimi, S., 2015. Mitochondrial dysfunction and longevity in animals: Untangling the knot. *Science*, 350(6265), pp.1204–1207. Available at: http://www.sciencemag.org/cgi/doi/10.1126/science.aac4357.

Ward, W. & Richardson, A., 1991. Effect of age on liver protein synthesis and degradation. *Hepatology (Baltimore, Md.)*, 14(5), pp.935–948.

Ward, W.F., 2000. The relentless effects of the aging process on protein turnover. *Biogerontology*, 1(3), pp.195–199.

Waterlow, J.C., 1986. Metabolic adaptation to low intakes of energy and protein. *Annual review of nutrition*, 6, pp.495–526.

Wei, Y.H. et al., 2001. Mitochondrial theory of aging matures--roles of mtDNA mutation and oxidative stress in human aging. *Zhonghua yi xue za zhi = Chinese medical journal; Free China ed*, 64(5), pp.259–270.

Weindruch, R. et al., 2001. Microarray profiling of gene expression in aging and its alteration by caloric restriction in mice. *The Journal of nutrition*, 131(3), p.918S–923S.

Weindruch, R. et al., 1986. The retardation of aging in mice by dietary restriction: longevity, cancer, immunity and lifetime energy intake. *The Journal of nutrition*, 116(4), pp.641–654.

Weindruch, R. & Sohal, R.S., 1997. Caloric Intake and Aging. *New England Journal of Medicine*, 337(14), pp.986–994.

Weindruch, R. & Sohal, R.S., 1997. Seminars in medicine of the Beth Israel Deaconess Medical Center. Caloric intake and aging. *The New England journal of medicine*, 337(14), pp.986–994.

Weindruch, R. & Walford, R., 1982. Dietary restriction in mice beginning at 1 year of age: effect on life-span and spontaneous cancer incidence. *Science*, 215(4538), pp.1415– 1418.

Weindruch, R. & Walford, R., 1988. The Retardation of Aging and Disease by Dietary Restriction.

Weindruch, R.H. et al., 1979. Influence of controlled dietary restriction on immunologic function and aging. *Federation proceedings*, 38(6), pp.2007–2016.

Weindruch, R.H. et al., 1980. Modification of mitochondrial respiration by aging and dietary restriction. *Mechanisms of Ageing and Development*, 12(4), pp.375–392.

Weindruch, R.S.S. and R., 1996. Oxidative Stress, Caloric Restriction, and Aging.

Weiss, E.P. et al., 2006. Improvements in glucose tolerance and insulin action induced by increasing energy expenditure or decreasing energy intake: a randomized controlled trial. *Am J Clin Nutr*, 84(5), pp.1033–1042. Available at: http://ajcn.nutrition.org/content/84/5/1033.short.

Williams, R.W. et al., 2004. Genetic structure of the LXS panel of recombinant inbred mouse strains: a powerful resource for complex trait analysis. *Mammalian genome : official journal of the International Mammalian Genome Society*, 15(8), pp.637–647. Available at: http://www.ncbi.nlm.nih.gov/pubmed/15457343.

Wolff, S., Weissman, J.S. & Dillin, A., 2014. Differential scales of protein quality control. *Cell*, 157(1), pp.52–64.

Yan, L. et al., 2012. Common mechanisms for calorie restriction and adenylyl cyclase type 5 knockout models of longevity. *Aging cell*, 11(6), pp.1110–1120.

Yeni-Komshian, H. et al., 2000. Relationship between several surrogate estimates of insulin resistance and quantification of insulin-mediated glucose disposal in 490 healthy nondiabetic volunteers. *Diabetes care*, 23(2), pp.171–175.

Yoneshiro, T. et al., 2013. Recruited brown adipose tissue as an antiobesity agent in humans. *The Journal of clinical investigation*, 123(8), pp.3404–3408.

Zangarelli, A. et al., 2006. Synergistic effects of caloric restriction with maintained protein intake on skeletal muscle performance in 21-month-old rats: a mitochondria-mediated pathway. *The FASEB Journal*, 20(14), pp.2439–2450. Available at: http://www.fasebj.org/content/20/14/2439.abstract.

Zhang, H. et al., 2016. NAD(+) repletion improves mitochondrial and stem cell function and enhances life span in mice. *Science (New York, N.Y.)*,

352(6292), pp.1436–1443.

Zhou, M. et al., 1997. A stable nonfluorescent derivative of resorufin for the fluorometric determination of trace hydrogen peroxide: applications in detecting the activity of phagocyte NADPH oxidase and other oxidases. *Analytical biochemistry*, 253(2), pp.162–168.

Zid, B.M. et al., 2009. 4E-BP Extends Lifespan upon Dietary Restriction by Enhancing Mitochondrial Activity in Drosophila. *Cell*, 139(1), pp.149–160. Available at: http://dx.doi.org/10.1016/j.cell.2009.07.034.